HYDROPHILIC SEGMENTED BLOCK COPOLYMERS BASED ON POLY(ETHYLENE OXIDE)

PROEFSCHRIFT

ter verkrijging van
de graad van doctor aan de Universiteit Twente,
op gezag van de rector magnificus,
prof. dr. W.H.M. Zijm,
volgens besluit van het College voor Promoties
in het openbaar te verdedigen
op donderdag 7 december 2006 om 15.00 uur

door

Debby Husken

geboren op 14 april 1978
te Enschede

Dit proefschrift is goedgekeurd door:

Promotor:	prof. dr. J. Feijen
Assistent-promotor:	dr. R.J. Gaymans

“De mens moet wel blijven geloven, dat het onbegrijpelijke onbegrijpelijk is,
anders ging hij niet verder met onderzoeken.”

(Johan Wolfgang von Goethe)

The research described in this thesis is part of the Research Program of the Dutch Polymer Institute (DPI), the Netherlands (project #313)

Hydrophilic segmented block copolymers based on poly(ethylene oxide) / D. Husken
Thesis, University of Twente, the Netherlands
December 2006

ISBN 90-365-2438-5

Cover design by: Ype van der Zijpp and Debby Husken

Copyright © D. Husken

Printed by: PrintPartners Ipskamp, Enschede, the Netherlands

Voorwoord

“How time flies when you’re having fun”

Tijdens het schrijven van dit voorwoord komen vele leuke herinneringen aan mijn promotietijd naar boven. Ik kan wel zeggen dat deze tijd voorbij is gevlogen. Dit heb ik mede te danken aan verschillende mensen.

Allereerst wil ik Reinoud Gaymans bedanken. Na een jaar gewerkt te hebben als technicus zag jij voldoende potentie in mij en hebt mij een promotieplaats aangeboden. De deur stond altijd open voor vragen en eventuele problemen. We waren het wel niet altijd eens met elkaar maar ik kijk met plezier terug op alle gesprekken en discussie die we hebben gehad.
Tevens wil ik mijn promotor prof. Jan Feijen bedanken voor alle besprekingen en discussies tijdens mijn promotietijd. U heeft me vaak aan nieuwe ideeën geholpen om ook eens vanuit een andere hoek naar de behaalde resultaten te kijken.

Speciale dank gaat uit naar mijn twee paranimfen, Edwin Biemond en Ingrid Velthoen. Edwin, sinds jij na je promotie de STEP-groep en ons kantoor hebt verlaten, is het een stuk “leger” geworden. Jij was altijd graag bereid een weddenschap met me aan te gaan: waarschijnlijk omdat ik er in de afgelopen vier jaar slechts één heb gewonnen! Ik heb de thee met Sambuca gemist. Ingrid, ondanks dat je in een andere groep zit hebben we tijdens de vele koffiepauzes altijd gezellige (vrouwen)gesprekken gehad. Tevens heb ik altijd genoten tijdens de volleybalwedstrijden, ladies nights en beauty evenings.

Natuurlijk wil ik ook mijn drie afstudeerders bedanken voor hun bijdrage: Marc Rijsdijk, Niels Sijbrandi en Sander Reijerkerk. Bedankt voor jullie inzet en vaak ‘verfrissende’ kijk op de resultaten. Marc en Sander, jullie zal een groot deel van hoofdstuk 9 wel bekend voorkomen. Niels, jou werk staat helaas niet in dit proefschrift beschreven, maar de geplande artikelen met jouw naam erbij zullen zeker komen!

Verder bedank ik de gehele STEP-groep: Wilco, Josien, Martijn, Edwin (wederom), Arun, Debassish en alle afstudeerders natuurlijk. Het was altijd erg gezellig: de ontspannende

fietstochtjes (met een gemiddelde snelheid van zo’n 28 km/uur), (Sambuca-)borrels, jaarlijkse oliebollen feestjes, diverse etentjes, bedrijfsbezoeken en memorabele congressen. Daarbij vergeet ik uiteraard niet alle Artecs-mensen: Wilco, Ype, Niels en Kai. Bedankt voor alle hulp bij mijn experimenten en koppen koffie. Inmiddels zijn jullie vast ook (noodgedwongen) fans van Robbie Williams geworden!

Iedereen van de groepen PBM, MTP en RBT bedank ik voor de gezelligheid tijdens de koffiepauzes, vele borrels, ladies nights, volleybalwedstrijden en natuurlijk de beruchte jaarlijkse triathlon. Ik zal de spannende soap over het leven van Mark ten B. tijdens de lunch gaan missen en kan niet wachten op de autobiografie.
Zlata en Karin: bedankt voor alle gezellige gesprekken en hulp bij mijn ontelbare bestellingen en het regelen van allerlei formaliteiten in de afgelopen jaren. Hetty: bedankt voor je hulp bij het opnemen van de AFM-plaatjes. Tijmen: bedankt voor het uitvoeren van de gastransport-metingen en vele discussies die we hebben gehad over de resultaten.

Mijn speciale dank gaat uit naar Mark.
Zonder jou lag dit boekje er niet! Bedankt voor je groot vertrouwen in mij. Jouw eeuwig positieve en rustige kijk op de dingen heeft mij zover gebracht als ik nu ben. Je aanzoek had op geen beter moment kunnen komen. Ik hou van je!

Debby

Contents

Chapter 1	General introduction	1
Chapter 2	Synthesis and characterisation of segmented block copolymers based on poly(ethylene oxide) and monodisperse crystallisable segments	7
Chapter 3	Segmented block copolymers with terephthalic extended PEO segments	33
Chapter 4	Segmented block copolymers based on mixed polyether segments	51
Chapter 5	Water in polyether-based segmented block copolymers	73
Chapter 6	Surface properties of polyether-based segmented block copolymers	101
Chapter 7	Gas permeation properties of PEO-based segmented block copolymers	117
Chapter 8	Water vapour transmission of polyether-based segmented block copolymers	135
Chapter 9	Use of monofunctional PEO in segmented block copolymers containing monodisperse crystallisable segments	155
Summary		183
Samenvatting		187
Curriculum Vitae		191

Chapter 1

General introduction

Introduction

Thermoplastic elastomers (TPE's) are polymers that show elastomeric behaviour at their service temperature and can be melt-processed at elevated temperatures [1,2]. TPE's contain thermally reversible physical crosslinks and can be melt-processed repeatedly. The main advantages of TPE's compared to conventional elastomers are the ease of processing and the ability to recycle production scrap. However, TPE's are usually not as effective as chemical crosslinked elastomers in solvent resistance and resistance to deformation at high temperature. TPE's can be roughly divided into three main groups. The largest group comprises the styrenic triblock copolymers, followed by the second largest group containing thermoplastic polyolefins (TPO and TPV) and finally the last group consisting of multi-block copolymers. This last group can be divided in thermoplastic polyurethanes, polyesters and polyamides.

The global demand for TPE's is expected to grow 6.4 percent per year, to 2.15 million metric tons in 2006 [3]. This growth is due to the replacement of natural and synthetic rubber as well as rigid plastics and metals by TPE's.

Segmented block copolymers

Segmented block copolymers or multi-block copolymers consist of alternating flexible soft segments and crystallisable rigid segments [2]. The flexible segments have a low glass transition temperature and provide the material its flexibility. The rigid segments act as physical crosslinks for the soft phase and give the material dimensional stability and solvent resistance. The properties of segmented block copolymers can be varied by changing the block lengths of the flexible and rigid segments.

The rigid segments can contain ester, urethane or amide groups, while the flexible segments are usually polyesters or polyethers. The rigid and flexible segments are thermodynamically immiscible and, therefore, phase separation occurs. Phase separation can occur through liquid-liquid demixing or crystallisation. Polyurethanes phase separate through liquid-liquid

demixing, often followed by partial crystallisation of the rigid segments. Fast crystallising segments, such as polyesters or polyamides, usually phase separate through crystallisation.

The generally accepted morphology of segmented block copolymers that contain fast crystallisable segments is proposed by Cella [4] and is schematically shown in Figure 1.1. The amorphous phase (D) is the continuous phase that consists of flexible segments and some amorphous rigid segments dissolved in it (C). Part of the rigid segments has crystallised into lamellae (A).

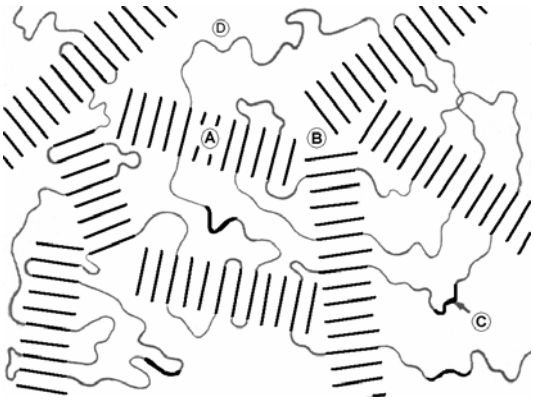

Figure 1.1: Schematic representation of the morphology of a segmented block copolymer with crystallised rigid segments as proposed by Cella [4]: A, crystalline domain; B, junction of crystalline lamellae; C, amorphous rigid segment, D, amorphous phase.

Film applications

There is a growing demand for films of segmented block copolymers that combine a number of properties including flexibility, elasticity, permeability to water vapour, chemical resistance, and thermal stability. The nature of the flexible segments has a strong influence on the type of application. Copolymers composed of hydrophilic polyether segments, like poly(ethylene oxide) (PEO), can be used for breathable film applications. These films must be permeable for water vapour while being a barrier for liquid water. One can think of a wide range of application markets for breathable films, as summarised in Table 1.1.

There are several commercially available segmented block copolymers that can be used for breathable film applications. The combination of a high water vapour permeability, water impermeability and elasticity makes these materials suitable for breathable film applications.

A well-known commercial breathable copolyester elastomer is Arnitel (DSM), which contains flexible polyether segments and poly(butylene terephthalate) (PBT) rigid segments. Thermoplastic polyamides, like PEBAX, are supplied by Atofina. These segmented block copolymers consist of polyether flexible segments and PA-6 or PA-12 rigid segments.

Important commercial segmented polyurethanes are Elastollan (Elastogran) and Pellethane (DOW). Thermoplastic polyurethanes can be synthesised from a long-chain diol (polyether or polyester), diisocyanate and a chain extender (usually a low molecular weight component like a diol or diamine).

Table 1.1: Breathable film applications. [5,6]

Medical / hygiene	Surgical garments
	Mattress cover dressings
	Adult incontinence articles / babies diapers
Textile	Films for textile lamination for sports, leisure and work-wear
	Footwear
Construction	Roofing membranes
	Wall coverings
Food packaging	Fruit, vegetables, mushrooms
Industry	Gas separation membranes
	Antistatic film
	Membranes for fuel cells

Monodisperse crystallisable segments

In general, segmented block copolymers have an incomplete phase separation, indicating that a large amount of non-crystallised rigid segments is present in the soft phase. The glass transition temperature of the soft phase increases with increasing amount of non-crystallised rigid segment present. A relatively high rigid segment concentration is required to obtain a segmented block copolymer with good mechanical properties, since the rigid segment crystallinity is rather low.

An effective way to improve phase separation in segmented block copolymers is by using monodisperse crystallisable segments [7,8]. These segments crystallise over their full length and, therefore, even short segments (i.e. low molecular weight) are able to crystallise. Moreover, the crystallisation of these segments is almost complete indicating that only a small amount of non-crystallised rigid segments is present in the soft phase.

The use of monodisperse crystallisable segments containing urethane(urea) [7-12] or amide groups [9,10,13-17] in segmented block copolymers has been studied previously. The rigid segments crystallise and form lamellae in the continuous soft phase, acting as thermo-reversible physical crosslinks, giving the material dimensional stability and solvent resistance.

Krijgsman et al. reported the synthesis and characterisation of monodisperse crystallisable bisester tetra-amide segments (T6T6T) [18]. These segments are composed of dimethyl terephthalate (T) and hexamethylenediamine (6) (Figure 1.2).

The monodisperse crystallisable T6T6T segments have been incorporated in hydrophobic polyether-based copolymers. The synthesis and characterisation of poly(tetramethylene oxide) (PTMO)-T6T6T [10,13,14] and poly(propylene oxide) (PPO)-T6T6T [9] segmented block copolymers have been previously reported. The polyether-T6T6T copolymers crystallise fast, have a relative high modulus, an almost temperature independent rubbery plateau and a sharp melting temperature. Besides, these copolymers are highly elastic and have high fracture strains.

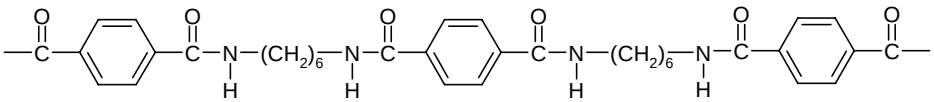

Figure 1.2: Structure of monodisperse crystallisable bisester tetra-amide (T6T6T) segment.

For breathable film applications it is interesting to synthesise a segmented block copolymer with a high soft phase concentration, as the gas vapour is transported mainly through the soft phase. By using monodisperse rigid segments, segmented block copolymers with a polyether concentration up to 97 wt% can be achieved while the copolymer still possesses good thermal mechanical properties. These copolymers can achieve a fracture stress and strain of 11 MPa and 870% respectively [10].

Research aim

The aim of the research described in this thesis, is to study the synthesis and structure-property relations of segmented block copolymers based on flexible polyether segments and monodisperse crystallisable segments. The polyether phase consists of hydrophilic poly(ethylene oxide) (PEO) and/or more hydrophobic poly(tetramethylene oxide) (PTMO) segments. Well phase-separated polymer structures are obtained by using monodisperse crystallisable segments, resulting in a rather pure polyether phase. The influence of the soft phase composition of the copolymers on the thermal mechanical properties, water absorption, surface hydrophilicity, gas permeation properties and water vapour transmission is studied.

Outline of this thesis

This thesis is directed to the research on segmented block copolymers with poly(ethylene oxide) (PEO) and/or poly(tetramethylene oxide) (PTMO) flexible segments and monodisperse crystallisable T6T6T segments.

In **Chapter 2** the synthesis of segmented block copolymers with different PEO molecular weights is reported. The thermal mechanical properties and crystallisation behaviour of these copolymers are investigated.

Chapter 3 describes the synthesis of segmented block copolymers where the PEO segments are extended with terephthalic units to create long flexible segments. The soft phase composition is varied by changing the PEO molecular weight and/or the molecular weight of the total flexible segment. The morphology and thermal mechanical properties of these copolymers are studied.

The synthesis of segmented block copolymers consisting of a mixture of hydrophilic PEO and hydrophobic PTMO segments is given in **Chapter 4**. The effect of the incorporated PTMO segments on the thermal mechanical properties and crystallisation behaviour of the copolymers is examined.

Parameters affecting the water absorption of polyether-based segmented block copolymers are determined in **Chapter 5.** Furthermore, the influence of water on the physical properties and tensile properties of polyether-based segmented block copolymers is discussed.

The surface hydrophilicity, determined by contact angle measurements, and the water vapour transmission through films of the polyether-based segmented block copolymers are reported in **Chapter 6** and **Chapter 7** respectively. The relation between the soft phase composition of the copolymer on both the surface hydrophilicity and the water vapour transmission is investigated.

Gas permeation properties and pure gas selectivity values of these well phase-separated PEO-based segmented block copolymers are discussed in **Chapter 8**.

In **Chapter 9** the synthesis and characterisation of segmented block copolymers, which are end-capped with monofunctional PEO segments, are reported. Furthermore, branched polymer structures are created by incorporating a trifunctional carboxylate ester to increase the polymer molecular weight while the mPEO concentration remains relatively high. The influence of PEO end-blocks on the polymer molecular weight, the thermal mechanical properties, the water absorption, the surface properties and the tensile properties is studied.

References

1. Fakirov, S., in *Handbook of condensation thermoplastic elastomers*, Wiley-VCH Verlag GmbH & Co., Weinheim **2005**.
2. Holden, G., Legge, N.R., Quirk, R.P. and Schroeder, H.E., in *Thermoplastic elastomers*, Hanser Publishers, Munich **1996**.
3. World thermoplastic elastomers to 2009, The Freedonia Group, http://www.freedoniagroup.com.
4. Cella, R.J., *J. Polym. Sci., Symp.* **1973**, 42, p. 727-740.
5. PEBAX General Brochure; PEBAX® Breathable Film Grades.
6. Arnitel Brochure; Arnitel® copolyester elastomers.
7. Harrell, L.L., *Macromolecules* **1969**, 2, p. 607-612.
8. Miller, J.A., Lin, S.B., Hwang, K.K.S., Wu, K.S., Gibson, P.E. and Cooper, S.L., *Macromolecules* **1985**, 18, p. 32-44.
9. Van der Schuur, M., Ph.D. Thesis '*Poly(propylene oxide) based segmented blockcopolymers*', University of Twente, The Netherlands **2004**.
10. Biemond, G.J.E., Ph.D. Thesis '*Hydrogen bonding in segmented blockcopolymers*', University of Twente, The Netherlands **2006**.
11. Versteegen, R.M., Kleppinger, R., Sijbesma, R.P. and Meijer, E.W., *Macromolecules* **2006**, 39, p. 772-783.
12. Versteegen, R.M., Sijbesma, R.P. and Meijer, E.W., *Macromolecules* **2005**, 38, p. 3176-3184.
13. Krijgsman, J., Husken, D. and Gaymans, R.J., *Polymer* **2003**, 44, p. 7573-7588.
14. Krijgsman, J. and Gaymans, R.J., *Polymer* **2004**, 45, p. 437-446.
15. Husken, D., Krijgsman, J. and Gaymans, R.J., *Polymer* **2004**, 45, p. 4837-4843.
16. Gaymans, R.J. and de Haan, J.L., *Polymer* **1993**, 34, p. 4360-4364.
17. Niesten, M.C.E.J., Ph.D. Thesis '*Polyether based segmented copolymers with uniform aramid segments*', University of Twente, The Netherlands **2000**.
18. Krijgsman, J., Husken, D. and Gaymans, R.J., *Polymer* **2003**, 44, p. 7043-7053.

Chapter 2

Synthesis and characterisation of segmented block copolymers based on PEO and monodisperse crystallisable segments

---

Abstract

Segmented block copolymers based on poly(ethylene oxide) (PEO) flexible segments and monodisperse crystallisable bisester tetra-amide segments were made via a polycondensation reaction. The molecular weight of the PEO segments was varied from 600 to 4600 g/mol and a bisester tetra-amide segment (T6T6T) based on dimethyl terephthalate (T) and hexamethylenediamine (6) was used. The resulting copolymers are melt-processable and transparent.

The crystallinity of the copolymers was investigated by DSC and FTIR. The thermal properties were studied by DSC, temperature modulated SAXS and DMA. The elastic properties were evaluated by the compression set test.

The crystallinity of the T6T6T segments in the copolymers is high (>84%) and the crystallisation is fast due to the use of monodisperse tetra-amide segments. DMA experiments show that the materials have a low T_g, a broad and almost temperature independent rubbery plateau and a sharp flow temperature. With decreasing amide content the storage modulus and flow temperature of the copolymers decrease.

With increasing PEO segment length both the PEO melting temperature and the PEO crystallinity increase. When the PEO segment length is longer than 2000 g/mol, the PEO melting temperature is above room temperature. The presence of a semi-crystalline PEO phase in the copolymer increases the modulus and results in higher compression set values at room temperature.

The properties of PEO-T6T6T copolymers are compared to similar polyether-T6T6T segmented block copolymers.

Introduction

Thermoplastic elastomers (TPE's) are polymers that show elastomeric behaviour at their service temperature and can be melt-processed at elevated temperatures. Segmented block copolymers are a kind of TPE's. Generally, segmented block copolymers, composed of alternating rigid and flexible segments, have a two-phase structure. One phase consists of mobile segments containing a low glass transition temperature, the other of crystalline domains with a high melting temperature. The crystalline domains act as physical crosslinks and can be considered as filler, reinforcing the amorphous matrix. Due to the presence of physical crosslinks the materials have good elastic properties.

The glass transition temperature (T_g) of the soft phase depends on the type and length of the flexible segments and on the amount of rigid segment dissolved in the soft phase. Materials of interest have a low T_g and a high melting temperature and, therefore, they posses a broad rubbery plateau. Often used flexible segments with a low T_g are polyethers, like poly(tetramethylene oxide) (PTMO), poly(propylene oxide) (PPO) or poly(ethylene oxide) PEO. The crystalline domains provide the material dimensional stability, heat stability and solvent resistance. Crystallisable segments that have a high melting temperature contain usually urethane, ester or amide groups.

In literature several segmented block copolymers based on flexible PEO segments and ester [1-4], amide [5-7] or urethane [7-13] type of rigid segments are reported. The PEO-based copolymers are used for breathable film applications, like gloves, laminates on textile, roofing membranes, gas separation membranes or food packaging materials. Furthermore, these copolymers might be considered as biomaterials for various biomedical applications, like tissue engineering [14-18] and controlled drug release systems [19,20].

The crystallinity of the rigid segments in these PEO-based segmented block copolymers is usually low (~30%) [21,22], which means that a large amount of the rigid segments is amorphous and partially dissolved in the PEO matrix. Therefore, these copolymers have at least a three-phase morphology; a crystalline rigid phase and two amorphous phases. The glass transition temperature of the PEO phase is low but increases when the content of non-crystallised rigid segments dissolved in the PEO matrix increases. Besides, a second glass transition temperature is observed that originates from the amorphous rigid phase. When the concentration and length of the PEO segments increase, the PEO segments tend to crystallise, creating an extra crystalline phase in the copolymer [23].

The crystallisation of the rigid segments can be improved by using monodisperse crystallisable segments [24,25]. These monodisperse segments crystallise fast and almost complete. Consequently, there is hardly any non-crystallised rigid segment dissolved in the soft phase. A low amount of monodisperse rigid segments (~5 wt%) is already sufficient for good mechanical and elastic properties of the copolymer.

The use of monodisperse crystallisable segments in segmented block copolymers containing urethane(urea) [26-29] or amide groups [26,29-32] has been previously studied. These copolymers have a low under-cooling, a relatively high modulus and an almost temperature independent rubbery plateau. Besides, these polymers have a high elasticity and high fracture strains. The copolymers can consist of PTMO or PPO flexible segments and bisester tetra-amide rigid segments (T6T6T) [26,30-33]. The T6T6T segments are based on dimethyl terephthalate (T) and hexamethylenediamine (6) (Figure 2.1) [34].

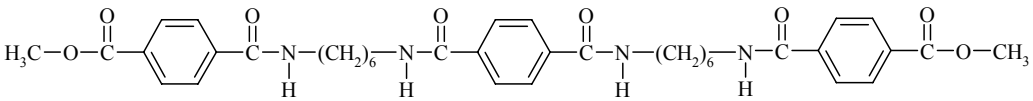

Figure 2.1: Structure of bisester tetra-amide segment T6T6T-dimethyl.

The PTMO-T6T6T [26,30-32] and PPO-T6T6T [33] copolymers show good solvent resistance, are melt-processable and transparent. DMA experiments revealed that the copolymers have a low glass transition temperature, a broad and almost temperature independent rubbery plateau and a sharp flow temperature. The crystallised T6T6T segments have a ribbon-like structure with a high aspect ratio (L/D ≈ 1000) dispersed in the polyether matrix. The strong increase in modulus with T6T6T content can be described by the composite model of Halpin-Tsai [26,35,36]. This model suggests that the function of the crystalline segments as reinforcing filler is important for obtaining a copolymer with a high modulus. By increasing the T6T6T concentration in the PTMO-T6T6T and PPO-T6T6T copolymers, the storage modulus of the rubbery plateau and the flow temperature were increased. The storage moduli of the rubbery plateau were similar for both polyether-T6T6T copolymers, but the flow temperatures of PPO-T6T6T were lower than those of PTMO-T6T6T. Furthermore, both copolymers have comparable low compression set values (6 – 17%).

Both PTMO and PPO polyether segments are hydrophobic and it would be interesting to study segmented block copolymers based on hydrophilic PEO segments and monodisperse T6T6T segments. Generally, PEO refers to polyols of a molecular weight above 20,000 g/mol. Below this molecular weight it is known as poly(ethylene glycol) (PEG).

However, when PEG segments are build into the copolymer the term PEO is used. To prevent confusion, only the term PEO is used, for both the prepolymers as well as the copolymers.

Aim

This chapter is directed to the synthesis and characterisation of segmented block copolymers based on PEO segments and monodisperse crystallisable T6T6T segments. A polymer series, denoted as PEO_x-T6T6T, will be prepared where the molecular weight of the PEO segments (x) is varied between 600 and 4600 g/mol. As the PEO length increases the T6T6T content in the copolymer decreases.

The T6T6T-dimethyl segments are analysed by DSC and MALDI-TOF. The molecular weight of the block copolymers is determined with inherent viscosity measurements. By using FTIR, information is obtained about the PEO and T6T6T crystallisation in the copolymer. SAXS experiments are used to study the polymer morphology. Phase transitions and thermal mechanical behaviour are studied with DSC and DMA respectively. The elastic behaviour is investigated with compression set tests.

Experimental

Materials. 1,6-Hexamethylenediamine (HMDA) was obtained from Aldrich. Dimethyl terephthalate (DMT) and *N*-methyl-2-pyrrolidone (NMP) were purchased from Merck. Tetra-isopropyl orthotitanate ($Ti(i\text{-}OC_3H_7)_4$) was obtained from Aldrich and diluted in *m*-xylene (0.05 M) received from Fluka. Irganox 1330 was obtained from CIBA. Methyl phenyl terephthalate (MPT) was synthesized from phenol (obtained from Aldrich) and methyl-(4-chlorocarbonyl)benzoate (obtained from Dalian) [34]. Difunctional poly(ethylene glycol)s (M_n of 600, 1000, 1500, 2000, 3400 and 4600 g/mol) were obtained from Aldrich.

Synthesis of T6T6T-dimethyl. Krijgsman et al. describe the synthesis of T6T6T-dimethyl [34]. First, 6T6-diamine was made by the reaction between an excess of HMDA and DMT (8:1 molar ratio). A mixture of HMDA (1.2 mol, 139 g) and DMT (0.15 mol, 29 g) was heated to 80 ºC in a 1 L stirred round bottomed flask with nitrogen inlet and a reflux condensor. After approximately 1 h the 6T6-diamine started to precipitate. After 4 h ~500 mL toluene was added to the mixture to improve stirring. The product was collected by filtration and washed twice with warm toluene (80 ºC) to remove the excess of HMDA. Finally, the product was washed with diethyl ether and dried at room temperature. The product contained impurities (mainly 6T6T6) as analysed by ^{1}H NMR [34]. After recrystallisation from *n*-butyl acetate at 110 ºC (15 g/L) the purity of the product became 98%.

Second, a mixture of 6T6-diamine (0.02 mol, 7.2 g) and MPT (0.08 mol, 20.5 g) was dissolved in 400 mL NMP in a 1 L stirred round bottomed flask with nitrogen inlet and a reflux condensor. The mixture was heated to 120 ºC for 16 h. After cooling, the precipitated product was collected by filtration and washed with NMP, warm toluene (80 ºC) and diethyl ether [34]. The purity of the final product was >95% as analysed by ^{1}H NMR [34].

PEO_x-T6T6T block copolymers. PEO_x-T6T6T block copolymers were synthesised by a polycondensation reaction using PEO segments and T6T6T-dimethyl. The synthesis of PEO_{2000}-T6T6T is given as an example.

The reaction was carried out in a 250 mL stainless steel vessel equipped with a magnetic stirrer and nitrogen inlet. The vessel contained T6T6T-dimethyl (10 mmol, 6.86 g), PEO_{2000} (10 mmol, 20.0 g), Irganox 1330 (0.20 g), 50 mL NMP and catalyst solution (1.0 mL of 0.05 M Ti-(*i*-$(OC_3H_7)_4$) in *m*-xylene). The reaction mixture was heated to 180 °C under a nitrogen flow in an oil bath. After 30 min the temperature was increased to 250 °C in 1 h. After 2 h at 250 °C the pressure was slowly reduced (P < 21 mbar) to remove all NMP. Than, the pressure was further reduced (P < 1 mbar) to allow melt polycondensation for 1 h. The polymer was cooled to room temperature while maintaining the vacuum. Liquid nitrogen was added to the reaction vessel to isolate the polymer. Before analysis, the polymer was dried in a vacuum oven at 50 °C for 24 h.

Injection-moulding. Samples for dynamic mechanical analysis, differential scanning calorimetry and compression set were prepared on an Arburg-H manual injection-moulding machine. The barrel temperature was set approximately 80 °C above the melting temperature of the copolymer and the mould temperature was set at 70 °C.

MALDI-TOF. Matrix Assisted Laser Desorption Ionization Time-Of-Flight experiments were performed using a Voyager (Applied Biosystems) mass spectrometer. A 337 nm UV nitrogen laser producing 3 ns pulses was used and the mass spectra were obtained in the linear mode. Samples were dissolved in TFA (0.1 wt%) and added to 30 µL acetonitril/water solution (50/50 mol%) with 0.1 mg/L 2,5-dihydroxybenzoic acid (DHB) as the matrix. One µL of solution was placed on a gold-sample plate. After that, the solvent was evaporated and the sample transferred to the MALDI-TOF for analysis.

Fourier Transform InfraRed (FTIR). FTIR spectra were recorded on a Nicolet 20SXB FTR spectrometer with a resolution of 4 cm^{-1}. The polymer was dissolved in TFA (0.1 wt%) and by spin coating, a thin polymer film (~15 µm) was formed on a silicon wafer. The polymer film was placed between two pressed KBr tablets. The FTIR data were collected between 700 and 4000 cm^{-1}. For temperature-dependent FTIR, a heating rate of 10 °C/min was used under a constant helium flow.

Small Angle X-ray (SAXS). Synchrotron SAXS measurements were performed at the Dutch-Belgium (DUBBLE-BM26) beamline, at the European Synchrotron Radiation Facility (ESRF) in Grenoble. The wavelength of the beam was 1.2 Å. A two-dimensional SAXS detector was used and a q-range of 0 – 1.8 nm^{-1} was measured. Temperature dependent profiles were recorded at a heating and cooling rate of 10 ºC/min using a remote controlled LINKAM DSC. Two dimensionally SAXS intensity was azimuthally integrated to obtain the scattering pattern as a function of $q = 4\pi \sin \theta/\lambda$, where q is the scattering vector, 2θ the scattering angle and λ is the X-ray wavelength.

Differential Scanning Calorimetry (DSC). DSC spectra were recorded on a Perkin Elmer DSC7 apparatus, equipped with a PE7700 computer and TAS-7 software. Dry polymer samples (5 – 10 mg) were heated from -50 to 250 °C at a rate of 20 °C/min. Subsequently, a cooling scan from 250 to -50 °C at a rate of 20 °C/min followed by a second heating scan under the same conditions as the first heating were performed. The melting temperature (T_m) was determined from the maximum of the endothermic peak in the second heating scan and the crystallisation temperature (T_c) from the peak maximum of the exothermic peak in the cooling scan. The under-cooling of the copolymer was defined as the difference between the melting and crystallisation temperature.

Viscometry. The inherent viscosity (η_{inh}) of the polymers was determined at 25 °C using a capillary Ubbelohde type 1B. The polymer solution had a concentration of 0.1 dL/g in a 1/1 (molar ratio) mixture of phenol/1,1,2,2-tetrachloroethane.

Dynamic mechanical analysis (DMA). The torsion behaviour (storage modulus G' and loss modulus G" as a function of temperature) was measured using a Myrenne ATM3 torsion pendulum at a frequency of 1 Hz and 0.1% strain. Before use, samples (70x9x2 mm) were dried in a vacuum oven at 50 °C overnight. Samples were cooled to -100 °C and then heated at a rate of 1 °C/min. The glass transition temperature (T_g) was defined as the maximum of the loss modulus and the flow temperature (T_{flow}) as the temperature where the storage modulus reached 1 MPa. The temperature where the rubber plateau starts is denoted as the flex temperature (T_{flex}) and the storage modulus at 20 ºC is given as $G'_{20\,°C}$.

Compression set (CS). Samples for compression set experiments were cut from injection-moulded bars with a thickness of ~ 2.2 mm. The compression set was measured according to the ASTM 395B at 20 °C. Samples were compressed (25%) for 24 h and after 30 min of relaxation the thickness of the samples was measured. The compression set (CS) was defined as;

$$CS = \frac{d_0 - d_2}{d_0 - d_1} \times 100\% \quad [\%] \qquad \text{(Equation 2.1)}$$

where, d_0 = thickness before compression [mm]

d_1 = thickness during compression [mm]

d_2 = thickness 30 min after release of the compression [mm]

Results and discussion

Synthesis and characterisation of T6T6T-dimethyl

T6T6T-dimethyl was synthesised from 6T6-diamine and methyl phenyl terephthalate using NMP as a solvent, according to the method described by Krijgsman et al [34]. The obtained product was a white powder and the yield of the reaction was around 95%.

The purity of the T6T6T-dimethyl segments is important as it affects the monodispersity of the rigid segments in the polymer. Previous research on the use of tetra-amide rigid segments in segmented block copolymers shows that with an increased dispersity of the rigid segments, the mechanical and elastic properties of the copolymers deteriorate [26,30,31]. The purity of the T6T6T-dimethyl was calculated by using the method described by Krijgsman et al. [34] and a purity of 98% was found. This purity is comparable to the value found by Krijgsman et al.

Figure 2.2 shows the DSC results of the first heating and cooling scan of T6T6T-dimethyl. One sharp melting peak and two crystallisation peaks are observed. Most likely, the second crystallisation temperature (at lower temperature) can be ascribed to a crystalline transition. Such a transition was also found for 6T6-diamine [34] and is quite common for polyamides like nylon-6,6 [37].

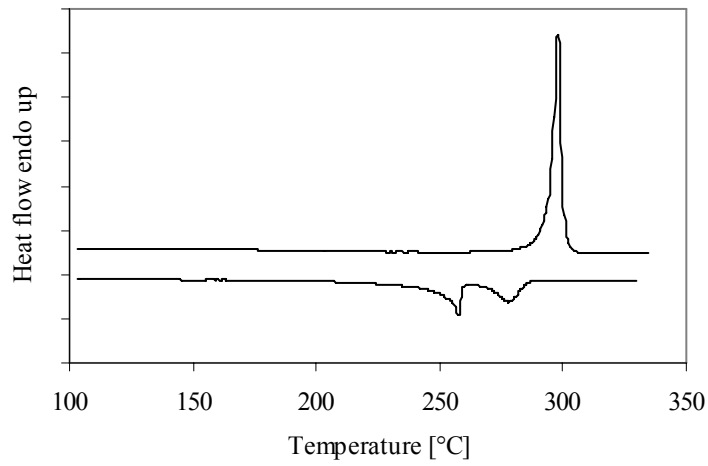

Figure 2.2: First heating scan and cooling scan of T6T6T-dimethyl at a scan rate of 20 ºC/min.

A melting temperature of 298 ºC and a melting enthalpy of 180 J/g were observed for T6T6T-dimethyl. Literature reported values for the melting temperature of T6T6T-dimethyl of 303 ºC and melting enthalpies of 152 – 170 J/g [26,34].

MALDI-TOF was used to further evaluate the purity of T6T6T-dimethyl. The analysed product can contain a proton (H^+), a sodium ion (Na^+) or a potassium ion (K^+). The molecular weight of the positively charged element must be added to the molecular weight of the product. The matrix used for the MALDI-TOF experiments was DHB (2,5-dihydroxybenzoic acid) and this compound can induce peaks at 273, 413, 551 and 727 m/z. In Figure 2.3 the MALDI-TOF spectrum of T6T6T-dimethyl is given.

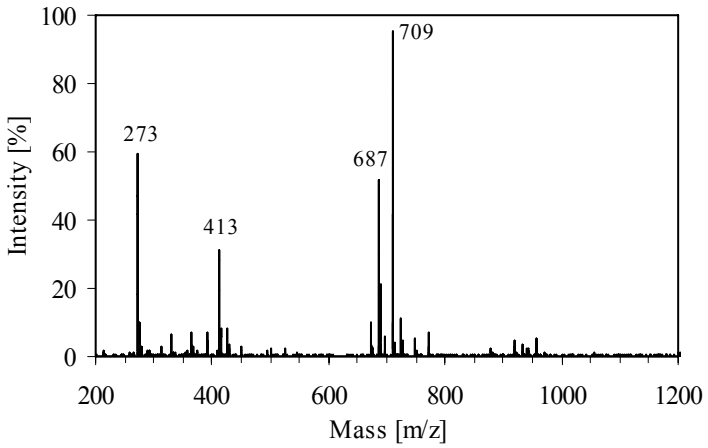

Figure 2.3: MALDI-TOF spectrum of T6T6T-dimethyl.

Besides the two peaks of the matrix (273 and 413 m/z), the MALDI-TOF spectrum of T6T6T-dimethyl shows two clear peaks at 687 and 709 m/z (687 m/z = T6T6T-dimethyl + H, 709 m/z = T6T6T-dimethyl + Na). No peaks were observed of di-amide (T6T) or hexa-amide (T6T6T6T). Therefore, it is concluded that T6T6T is monodisperse.

Polymerisation of PEO$_x$-T6T6T copolymers

Segmented block copolymers based on PEO and T6T6T-dimethyl were prepared via a polycondensation reaction using a titanium-based catalyst. As T6T6T-dimethyl units have a high melting temperature (303 °C) [34], NMP was used in the first step. The maximum reaction temperature was limited as PEO degrades at high temperatures. In nitrogen surroundings PEO starts to decompose at around 350 ºC [38,39] and when air (oxygen) is present the decomposition starts already at 220 ºC [39]. Therefore, Irganox 1330 was added to the reactor as antioxidant. In the first step the T6T6T units were coupled to the PEO, thereby lowering the melting temperature of T6T6T, so that the polycondensation reaction could be carried out in the melt at 250 ºC. During the polycondensation reaction, methanol was formed and the removal of methanol yields high molecular weight polymers.

Throughout the polymerisation the reaction mixture was transparent, which indicated that melt phasing did not take place. Even in the solid state the polymers were transparent, while being semi-crystalline. This suggests that the T6T6T crystals are too small to scatter light. The materials had a slight yellow/brown colour. Previously, it was observed that the colour of NMP changes from slightly yellow to brown with increasing temperature [26]. The monodispersity of the T6T6T units in the polymer was maintained during melt synthesis and processing [26].

FTIR

One way of studying the crystallinity of the PEO$_x$-T6T6T copolymers is by Fourier Transform Infrared Spectroscopy (FTIR). This can be done by looking at the absorption peaks of the carbonyl groups present in the copolymer, which are the amide carbonyl in the crystalline and amorphous state, respectively 1630 and 1660-1670 cm^{-1}, and the ester carbonyl at 1720-1730 cm^{-1} (Table 2.1).

Table 2.1: Peak assignments of IR bands of PEO_{2000}-T6T6T in the wave number region 1580 – 1760 cm^{-1}.

Peak	Description
1720 – 1730 cm^{-1}	Stretching C=O of ester bond
1660 - 1670 cm^{-1}	Stretching C=O of amide bond; amorphous
1630 cm^{-1}	Stretching C=O of amide bond; crystalline

The crystallinity can be obtained by comparing the intensity of crystalline amide carbonyl with amorphous amide carbonyl. In the melt, the amide segments are in the amorphous state and the amount of the amide carbonyl in the crystalline state is expected to be zero. Similar calculations were performed on nylon-6,6 [40]. An increase in the crystallinity of nylon-6,6, expressed as an increase in the density, was linearly related to the decrease of the amorphous band and the increase of the crystalline band. In Figure 2.4 the FTIR spectra of PEO_{2000}-T6T6T at different temperatures are given.

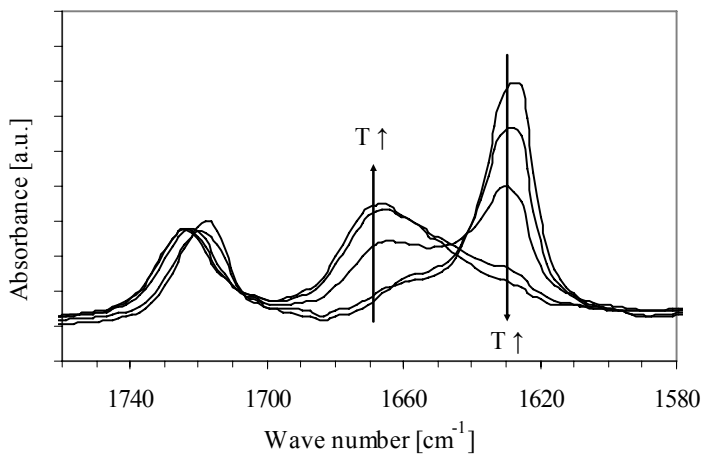

Figure 2.4: FTIR spectra of PEO_{2000}-T6T6T recorded at different temperatures: 50, 100, 150, 170 and 190 ºC.

The absorbance peak of the crystalline amide C=O decreases and the absorbance peak of amorphous amide C=O increases with increasing temperature. This change is particularly strong when the temperature approaches the melting temperature of the copolymer (T_m PEO_{2000}-T6T6T is 167 °C). In the melt, the peak at 1630 cm^{-1} has almost completely disappeared, while the peak at 1670 cm^{-1} is maximal. At temperatures higher than the melting temperature of the copolymer, the intensity of the 1630 cm^{-1} peak is very low and no further changes in the FTIR spectra are observed. The wave number of the amorphous amide carbonyl band increases with temperature from 1660 to 1670 cm^{-1}. The absorbance peak of the ester carbonyl shifts from 1720 to 1730 cm^{-1} with increasing temperature but the intensity is hardly affected.

The crystallinity of the rigid segments can be calculated using the 1630 and 1670 cm^{-1} peak intensities (Equation 2.2 and 2.3) [26].

$$X_c = \frac{h_{(1630\,cm^{-1})}}{(C \times h_{(1670\,cm^{-1})}) + h_{(1630\,cm^{-1})}} \times 100\% \quad [\%]$$

(Equation 2.2)

$$C = \frac{h_{(1630\,cm^{-1}\,at\,50°C)} - h_{(1630\,cm^{-1}\,melt)}}{h_{(1670\,cm^{-1}\,melt)} - h_{1670\,cm^{-1}\,at\,50°C)}}$$

(Equation 2.3)

where X_c is the T6T6T crystallinity in copolymer, and $h_{(1630\ cm^{-1})}$ and $h_{(1670\ cm^{-1})}$ the height absorbance peaks at 1630 cm^{-1} and 1660 - 1670 cm^{-1} respectively.

For calculating the constant *C*, the peak intensities determined at 50 ºC and in the melt are used. The peak intensities are taken at 50 ºC as this is above the melting temperature of the crystalline PEO segments. The constant *C* for PEO_{2000}-T6T6T, calculated by using Equation 2.3, has a value of 2.35. This is in agreement with the constant found for PTMO-T6T6T copolymers [26]. The value of *C* is assumed to be similar for all PEO_x-T6T6T copolymers. By using Equation 2.2 the crystallinity of the copolymers as a function of temperature can be determined. In Figure 2.5 the T6T6T crystallinity of PEO_{2000}-T6T6T is given as a function of temperature.

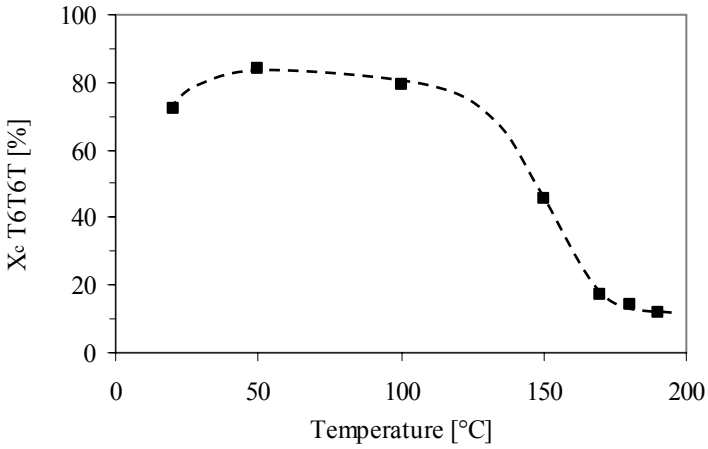

Figure 2.5: T6T6T crystallinity as a function of temperature for PEO_{2000}-T6T6T.

A small increase in T6T6T crystallinity is observed, followed by a decrease in T6T6T crystallinity above 100 °C. This decrease is small up to 130 ºC and approaches zero at 190 ºC.

For the copolymers with a PEO segment length of 2000 and 4600 g/mol the crystallinity at 50 °C was 84 and 87%, respectively. These high values for T6T6T crystallinities are in accordance with the values found for PTMO-T6T6T [26,30] and PPO-T6T6T [33] copolymers.
The T6T6T crystallinity of PEO_{2000}-T6T6T at room temperature is lower than that at 50 °C. FTIR spectra of all PEO_x-T6T6T copolymers recorded at room temperature are given in Figure 2.6.

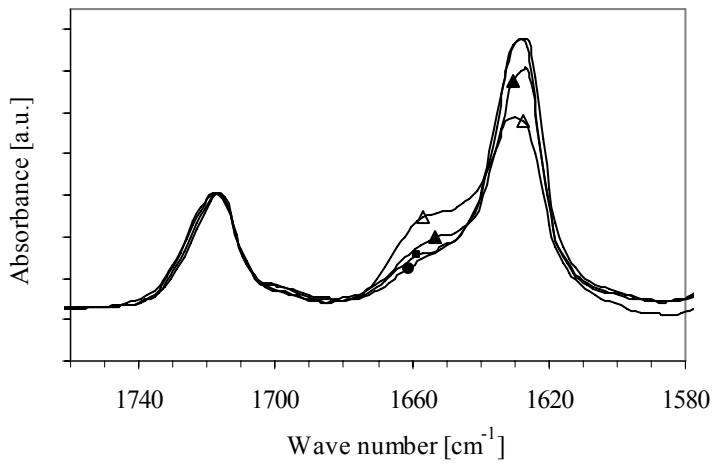

Figure 2.6: FTIR spectra of PEO_x-T6T6T recorded at room temperature with different PEO lengths (x): ●, 1500; ■, 2000; ▲, 3400; Δ, 4600.

With increasing PEO length, the peak at 1630 cm^{-1} decreases, the peak at 1660 cm^{-1} increases and the peak at 1720 cm^{-1} remains constant. This suggests that at room temperature the crystallinity of the T6T6T segments decreases as the PEO length increases. To study this in more detail, FTIR spectra of PEO_{4600}-T6T6T are recorded in a temperature range of 20 to 70 ºC (Figure 2.7).

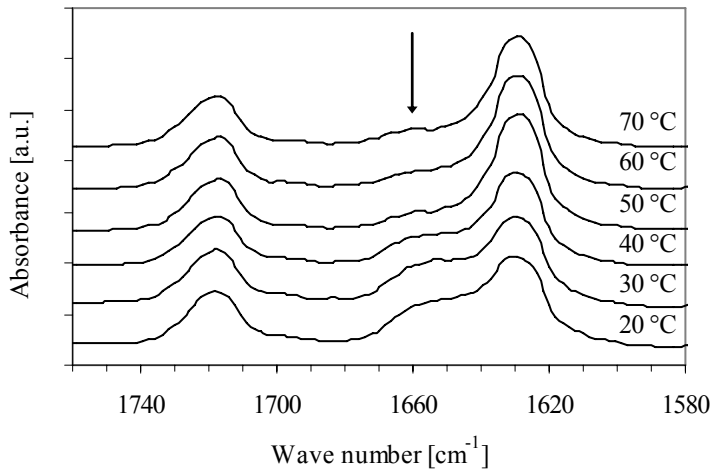

Figure 2.7: FTIR spectra of PEO_{4600}-T6T6T recorded at different temperatures (20 - 70 ºC) for the wave number region 1580 – 1760 cm^{-1}.

On heating from 20 to 50 ºC, the solution cast films showed a decrease in the peak intensity at 1660 cm^{-1}. Above 50 ºC the peak intensity does not change anymore. In Figure 2.8 the T6T6T crystallinity of PEO_{4600}-T6T6T is given as a function of the temperature.

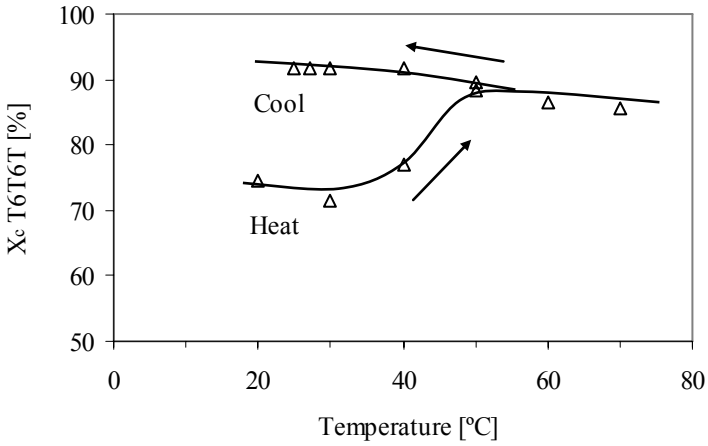

Figure 2.8: T6T6T crystallinity of PEO_{4600}-T6T6T as a function of temperature: heating-cooling cycle at 10 ºC/min.

On heating from 20 to 50 ºC the T6T6T crystallinity increases and at temperatures above 50 ºC the crystallinity decreases slowly. The maximum T6T6T crystallinity at 50 ºC coincides with the melting temperature of PEO_{4600} crystals in the copolymer (T_m PEO = 53 ºC). In the subsequent cooling scan from 70 to 20 ºC the T6T6T crystallinity only increases. These results suggest that the T6T6T crystallisation in a solution-cast film is not complete.

With FTIR it is also possible to study the melting and crystallisation of the PEO segments. The absorbance peaks of PEO_{4600}-T6T6T in the wave number region between 700 and 1400 cm^{-1} are taken at different temperatures (Figure 2.9). With increasing temperature some absorbance peaks shift and these peaks are indicated by arrows. The assignments and descriptions of the changing absorbance peaks are given in Table 2.2. From these spectra it is clear that the PEO crystals in the PEO_{4600}-T6T6T copolymer melt at about 50 °C.

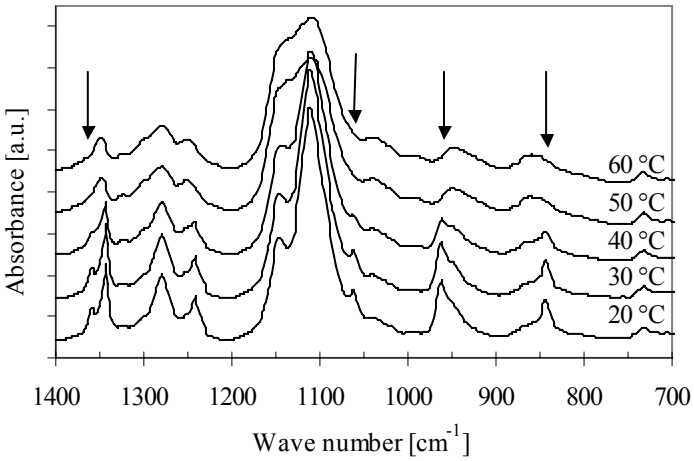

Figure 2.9: FTIR spectra of PEO_{4600}-T6T6T recorded at different temperatures for the wave number region 700 – 1400 cm^{-1}.

Table 2.2: Assignments and description of the most distinguishable FTIR absorbance peaks of amorphous and crystalline PEO [41].

Amorphous PEO	Crystalline PEO	Description
1350 cm^{-1}	1360 / 1343 cm^{-1}	Wagging CH_2
1250 / 1280 cm^{-1}	1240/ 1280 cm^{-1}	Twisting CH_2
	1150 cm^{-1}	Stretching C-O, Stretching C-C
1110 cm^{-1}	1111 cm^{-1}	Stretching C-O
	1061 cm^{-1}	Stretching C-O, Stretching C-C, rocking CH_2
	960 cm^{-1}	Rocking CH_2
950 cm^{-1}	950 cm^{-1}	Stretching C-O, rocking CH_2
860 cm^{-1}	843 cm^{-1}	Rocking CH_2

SAXS

SAXS experiments were performed to obtain information about the morphology of the segmented block copolymers. The long-spacing (L) can be determined from SAXS measurements on materials that possess a lamellar structure. This spacing corresponds to the lamellar thickness plus the thickness of the inter-lamellar (amorphous) region. The L-spacing is an average value of a two dimensional ordering of the lamellae in the matrix. The temperature modulated SAXS studies were carried out on PEO_{1000}-T6T6T. The T6T6T crystallites in this copolymer have a ribbon-like structure dispersed in the amorphous matrix.

In the intensity plots, where the scattering intensity *I(q)* is given as a function of the scattering vector *q*, a scattering maximum is observed which indicates the presence of phase-separated domains (Figure 2.10).

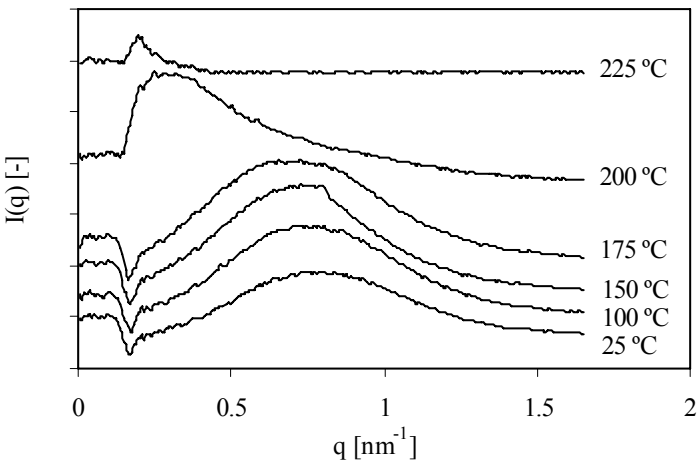

Figure 2.10: SAXS curves of PEO_{1000}-T6T6T at different temperatures.

The small drop in intensity in the beginning of the curve is due to scattering of the beam. The L-spacing can be derived from the scattering data;

$$L = \frac{2\pi}{q} \qquad \text{(Equation 2.4)}$$

As the temperature increases, the scattering maximum and intensity decrease at the same time. These changes are due to melting of the T6T6T crystals. Above the melting temperature of the copolymer (T_m of PEO_{1000}-T6T6T is 195 ºC) there was no peak observed anymore, which indicates that there was no crystalline order present in the melt. The SAXS curves show only one broad scattering maximum. Therefore, it is assumed that the T6T6T lamellae have a comparable thickness and width. In Figure 2.11 the long-spacing of PEO_{1000}-T6T6T as a function of temperature is given, during a heating and cooling cycle.

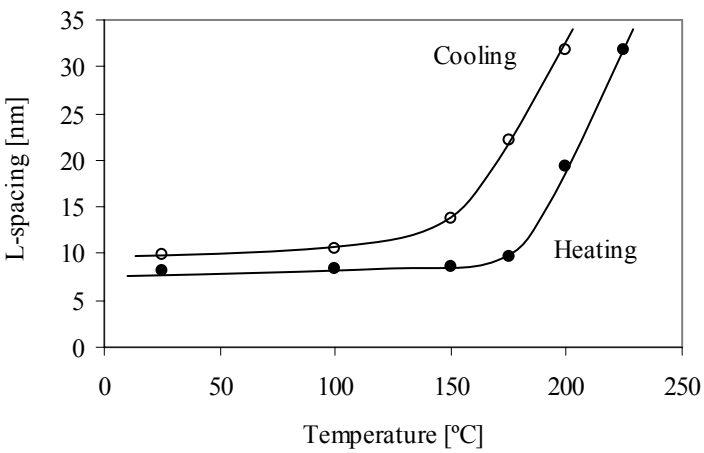

Figure 2.11: Long-spacing of PEO_{1000}-T6T6T as a function of temperature: heating-cooling cycle at 10 ºC/min.

The long-spacing of PEO_{1000}-T6T6T at 25 ºC is 8.2 nm and remains almost constant upon heating till a temperature of approximately 170 ºC. This is due to the monodisperse segments that all melt at the same temperature. As the temperature reaches the melting temperature of the copolymer the L-spacing increases tremendously. Upon cooling, the L-spacing decreases again with a temperature lag of 30 ºC. This small temperature lag indicates a high rate of crystallisation of the monodisperse segments. At 25 ºC the L-spacing was 9.9 nm which is close to the starting value.

The lamellar thickness can be determined from the SAXS data by using the linear correlation function, which is obtained via cosine transformation of the SAXS data [42] (Equation 2.5).

$$\gamma(r) = \frac{1}{Q}\int_0^\infty I(q)\,q^2\,(\cos 2\pi qr)\,dq$$

$$Q = \int_0^\infty I(q)\,q^2\,dq \qquad \text{(Equation 2.5)}$$

where Q is the invariant, $I(q)$ the scattering intensity, q the scattering vector and r the radius. This function is based on a two-phase lamellar morphology with periodically stacked crystalline domains. The use of the linear correlation function yields the average crystalline lamellar thickness (l_c). In Figure 2.12 the correlation function of PEO_{1000}-T6T6T is given.

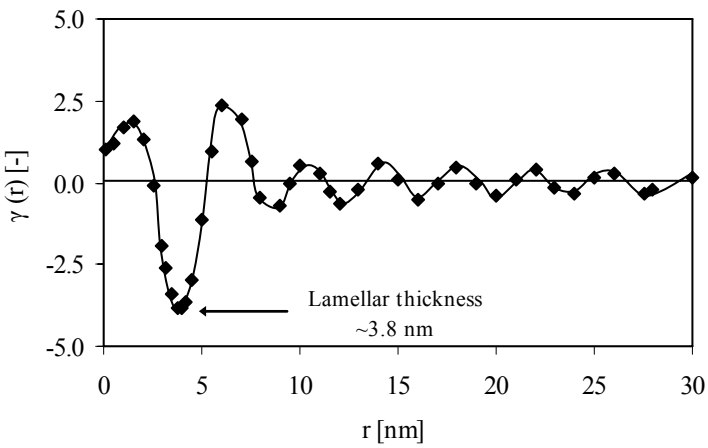

Figure 2.12: Correlation function of PEO_{1000}-T6T6T.

The calculated correlation function of PEO_{1000}-T6T6T reveals a lamellar thickness of 3.8 nm at room temperature. The value of the lamellar thickness is in good agreement with the

extended T6T6T chain segment length (3.7 nm) and comparable to previous results on $PTMO_{1000}$-T6T6T [26] and PPO_{1000}-T6T6T block copolymers. From these results the amorphous layer thickness (l_a) can be calculated ($L = l_a + l_c$) and this is 4.4 nm. The amorphous layer thickness depends on the polyether length, the T6T6T crystallinity and the chain conformation.

DSC

By using DSC the melting and crystallisation temperatures and enthalpies of PEO_x-T6T6T copolymers were determined. The second heating scan and first cooling scan of the copolymers are plotted in Figure 2.13 and the corresponding results are given in Table 2.3.

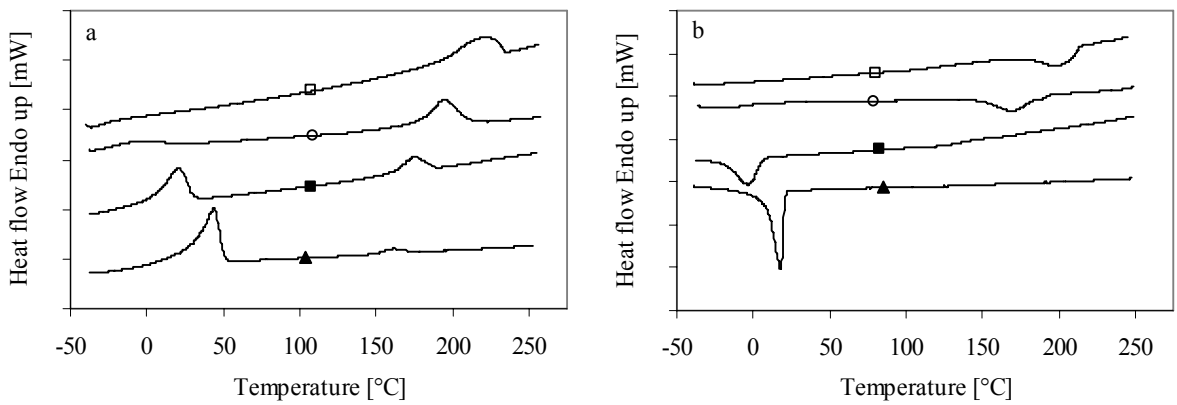

Figure 2.13: (a) Second heating scan and (b) first cooling scan of PEO_x-T6T6T with different PEO lengths (x): □, 600; ○, 1000; ■, 2000; ▲, 3400.

Table 2.3: DSC results of PEO_x-T6T6T copolymers.

			PEO		T6T6T			
PEO length (x) [g/mol]	Conc. T6T6T [wt%]	Conc. PEO [wt%]	T_m [°C]	ΔH_m [J/g PEO]	T_m [°C]	ΔH_m [J/g T6T6T]	T_c [°C]	T_m-T_c [°C]
600	51.0	49.0	-	-	219	81	201	18
1000	38.4	61.6	-2	20	195	104	169	26
1500	29.4	70.6	7	49	181	81	144	37
2000	23.8	76.2	21	53	167	73	161	6
3400	15.5	84.5	44	89	162	37	-	-
4600	11.9	88.1	53	103	161	42	-	-

The copolymer with a PEO length of 600 g/mol shows no melting peak of PEO since these segments are too short to crystallise. As the PEO length and thus the concentration increases the melting temperature and enthalpy of the PEO crystals increase, which indicates that the

PEO crystallinity increases. For the copolymers with x is 3400 and 4600 g/mol no crystallisation peak of T6T6T is observed as most likely the T6T6T concentration is too low to give a measurable peak. The melting enthalpy of T6T6T in the copolymer is lower than observed for the T6T6T-dimethyl segments (152 – 180 J/g). Furthermore, the melting enthalpy of T6T6T shows a decrease as the PEO concentration increases. This suggests that the T6T6T segments are not fully crystallised or that due to exothermic mixing energies the melting endotherms are not simply related to crystallinities. The copolymers have a low under-cooling, 6 – 37 ºC, since monodisperse crystallisable rigid segments crystallise fast.

Dynamic mechanical analysis

The storage and loss moduli of the PEO_x-T6T6T copolymers, determined by DMA measurements, are plotted as a function of temperature in Figure 2.14 and the corresponding data are given in Table 2.4.

All copolymers have a broad and almost temperature independent rubbery plateau and a sharp melting temperature. This is typical for crystallisable segments of monodisperse length. The storage modulus and flow temperature increase with decreasing PEO_x length due to an increased T6T6T content.

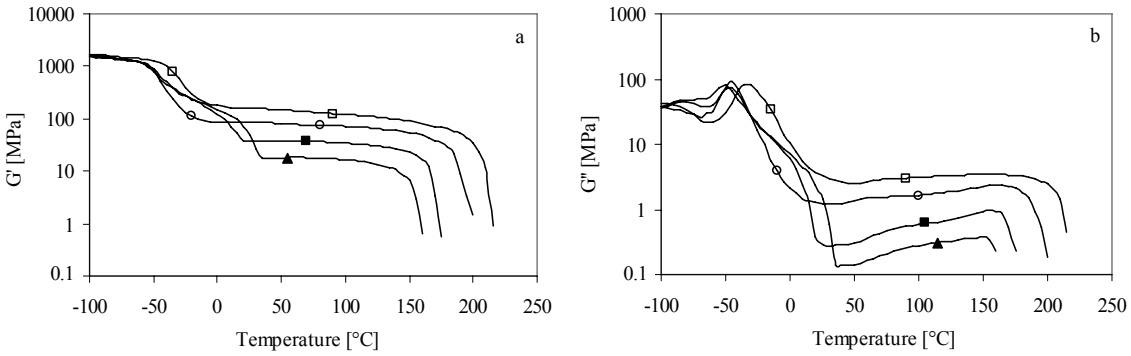

Figure 2.14: Storage (a) and loss (b) modulus of PEO_x-T6T6T with different PEO lengths (x): □, 600; ○, 1000; ■, 2000; ▲, 3400.

The synthesised PEO_x-T6T6T copolymers have a high inherent viscosity (>1.4 dL/g) and, therefore, a relatively high molecular weight (Table 2.4). An inherent viscosity of 1.0 dL/g for similar polymers corresponds to a polymer molecular weight of ~10,000 g/mol [43].

Table 2.4: Dynamic mechanical properties of PEO$_x$-T6T6T copolymers.

PEO length (x) [g/mol]	Conc. T6T6T [wt%]	Conc. PEO [wt%]	η_{inh} [dL/g]	T_g [°C]	T_{flex} [°C]	$G'_{20\,°C}$ [MPa]	T_{flow} [°C]	$CS_{25\%}$ (20 °C) [%]	$CS_{25\%}$ (70 °C) [%]
600	51.0	49.0	1.4	-33	-4	160	216	34	55
1000	38.4	61.6	1.4	-45	-13	86	199	22	-
1500	29.4	70.6	1.5	-46	7	57	180	23	-
2000	23.8	76.2	2.1	-48	20	38	174	17	45
3400	15.5	84.5	2.5	-50	33	72 (18[1])	159	49	-
4600	11.9	88.1	2.1	-45	55	201 (12[1])	154	32	-

[1] *Storage modulus of the rubbery plateau determined at 55 °C*

Glass transition temperature

The plot of the loss moduli as a function of the temperature of the PEO$_x$-T6T6T copolymers (Figure 2.14b) shows a low glass transition temperature (T_g), which originates from the polyether phase. A T_g of an amorphous T6T6T phase is not observed (T_g of nylon-6,T is 125 ˚C [44]), which suggests that there is no separate amorphous T6T6T phase present in the copolymers. In Figure 2.15 the T_g and flex temperature (T_{flex}) of PEO$_x$-T6T6T are given as a function of the PEO length.

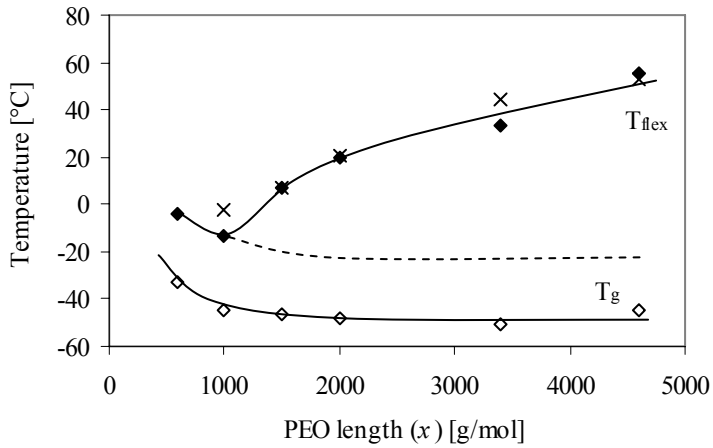

Figure 2.15: Transitions of the soft phase in PEO$_x$-T6T6T as a function of PEO length (x): ◊, glass transition; ♦, flex temperature; ×, melting temperature of PEO (DSC results) (dotted line: expected flex temperature in absence of PEO crystallisation).

The PEO segments in copolymers have higher glass transition temperatures than the T_g of the PEO prepolymers (–72 to –65 ˚C [41]). This effect is due to the reduced mobility of a bound segment, which can decrease the T_g of the polyether phase with approximately 20 ºC [33]. The

T_g of the polyether phase increases also with increasing amount of amorphous rigid segments dissolved in the polyether phase. When the T_g of the copolymers with $x \geq 1000$ g/mol is corrected for the reduced mobility, the T_g is close to the T_g of the PEO prepolymers. This suggests that only a low amount of amorphous T6T6T is dissolved in the PEO phase, which is in accordance with the expectation that the T6T6T crystallisation is almost complete. The high T_g for PEO_{600} can be explained by the high physical crosslink density in this copolymer.

The shoulder in the storage modulus after the glass transition temperature is a result of the melting of the PEO crystalline phase (Figure 2.14a). An increase in PEO length leads to a higher PEO melting temperature and crystallinity (Table 2.3). The flex temperature (T_{flex}), defined as the temperature where the rubbery plateau starts, is related to the melting temperature of PEO (Figure 2.15). In the case of a complete amorphous PEO phase, the T_{flex} would have followed the same trend as the T_g, indicated by the dotted line in Figure 2.15.

Storage modulus

The modulus of the rubbery plateau of PEO_x-T6T6T copolymers increases with T6T6T content (Figure 2.16a). As the copolymers have a comparable T6T6T crystallinity one can conclude that the modulus increases with crystalline content. With an increase in T6T6T content, the physical crosslink density and the reinforcing filler effect of the crystalline domains increase.

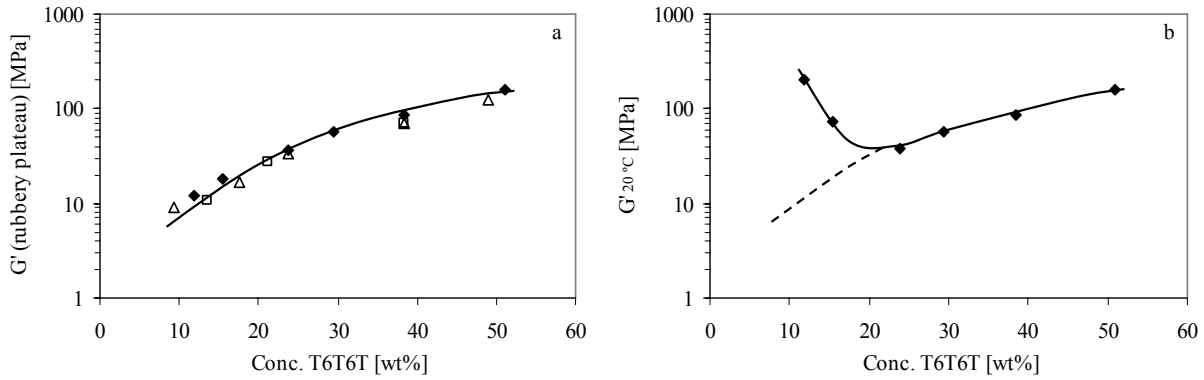

Figure 2.16: (a) Storage modulus of the rubbery plateau and (b) the storage modulus at 20 ºC of polyether-T6T6T copolymers as a function of the T6T6T content: ♦, PEO; □, PPO [33]; Δ, PTMO [30].

The moduli of the rubbery plateau of PEO-T6T6T copolymers are compared to the corresponding moduli of PPO- [33] and PTMO-T6T6T [30] copolymers (Figure 2.16a). The

increase in modulus with T6T6T content is similar for the polyether-T6T6T copolymers. This suggests that the reinforcing filler effect of the T6T6T crystallites is comparable in all three types of polyether-T6T6T copolymers and that the lamellae have a high aspect ratio (L/D of ~1000) [33].

The strong increase in modulus of the polyether-T6T6T copolymers is well described by the fibre composite model of Halpin-Tsai [26,35,36]. This model suggests that the crystalline ribbons in the copolymer can be considered as reinforcing nano-fillers for the amorphous matrix.

Besides the T6T6T concentration, the storage modulus is also influenced by the presence of a semi-crystalline PEO phase. In Figure 2.16b the storage modulus of PEO_x-T6T6T copolymers is given at 20 ºC. When the PEO segment length is >2000 g/mol, the PEO melting temperature is above 20 ºC, which results in a higher $G'_{20\ ºC}$. Copolymers with long PEO segments have a relatively low T6T6T concentration but since a semi-crystalline PEO phase is present at room temperature, the modulus is higher than when the copolymer contains an amorphous PEO phase (indicated by the dotted line in Figure 2.16b). Therefore, it is not possible to obtain a low modulus (G' < 15 MPa) PEO_x-T6T6T copolymer.

Flow temperature

The flow temperature of PEO_x-T6T6T copolymers increases with the rigid segment content. The melting temperature of the copolymers, measured with DSC, corresponds well to the flow temperature determined with DMA. The decrease in melting temperature with increasing PEO length can be explained by the solvent effect theory proposed by Flory. This theory describes that the amorphous phase acts as a solvent for the crystallisable phase [45,46]. An increase in amorphous phase content leads to a decrease in the melting temperature of the copolymer. The melting point depression of a semi-crystalline polymer by adding a solvent or plasticizer can be described according to the following equation [45,46];

$$\frac{1}{T_m} - \frac{1}{T_m^0} = \frac{R}{\Delta H_m} \times \frac{V_p}{V_s} \times \left(v_s - \chi v_s^2\right) \qquad \text{(Equation 2.6)}$$

where T_m is the melting temperature of the copolymer, T_m^0 the melting temperature of the crystalline homopolymer, R the gas constant, ΔH_m the melting enthalpy of the crystalline segment, V_p the molar volume of the crystalline segment, V_s the molar volume of the solvent, χ the Flory interaction parameter and v_s the volume fraction of the solvent. Equation 2.6 is

based on the assumption that the enthalpy and entropy of melting are temperature independent. So, the depression of the melting temperature of the copolymer by the presence of a solvent depends on the melting enthalpy, the ratio of molar volumes and/or the Flory interaction parameter.

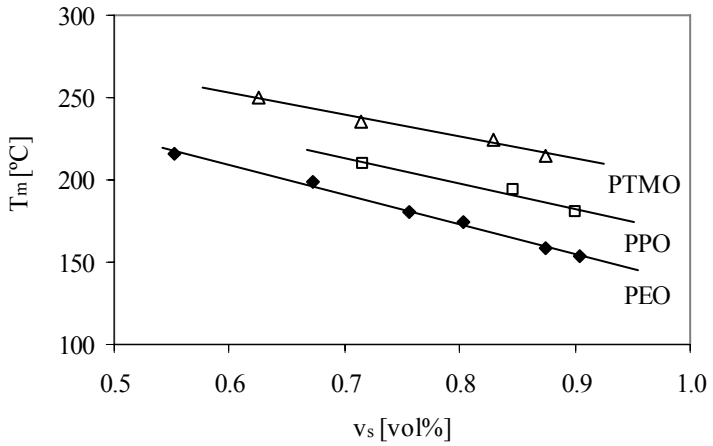

Figure 2.17: Melting temperature of polyether-T6T6T copolymers as a function of volume fraction of polyether: ♦, PEO; □, PPO [33]; Δ, PTMO [30].

In Figure 2.17 the melting temperatures of the polyether-T6T6T copolymers are plotted against the volume fraction of polyether (v_s). The densities of PEO, PPO and PTMO, respectively 1.13, 1.00 and 0.98 g/cm^3, and the calculated density of T6T6T (1.32 g/cm^3) are used to determine the volume fraction of polyether in the copolymers [47]. At a similar PEO concentration the flow temperature of PEO-T6T6T is lower that of PTMO-T6T6T [30] or PPO-T6T6T [33] copolymers. This suggests that PEO is more effective in lowering the melting temperature than PPO and PTMO.

The proposed relationship between T_m and v_s according to Equation 2.6 is not simple and a linear extrapolation to $v_s = 0$, in order to determine T_m^0, is not accurate. Besides the T_m^0, also the V_p/V_s ratio and χ parameter are unknown. This means that three parameters are unknown, which makes it complicated and so far impossible to solve Equation 2.6. Most likely, the difference in melting temperature between the polyether-T6T6T copolymers, at similar polyether concentrations, can be explained by different interaction parameters between the polyether and T6T6T segments.

Compression set

The compression set (CS) is a measure for the recovery of a material after compression. Ideal elastomers show a perfect recovery after compression, which means that no visco-elastic and plastic deformation occur. In segmented block copolymers two processes are involved in the relaxation; an elastic and visco-elastic process and a process of plastic deformation [26,36]. Biemond et al. found that at room temperature the CS values of segmented block copolymers slightly decrease in time, indicating that the effect of visco-elastic deformation in this CS test is small [26]. Moreover, the stress relaxation experiments show that the copolymers relax at a low rate. At higher temperatures, the visco-elastic relaxation is faster and possibly also stronger [26]. So, the CS at room temperature is mainly determined by the plastic deformation. Generally, the CS values of segmented block copolymers with monodisperse rigid segments increase with increasing rigid segment concentration [26,30,36]. In Figure 2.18 the CS values of polyether-T6T6T copolymers is given as a function of the T6T6T concentration.

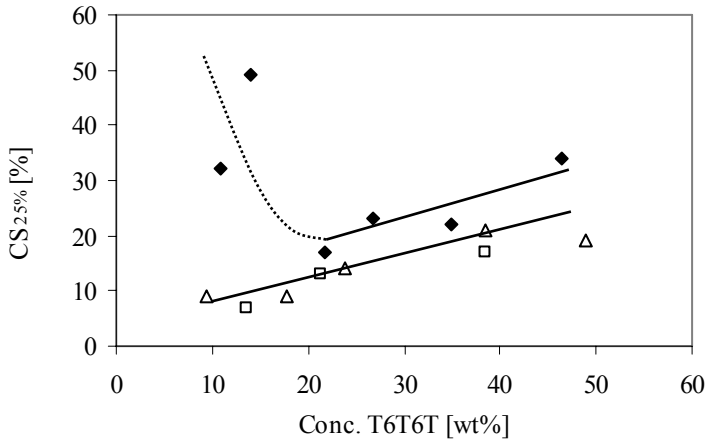

Figure 2.18: Compression set at 20 ºC of polyether-T6T6T copolymers as a function of the T6T6T content: ♦, PEO; □,PPO [33] ; Δ, PTMO [30].

At low T6T6T contents, the CS values of PTMO- and PPO-T6T6T copolymers are very low. However, the CS values of PEO_x-T6T6T copolymers at room temperature increase when the T6T6T content is below 20 wt%. In this case the PEO segment length is >2000 g/mol and these long PEO segments are partly crystalline and have a melting temperature above 20 ºC (Table 2.3). The crystalline PEO phase restricts the recovery and thus the elasticity of the copolymer at room temperature. When the CS is measured at 70 ºC, above the PEO melting temperature, the high CS values at low T6T6T contents are absent (Table 2.4). The PPO segments do not crystallise and the PTMO segments can crystallise but the melting

temperature of these crystals is below room temperature. Thus, the CS values of PPO-T6T6T and PTMO-T6T6T copolymers are not influenced by the presence of polyether crystals.

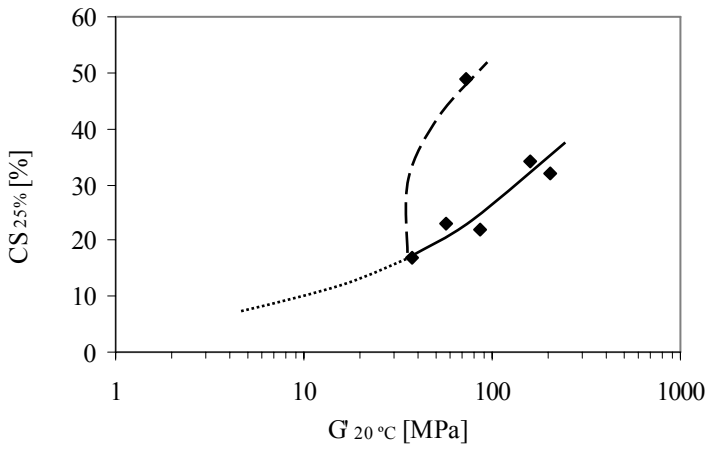

Figure 2.19: Compression set at 20 ºC of PEO-T6T6T copolymers as a function of the storage modulus at 20 ºC (dotted line; expected trend in absence of PEO crystallisation).

The PEO crystalline phase interferes not only in the CS at 20 °C but also in the modulus at 20 °C. The relationship between the modulus and compression is characteristic for segmented block copolymers. However, the PEO_x-T6T6T copolymers contain a rather complex modulus-CS relationship (Figure 2.19). The CS values of copolymers with a PEO length of 600 to 2000 g/mol decrease with decreasing storage modulus. This behaviour is known for other polyether-T6T6T copolymers [26,30,36]. However, the copolymers with x = 3400 and 4600 g/mol show no further decrease in CS values with decreasing modulus, which is due to the presence of high melting PEO crystals. This indicates that at room temperature the copolymers with PEO_{3400} and PEO_{4600} have poor elastic properties.
So, it is impossible to create a low modulus material (G' < 15 MPa) based on PEO_x-T6T6T block copolymers with good elastic properties.

Conclusions

Segmented block copolymers based on poly(ethylene oxide) (PEO) flexible segments and monodisperse crystallisable tetra-amide segments (T6T6T) have been synthesised via a polycondensation reaction. A polymer series is prepared where the molecular weight of PEO segments is varied from 600 to 4600 g/mol, thereby changing the T6T6T concentration from 51.0 to 11.9 wt%. The copolymers have a high molecular weight, are melt-processable and

transparent. By using monodisperse rigid segments the crystallisation of the copolymers is fast and almost complete. The under-cooling of the copolymers is low (20 – 30 °C) and the T6T6T crystallinity high (>84%). Besides, the T6T6T crystallinity remains high up to approximately 30 ºC below the melting temperature of the copolymer. SAXS experiments reveal a lamellar thickness of 3.8 nm, which corresponds to the calculated extended length of T6T6T. The L-spacing of the copolymer remains almost constant upon heating due to the use of monodisperse segments.

DMA experiments show that the materials have a low T_g, a broad and almost temperature independent rubbery plateau, and a sharp melting temperature. Due to the use of monodisperse rigid segments the phase-separation between the hard and soft phase is almost complete and only a small amount of non-crystallised rigid segments is dissolved in the PEO matrix. As the T6T6T content increases (11.9 – 51.0 wt%), the storage modulus of the rubbery plateau (12 – 159 MPa) and the flow temperature (154 – 216 °C) increase.

The PEO melting temperature and enthalpy increase when the molecular weight of the PEO segments increases. When the PEO length is >2000 g/mol the melting temperature of the PEO crystals is above room temperature, which results in a reduced elasticity of the copolymer. So far, it is impossible to create a low modulus material (G' < 15 MPa) based on PEO_x-T6T6T copolymers with good elastic properties due to the PEO crystallisation.

The PEO-T6T6T copolymers have similar modulus-composition behaviour as PPO-T6T6T and PTMO-T6T6T copolymers, indicating that the reinforcing effect of the T6T6T crystals is comparable. However, at equal T6T6T concentration the melting temperature of the polyether-T6T6T copolymers decreases in the order of PTMO > PPO > PEO.

References

1. Gebben, B., *J. Membr. Sci.* **1996**, 113, p. 323-329.
2. Metz, S.J., Potreck, J., Mulder, M.H.V. and Wessling, M., *Desalination* **2002**, 148, p. 303-307.
3. Stroeks, A. and Dijkstra, K., *Polymer* **2001**, 42, p. 117-127.
4. Metz, S.J., Mulder, M.H.V. and Wessling, M., *Macromolecules* **2004**, 37, p. 4590-4597.
5. Bondar, V.I., Freeman, B.D. and Pinnau, I., *J. Polym. Sci., Part B: Polym. Phys.* **1999**, 37, p. 2463-2475.
6. Bondar, V.I., Freeman, B.D. and Pinnau, I., *J. Polym. Sci., Part B: Polym. Phys.* **2000**, 38, p. 2051-2062.
7. Johnson, L. and Schultze, D., *Medical Device & Diagnostic Industry*, Breathable TPE films for medical applications, **2000**.
8. Schneider, N.S., Illinger, J.L. and Karasz, F.E., in *Polymers of biological and biomedical significance,* American Chemical Society, Washington D.C. **1994**.
9. Lee, D., Lee, S., Kim, S., Char, K., Park, J.H. and Bae, Y.H., *J. Polym. Sci., Part B: Polym. Phys.* **2003**, 41, p. 2365-2374.
10. Schneider, N.S., Langlois, D.A. and Byrne, C.A., *Polym. Mater. Sci. Eng.* **1993**, 69, p. 249-250.
11. Chen, C.T., Eaton, R.F., Chang, Y.J. and Tobolsky, A.V., *J. Appl. Polym. Sci.* **1972**, 16, p. 2105-2114.
12. Schneider, N.S., Illinger, J.L. and Karasz, F.E., *J. Appl. Polym. Sci.* **1993**, 47, p. 1419-1425.

13. Yilgör, I. and Yilgör, E., *Polymer* **1999**, 40, p. 5575-5581.
14. Claase, M.B., Grijpma, D.W., Mendes, S.C., de Bruijn, J.D. and Feijen, J., *J. Biomed. Mater. Res.* **2003**, 64A, p. 291-300.
15. Deschamps, A.A., Grijpma, D.W. and Feijen, J., *J. Controlled Release* **2003**, 87, p. 302-304.
16. Deschamps, A.A., van Apeldoorn, A.A., de Bruijn, J.D., Grijpma, D.W. and Feijen, J., *Biomaterials* **2003**, 24, p. 2643-2652.
17. Van Dorp, A.G.M., Verhoeven, M.C.H., Koerten, H.K., Blitterswijk, v., C.A. and Ponec, M., *J. Biomed. Mater. Res.* **1999**, 47, p. 292-300.
18. Deschamps, A.A., Claase, M.B., Sleijster, W.J., Bruijn, d., J.D., Grijpma, D.W. and Feijen, J., *J. Controlled Release* **2002**, 78, p. 175-186.
19. Van Dijkhuizen-Radersma, R., Metairie, S., Roosma, J.R., de Groot, K. and Bezemer, J.M., *J. Controlled Release* **2005**, 101, p. 175-186.
20. Van Dijkhuizen-Radersma, R., Roosma, J.R., Kaim, P., Metairie, S., Peters, F., de Wijn, J., Zijlstra, P.G., de Groot, K. and Bezemer, J.M., *J. Biomed. Mater. Res.* **2003**, 67A, p. 1294-1304.
21. Fakirov, S. and Gogeva, T., *Makromol. Chem.* **1990**, 191, p. 603-614.
22. Fakirov, S. and Gogeva, T., *Makromol. Chem.* **1990**, 191, p. 615-624.
23. Fakirov, S., Goranov, K., Bosvelieva, E. and Du Chesne, A., *Makromol. Chem.* **1992**, 193, p. 2391-2404.
24. Miller, J.A., Lin, S.B., Hwang, K.K.S., Wu, K.S., Gibson, P.E. and Cooper, S.L., *Macromolecules* **1985**, 18, p. 32-44.
25. Harrell, L.L., *Macromolecules* **1969**, 2, p. 607-612.
26. Biemond, G.J.E., Ph.D. Thesis '*Hydrogen bonding in segmented block copolymers*', University of Twente, The Netherlands **2006**.
27. Versteegen, R.M., Kleppinger, R., Sijbesma, R.P. and Meijer, E.W., *Macromolecules* **2006**, 39, p. 772-783.
28. Versteegen, R.M., Sijbesma, R.P. and Meijer, E.W., *Macromolecules* **2005**, 38, p. 3176-3184.
29. Van der Schuur, J.M., Noordover, B. and Gaymans, R.J., *Polymer* **2006**, 47, p. 1091-1100.
30. Krijgsman, J., Husken, D. and Gaymans, R.J., *Polymer* **2003**, 44, p. 7573-7588.
31. Krijgsman, J. and Gaymans, R.J., *Polymer* **2004**, 45, p. 437-446.
32. Husken, D., Krijgsman, J. and Gaymans, R.J., *Polymer* **2004**, 45, p. 4837-4843.
33. Van der Schuur, M. and Gaymans, R.J., *J. Polym. Sc., Part A: Polym. Chem.* **2006**, 44, p. 4769-4781.
34. Krijgsman, J., Husken, D. and Gaymans, R.J., *Polymer* **2003**, 44, p. 7043-7053.
35. Halpin, J.C. and Kardos, J.L., *J. Appl. Phys.* **1972**, 43, p. 2235-2241.
36. Van der Schuur, J.M., De Boer, J. and Gaymans, R.J., *Polymer* **2005**, 46, p. 9243-9256.
37. Todoki, M. and Kawaguchi, T., *J. Polym. Sc., Part B: Polym. Phys.* **1977**, 15, p. 1067-1075.
38. Cameron, G.G., Ingram, M.D., Qureshi, M.Y., Costa, L. and Camino, G., *Eur. Polym. J.* **1989**, 25, p. 779-784.
39. Costa, L., Gad, A.M., Camino, G., Cameron, G.G. and Qureshi, M.Y., *Macromolecules* **1992**, 25, p. 5512-5518.
40. Zbinden, R., in *Infrared Spectroscopy of High Polymers*, Academic Press, New York and London **1964**.
41. Bailey, J.F.E. and Koleske, J.V., in *Poly(ethylene oxide)*, Acedemic Press, New York **1976**.
42. Strobl, G.R. and Schneider, M., *J. Polym. Sc., Part B: Polym. Phys.* **1980**, 18, p. 1343-1359.
43. Chapter 9 of this thesis.
44. Morgan, P.W. and Kwolek, S.L., *Macromolecules* **1975**, 8, p. 104-111.
45. Flory, P.J., in *Principles of polymer chemistry*, Cornell University Press, Ithaca **1967**.
46. Flory, P.J., *Trans. Faraday Soc.* **1955**, 51, p. 848.
47. Van Krevelen, D.W., in *Properties of polymers*, Elsevier Science Publishers, New York **1990**.

Chapter 3

Segmented block copolymers with terephthalic extended PEO segments

---

Abstract

Segmented block copolymers based on poly(ethylene oxide) (PEO) flexible segments and monodisperse crystallisable bisester tetra-amide segments (T6T6T) were synthesised. The PEO segments, having a molecular weight of 300 to 2000 g/mol, were extended with terephthalic units up to flexible segment lengths of 1250 to 10,000 g/mol. The influence of terephthalic units in the soft phase on the polymer morphology, the thermal mechanical and the elastic properties was studied.

Copolymers consisting of PEO segments with a length >2000 g/mol contain a semi-crystalline PEO phase that melts above room temperature. The presence of a PEO semi-crystalline phase at room temperature increases the modulus and decreases the elasticity of the copolymer. Copolymers containing short PEO segments (M_n of 300 and 600 g/mol) that are extended with terephthalic units have a much lower PEO crystallinity and melting temperature than corresponding copolymers with long PEO segments.

The presence of terephthalic units in the copolymer increases the glass transition temperature of the soft phase by approximately 5 ºC. However, the low temperature flexibility of these copolymers is improved due to a lower PEO crystallinity and melting temperature. With the use of terephthalic extended PEO segments, segmented block copolymers with a low modulus (G' < 15 MPa) are obtained that have good elastic properties.

Introduction

Segmented block copolymers consist of alternating flexible and crystallisable rigid segments. The flexible segments have a low glass transition temperature, providing the polymer its flexibility. The rigid segments can crystallise into lamellae and act as physical crosslinks and reinforcing filler for the amorphous matrix.

The crystallinity of the rigid segments in segmented block copolymers is usually low (~30%), which means that a large amount of the rigid segments is amorphous and partially dissolved in the amorphous matrix [1]. This indicates that a relatively high amount of rigid segments is necessary to obtain good mechanical properties of the copolymer. The crystallisation of the rigid segments can be improved by using monodisperse crystalline segments [2,3]. These monodisperse segments crystallise fast and almost complete. Consequently, there are hardly any non-crystallised rigid segments dissolved in the amorphous matrix.

Several segmented block copolymers containing poly(tetramethylene oxide) (PTMO) flexible segments and monodisperse bisester rigid segments have been reported [4-7]. PTMO segments of 1000 g/mol or shorter are amorphous while longer PTMO segments are semi-crystalline. The presence of a semi-crystalline PTMO phase reduces the low temperature flexibility and elasticity of the copolymer. The PTMO crystallinity increases upon straining (strain-induced crystallisation) resulting in a strain-hardening behaviour of the copolymer. Copolymers that show (PTMO) strain-hardening have relatively high tensile strengths but reduced elasticity. The PTMO crystallinity can be suppressed by extending PTMO segments with terephthalic units, which results in improved low temperature flexibility [8,9].

Krijgsman et al. [6,8] studied copolymers based on $PTMO_{1000}$ extended with terephthalic units to segment lengths of 3000 – 10,000 g/mol and monodisperse bisester tetra-amides (T6T6T) segments. The T6T6T segments are based on dimethyl terephthalate (T) and hexamethylene-diamine (6) [10]. The PTMO-T6T6T copolymers have a fast crystallisation and a high crystallinity (~85%). A low amount of T6T6T (~5 wt%) is already sufficient to obtain good mechanical and elastic properties of the copolymer. Besides, the modulus of the material is relatively high and constant over a wide temperature range and the material melts in a narrow temperature range. By incorporating terephthalic units in the PTMO phase the glass transition temperature of this phase was increased by approximately 5 ºC.

Copolymers based on poly(ethylene oxide) (PEO) flexible segments have a hydrophilic character and can be used in breathable films applications [11-15]. The synthesis and

characterisation of PEO_x-T6T6T segmented block copolymers, where *x* represents the PEO molecular weight, have been discussed in Chapter 2 of this thesis. Copolymers with PEO segment lengths >2000 g/mol have a semi-crystalline PEO phase that melts above room temperature. The presence of a semi-crystalline PEO phase at room temperature results in copolymers with a relatively high modulus but reduced elastic properties. Therefore, the presence of a semi-crystalline PEO phase at room temperature is often undesirable.

It is expected that the PEO segments can be extended with terephthalic units without increasing the PEO melting temperature and crystallinity too much. These copolymers are denoted as $(PEO_x/T)_y$-T6T6T, where *y* represents the molecular weight of the total flexible segment. The morphology of the copolymers is investigated with AFM and the thermal mechanical properties are studied with DSC and DMA. The elastic behaviour of the copolymers is evaluated by compression set measurements. The thermal mechanical and elastic properties of $(PEO_x/T)_y$-T6T6T copolymers are compared to PEO_x-T6T6T copolymers, to study the influence of terephthalic units in the PEO phase.

Experimental

Materials. Dimethyl terephthalate (DMT) and *N*-methyl-2-pyrrolidone (NMP) were purchased from Merck and used as received. Tetra-isopropyl orthotitanate ($Ti(i\text{-}OC_3H_7)_4$) was obtained from Aldrich and diluted in *m*-xylene (0.05 M) received from Fluka. Irganox 1330 was obtained from CIBA. Difunctional poly(ethylene glycol)s (M_n of 300, 600, 1000 and 2000 g/mol) were obtained from Aldrich and used as received.

PEO_x-T6T6T block copolymers. The PEO_x-T6T6T copolymers were synthesised by a polycondensation reaction using PEO segments with a molecular weight of 600 – 4600 g/mol and T6T6T-dimethyl. See chapter 2 of this thesis.

$(PEO_x/T)_y$-T6T6T block copolymers. The preparation of $(PEO_{600}\text{-}T)_{5000}$-T6T6T is given as an example of the synthesis of a polymer containing PEO segments extended with terephthalic units, where PEO of a molecular weight of 600 g/mol is extended with DMT to a flexible segment length of 5000 g/mol.

The reaction was carried out in a 250 mL stainless steel vessel equipped with a magnetic stirrer and nitrogen inlet. The vessel contained T6T6T-dimethyl (5 mmol, 3.43 g), PEO_{600} (35.15 mmol, 21.09 g), DMT (30.15 mmol, 5.85 g), Irganox 1330 (0.21 g), 50 mL NMP and catalyst solution (3.5 mL of 0.05 M $Ti\text{-}(i\text{-}(OC_3H_7)_4)$ in *m*-xylene). The reaction mixture was heated to 180 °C under a nitrogen flow in an oil bath. After 30 min the temperature was increased to 250 °C in 1 h. After 2 h at 250 °C the pressure was slowly reduced (P < 21 mbar) to remove all NMP and the reaction product methanol. Subsequently, the pressure was further reduced (P < 1 mbar) to allow melt polycondensation for 1 h. The polymer melt was cooled down to room temperature, while maintaining the vacuum. Then the reaction vessel was filled with liquid nitrogen and the polymer was removed. The copolymer was then dried in a vacuum oven at 50 ºC for 24 h.

Injection-moulding. Samples for dynamic mechanical analysis, differential scanning calorimetry and compression set were prepared on an Arburg-H manual injection-moulding machine. The barrel temperature was set approximately 80 °C above the melting temperature of the block copolymer and the mould temperature was set on 70 °C.

Viscometry. The inherent viscosity (η_{inh}) of the polymers was determined at 25 °C using a capillary Ubbelohde type 1B. The polymer solution had a concentration of 0.1 dL/g in a 1/1 (molar ratio) mixture of phenol/1,1,2,2-tetrachloroethane.

Atomic Force Microscopy (AFM). AFM measurements were performed on a Bioscope AFM and Nanoscope IV controller. The AFM height and phase images were recorded in tapping mode using a TESP cantilever. The operating set point value (A/A_0) was 0.6 – 0.7 and the scan size was 1 μm. Solvent-cast samples of ~15 μm were prepared from a 10 wt% solution in TFA.

Differential scanning calorimetry (DSC). DSC thermograms were recorded on a Perkin Elmer DSC7 apparatus, equipped with a PE7700 computer and TAS-7 software. Dry polymer samples (5 – 10 mg) were heated from -50 to 250 °C at a rate of 20 °C/min. Subsequently, a cooling scan from 250 to -50 °C at a rate of 20 °C/min followed by a second heating scan, under the same conditions as the first heating scan, were performed. The melting temperature (T_m) was determined from the maximum of the endothermic peak in the second heating scan and the crystallisation temperature (T_c) from the peak maximum of the exothermic peak in the cooling scan. The under-cooling of the copolymer was defined as the difference between the melting and crystallisation temperature ($T_m - T_c$).

Dynamic mechanical analysis (DMA). The torsion behaviour (storage modulus G' and loss modulus G" as a function of temperature) was measured using a Myrenne ATM3 torsion pendulum at a frequency of 1 Hz and 0.1% strain. Before use, samples (70x9x2 mm) were dried in a vacuum oven at 50 °C overnight. Samples were cooled to -100 °C and then heated at a rate of 1 °C/min. The glass transition temperature (T_g) was defined as the maximum of the loss modulus and the flow temperature (T_{flow}) as the temperature where the storage modulus reached 1 MPa. The temperature where the rubber plateau starts is denoted as the flex temperature (T_{flex}). The storage modulus at 20 °C is given as $G'_{20\,°C}$.

Compression set (CS). Samples for compression set experiments were cut from injection-moulded bars with a thickness of ~2.2 mm. The compression set was measured according to the ASTM 395B at 20 °C. Samples were compressed (25%) for 24 h and after 30 min of relaxation the thickness of the samples was measured. The compression set (CS) is calculated according to Equation 3.1.

$$CS = \frac{d_0 - d_2}{d_0 - d_1} \times 100\% \quad [\%] \qquad \text{(Equation 3.1)}$$

where d_0 = thickness before compression [mm]

d_1 = thickness during compression [mm]

d_2 = thickness 30 min after release the compression [mm]

Results and discussion

PEO-based segmented block copolymers have been synthesised, where the PEO segments are extended with terephthalic units to create long flexible polyether segments. These copolymers are denoted as -[(PEO$_x$-T)$_n$-PEO$_x$]$_y$- or in brief (PEO$_x$/T)$_y$, where x is the PEO molecular weight, y the total flexible segment length expressed in molecular weight and n the number of repeating PEO/T units (Figure 3.1).

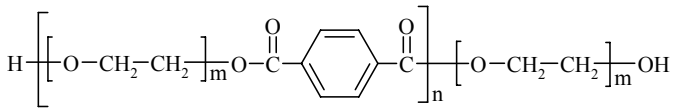

Figure 3.1: Structure of PEO extended with terephthalic units, where m represents the number of EO repeating units and n the number of PEO/T units.

The PEO segments have a molecular weight of 300 - 4600 g/mol and the total flexible segments (y) have lengths up to 10,000 g/mol. The compositions of these copolymers are given in Table 3.1. The thermal mechanical and elastic properties of (PEO$_x$/T)$_y$-T6T6T copolymers are compared to PEO$_x$-T6T6T copolymers to study the influence of terephthalic units in the PEO phase.

The PEO$_x$-T6T6T [16] and (PEO$_x$/T)$_y$-T6T6T copolymers were synthesised by a polycondensation reaction, using T6T6T-dimethyl that was synthesised prior to the polymerisation. The T6T6T concentration in the copolymer decreases with increasing flexible segment length.

At a constant rigid segment length the probability that melt phasing occurs increases with a higher molecular weight of the flexible segment [1]. During the polymerisation of (PEO$_x$/T)$_y$-T6T6T copolymers the melt remained transparent, indicating that melt phasing was absent. Moreover, hardly any sublimation of DMT was observed during the polymerisation, indicating that most of the DMT was used to extend the PEO segments.

The materials in the solid state were also transparent, indicating that the T6T6T crystals were too small to scatter light. The materials have a slightly yellow/brown colour, which is due to a change in the colour of NMP from yellow/brown to brown with increasing temperature [5]. All polymers had a high inherent viscosity (1.2 – 2.5 dL/g) and, therefore, a relatively high molecular weight (Table 3.2).

AFM

Phase angle images, recorded using AFM, show the difference between the flexible and crystalline phase at the surface. The morphology of $(PEO_{600}/T)_{5000}$-T6T6T is investigated and the light ribbons correspond to the T6T6T crystallites (Figure 3.2).

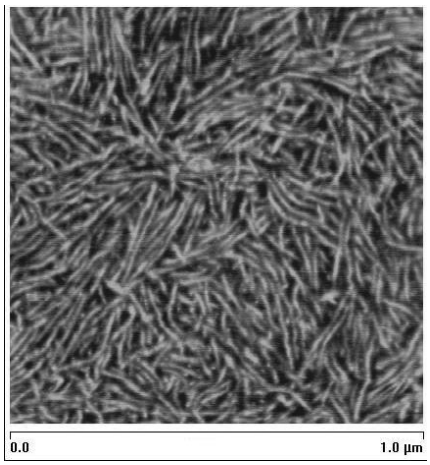

Figure 3.2: Morphology as measured by AFM at 1x1 µm for a solution-cast sample of $(PEO_{600}/T)_{5000}$-T6T6T (phase angle image).

Crystallites with long ribbon-like structures are observed. From AFM images it is difficult to determine the ribbon thickness accurately due to the dimensions of the AFM tip. It is expected that the ribbon thickness will correspond to the length of an extended T6T6T segment, which is around 3.7 nm [5,16,17]. The full length of the crystalline ribbons cannot be determined since only the surface morphology of a sample is scanned. The observed length of the ribbons at the surface is around 1000 nm. It is expected that the actual ribbon length is longer as the ribbons disappear out of the surface. Transmission Electron Microscopy (TEM) measurements of PPO-T6T6T copolymers reveal a ribbon length of 1000 - 5000 nm [17]. Therefore, the aspect ratio of the crystalline ribbons is expected to be between 300 and 1000.

DSC

The thermal properties of PEO_x-T6T6T and $(PEO_x/T)_y$-T6T6T copolymers were studied with DSC. The melting and crystallisation temperatures and corresponding melting enthalpies of the copolymers, obtained from the second heating and first cooling scan, are given in Table 3.1.

The PEO melting temperature and enthalpy of PEO_x-T6T6T copolymers increase with increasing PEO segment length. The PEO melting temperatures rise from -2 °C for PEO_{1000}-

T6T6T to 53°C for PEO_{4600}-T6T6T. The PEO melting enthalpy increases from 20 to 103 J/g with increasing the PEO length from 1000 to 4600 g/mol, which indicates an increase in the PEO crystallinity. The $(PEO_{300}/T)_{2500}$-T6T6T, $(PEO_{600}/T)_{1250}$-T6T6T and $(PEO_{600}/T)_{2500}$-T6T6T copolymers show no melting peak of PEO.

Table 3.1: DSC results of PEO_x-T6T6T [16] and $(PEO_x/T)_y$-T6T6T copolymers.

				PEO		T6T6T			
x or *y* [g/mol]	Conc. T6T6T [wt%]	Conc. PEO [wt%]	Conc. T [wt%]	T_m [°C]	ΔH_m [J/g PEO]	T_m [°C]	ΔH_m [J/g T6T6T]	T_c [°C]	T_m - T_c [°C]
PEO_x-T6T6T									
600	51.0	49.0	-	-	-	219	74	201	18
1000	38.4	61.6	-	-2	20	195	95	169	26
1500	29.4	70.6	-	7	49	181	74	144	37
2000	23.8	76.2	-	21	53	167	66	161	6
3400	15.5	84.5	-	44	89	162	34	-	-
4600	11.9	88.1	-	53	103	161	39	-	-
$(PEO_{300}/T)_y$-T6T6T									
2500	19.9	58.4	21.7	-	-	205	151	205	0
$(PEO_{600}/T)_y$-T6T6T									
600	51.0	49.0	-	-	-	219	74	201	18
1250	33.3	60.4	6.3	-	-	208	88	194	14
2500	20.0	69.0	11.0	-6	5	187	99	185	2
5000	11.1	74.8	14.2	-3	6	171	59	165	6
10,000	5.9	78.1	16.0	2	33	158	64	156	2
$(PEO_{1000}/T)_y$-T6T6T									
1000	38.4	61.6	-	-2	20	195	95	169	26
2500	20.0	74.4	5.6	15	48	181	93	144	37
3000	17.2	76.3	6.5	19	48	179	103	151	28
5000	11.1	80.6	8.3	26	65	170	90	135	35
$(PEO_{2000}/T)_y$-T6T6T									
2000	23.8	76.2	-	21	53	167	66	161	6
4000	13.5	83.8	2.7	39	78	165	54	130	35
6000	9.5	86.8	3.7	42	80	158	40	140	18
8000	7.2	88.5	4.3	46	82	154	35	133	21

The PEO melting temperature of the $(PEO_x/T)_y$-T6T6T copolymers is affected by the PEO segment length (*x*) and the total flexible segment length (*y*). In Figure 3.3 the PEO melting

temperature of PEO_x-T6T6T and $(PEO_x/T)_y$-T6T6T copolymers is given as a function of the flexible segment length.

The PEO melting temperature increases with the PEO length in the $(PEO_x/T)_y$-T6T6T and PEO_x-T6T6T copolymers. However, there is a difference in PEO melting temperature between both types of copolymers. The presence of terephthalic units in the PEO phase influences the PEO melting temperature. A less strong increase in PEO melting temperature (and melting enthalpy) with increasing flexible segment length is observed when terephthalic units are present. A similar increase in PEO melting temperature with flexible segment length is observed for the PEO_{600}/T, PEO_{1000}/T and PEO_{2000}/T series.

The PEO_x-T6T6T copolymers have a semi-crystalline PEO phase at room temperature when the PEO length is >2000 g/mol. By extending the PEO segments with terephthalic units it is possible to create a copolymer with long flexible segments and a reduced PEO melting temperature and crystallinity.

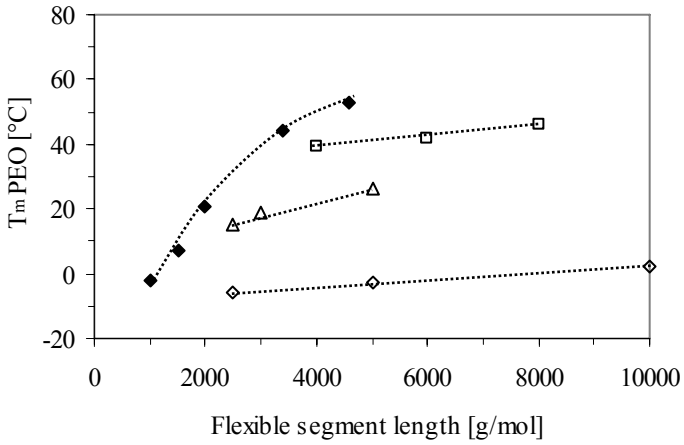

Figure 3.3: PEO melting temperature as a function of flexible segment length: ♦, PEO_x-T6T6T [16]; ◊, $(PEO_{600}/T)_y$-T6T6T; Δ, $(PEO_{1000}/T)_y$-T6T6T; □, $(PEO_{2000}/T)_y$-T6T6T.

The melting temperature of the crystalline T6T6T phase in these copolymers depends on the polyether concentration [16]. The melting temperatures of the PEO_x-T6T6T copolymers decrease ~60 ºC by increasing the PEO segment length from 600 to 4600 g/mol due to an increase in the polyether content from 49 to 88 wt% (Table 3.1). The melting enthalpies showed considerable scattering in the data and at low T6T6T concentrations the enthalpies were difficult to measure accurately with DSC. In Chapter 2 it was reported that the T6T6T crystallinity in PEO_x-T6T6T copolymers, as measured by FTIR, is ~84%. Since the $(PEO_x/T)_y$-T6T6T copolymers have similar T6T6T melting enthalpies as the PEO_x-T6T6T

copolymers, it is expected that the T6T6T crystallinity in the PEO/T extended copolymers is also high.

The under-cooling (T_m - T_c) of the rigid phase in the $(PEO_x/T)_y$-T6T6T copolymers is low, between 2 - 35 ºC, due to the use of monodisperse rigid segments.

Dynamic mechanical analysis

The storage moduli of $(PEO_{600}/T)_y$-T6T6T copolymers with different flexible segment lengths (y) are given as a function of the temperature in Figure 3.4. All $(PEO_{600}/T)_y$-T6T6T copolymers have a low T_g and some copolymers show a melting transition of PEO. Furthermore, a broad and almost temperature independent rubbery plateau and a sharp flow temperature were observed. The storage modulus and the flow temperature increase with increasing T6T6T concentration due to an increased crystalline T6T6T content.

The thermal mechanical properties of all $(PEO_x/T)_y$-T6T6T copolymers studied are reported in Table 3.2.

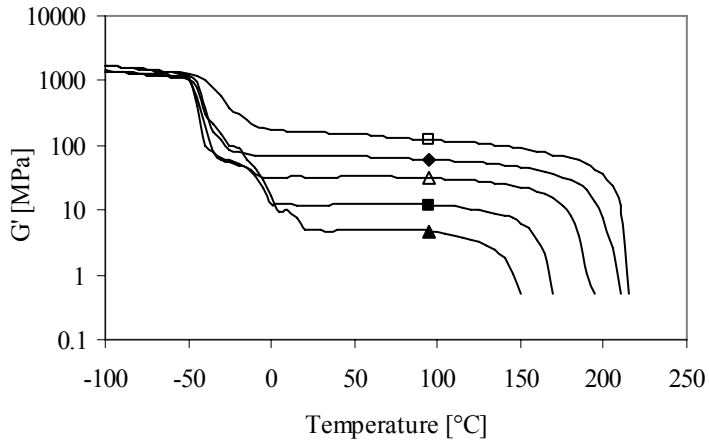

Figure 3.4: Storage modulus of $(PEO_{600}/T)_y$-T6T6T copolymers with different flexible segments lengths (y): □, 600; ♦, 1250; Δ, 2500; ■, 5000; ▲, 10,000.

Low temperature properties

All $(PEO_x/T)_y$-T6T6T copolymers have a low and sharp glass transition temperature. The T_g of the soft phase depends on the composition of the soft phase and the physical crosslink density. The soft phase of the $(PEO_x/T)_y$-T6T6T copolymers consists of PEO, terephthalic units and non-crystallised T6T6T units. The terephthalic units do not crystallise and belong to the amorphous phase [6,7]. Since the T6T6T crystallinity is high (~85%) the amount of amorphous T6T6T dissolved in the soft phase is low.

Table 3.2: Dynamic mechanical properties of PEO_x-T6T6T [16] and $(PEO_x/T)_y$-T6T6T copolymers.

x or *y* [g/mol]	Conc. T6T6T [wt%]	Conc. PEO [wt%]	Conc. T [wt%]	η_{inh} [dL/g]	T_g [ºC]	T_{flex} [ºC]	$G'_{20\,°C}$ [MPa]	$G'_{55\,°C}$ [MPa]	T_{flow} [ºC]	$CS_{25\%}$ (20 °C) [%]	$CS_{25\%}$ (70 °C) [%]
PEO_x-T6T6T											
600	51.0	49.0	-	1.4	-33	-4	160	159	216	34	55
1000	38.4	61.6	-	1.4	-45	-13	86	85	199	22	-
1500	29.4	70.6	-	1.5	-46	7	57	57	180	23	-
2000	23.8	76.2	-	2.1	-48	20	38	37	174	17	45
3400	15.5	84.5	-	2.5	-50	33	72	18	159	49	-
4600	11.9	88.1	-	2.1	-45	55	201	12	154	32	-
$(PEO_{300}/T)_y$-T6T6T											
2500	19.9	58.4	21.7	1.7	-28	-17	46	46	210	13	46
$(PEO_{600}/T)_y$-T6T6T											
600	51.0	49.0	-	1.4	-33	-4	160	159	216	34	55
1250	33.3	60.4	6.3	1.9	-40	-23	68	68	208	23	49
2500	20.0	69.0	11.0	1.7	-44	-4	32	33	190	15	52
5000	11.1	74.8	14.2	1.4	-43	2	12	12	170	10	47
10000	5.9	78.1	16.0	1.5	-44	21	5	5	145	5	50
$(PEO_{1000}/T)_y$-T6T6T											
1000	38.4	61.6	-	1.4	-45	-13	86	85	199	22	-
2500	20.0	74.4	5.6	1.4	-43	16	34	34	180	15	55
3000	17.2	76.3	6.5	1.3	-45	17	30	31	178	13	-
5000	11.1	80.6	8.3	1.2	-44	25	35	17	167	10	-
$(PEO_{2000}/T)_y$-T6T6T											
2000	23.8	76.2	-	2.1	-48	20	38	37	174	17	45
4000	13.5	83.8	2.7	2.1	-45	35	87	17	161	45	66
6000	9.5	86.8	3.7	2.3	-44	41	115	11	153	49	52
8000	7.2	88.5	4.3	2.0	-44	45	110	4	143	52	- [1]

[1] *CS could not be determined as the sample was pulverised*

The flexible segment length of $(PEO_x/T)_y$-T6T6T copolymers is assumed to be the length between network points. An increase in flexible segment length results in a decrease in T_g of the copolymer due to a reduction in network density (Figure 3.5). The T_g's of $(PEO_x/T)_y$-T6T6T copolymers are slightly higher (~5 ºC) than those of the PEO_x-T6T6T copolymers as the presence of terephthalic units in the soft phase restricts the mobility of the PEO segments. This was also observed for PTMO/T-T6T6T segmented block copolymers [6,18]. The T_g of $(PEO_{300}/T)_{2500}$-T6T6T is higher than corresponding copolymers with PEO_{600}/T or PEO_{1000}/T

extended to a length of 2500 g/mol. This can be explained by a combination of a relatively high terephthalic unit content and low molecular weight of PEO used (300 g/mol).

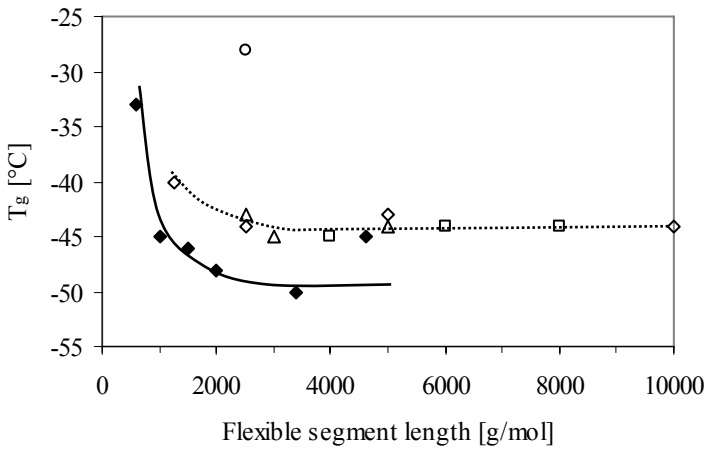

Figure 3.5: Glass transition temperature as a function of flexible segment length: ♦, PEO_x-T6T6T; ○,$(PEO_{300}/T)_y$-T6T6T; ◊, $(PEO_{600}/T)_y$-T6T6T; Δ, $(PEO_{1000}/T)_y$-T6T6T; □, $(PEO_{2000}/T)_y$-T6T6T.

In the case of fully amorphous flexible segments the flex temperature is related to the T_g of the copolymer. However, the flex temperature of copolymers containing a semi-crystalline PEO phase is related to the melting temperature of this segment.

The shoulder in the storage modulus after the glass transition temperature is the result of the melting of the PEO crystalline phase (Figure 3.4). An increase in flexible segment length leads to a higher PEO melting temperature and crystallinity (Table 3.1). The T_{flex} of PEO_x-T6T6T and $(PEO_x/T)_y$-T6T6T copolymers increases strongly with increasing PEO segment length (*x*) and total flexible segment length (*y*) (Figure 3.6).

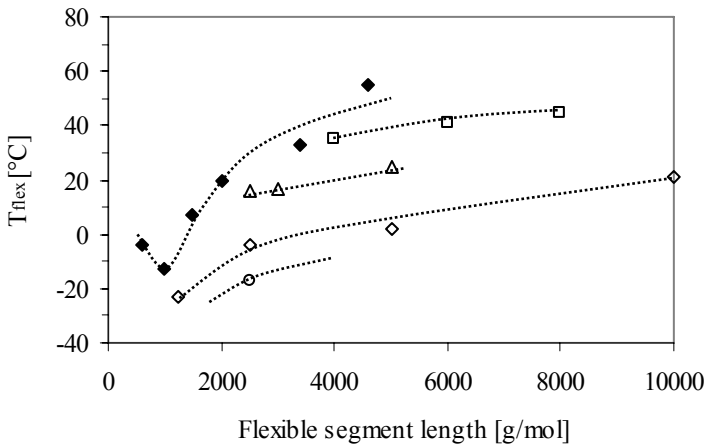

Figure 3.6: Flex temperature as a function of flexible segment length: ♦, PEO_x-T6T6T; ○,$(PEO_{300}/T)_y$-T6T6T; ◊, $(PEO_{600}/T)_y$-T6T6T; Δ, $(PEO_{1000}/T)_y$-T6T6T; □, $(PEO_{2000}/T)_y$-T6T6T.

The increase in T_{flex} with flexible segment length is stronger for PEO_x-T6T6T copolymers than for $(PEO_x/T)_y$-T6T6T copolymers. When terephthalic units are present in the flexible segment, the increase in PEO melting temperature with increasing flexible segment length is less strong, which is due to a reduced PEO crystallinity.
Copolymers with long flexible segments and good low temperature flexibility can be obtained by extending short PEO segments (300 or 600 g/mol) with terephthalic units.

Storage modulus

The increase in modulus of polyether-T6T6T copolymers with increasing T6T6T content can be described by the fibre composite model of Halpin-Tsai, which states that the crystalline ribbons act as reinforcing fillers for the soft phase [5,17,19]. This reinforcing filler effect depends on the crystalline content and the aspect ratio of the lamellae. The use of monodisperse T6T6T crystallisable segments results in crystallites that have a ribbon-like structure with a high aspect ratio [17]. Previous results discussed in Chapter 2 showed that the type of polyether has no effect on the modulus of polyether-T6T6T copolymers since these copolymers have a comparable morphology and T6T6T crystallinity.
In Figure 3.7 the storage modulus at 20 ºC of PEO_x-T6T6T and $(PEO_x/T)_y$-T6T6T copolymers is given.

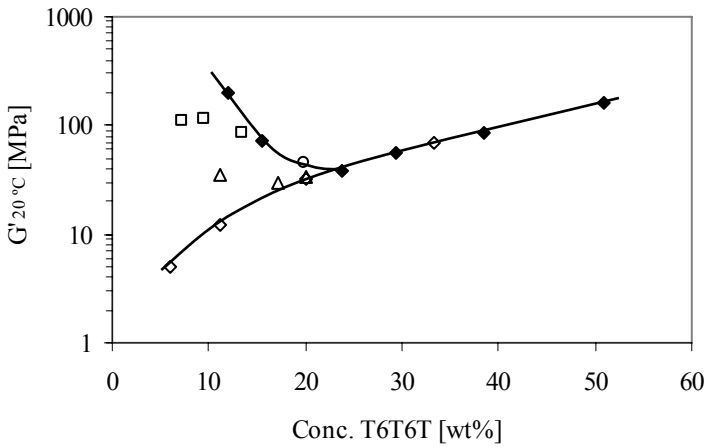

Figure 3.7: Storage modulus at 20 ºC as a function of T6T6T content: ♦, PEO_x-T6T6T; ○, $(PEO_{300}/T)_y$-T6T6T; ◊, $(PEO_{600}/T)_y$-T6T6T; Δ, $(PEO_{1000}/T)_y$-T6T6T; □, $(PEO_{2000}/T)_y$-T6T6T.

The storage modulus at 20 ºC of PEO_x-T6T6T copolymers decreases as the PEO length increases due to a reduced T6T6T content. However, as the PEO length is >2000 g/mol the T6T6T content is low but the $G'_{20\ °C}$ increases as a result of a semi-crystalline PEO phase

(Figure 3.7). When the PEO phase is completely amorphous at room temperature, the $G'_{20\,°C}$ values of $(PEO_x/T)_y$-T6T6T and PEO_x-T6T6T copolymers are comparable (Figure 3.7). This indicates that the terephthalic units have no effect on the modulus of the copolymers, which is in line with previous research on PTMO-based copolymers with monodisperse rigid segments [5,6,18]. The $(PEO_x/T)_y$-T6T6T copolymers with long PEO segment (*x* of 1000 and 2000) have relatively high storage moduli at room temperature despite the low T6T6T contents, which is due to the presence of a semi-crystalline PEO phase. Only $(PEO_{600}/T)_y$-T6T6T copolymers have a low storage modulus at room temperature since the PEO phase of these copolymers is completely amorphous.

For segmented block copolymers it is interesting to have good elastic properties even at low temperatures. This means that the material should have a low modulus combined with a low flex temperature. Low temperature flexibility can be obtained when the crosslink density in the copolymer is not too high and when the PEO melting temperature is suppressed. The relation between the T_{flex} and storage modulus at 20 ºC of PEO_x-T6T6T and $(PEO_x/T)_y$-T6T6T copolymers is given in Figure 3.8 and shows a rather complex behaviour.

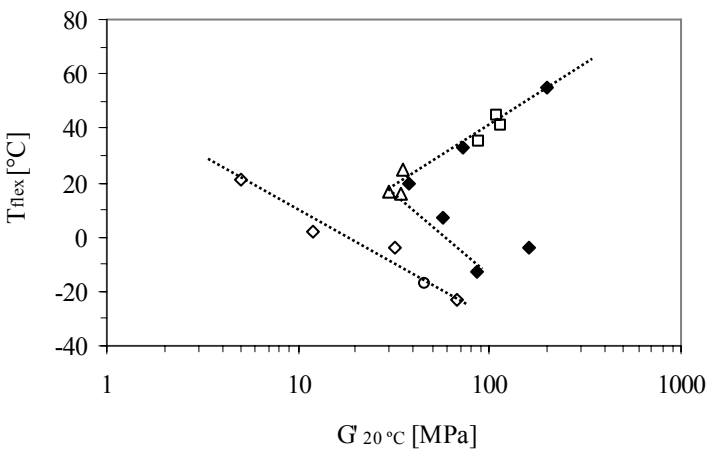

Figure 3.8: Flex temperature as a function of storage modulus at 20 ºC: ♦, PEO_x-T6T6T; ○,$(PEO_{300}/T)_y$-T6T6T; ◊, $(PEO_{600}/T)_y$-T6T6T; Δ, $(PEO_{1000}/T)_y$-T6T6T; □, $(PEO_{2000}/T)_y$-T6T6T.

It is not possible to obtain a PEO_x-T6T6T copolymer with a low modulus (G' < 15 MPa) and a T_{flex} below room temperature as was discussed before in Chapter 2. $(PEO_x/T)_y$-T6T6T copolymers based on PEO segments with a length of 1000 and 2000 g/mol cannot be used to obtain a low modulus material since these copolymers with follow the same trend in T_{flex} versus modulus as PEO_x-T6T6T copolymers with PEO segments longer than 2000 g/mol. The

$(PEO_{300}/T)_y$-T6T6T copolymer has a low flex temperature and low storage modulus at 20 ºC but the glass transition temperature is relatively high (-28 ºC). Therefore, only $(PEO_{600}/T)_y$-T6T6T copolymers can be used to create a low modulus material (G' < 15 MPa) combined with low temperature flexibility.

Flow temperature

The flow temperature of T6T6T in polyether-T6T6T segmented block copolymers decreases with increasing polyether content [16]. This decrease in flow temperature of polyether-T6T6T segmented block copolymers can be explained by the solvent effect theory of Flory, which states that the amorphous phase in a copolymer, i.e. the polyether phase, acts as solvent for the crystallisable phase [20,21]. The melting point depression depends on the type of polyether and the volume fraction of polyether [16]. In Figure 3.9 the flow temperature of PEO_x-T6T6T and $(PEO_x/T)_y$-T6T6T copolymers is given as a function of the polyether concentration. To determine the volume fraction of PEO in the copolymers, the concentrations and densities of PEO, T and T6T6T (1.13, 1.20 and 1.32 g/cm^3 respectively) are used [22].

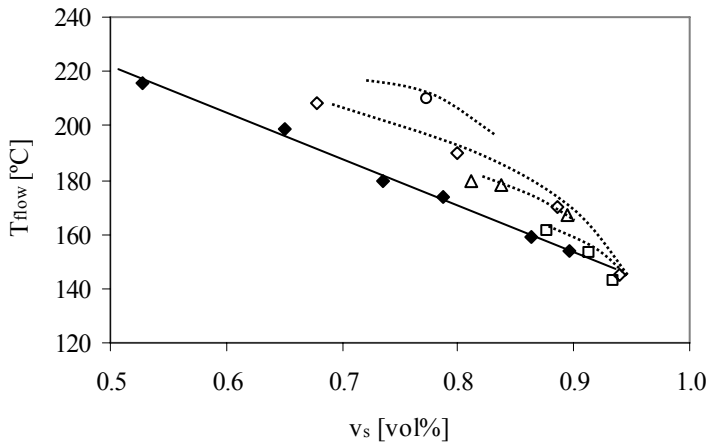

Figure 3.9: Flow temperature as a function of volume fraction PEO: ♦, PEO_x-T6T6T; ○,$(PEO_{300}/T)_y$-T6T6T; ◊, $(PEO_{600}/T)_y$-T6T6T; Δ, $(PEO_{1000}/T)_y$-T6T6T; □, $(PEO_{2000}/T)_y$-T6T6T.

With increasing volume fraction of PEO the flow temperature decreases for both PEO_x-T6T6T as well as $(PEO_x/T)_y$-T6T6T copolymers. The flow temperatures of $(PEO_x/T)_y$-T6T6T copolymers are slightly higher than those of PEO_x-T6T6T copolymers. The presence of terephthalic units in the flexible segments results in a less lowered melting temperature of the copolymer. Most likely, the terephthalic units present in the amorphous phase restrict the function of the amorphous phase as solvent for the crystalline T6T6T phase.

Compression set

Important for segmented block copolymers is the elasticity of the material. A measure for the elasticity is the compression set (CS). Generally, the CS values of polyether-T6T6T copolymers decrease as the rigid segment content decreases [5,6,16,17]. This trend is also observed for the $(PEO_x/T)_y$-T6T6T copolymers when the PEO phase is amorphous at room temperature (Figure 3.10, Table 3.2). When this is the case, there is hardly any difference between the CS values of PEO_x-T6T6T and $(PEO_x/T)_y$-T6T6T copolymers, indicating that the presence of terephthalic units in the flexible segments does not affect the CS values.

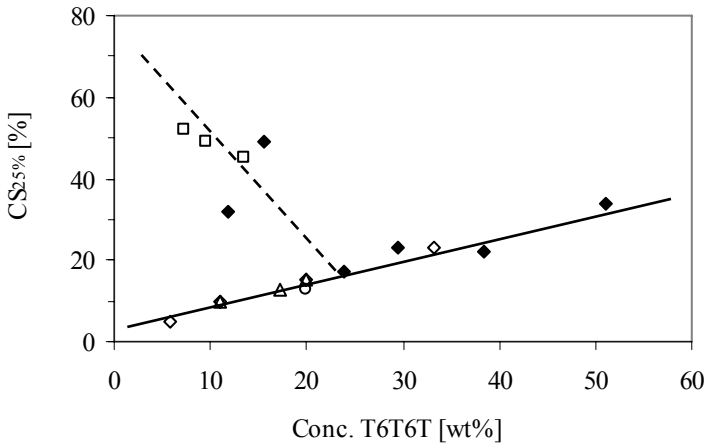

Figure 3.10: Compression set at 20 ºC as a function of T6T6T content: ♦, PEO_x-T6T6T; ○, $(PEO_{300}/T)_y$-T6T6T; ◊, $(PEO_{600}/T)_y$-T6T6T; Δ, $(PEO_{1000}/T)_y$-T6T6T; □, $(PEO_{2000}/T)_y$-T6T6T.

Copolymers containing a PEO crystalline phase above room temperature have higher CS values than copolymers containing an amorphous PEO phase at room temperature. The presence of semi-crystalline PEO phase at room temperature restricts the recovery of the copolymer and thus the elasticity. The CS values have also been determined at 70 ºC, well above the PEO melting temperature. At 70 ºC, the CS values are higher than at room temperature due to more plastic deformation (Table 3.2). At this temperature no trend between CS and T6T6T content is apparent.

Generally, a high polyether concentration is necessary to create a low modulus material. In Figure 3.11 the compression set is given as a function of the storage modulus, both determined at 20 ºC.

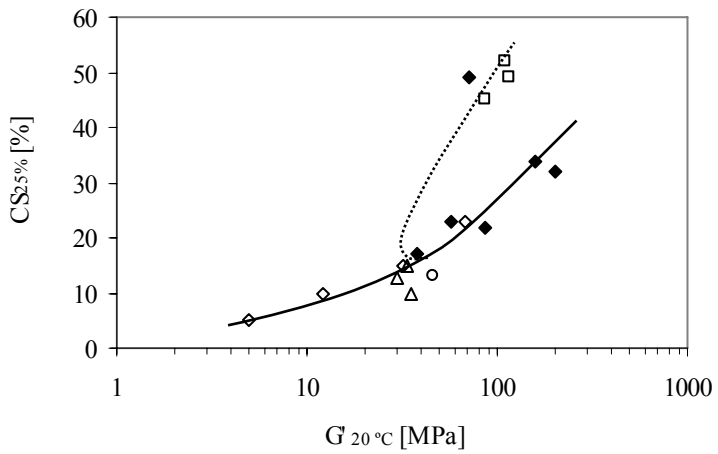

Figure 3.11: Compression set at 20 ºC as a function of the storage modulus at 20ºC: ♦, PEO$_x$-T6T6T; ○, (PEO$_{300}$/T)$_y$-T6T6T; ◊, (PEO$_{600}$/T)$_y$-T6T6T; Δ, (PEO$_{1000}$/T)$_y$-T6T6T; □, (PEO$_{2000}$/T)$_y$-T6T6T.

For PEO$_x$-T6T6T copolymers, a high PEO concentration corresponds to a long PEO segment length. However, copolymers with a PEO length >2000 g/mol contain a semi-crystalline PEO phase at room temperature, which results in copolymers with a high G'$_{20\ °C}$. A similar behaviour was observed for (PEO$_{2000}$/T)$_y$-T6T6T copolymers. The (PEO$_x$/T)$_y$-T6T6T copolymers with a PEO segment length smaller than 2000 g/mol have a PEO melting temperature below room temperature and the corresponding CS values decrease with decreasing storage modulus.

Conclusions

Segmented block copolymers based on poly(ethylene oxide) (PEO) flexible segments and monodisperse crystallisable bisester tetra-amide segments (T6T6T) were made. The PEO segments, having molecular weights from 300 to 2000 g/mol, were extended with terephthalic units to flexible segments lengths up to 10,000 g/mol. These copolymers are denoted as (PEO$_x$/T)$_y$-T6T6T and are compared to PEO$_x$-T6T6T copolymers. All copolymers have a high molecular weight, are transparent and melt-processable.

By using monodisperse rigid segments the crystallisation is fast and almost complete. AFM experiments show that the crystallised T6T6T segments in the polymer have a ribbon-like structure with a high aspect ratio. DMA experiments revealed that the copolymers have a low glass transition temperature, a broad and almost temperature independent rubbery plateau and a sharp melting temperature.

The presence of terephthalic units in the soft phase has no disturbing effect on the modulus of the copolymer but the flow temperature is slightly higher. The soft phase composition has influence on the low temperature properties like the glass transition temperature, the PEO melting temperature and crystallinity. An increase in glass transition temperature of approximately 5 ºC is observed when terephthalic units are present in the soft phase, which is due to a reduced mobility.

PEO_x-T6T6T copolymers contain a semi-crystalline PEO phase at room temperature when the PEO segment length is above 2000 g/mol. The presence of PEO crystals at room temperature results in a relative high modulus and a reduced elasticity of the copolymer. This is also observed for $(PEO_x/T)_y$-T6T6T copolymers with PEO segment lengths of 1000 or 2000 g/mol. The $(PEO_{300}/T)_y$-T6T6T copolymers have a low PEO melting temperature and low storage modulus at 20 ºC, but the glass transition temperature is relatively high (-28 ºC). Only $(PEO_{600}/T)_y$-T6T6T copolymers can be used to obtain a low modulus material (G' < 15 MPa) combined with low temperature flexibility.

References

1. Holden, G., Legge, N.R., Quirk, R.P. and Schroeder, H.E., in *Thermoplastic elastomers*, Hanser Publishers, Munich **1996**.
2. Miller, J.A., Lin, S.B., Hwang, K.K.S., Wu, K.S., Gibson, P.E. and Cooper, S.L., *Macromolecules* **1985**, 18, p. 32-44.
3. Harrell, L.L., *Macromolecules* **1969**, 2, p. 607-612.
4. Husken, D., Krijgsman, J. and Gaymans, R.J., *Polymer* **2004**, 45, p. 4837-4843.
5. Biemond, G.J.E., Ph.D. Thesis '*Hydrogen bonding in segmented block copolymers*', University of Twente, The Netherlands **2006**.
6. Krijgsman, J., Husken, D. and Gaymans, R.J., *Polymer* **2003**, 44, p. 7573-7588.
7. Niesten, M.C.E.J., Feijen, J. and Gaymans, R.J., *Polymer* **2000**, 41, p. 8487-8500.
8. Krijgsman, J. and Gaymans, R.J., *Polymer* **2004**, 45, p. 437-446.
9. Niesten, M.C.E.J. and Gaymans, R.J., *Polymer* **2001**, 42, p. 6199-6207.
10. Krijgsman, J., Husken, D. and Gaymans, R.J., *Polymer* **2003**, 44, p. 7043-7053.
11. Gebben, B., *J. Membr. Sci.* **1996**, 113, p. 323-329.
12. Metz, S.J., Mulder, M.H.V. and Wessling, M., *Macromolecules* **2004**, 37, p. 4590-4597.
13. Bondar, V.I., Freeman, B.D. and Pinnau, I., *J. Polym. Sci., Part B: Polym. Phys.* **1999**, 37, p. 2463-2475.
14. Johnson, L. and Schultze, D., *Medical Device & Diagnostic Industry*, Breathable TPE films for medical applications, **2000**.
15. Stroeks, A. and Dijkstra, K., *Polymer* **2001**, 42, p. 117-127.
16. Chapter 2 of this thesis.
17. Van der Schuur, M. and Gaymans, R.J., *J. Polym. Sc., Part A: Polym. Chem.* **2006**, 44, p. 4769-4781.
18. Niesten, M.C.E.J., ten Brinke, J.W. and Gaymans, R.J., *Polymer* **2001**, 42, p. 1461-1469.
19. Halpin, J.C. and Kardos, J.L., *J. Appl. Phys.* **1972**, 43, p. 2235-2241.
20. Flory, P.J., *Trans. Faraday Soc.* **1955**, 51, p. 848.
21. Flory, P.J., in *Principles of polymer chemistry*, Cornell University Press, Ithaca **1967**.
22. Van Krevelen, D.W., in *Properties of polymers*, Elsevier Science Publishers, New York **1990**.

Chapter 4

Segmented block copolymers based on mixed polyether segments

Abstract

The synthesis and characterisation of segmented block copolymers based on mixed hydrophilic poly(ethylene oxide) (PEO) and hydrophobic poly(tetramethylene oxide) (PTMO) polyether segments and monodisperse crystallisable bisester tetra-amide segments (T6T6T) are discussed in this chapter. Several series of PEO/PTMO-T6T6T copolymers are reported, which have different PEO/PTMO ratios and/or polyether segment lengths. The influence of the composition of the polyether phase on the thermal mechanical and the elastic properties of the resulting copolymers is studied.

The thermal transitions and T6T6T crystallinity of the copolymers are evaluated with DSC. Additional information about the T6T6T crystallinity of the copolymers is obtained by FTIR measurements. The thermal mechanical properties are studied by DMA and the elastic properties are evaluated by compression set experiments.

The use of monodisperse T6T6T segments results in a fast and almost complete crystallisation. Above the glass transition temperature, the storage modulus of the copolymers is almost temperature independent up to the melting temperature of the copolymer. The PEO/PTMO-T6T6T copolymers have only one glass transition temperature, which suggests that the amorphous polyether segments are homogenously mixed. Using a mixture of polyether segments reduces both the melting temperature and the crystallinity of the polyether phase. Copolymers with short polyether segments (2000 g/mol or shorter) contain one mixed polyether crystalline phase, while two separate crystalline polyether phases are observed when the polyether lengths are longer.

Introduction

Segmented block copolymers consist of alternating flexible and crystallisable rigid segments [1]. The rigid segments crystallise into ribbons dispersed in the amorphous matrix and act as physical crosslinks and as a reinforcing filler for the amorphous matrix. The presence of physical crosslinks, instead of chemical crosslinks, allows solvent casting and thermal processing of the material. The rigid segments provide the copolymer dimensional and thermal stability while the flexible segments give the material elasticity. Polyethers are often used as flexible segments due to their low glass transition temperature.

Hydrophilic segmented block copolymers based on poly(ethylene oxide) (PEO) find applications in many different fields like textile industry, packaging materials, construction industry and gas separation processes. Moreover, these materials have gained increasing attention for biomedical applications like drug delivery systems, contact lenses, catheters and wound dressings. Several PEO-based segmented block copolymers with ester [2-4], amide [5-7] or urethane [7-13] types of rigid segments were previously reported.

PEO can easily crystallise and an increase in PEO molecular weight results in a higher PEO melting temperature and crystallinity. The presence of a semi-crystalline PEO phase in the block copolymer results in reduced low temperature flexibility [14,15].

The use of PEO flexible segments results in a strong increase in water absorption of the copolymer. Generally, the tensile properties of PEO-based copolymers reduce when the material is swollen with water [16-18]. The swelling of the material can be controlled by using mixtures of hydrophilic and hydrophobic soft segments. Often a combination of hydrophilic PEO blocks and hydrophobic poly(tetramethylene oxide) (PTMO) or poly(propylene oxide) (PPO) blocks is used.

The physical properties of polyurethanes based on hydrophilic PEO and hydrophobic PTMO blocks were investigated for possible applications in biomedical devices [19,20]. Polyurethanes based on $PEO_{2000}/PTMO_{2000}$ had two glass transition temperatures (-38 and -80 ºC) and two melting temperatures (39 and 5 ºC) of PEO and PTMO respectively. Two glass transition temperatures were also observed for polyurethanes based on $PEO_{2000}/PTMO_{1000}$ and $PEO_{1450}/PTMO_{2000}$ [10]. However, one glass transition temperature was found for polyurethane copolymers containing shorter PEO and PTMO segments with 1000 g/mol.

Polyurethanes with mixed PTMO and PPO segments, which both have a molecular weight of 1000 or 2000 g/mol, had only one glass transition temperature [12,21]. This suggests that these PPO/PTMO polyurethane systems have a homogeneous amorphous polyether phase.

However, the glass transition temperatures of pure PTMO and PPO are close together and, therefore, two separate glass transition temperatures are difficult to distinguish.

The crystallinity of the rigid segments in block copolymers is often low and part of the non-crystallised rigid segments is dissolved in the amorphous phase. The crystallisation of the rigid segments can be improved by using monodisperse crystalline segments [22,23]. With monodisperse crystallisable segments a fast and more complete crystallisation can be obtained and, as a result, there is hardly any amorphous rigid segment dissolved in the amorphous matrix.
Segmented block copolymers with monodisperse crystalline bisester tetra-amide segments (T6T6T) and flexible polyether segments have been studied extensively [14,15,24-28]. The bisester tetra-amide is based on dimethyl terephthalate (T) and hexamethylenediamine (6) [26]. Copolymers with monodisperse crystallisable T6T6T segments crystallise fast, have a relatively high modulus and an almost temperature independent rubbery plateau. The flexible polyether segments consist of PTMO [24,25,27], PPO [28] or PEO [14,15]. So far, no segmented block copolymers with mixed polyether segments and monodisperse crystallisable segments have been investigated.

In this chapter, the synthesis and characterisation of segmented block copolymers based on mixed hydrophilic PEO and hydrophobic PTMO flexible segments and monodisperse T6T6T segments will be reported. These copolymers are denoted as $PEO_x/PTMO_z$-T6T6T, where x and z represent the PEO and PTMO molecular weights respectively. Several series of copolymers have been made where the PEO_x length, the $PTMO_z$ length and/or the T6T6T content are varied. The influence of the polyether phase composition on the thermal mechanical and elastic properties will be studied.
The polymer molecular weight is determined by measuring the inherent viscosity. The thermal transitions and crystallinity of the polyether and T6T6T are evaluated by DSC. Additional results concerning the T6T6T crystallinity are obtained from FTIR measurements. The thermal mechanical properties are studied by DMA and the elastic properties are evaluated by compression set experiments.

Experimental

Materials. *N*-methyl-2-pyrrolidone (NMP) was purchased from Merck. Tetra-isopropyl orthotitanate (Ti(*i*-$OC_3H_7)_4$) was obtained from Aldrich and diluted in *m*-xylene (0.05 M) received from Fluka. Irganox 1330 was obtained from CIBA. Difunctional poly(ethylene glycol)s (M_n of 600, 1000, 2000, 3400, 4600 and 8000 g/mol) were obtained from Aldrich and difunctional poly(tetramethylene oxide)s (PTMO) (M_n of 650, 1000, 2000 and 2900 g/mol) were a gift from Dupont. T6T6T-dimethyl was synthesised as described before [26].

PEO_x/$PTMO_z$-T6T6T block copolymers. The preparation of PEO_{2000}/$PTMO_{2000}$-T6T6T block copolymers, with a PEO/PTMO weight percentage ratio of 60/40, is given as an example.

The reaction was carried out in a 250 mL stainless steel vessel equipped with a magnetic stirrer and nitrogen inlet. The vessel contained T6T6T-dimethyl (10 mmol, 6.86 g), PEO_{2000} (6 mmol, 12.00 g), $PTMO_{2000}$ (4 mmol, 8.00 g), Irganox 1330 (0.20 g), 50 mL NMP and catalyst solution (1 mL of 0.05 M Ti-(*i*-$(OC_3H_7)_4$) in *m*-xylene). The reaction mixture was heated to 180 °C under a nitrogen flow in an oil bath and after 30 min the temperature was increased to 250 °C in 1 h. After 2 h at 250 °C the pressure was slowly reduced (P < 21 mbar) to remove all NMP. Subsequently, the pressure was further reduced (P < 1 mbar) to allow melt polycondensation for 1 h. The polymer melt was cooled down to room temperature while maintaining the vacuum. Then the reaction vessel was filled with liquid nitrogen and the polymer was removed. The copolymer was crushed and dried in a vacuum oven at 50 ºC for 24 h.

Viscometry. The inherent viscosity (η_{inh}) of the polymers was determined at 25 °C using a capillary Ubbelohde type 1B. The polymer solution had a concentration of 0.1 dL/g in a 1/1 (molar ratio) mixture of phenol/1,1,2,2-tetrachloroethane.

Injection-moulding. Samples for dynamic mechanical analysis, differential scanning calorimetry and compression set were prepared on an Arburg-H manual injection-moulding machine. The barrel temperature was set approximately 80 °C above the melting temperature of the block copolymer and the mould temperature was set at 70 °C.

Differential scanning calorimetry (DSC). DSC spectra were recorded on a Perkin Elmer DSC7 apparatus, equipped with a PE7700 computer and TAS-7 software. Dry polymer samples (5 – 10 mg) were heated from -50 to 250 °C at a rate of 20 °C/min. Subsequently, a cooling scan from 250 to -50 °C at a rate of 20 °C/min followed by a second heating scan under the same conditions as the first heating scan were performed. The melting temperature (T_m) was determined from the maximum of the endothermic peak in the second heating scan and the crystallisation temperature (T_c) from the peak maximum of the exothermic peak in the cooling scan. The under-cooling of the copolymer was defined as the difference between the melting and crystallisation temperature.

Fourier Transform InfraRed (FTIR). FTIR spectra were recorded on a Nicolet 20SXB FTR spectrometer with a resolution of 4 cm^{-1}. The polymer was dissolved in TFA (0.1 wt%) and by spin coating a thin polymer film (~15 μm) was formed on a silicon wafer. The polymer film was placed between two pressed KBr tablets. The FTIR data were collected between 700 and 4000 cm^{-1}. For temperature-dependent FTIR a heating rate of 10 °C/min was used under a constant helium flow. The crystallinity (X_c) of T6T6T in the copolymer was calculated using the following equations;

$$X_c = \frac{h_{(1630\,cm^{-1})}}{(C \times h_{(1670\,cm^{-1})}) + h_{(1630\,cm^{-1})}} \times 100\% \quad [\%] \qquad \text{(Equation 4.1)}$$

and $$C = \frac{h_{(1630\,cm^{-1}\,at\,50°C)} - h_{(1630\,cm^{-1}\,melt)}}{h_{(1670\,cm^{-1}\,melt)} - h_{(1670\,cm^{-1}\,at\,50°C)}} \qquad \text{(Equation 4.2)}$$

where $h_{(1630\,cm^{-1})}$ and $h_{(1670\,cm^{-1})}$ are the intensities of the absorbance peaks at 1630 cm^{-1} and 1660 - 1670 cm^{-1} respectively.

Dynamic mechanical analysis (DMA). The torsion behaviour (storage modulus G' and loss modulus G" as a function of temperature) was measured using a Myrenne ATM3 torsion pendulum at a frequency of 1 Hz and 0.1% strain. Before use, samples (70x9x2 mm) were dried in a vacuum oven at 50 °C overnight. Samples were cooled to –100 °C and then heated at a rate of 1 °C/min. The glass transition temperature (T_g) was defined as the maximum of the loss modulus and the flow temperature (T_{flow}) as the temperature where the storage modulus reached 1 MPa. The temperature where the rubbery plateau starts is denoted as the flex temperature (T_{flex}) and the storage modulus at 20 ºC is given as $G'_{20\,°C}$.

Compression set (CS). Samples for compression set experiments were cut from injection-moulded bars with a thickness of ~2.2 mm. The compression set was measured according to the ASTM 395B at 20 °C. Samples were compressed (25%) for 24 h and after 30 min of relaxation the thickness of the samples was measured. The compression set (CS) was calculated using Equation 4.3.

$$CS = \frac{d_0 - d_2}{d_0 - d_1} \times 100\% \quad [\%] \qquad \text{(Equation 4.3)}$$

where d_0 = thickness before compression [mm]
d_1 = thickness during compression [mm]
d_2 = thickness 30 min after release of the compression [mm]

Results and discussion

The copolymers discussed in this chapter are based on a mixture of hydrophilic PEO and hydrophobic PTMO segments and monodisperse crystallisable T6T6T segments. The copolymers are denoted as $PEO_x/PTMO_z$-T6T6T where *x* and *z* represent the PEO and PTMO molecular weights respectively. The T6T6T segments were synthesised prior to the polycondensation reaction to obtain monodisperse segments in the copolymers.

First, the synthesis and characterisation of $PEO_{2000}/PTMO_{2000}$-T6T6T will be discussed and, second, two copolymer series will be discussed where the PEO_x and $PTMO_z$ segment lengths and T6T6T concentrations are varied.

$PEO_{2000}/PTMO_{2000}$-T6T6T block copolymers

Segmented block copolymers based on mixed PEO_{2000} and $PTMO_{2000}$ polyether segments and monodisperse T6T6T segments have been prepared. The PEO/PTMO ratio is varied while the T6T6T remains constant (23.8 wt%). The copolymers with a ratio of 0/100 and 100/0 can also be denoted as $PTMO_{2000}$-T6T6T and PEO_{2000}-T6T6T respectively, and have been discussed before [14,25,27]. The composition of these copolymers is given in Table 4.1.

During the polymerisation the polymer melt was homogeneous and transparent, indicating that no melt phasing between the segments occurred. The copolymers have a high inherent viscosity and, therefore, a relatively high molecular weight (Table 4.1).

Table 4.1: Composition and inherent viscosity of $PEO_{2000}/PTMO_{2000}$-T6T6T copolymers.

PEO/PTMO ratio	Conc. T6T6T [wt%]	Conc. PEO [wt%]	Conc. PTMO [wt%]	η_{inh} [dL/g]
0/100	23.8	0.0	76.2	2.2
20/80	23.8	15.2	61.0	2.0
40/60	23.8	30.5	45.7	2.1
50/50	23.8	38.1	38.1	1.7
60/40	23.8	45.7	30.5	1.8
80/20	23.8	61.0	15.2	1.9
100/0	23.8	76.2	0.0	2.1

DSC

The melting and crystallisation behaviour of $PEO_{2000}/PTMO_{2000}$-T6T6T copolymers was investigated with DSC and the obtained data are given in Table 4.2. Data obtained from the second heating scan were used to exclude the influence of the thermal history of the polymer.

Table 4.2: DSC results of $PEO_{2000}/PTMO_{2000}$-T6T6T copolymers.

	Polyether			T6T6T					
PEO/PTMO ratio	T_m [°C]	ΔH_m [J/g]	X_c [%]	T_m [°C]	ΔH_m [J/g]	T_c [°C]	T_m-T_c [°C]	X_c (DSC) [%]	X_c (IR) [%]
0/100	2	17	11	227	32	222; 145	5	88	85
20/80	0	15	10	220	25	208; 129	12	69	86
40/60	7	16	11	207	20	197; 122	10	56	87
50/50	10	21	14	203	27	200; 116	3	74	86
60/40	12	25	17	196	23	193; -	3	62	87
80/20	15	30	20	184	20	178; 120	6	56	84
100/0	21	40	27	167	16	161; 114	6	45	84

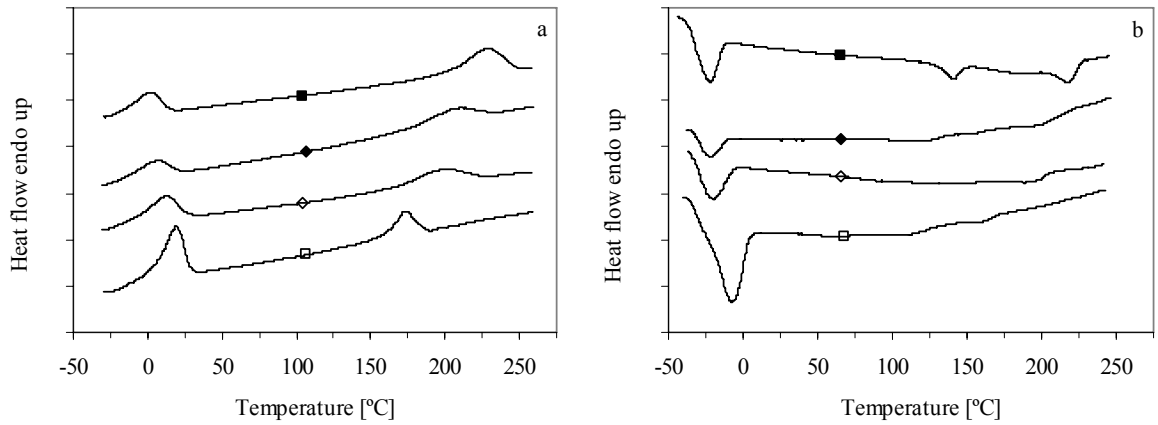

Figure 4.1: DSC thermogram during (a) heating and (b) cooling of $PEO_{2000}/PTMO_{2000}$-T6T6T copolymers with different PEO/PTMO ratios: ■, 0/100; ♦, 40/60; ◊, 60/40; □, 100/0.

During heating, two melting peaks for $PEO_{2000}/PTMO_{2000}$-T6T6T copolymers are observed, corresponding to the polyether and T6T6T phase (Figure 4.1a). PEO_{2000}-T6T6T has a higher polyether melting temperature than $PTMO_{2000}$-T6T6T, 21 and 2 ºC respectively. Copolymers with mixed PEO and PTMO segments show one polyether melting peak. This value is lower than in the case of ideal co-crystallisation. When ideal co-crystallisation had taken place, a linear increase in polyether melting temperature with increasing PEO/PTMO ratio would have been observed.

In Figure 4.2 the polyether melting temperature is given as a function of the PEO/PTMO ratio. The polyether melting temperature remains almost constant at low PEO/PTMO ratios, while above a ratio of approximately 30/70 the polyether melting temperature increases.

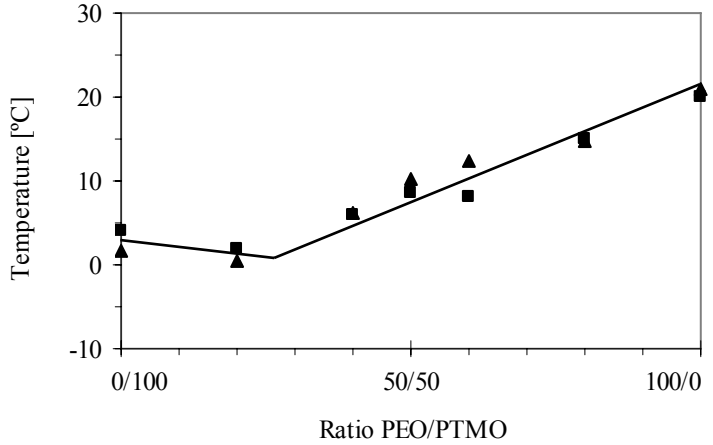

Figure 4.2: (■) Flex temperature and (▲) polyether melting temperature of $PEO_{2000}/PTMO_{2000}$-T6T6T copolymers as a function of the PEO/PTMO ratio.

The crystallinity of the polyether phase can be calculated assuming that pure crystalline PEO and PTMO have a melting enthalpy of 197 and 200 J/g respectively [29]. The calculated polyether crystallinity of PEO_{2000}-T6T6T is 27% and of $PTMO_{2000}$-T6T6T 11%. These results indicate that PEO is more crystalline than PTMO despite the same molecular weight. The polyether crystallinity of copolymers with mixed PEO and PTMO segments can be calculated using the polyether concentrations. In Figure 4.3 the polyether crystallinity of PEO_{2000}/$PTMO_{2000}$-T6T6T copolymers is given as a function of the PEO/PTMO ratio. The polyether crystallinity is lower than in the case of ideal co-crystallisation, with a minimum at a PEO/PTMO ratio of approximately 30/70.

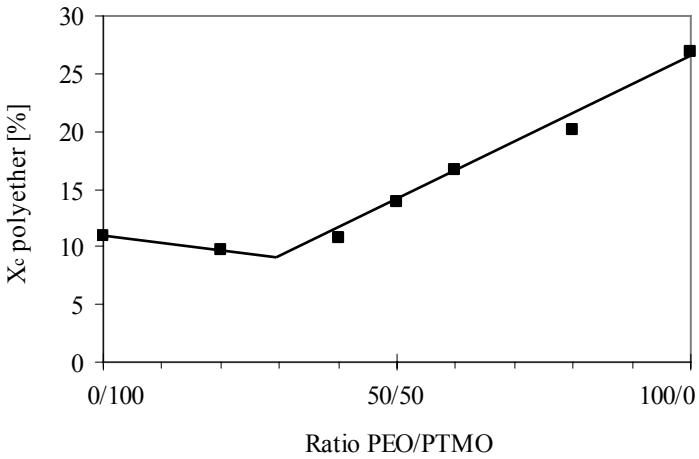

Figure 4.3: Polyether crystallinity in PEO_{2000}/$PTMO_{2000}$-T6T6T copolymers, as determined with DSC, as a function of the PEO/PTMO ratio.

By using a mixture of polyethers both the melting temperature and the crystallinity of the polyether phase is reduced by the presence of the other polyether segment. As only one melting temperature of the polyether phase is observed it is expected that one crystalline polyether phase is present in these copolymers.

The T6T6T melting temperature and melting enthalpy is lower for PEO_{2000}-T6T6T than for $PTMO_{2000}$-T6T6T (Table 4.2) and this effect was already discussed in Chapter 2. The flow temperatures of copolymers with mixed polyether segments show a linear decrease with increasing PEO content. This decrease in melting temperature of the copolymer can be explained by a solvent effect described by Flory [30,31], which states that the soft phase acts as a solvent for the crystallisable phase. According to this theory, the melting point depression depends on the volume fraction of polyether and the interaction parameter (χ) between the polyether and T6T6T [14]. The stronger melting temperature depression for the PEO-T6T6T

copolymer suggests that the PEO-T6T6T interaction is stronger than the PTMO-T6T6T interaction. Therefore, it is expected that the PEO-T6T6T copolymer has a lower interaction parameter than the PTMO-T6T6T copolymer. Surprisingly, the heat of fusion of T6T6T also decreases with increasing PEO content.

An estimation of the T6T6T crystallinity in the copolymer can be made by assuming that the melting enthalpy of pure T6T6T is 152 J/g [25]. The T6T6T crystallinity in $PTMO_{2000}$-T6T6T copolymer is around 88% but for PEO_{2000}-T6T6T the calculated T6T6T crystallinity is only 45% (Table 4.2). The copolymers with mixtures of $PEO_{2000}/PTMO_{2000}$ have a constant T6T6T concentration of 23.8 wt% but the heat of fusions decrease with increasing PEO content. The lower T6T6T heat of fusion in PEO-based copolymer suggests that either the T6T6T is less crystalline or that the heat of fusion is lower due to exothermic mixing between PEO and T6T6T. Therefore, studying the T6T6T crystallinity with a different method (e.g. FTIR) might give more insight in what is happening.

On cooling, most of the $PEO_{2000}/PTMO_{2000}$-T6T6T copolymers show two crystallisation peaks of T6T6T (Figure 4.1b). Two crystallisation peaks were also observed for the T6T6T-dimethyl starting material and is most likely due to a change in crystalline structure [14,26].

FTIR

Another method to determine the crystallinity of T6T6T in the copolymer is by Fourier Transform InfraRed spectroscopy (FTIR) [14,27]. The wave number of the amide carbonyl absorbance band in T6T6T is sensitive to the transition from the crystalline state to the amorphous state. In Figure 4.4 the FTIR spectra of $PEO_{2000}/PTMO_{2000}$-T6T6T (50/50) are given at different temperatures.

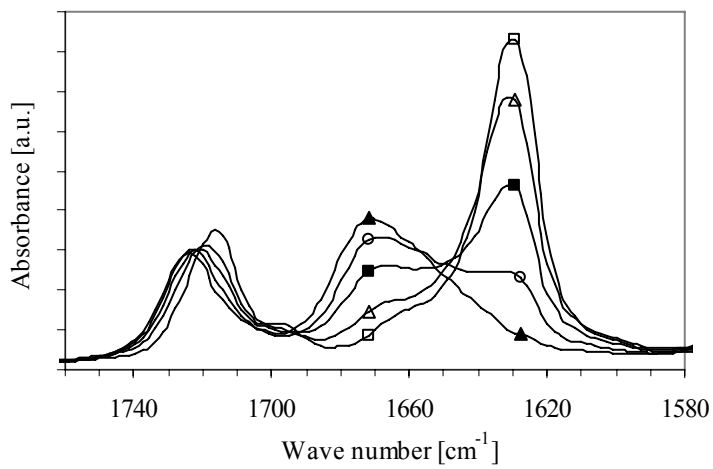

Figure 4.4: FTIR spectra of $PEO_{2000}/PTMO_{2000}$-T6T6T (50/50) recorded at different temperatures: □, 50 ºC; Δ, 150 ºC; ■, 190 ºC; ○, 210 ºC; ▲ 250 ºC.

With increasing temperature, the absorbance peak of the crystalline amide C=O (1630 cm^{-1}) decreases and the absorbance peak of the amorphous amide C=O (1660 – 1670 cm^{-1}) increases. This change is particularly strong when the temperature approaches the melting temperature of the copolymer (T_m is 203 °C). In the melt, the peak at 1630 cm^{-1} has almost completely disappeared, while the peak at 1670 cm^{-1} is maximal. With increasing temperature the wave number of the amorphous amide C=O increases slightly from 1660 to 1670 cm^{-1}. Besides, the absorbance peak of the ester carbonyl shifts from 1720 to 1730 cm^{-1} but the intensity of the ester carbonyl is hardly affected by the temperature.

The T6T6T crystallinity in the copolymers is calculated by using Equations 4.1 and 4.2. The intensity of the crystalline amide carbonyl is compared to the intensity of the amorphous amide carbonyl. The T6T6T crystallinity is determined at 50 ºC to exclude the presence of a crystalline PEO phase in the copolymer. The constant *C* for PEO_{2000}-T6T6T, $PEO_{2000}/PTMO_{2000}$-T6T6T (50/50) and $PTMO_{2000}$-T6T6T is about the same (~2.3) and corresponds to values reported in previous research on PEO-T6T6T [14] and PTMO-T6T6T copolymers [27].

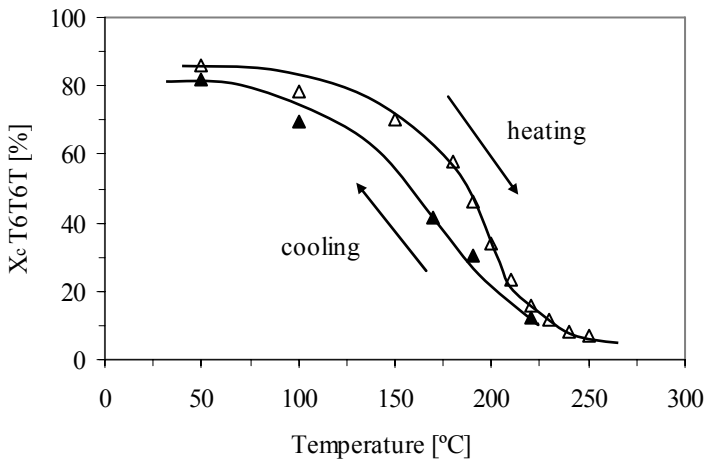

Figure 4.5: T6T6T crystallinity as a function of temperature at 10 ºC/min for $PEO_{2000}/PTMO_{2000}$-T6T6T (50/50): Δ, heating; ▲, cooling

In Figure 4.5 the T6T6T crystallinity in $PEO_{2000}/PTMO_{2000}$-T6T6T (50/50) as a function of temperature is given during a heating and cooling cycle. On heating, the T6T6T crystallinity remains high up to temperatures close to the melting point (T_m is 203 ºC). Upon cooling from the melt, the crystallinity returns relatively fast and is almost complete. The T6T6T crystallinity at 50 ºC of all $PEO_{2000}/PTMO_{2000}$-T6T6T copolymers is around 85% (Table 4.2). The FTIR results reveal that the PEO-based copolymers have a high T6T6T crystallinity.

Dynamic mechanical analysis

Thermal mechanical properties of the $PEO_{2000}/PTMO_{2000}$-T6T6T copolymers are studied by dynamic mechanical analysis (DMA) in torsion. The storage and loss moduli as a function of temperature are represented in Figure 4.6 and the results are summarised in Table 4.3.

All copolymers have a broad and an almost temperature independent rubbery plateau and a sharp flow temperature. This is common for polymers with crystallisable segments of monodisperse length. The modulus of the rubbery plateau is independent of the PEO/PTMO ratio and is mainly determined by the T6T6T content.

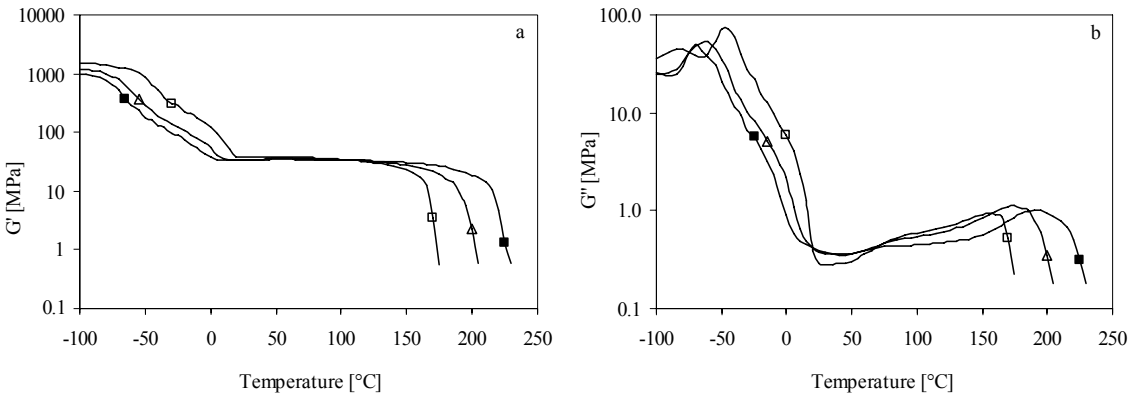

Figure 4.6: Storage (a) and loss (b) modulus as a function of temperature of $PEO_{2000}/PTMO_{2000}$-T6T6T copolymers with different PEO/PTMO ratios: ■, 0/100; Δ, 50/50; □, 100/0.

Table 4.3: Dynamic mechanical properties of $PEO_{2000}/PTMO_{2000}$-T6T6T copolymers.

PEO/PTMO ratio	Conc. T6T6T [wt%]	Conc. PEO [wt%]	Conc. PTMO [wt%]	T_g [°C]	T_{flex} [°C]	$G'_{20\,°C}$ [MPa]	T_{flow} [°C]	$CS_{25\%}$ [%]
0/100	23.8	0.0	76.2	-70	4	34	226	13
20/80	23.8	15.2	61.0	-67	2	38	217	12
40/60	23.8	30.5	45.7	-63	6	31	212	13
50/50	23.8	38.1	38.1	-61	9	33	204	13
60/40	23.8	45.7	30.5	-57	8	33	199	15
80/20	23.8	61.0	15.2	-52	15	33	187	16
100/0	23.8	76.2	0.0	-48	20	38	174	17

The T_g of $PTMO_{2000}$-T6T6T and PEO_{2000}-T6T6T is -70 and -48 °C respectively. This difference is due to a higher T_g of pure PEO (-72 to -65 ºC) [32] compared to pure PTMO (-86 ºC) [33]. In the loss modulus of the $PEO_{2000}/PTMO_{2000}$-T6T6T copolymers only one maximum is observed, indicating that the copolymers have one T_g (Figure 4.6b).

In Figure 4.7 the T_g of $PEO_{2000}/PTMO_{2000}$-T6T6T copolymers is given as a function of the PEO/PTMO ratio. The T_g's increase linearly with PEO/PTMO ratio and thus PEO content. As only one T_g is observed that increases linearly with the PEO content, a homogenous amorphous mixed ether phase is expected.

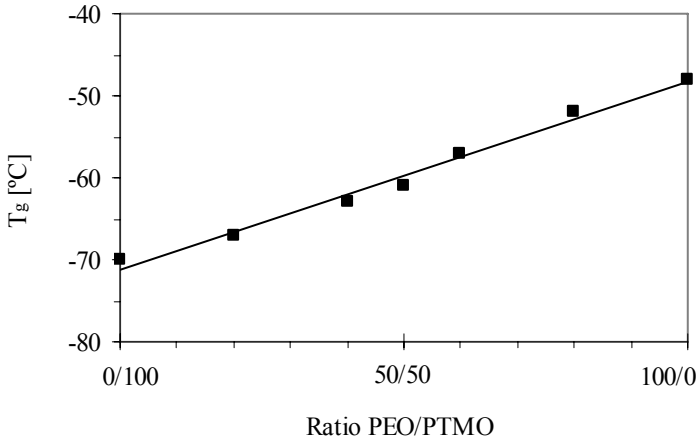

Figure 4.7: Glass transition temperature of $PEO_{2000}/PTMO_{2000}$-T6T6T copolymers as a function of the PEO/PTMO ratio.

The flex temperature (T_{flex}) of copolymers with an amorphous polyether phase is mainly determined by the glass transition temperature. However, the flex temperature of copolymers with a semi-crystalline ether phase depends on the melting temperature of the crystalline polyether phase [14,15]. The T_{flex} of the $PEO_{2000}/PTMO_{2000}$-T6T6T copolymers seems to be a singular transition that follows the trend of the polyether melting temperature (Figure 4.2). However, the increase in T_{flex} with PEO content is not linear. The crystalline polyether melting temperature (and crystallinity) is disturbed by the presence of the other polyether segment.

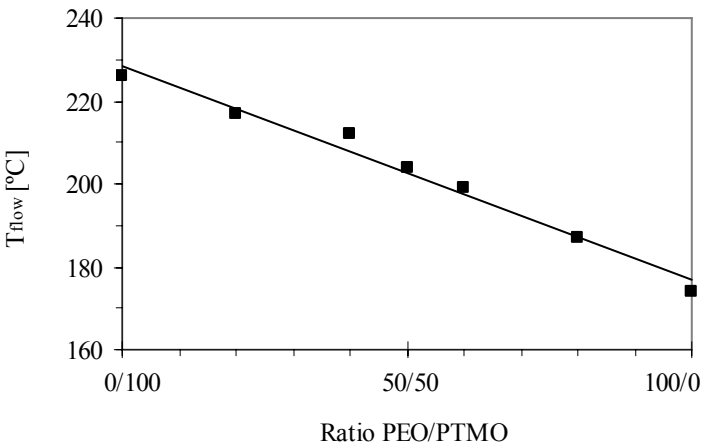

Figure 4.8: Flow temperature of $PEO_{2000}/PTMO_{2000}$-T6T6T copolymers as a function of the PEO/PTMO ratio.

In Figure 4.8 the flow temperature of the $PEO_{2000}/PTMO_{2000}$-T6T6T copolymers is given as a function of the PEO/PTMO ratio. The T_{flow} decreases linearly with increasing PEO content, despite the fact that the T6T6T content is constant in all copolymers. The flow temperatures have comparable values as the melting temperatures obtained with DSC experiments. As discussed before, the decrease in T_{flow} with PEO content can be explained by a stronger interaction between PEO and T6T6T compared to the interaction between PTMO and T6T6T.

Compression set

The elastic properties are investigated with compression set tests. The compression set (CS) is a measure for the recovery of a material after compression. At room temperature, the CS values are mainly determined by plastic deformation [27]. The CS values of copolymers usually increase with increasing modulus as the network density increases. The CS values increase also strongly with increasing polyether crystallinity [14,15].

In Figure 4.9 the CS values of $PEO_{2000}/PTMO_{2000}$-T6T6T copolymers are given as a function of the PEO/PTMO ratio.

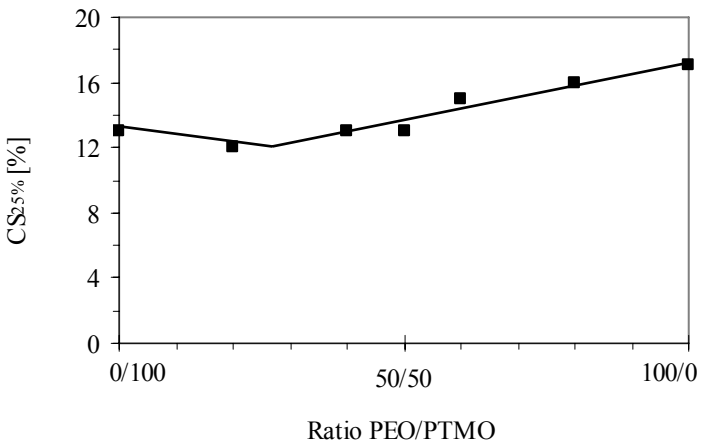

Figure 4.9: Compression set measured at 20 °C for $PEO_{2000}/PTMO_{2000}$-T6T6T copolymers as a function of the ratio PEO/PTMO.

Despite the fact that the T6T6T concentration in all copolymers is constant, the CS values increase with PEO content and, thereby, going through a minimum at a ratio of approximately 30/70. This minimum corresponds to the minimum observed for the polyether crystallinity determined with DSC experiments (Figure 4.3). The higher CS of PEO_{2000}-T6T6T compared to $PTMO_{2000}$-T6T6T is most likely due to the presence of some polyether crystals.

Influence of the molecular weight of polyether segments

The polyether crystallinity in $PEO_{2000}/PTMO_{2000}$-T6T6T copolymers is relatively high. When using shorter polyether segments the polyether crystallinity is reduced but the T6T6T contents are higher. A $PEO_{1000}/PTMO_{1000}$-T6T6T copolymer series is made, where the T6T6T concentration is 38.4 wt%, and the thermal mechanical and elastic properties of these copolymers are compared with the $PEO_{2000}/PTMO_{2000}$-T6T6T series where the T6T6T concentration is 23.8 wt%.

Two other copolymer series are made to study the effect of the polyether molecular weight on thermal mechanical and elastic properties. One series is made where the $PEO_x/PTMO_{1000}$ ratio is kept 30/70 but the PEO_x length changes from 600 to 8000 g/mol. Another series is based on $PEO_{1000}/PTMO_z$ where the PEO_{1000} content is kept constant at 37 wt% and the $PMTO_z$ length changes from 650 to 2900 g/mol.

The copolymer compositions of the $PEO_{1000}/PTMO_{1000}$-T6T6T, $PEO_x/PTMO_{1000}$-T6T6T and $PEO_{1000}/PTMO_z$-T6T6T series are given in Table 4.4.

Table 4.4: Dynamic mechanical properties and inherent viscosity of $PEO_x/PTMO_z$-T6T6T copolymers

PEO_x / $PTMO_z$ [ratio]	M_n PEO [g/mol]	M_n PTMO [g/mol]	Conc. T6T6T [wt%]	Conc. PEO [wt%]	Conc. PTMO [wt%]	η_{inh} [dL/g]	T_g [°C]	T_{flex} [°C]	$G'_{20\,°C}$ [MPa]	T_{flow} [°C]	$CS_{25\%}$ [%]
$PEO_{1000}/PTMO_{1000}$-T6T6T											
0/100	1000	1000	38.4	0.0	61.5	2.1	-63	-22	89	239	18
30/70	1000	1000	38.4	18.5	43.1	1.7	-60	-25	80	225	- [1]
40/60	1000	1000	38.4	24.6	36.9	1.4	-57	-25	111	220	23
60/40	1000	1000	38.4	36.9	24.6	1.1	-56	-20	103	219	23
100/0	1000	1000	38.4	61.5	0.0	1.4	-45	-13	85	199	22
$PEO_x/PTMO_{1000}$-T6T6T											
30/70	600	1000	42.9	17.1	40.0	2.3	-56	-10	113	229	20
30/70	1000	1000	38.4	18.5	43.1	1.7	-60	-25	80	225	- [1]
30/70	3400	1000	33.0	20.1	46.9	2.0	-62	-27; -5	73	230	22
30/70	4600	1000	32.3	20.3	47.3	1.8	-61	-25; 9	85	229	19
30/70	8000	1000	31.5	20.6	47.9	1.8	-60	-20; 51	109	234	14
$PEO_{1000}/PTMO_z$-T6T6T											
64/36	1000	650	42.7	36.9	20.4	2.5	-45	-10	74	232	21
60/40	1000	1000	38.4	36.9	24.6	1.1	-56	-20	103	219	23
55/45	1000	2000	32.6	37.1	30.3	1.6	-53	-27	49	213	17
53/47	1000	2900	30.2	37.0	32.8	1.7	-50	-28; 15	41	208	14

[1] *CS experiments were not performed*

During the polymerisation, the polymer melt of all the copolymers was transparent, indicating that no melt phasing between the segments occurred. All copolymers have a high inherent viscosity and, therefore, a high molecular weight (Table 4.4).

Low temperature properties

DMA results of the $PEO_x/PTMO_z$-T6T6T copolymers reveal only one glass transition temperature of the mixed polyether phase. This suggests that the amorphous PEO and PTMO segments are mixed homogeneously. In Figure 4.10a the T_g's of $PEO_{1000}/PTMO_{1000}$-T6T6T and $PEO_{2000}/PTMO_{2000}$-T6T6T copolymers are given as a function of the PEO/PTMO ratio.

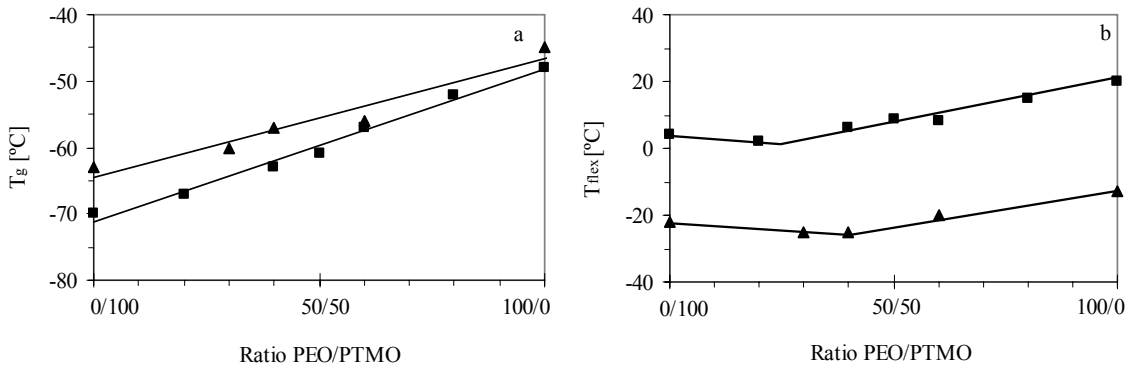

Figure 4.10: The (a) glass transition temperature and (b) flex temperature as a function of the PEO/PTMO ratio: ■, $PEO_{2000}/PTMO_{2000}$-T6T6T; ▲, $PEO_{1000}/PTMO_{1000}$-T6T6T.

All copolymers have a low T_g, which increases linearly with increasing PEO/PTMO ratio. The T_g's of $PEO_{1000}/PTMO_{1000}$-T6T6T copolymers are higher than those of the $PEO_{2000}/PTMO_{2000}$-T6T6T copolymers due to a higher physical crosslink density.

The flex temperature of copolymers, containing a semi-crystalline polyether phase, is related to the melting temperature of the polyether segments. The $PEO_{1000}/PTMO_{1000}$-T6T6T copolymers have lower flex temperatures than those of the $PEO_{2000}/PTMO_{2000}$-T6T6T copolymers (Figure 4.10b). Shorter polyether segments are less crystalline and have a lower melting temperature. Both copolymer series show no linear increase in flex temperature with increasing PEO/PTMO ratio, indicating that the polyether segments hinder each other in their crystallisation. Both the $PEO_{2000}/PTMO_{2000}$-T6T6T and $PEO_{1000}/PTMO_{1000}$-T6T6T copolymers contain the lowest polyether crystallinity at a PEO/PTMO ratio of approximately 30/70.

In another series, based on $PEO_x/PTMO_{1000}$-T6T6T copolymers, the $PEO_x/PTMO_{1000}$ ratio is kept constant at 30/70 and the PEO length was varied from 600 to 8000 g/mol. In Figure 4.11a the glass transition temperatures and flex temperatures of these copolymers are given as a function of the PEO segment length.

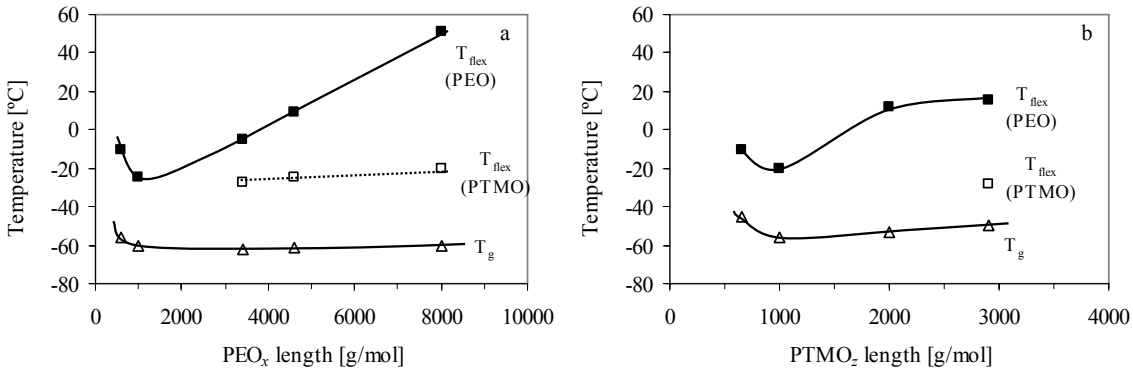

Figure 4.11: The glass transition temperature and flex temperature as a function of the polyether length of (a) $PEO_x/PTMO_{1000}$-T6T6T and (b) $PEO_{1000}/PTMO_z$-T6T6T: Δ, T_g; □, T_{flex} of PTMO phase; ■, T_{flex} of PEO phase.

The $PEO_x/PTMO_{1000}$-T6T6T copolymers have one glass transition temperature that remains almost constant despite the increasing PEO length. An exception is $PEO_{600}/PTMO_{1000}$-T6T6T, which has a slightly higher T_g due to a higher crosslink density.

The $PEO_x/PTMO_{1000}$-T6T6T copolymers with PEO_x of 600 or 1000 g/mol show one polyether melting transition while copolymers with PEO_x of 3400 g/mol or higher show two transitions at low temperatures. These two melting transitions correspond to a PEO and PTMO crystalline phase. The copolymer with a PEO length of 8000 g/mol has a flex temperature far above room temperature.

The DSC heating scan of $PEO_x/PTMO_{1000}$-T6T6T copolymers show one glass transition and a broad polyether melting peak (Figure 4.12). The melting transition can be divided in a PTMO and PEO melting peak. The glass transition temperature of the polyether phase and PTMO melting temperature remain unaffected when the PEO length increases. However, the PEO melting temperature shows a strong increase. These extra transitions suggest that with long polyether segments the PEO/PTMO-T6T6T copolymers contain two polyether crystalline phases.

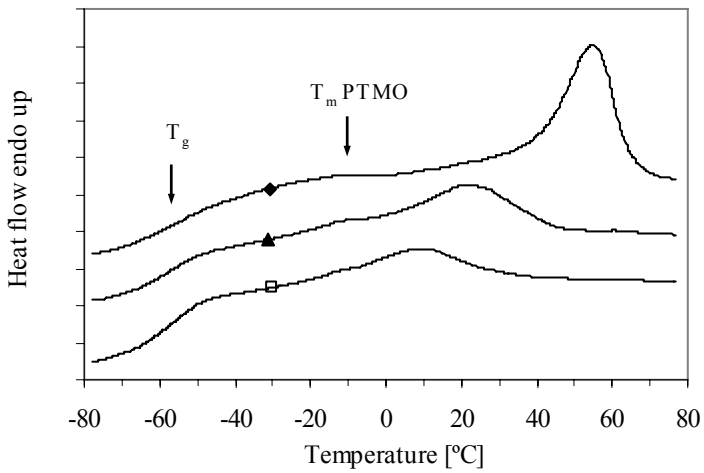

Figure 4.12: DSC heating scan of $PEO_x/PTMO_{1000}$-T6T6T copolymers: □, x = 3400 g/mol; ▲, x = 4600 g/mol; ♦, x = 8000 g/mol.

In the other series, based on $PEO_{1000}/PTMO_z$-T6T6T copolymers, the PTMO length is varied from 650 to 2900 g/mol. The glass transition temperatures and flex temperatures of these copolymers are given as a function of the PTMO segment length in Figure 4.11b. The $PEO_{1000}/PTMO_z$-T6T6T copolymers have one glass transition temperature that slightly increases with increasing the PTMO length. The T_g of $PEO_{1000}/PTMO_{650}$-T6T6T is higher due to a higher crosslink density in the copolymer. A single flex temperature is observed for the copolymers when the $PTMO_z$ segment length is 2000 g/mol or lower, and two flex temperatures are observed when the $PTMO_z$ segment length is 2900 g/mol.

Storage modulus

The storage modulus at room temperature of polyether-T6T6T copolymers depends mainly on the T6T6T content. The type of polyether segments only has a small effect as discussed in Chapter 2. However, when the melting temperature (T_{flex}) of the polyether phase is above room temperature the modulus ($G'_{20\ °C}$) is higher. The storage moduli of the studied $PEO_x/PTMO_z$-T6T6T copolymers are given as a function of the T6T6T concentration in Figure 4.13.

As expected, the storage modulus increases with T6T6T content. The $PEO_x/PTMO_{1000}$-T6T6T copolymers with long PEO_x segments have a somewhat higher modulus than the observed trend in modulus versus T6T6T concentration of the other $PEO_x/PTMO_z$-T6T6T copolymers. This can be explained by the presence of a high melting PEO phase. At 20 ºC, the storage modulus of $PEO_{8000}/PTMO_{1000}$-T6T6T is 109 MPa while at 55 ºC, where the polyether phase is completely amorphous, the storage modulus is 76 MPa.

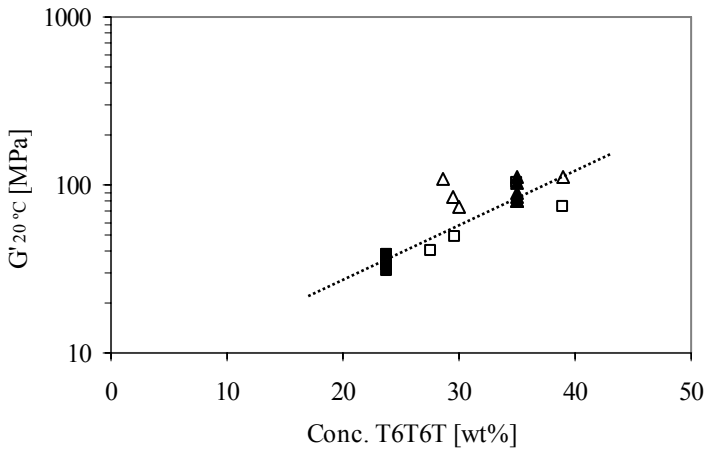

Figure 4.13: Storage modulus at 20 ºC as a function of the T6T6T concentration: ■, $PEO_{2000}/PTMO_{2000}$-T6T6T; ▲, $PEO_{1000}/PTMO_{1000}$-T6T6T; □, $PEO_{1000}/PTMO_{z}$-T6T6T; Δ, $PEO_{x}/PTMO_{1000}$-T6T6T.

Flow temperature

In Figure 4.14 the flow temperatures of $PEO_{1000}/PTMO_{1000}$-T6T6T and $PEO_{2000}/PTMO_{2000}$-T6T6T copolymers are given as a function of the PEO/PTMO ratio.

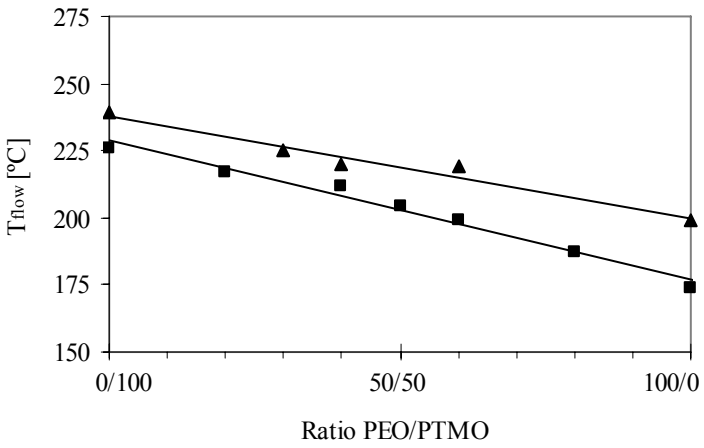

Figure 4.14: Flow temperature as a function of the PEO/PTMO ratio; ■, $PEO_{2000}/PTMO_{2000}$-T6T6T; ▲, $PEO_{1000}/PTMO_{1000}$-T6T6T.

As already discussed, the flow temperatures of $PEO_{2000}/PTMO_{2000}$-T6T6T copolymers decrease linearly with increasing PEO/PTMO ratio, while the T6T6T concentration is constant (Figure 4.8). The flow temperatures of $PEO_{1000}/PTMO_{1000}$-T6T6T copolymers show a similar decrease, however, at a higher temperature than the $PEO_{2000}/PTMO_{2000}$-T6T6T copolymers. This is due to a lower polyether content.

With increasing PEO segment length, the total polyether content of $PEO_x/PTMO_{1000}$-T6T6T copolymers increases from 57 to 68 wt%. However, the flow temperature of these copolymers does not change. It is expected that the melting temperature of the copolymer decreases due to the increased polyether content.

The PTMO content in the $PEO_{1000}/PTMO_z$-T6T6T copolymers increases from 20 to 33 wt% and, as a result, the flow temperature decreases.

Elasticity

The elasticity of the $PEO_x/PTMO_z$-T6T6T copolymers is investigated by compression set experiments performed at room temperature. The compression set (CS) of polyether-T6T6T copolymers mainly depends on the T6T6T concentration and thus on the storage modulus. However, the presence of a semi-crystalline polyether phase at room temperature reduces the elasticity of the copolymer [14,15]. The CS values of all the $PEO_x/PTMO_z$-T6T6T copolymers are given as a function of the storage modulus in Figure 4.15.

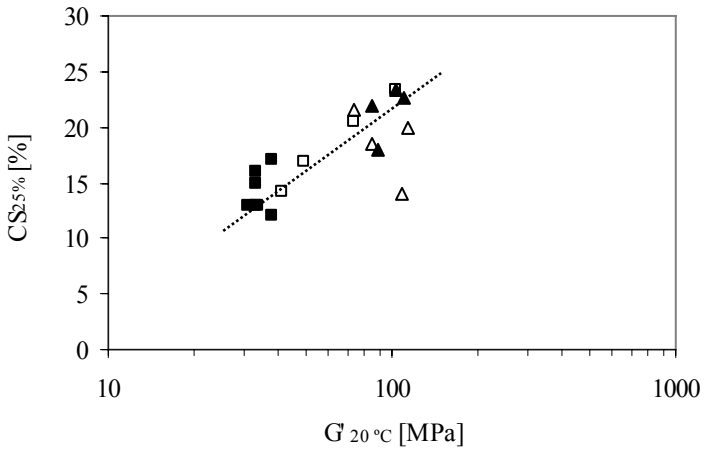

Figure 4.15: Compression set determined at 20 °C as a function of the PEO content; ■, $PEO_{2000}/PTMO_{2000}$-T6T6T; ▲, $PEO_{1000}/PTMO_{1000}$-T6T6T; □, $PEO_{1000}/PTMO_z$-T6T6T; Δ, $PEO_x/PTMO_{1000}$-T6T6T.

All the $PEO_x/PTMO_z$-T6T6T copolymers show an increase in elasticity (and thus lower CS values) with decreasing modulus. It is remarkable that the $PEO_{8000}/PTMO_{1000}$-T6T6T copolymer has a low CS value, while the polyether melting temperature of this copolymer is above room temperature (51 °C). The low CS value at a relative high modulus suggests that the crystallites of PEO_{8000} are more difficult to deform.

Conclusions

$PEO_x/PTMO_z$-T6T6T segmented block copolymers based on mixed hydrophilic poly(ethylene oxide) (PEO) and hydrophobic poly(tetramethylene oxide) (PTMO) polyether segments and monodisperse crystallisable T6T6T segments were made. The copolymers have a high molecular weight, are melt-processable and transparent. The $PEO_x/PTMO_z$-T6T6T copolymers show a broad and an almost temperature independent rubbery plateau and a sharp melting temperature due to the use of monodisperse T6T6T segments.

All investigated $PEO_x/PTMO_z$-T6T6T copolymers only have one glass transition temperature. This indicates that the amorphous polyether segments remain mixed when the rigid phase is highly crystalline, while in the case of copolymers with a low rigid segment crystallinity the amorphous polyether segments phase separate more easily. The T_g's of $PEO_x/PTMO_z$-T6T6T copolymers increase linearly with increasing PEO content since the T_g of the PEO prepolymer is higher than that of PTMO prepolymer.

Polyether segments can crystallise and with increasing crystallinity the polyether melting temperature increases. The $PEO_x/PTMO_y$-T6T6T copolymers have a single polyether melting transition when both PEO and PTMO have molecular weights of 2000 g/mol or less. When either PEO or PTMO is longer than 2000 g/mol, two polyether melting temperatures are observed. The polyether melting temperatures and crystallinities of $PEO_x/PTMO_y$-T6T6T copolymers are lower than in the case of ideal co-crystallisation, indicating that the polyether segments hinder each other in their crystallisation. A minimum in polyether melting temperature, crystallinity and compression set values is observed at a $PEO_x/PTMO_z$ ratio of approximately 30/70. An unusually low compression set value is observed for $PEO_{8000}/PTMO_{1000}$-T6T6T copolymers.

The T6T6T heat of fusion in the $PEO_x/PTMO_z$-T6T6T copolymers decreases with increasing PEO content, while FTIR results reveal a high T6T6T crystallinity in all copolymers (~85%). The lower values of heat of fusion might be due to exothermic mixing of T6T6T and PEO on melting.

References

1. Holden, G., Legge, N.R., Quirk, R.P. and Schroeder, H.E., in *Thermoplastic elastomers*, Hanser Publishers, Munich **1996**.
2. Gebben, B., *J. Membr. Sci.* **1996**, 113, p. 323-329.
3. Stroeks, A. and Dijkstra, K., *Polymer* **2001**, 42, p. 117-127.
4. Metz, S.J., Mulder, M.H.V. and Wessling, M., *Macromolecules* **2004**, 37, p. 4590-4597.
5. Bondar, V.I., Freeman, B.D. and Pinnau, I., *J. Polym. Sci., Part B: Polym. Phys.* **1999**, 37, p. 2463-2475.

6. Bondar, V.I., Freeman, B.D. and Pinnau, I., *J. Polym. Sci., Part B: Polym. Phys.* **2000**, 38, p. 2051-2062.
7. Johnson, L. and Schultze, D., *Medical Device & Diagnostic Industry*, Breathable TPE films for medical applications, **2000**.
8. Schneider, N.S., Illinger, J.L. and Karasz, F.E., in *Polymers of biological and biomedical significance,* American Chemical Society, Washington D.C. **1994**.
9. Lee, D., Lee, S., Kim, S., Char, K., Park, J.H. and Bae, Y.H., *J. Polym. Sci., Part B: Polym. Phys.* **2003**, 41, p. 2365-2374.
10. Schneider, N.S., Langlois, D.A. and Byrne, C.A., *Polym. Mater. Sci. Eng.* **1993**, 69, p. 249-250.
11. Chen, C.T., Eaton, R.F., Chang, Y.J. and Tobolsky, A.V., *J. Appl. Polym. Sci.* **1972**, 16, p. 2105-2114.
12. Schneider, N.S., Illinger, J.L. and Karasz, F.E., *J. Appl. Polym. Sci.* **1993**, 47, p. 1419-1425.
13. Yilgör, I. and Yilgör, E., *Polymer* **1999**, 40, p. 5575-5581.
14. Chapter 2 of this thesis.
15. Chapter 3 of this thesis.
16. Rault, J. and Le Huy, H.M., *J. Macromol. Sci., Phys.* **1996**, 35, p. 89-114.
17. Deschamps, A.A., Grijpma, D.W. and Feijen, J., *Polymer* **2001**, 42, p. 9335-9345.
18. Chapter 5 of this thesis.
19. Park, J.H. and Bae, Y.H., *J. Appl. Polym. Sci.* **2003**, 89, p. 1505-1514.
20. Park, J.H., Cho, Y.W., Kwon, I.C., Jeong, S.Y. and Bae, Y.H., *Biomaterials* **2002**, 23, p. 3991-4000.
21. Shibaya, M., Suzuki, Y., Doro, M., Ishihara, H., Yoshihara, N. and Enomoto, M., *J. Polym. Sci., Part B: Polym. Phys.* **2006**, 44, p. 573-583.
22. Miller, J.A., Lin, S.B., Hwang, K.K.S., Wu, K.S., Gibson, P.E. and Cooper, S.L., *Macromolecules* **1985**, 18, p. 32-44.
23. Harrell, L.L., *Macromolecules* **1969**, 2, p. 607-612.
24. Krijgsman, J. and Gaymans, R.J., *Polymer* **2004**, 45, p. 437-446.
25. Krijgsman, J., Husken, D. and Gaymans, R.J., *Polymer* **2003**, 44, p. 7573-7588.
26. Krijgsman, J., Husken, D. and Gaymans, R.J., *Polymer* **2003**, 44, p. 7043-7053.
27. Biemond, G.J.E., Ph.D. Thesis '*Hydrogen bonding in segmented block copolymers*', University of Twente, The Netherlands **2006**.
28. Van der Schuur, M. and Gaymans, R.J., *J. Polym. Sc., Part A: Polym. Chem.* **2006**, 44, p. 4769-4781.
29. Wunderlich, B., in *Thermal Analysis of Polymeric Materials*, Springer, Berlin Heidelberg New York **2005**.
30. Flory, P.J., *Trans. Faraday Soc.* **1955**, 51, p. 848.
31. Flory, P.J., in *Principles of polymer chemistry*, Cornell University Press, Ithaca **1967**.
32. Bailey, J.F.E. and Koleske, J.V., in *Poly(ethylene oxide)*, Acedemic Press, New York **1976**.
33. Van Krevelen, D.W., in *Properties of polymers*, Elsevier Science Publishers, New York **1990**.

Chapter 5

Water in polyether-based segmented block copolymers

Abstract

The segmented block copolymers described in this chapter are based on flexible polyether segments and monodisperse crystallisable tetra-amide segments (T6T6T). The polyether phase consists of hydrophilic poly(ethylene oxide) (PEO) and/or hydrophobic poly(tetramethylene oxide) (PTMO) segments. The influence of the soft phase composition of the copolymer on the water absorption was studied. The water absorption of the PEO-based copolymers depends on the PEO concentration. The number of water molecules per ethylene oxide unit (H_2O/EO) is determined by the crosslink density in the copolymer (i.e. the T6T6T concentration) and the presence of hydrophobic units (like PTMO or terephthalic units) in the PEO phase.

The effect of water on the physical properties of the copolymers was studied with DSC. A strong decrease in glass transition temperature of the soft phase is observed when the PEO-based copolymers are fully hydrated with water. This is due to the plasticizing effect of water on the PEO segments. The PEO melting temperature and crystallinity are strongly reduced when the copolymer absorbs water, while the PTMO phase remains unaffected by water. Freezing water is present in the PEO-based copolymer when the PEO phase contains approximately 30 vol% water. The amount of freezing water is almost independent of the PEO concentration, the PEO molecular weight and the presence of hydrophobic PTMO segments in the PEO phase.

The tensile properties of dry and hydrated PEO-based copolymers were evaluated. The hydrated copolymers have a lower E-modulus but a higher yield strain compared to dry copolymers. In an aqueous environment, the PEO melting temperature is strongly reduced and the strain-induced crystallisation of the polyether segments is lowered, resulting in a reduced fracture stress.

Introduction

The hydrophilicity and water vapour permeability of segmented block copolymers can be improved by using polar poly(ethylene oxide) (PEO) segments instead of hydrophobic flexible segments. Several PEO-based segmented block copolymers with ester [1-4], amide [5-7] or urethane(urea) [7-14] types of rigid segments have been reported. These hydrophilic PEO-based block copolymers can be used in many different application markets like textile, packaging, construction and gas separation.

PEO is completely soluble in water at room temperature, in contrast to other closely related polyethers, like poly(tetramethylene oxide) (PTMO) or poly(propylene oxide) (PPO). This can be explained by the strong interaction between water and PEO [15]. The high mobility of hydrated PEO segments present at a polymer surface and the large excluded volume will decrease the protein adsorption when contacting such a surface with a protein solution. Therefore, PEO-based block copolymers might also be interesting for biomedical applications.

The use of flexible PEO segments results in a strong increase in water absorption of the copolymer. An exponential increase of the water vapour sorption isotherm (volume fraction of water versus the water vapour activity) is usually observed for hydrophilic polymers, which can be explained by the formation of water clusters in the copolymer [16-19].

Water in hydrophilic polymers can be present in three states; bound water, freezing bound water and freezing water [20,21]. Water molecules can form hydrogen bonds with polar groups of the polymer. The mobility of these water molecules is restricted and, therefore, this water cannot crystallise and is known as bound water or non-freezing water. Freezing bound water, or interfacial water, is not directly bound to the polar groups of the polymer but forms hydration layers around the bound water molecules [22,23]. This freezing bound water can crystallise, but at a temperature below the crystallisation temperature of bulk water. Above a certain amount of (freezing) bound water, freezing water is observed and this water crystallises at the same temperature as bulk water.

It is known that absorbed water lowers the glass transition temperature of the polymer since water acts as plasticizer. Furthermore, water reduces the mechanical properties of the polymer, like the modulus and fracture stress [11,24-28]. The swelling of the polymer in water can be controlled by using mixtures of hydrophilic and hydrophobic polyether segments. Several segmented block copolymers with a mixture of flexible PEO/PTMO or PEO/PPO

segments and polyurethane(urea) rigid blocks have been reported [11-14,29,30]. These copolymers can be used to create an optimal hydrophilic-hydrophobic balance of the surface, which might be interesting for biomedical applications [31-35].

Polyurethane-based segmented block copolymers phase separate through liquid-liquid demixing, often followed by partial crystallisation of the rigid segments. Fast crystallising rigid segments, like polyesters and polyamides, usually phase separate by crystallisation. However, the crystallinity of these rigid segments in the copolymers is generally low. A large amount of non-crystallised rigid segments is present in the polyether matrix. The crystallisation of the rigid segments can be improved by using monodisperse segments [36,37]. Copolymers containing monodisperse rigid segments have a fast crystallisation and an almost complete phase separated polymer morphology. The polyether concentration in the copolymer can be high, up to 88 wt%, while the mechanical properties of the copolymer are still good [38,39].

Segmented block copolymers based on hydrophilic PEO and/or hydrophobic PTMO segments and monodisperse crystallisable tetra-amide segments (T6T6T) have been studied in this thesis. The influence of water on the physical and tensile properties of these copolymers will be discussed in this chapter. The physical properties like the glass transition temperature of the soft phase, the polyether melting temperature and the polyether crystallinity will be determined by DSC. Moreover, the state of water in the copolymers, i.e. bound or freezing water, will be determined.

Three different copolymer series will be studied, which vary in the PEO concentration, the hydrophobic concentration (PTMO or terephthalic units) and the T6T6T concentration. The first polymer series, denoted as PEO_x-T6T6T, is based on PEO flexible segments with varying PEO molecular weights (x) (600 to 4600 g/mol) [38]. The second series contains PEO segments that are extended with terephthalic units (T) to create long flexible polyether segments that will not phase separate by liquid-liquid demixing. These copolymers are denoted as $(PEO_x/T)_y$-T6T6T, where both the PEO molecular weight (x) as well as the total molecular weight of the flexible segments (y) are varied [39]. The third polymer series is based on a mixture of PEO and PTMO segments, denoted as $PEO_{2000}/PTMO_{2000}$-T6T6T, where the PEO/PTMO ratio is varied [40]. The dry and hydrated surface morphology of these PEO/PTMO-T6T6T copolymers will be investigated by AFM, to determine whether phase separation between the polyether segments occurs in an aqueous environment.

Experimental

PEO$_x$-T6T6T block copolymers. The PEO$_x$-T6T6T copolymers were synthesised by a polycondensation reaction using PEO segments with a molecular weight (x) of 600 – 4600 g/mol and T6T6T. See Chapter 2 of this thesis.

(PEO$_x$/T)$_y$-T6T6T block copolymers. These copolymers were synthesised by a polycondensation reaction using PEO segments that were extended with terephthalic units, and T6T6T. The PEO molecular weight (x) and the total molecular weight of the flexible segment (y) were varied. See Chapter 3 of this thesis.

PEO$_{2000}$/PTMO$_{2000}$-T6T6T block copolymers. These copolymers were synthesised by a polycondensation reaction using a mixture of PEO and PTMO flexible segments and T6T6T. Both polyether segments have a molecular weight of 2000 g/mol and the weight percentage ratio between PEO and PTMO was varied. See Chapter 4 of this thesis.

Water absorption (WA). The equilibrium water absorption was measured using pieces of injection-moulded polymer bars (70x9x2 mm). The samples were placed in a desiccator filled with demineralised water for four wks at room temperature. The water absorption was defined as the weight gain of the polymer according to;

$$Water\ absorption = \frac{m - m_0}{m_0} \times 100\% \quad [wt\%] \qquad \text{(Equation 5.1)}$$

where m_0 is the weight of dry sample and m the weight of the sample after conditioning to equilibrium. The measurements were performed in duplicate. After 4 wks the samples were dried and m_0 was measured again to exclude weight loss during the experiment. The volume fraction of water in the copolymer, denoted as φ_{water}, was determined by using a PEO, PTMO, DMT and T6T6T density of 1.13, 0.98, 1.20 and 1.32 g/cm^3 respectively [41].

Water vapour sorption isotherm. Water vapour sorption measurements were performed by determining the equilibrium water absorption of pieces of injection-moulded polymer bars at different relative humidities (RH), using desiccators filled with saturated salt solutions. Several different saturated salt solutions were used; KCl (85% RH), NaCl (75% RH), $Mg(NO_3)_2 \cdot 6H_2O$ (54% RH), KF (31% RH), LiCl (11% RH). The water absorption was determined after 4 wks at room temperature using Equation 5.1.

Differential scanning calorimetry (DSC). The thermal transitions of dry and hydrated copolymers were determined by DSC using a Pyris 1 (Perkin Elmer, USA). Small pieces of injection-moulded polymer bars (5 - 10 mg) were used. The samples were kept for 1 min at -100 ºC and subsequently heated from -100 to 80 °C at a heating rate of 10 °C/min. The heating scan was followed by a cooling scan from 80 to -100 °C at a rate of 10 °C/min and a subsequent second heating scan under the same conditions. The glass transition temperature was taken as the midpoint of the heat capacity change of the first heating scan. In the case of completely hydrated polymers, the samples were placed in demineralised water for 1 d to reach an equilibrium state of water absorption. The excess of water was gently removed using an absorbing tissue.

Tensile test. Samples for the tensile test were prepared by melt spinning the dried polymer into threads on a (4cc DSM res RD11H-1009025-4) co-rotating twin screw mini extruder. The extruder was set approximately 40 ºC above the flow temperature and the screw speed was 30 rpm. The titer of the threads (expressed in tex = 10^{-6} kg/m) was calculated assuming a polymer density of 1.0 g/cm^3. Tensile tests on threads were carried out on a Zwick Z020 universal tensile machine equipped with a 10 N load cell. The strain was measured by clamp displacement. Standard stress-strain curves were obtained at a strain rate of 250 mm/min with a starting clamp

distance of 25 mm. The test was preformed in 5-fold. Tensile tests were also performed on hydrated polymers threads. The threads were placed in demineralised water for 1 d to reach an equilibrium state of water absorption.

Atomic Force Microscopy (AFM). AFM measurements were performed on a Bioscope AFM and Nanoscope IV controller. The AFM height images were recorded in tapping mode. The operating set point value (A/A_0) was 0.6 – 0.7 and the scan size was 1 µm. Solvent-cast samples of ~15 µm were prepared from a 4 wt% solution in TFA. The AFM measurements were first performed on dry samples using a TESP cantilever (k ~ 40 N/m). Subsequently, a drop of demineralised water was placed on the film and the measurements were performed using a DNP cantilever (k ~ 0.58 N/m).

Results and discussion

PEO-based segmented block copolymers

The water absorption of two different PEO-based copolymer series, the PEO_x-T6T6T and $(PEO_x/T)_y$-T6T6T series, is discussed in this section. In Table 5.1 the compositions and water absorptions of both types of copolymers are given. Since the T6T6T crystallinity in all the copolymers is high (~85%) and crystalline nylon does not absorb water [42], it is assumed that water is only absorbed in the PEO phase of the copolymers.

Table 5.1: Water absorption (WA) of PEO_x-T6T6T and $(PEO_x/T)_y$-T6T6T copolymers.

x or *y* [g/mol]	Conc. T6T6T [wt%]	Conc. PEO [wt%]	Conc. T [wt%]	WA [wt%]	H_2O/EO [-]	φ_{water} [vol%]
PEO_x-T6T6T						
600	51.0	49.0	-	18	0.9	18
1000	38.4	61.6	-	35	1.4	30
1500	29.4	70.6	-	69	2.4	45
2000	23.8	76.2	-	91	2.9	51
3400	15.5	84.5	-	127	3.7	59
4600	11.9	88.1	-	170	4.7	66
$(PEO_{300}/T)_y$-T6T6T						
2500	19.9	58.4	21.7	14	0.6	14
$(PEO_{600}/T)_y$-T6T6T						
600	51.0	49.0	-	18	0.9	18
1250	33.3	60.4	6.3	30	1.2	26
2500	20.0	69.0	11.0	49	1.7	36
5000	11.1	74.8	14.1	66	2.2	43
10000	5.9	78.1	16.0	75	2.3	46

In Figure 5.1 the water absorption and volume fraction of water (φ_{water}) of PEO_x-T6T6T and $(PEO_x/T)_y$-T6T6T copolymers are given as a function of the PEO concentration.

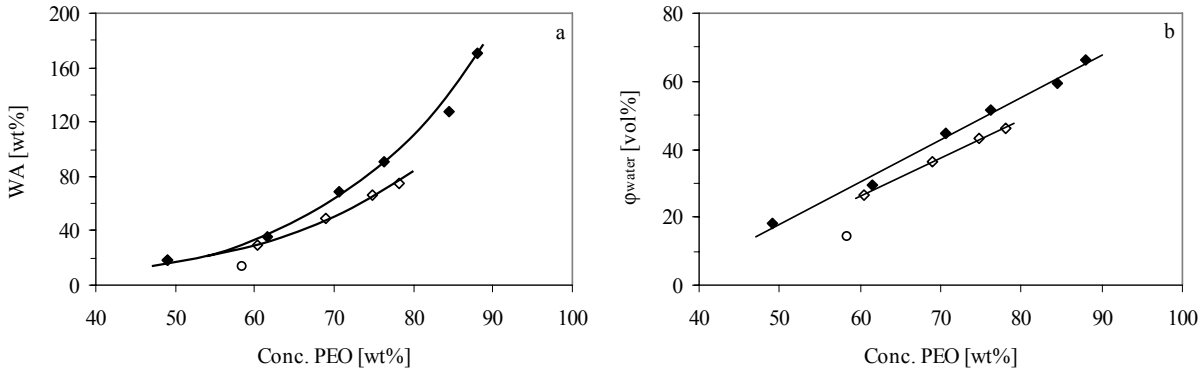

Figure 5.1: (a) Equilibrium water absorption (WA) and (b) volume fraction of water (φ_{water}) as a function of PEO concentration: ♦, PEO_x-T6T6T; ◊, $(PEO_{600}/T)_y$-T6T6T; ○, $(PEO_{300}/T)_{2500}$-T6T6T.

A strong increase in water absorption as a function of PEO content is found for PEO_x-T6T6T and $(PEO_x/T)_y$-T6T6T copolymers. This strong increase in water absorption with PEO content can be explained by an increase in the physical crosslink density (T6T6T concentration), which limits the swelling of the amorphous regions. Slightly lower water absorptions are observed for copolymers with terephthalic extended PEO segments, indicating that the presence of terephthalic units in the amorphous phase reduces the water absorption. This reduction in water absorption is stronger when copolymers contain a higher concentration of terephthalic units. The water absorption can also be given as volume fraction of water (φ_{water}) in the copolymer. A linear increase in φ_{water} is observed for both PEO_x-T6T6T and $(PEO_x/T)_y$-T6T6T copolymers when the PEO concentration is above approximately 50 wt%.

In Figure 5.2 the number of water molecules per ethylene oxide unit (H_2O/EO) is given as a function of the T6T6T concentration. The H_2O/EO ratio was calculated using the PEO and water concentration (Table 5.1). The H_2O/EO ratios of both copolymer series decrease with increasing T6T6T concentration. When hydrophobic terephthalic units are present in the PEO phase the H_2O/EO ratio is even more reduced. This indicates that the H_2O/EO ratio is influenced by the T6T6T concentration and the presence of hydrophobic terephthalic units in the PEO phase.

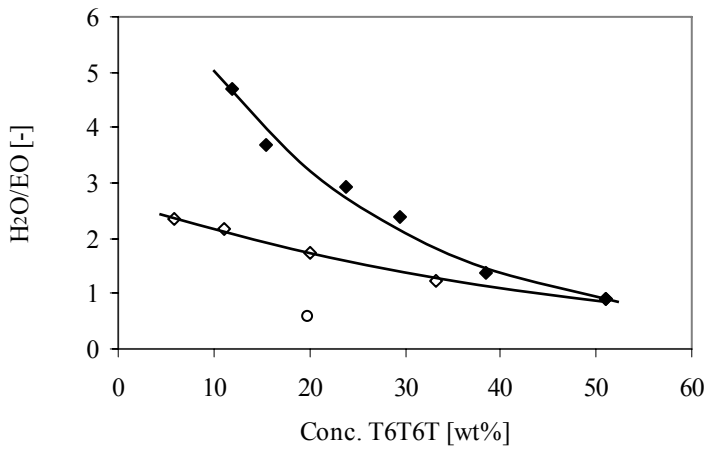

Figure 5.2: Number of water molecules per ethylene oxide unit (H_2O/EO) as a function of T6T6T concentration: ♦, PEO_x-T6T6T; ◊, $(PEO_{600}/T)_y$-T6T6T; ○, $(PEO_{300}/T)_{2500}$-T6T6T.

Sorption isotherm

The water vapour sorption isotherms (volume fraction of water versus the water vapour activity) of PEO_x-T6T6T copolymers at room temperature are given in Figure 5.3.

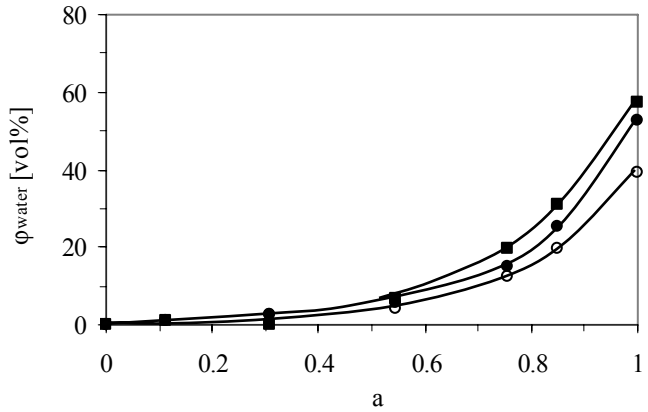

Figure 5.3: Equilibrium water sorption isotherms of PEO_x-T6T6T copolymers with different PEO segment lengths (x): ○, x = 1000; ●, x = 1500; ■, x = 2000.

An exponential increase in volume fraction of water with increasing water vapour activity is observed for the PEO_x-T6T6T copolymers. Comparable convex sorption isotherms were observed for PEO-based block copolymers containing polyester [2,43] or polyurethane [29,44-47] rigid segments. This exponential increase in volume fraction of water is often explained by the formation of water clusters in the copolymer.

Effect of water on PEO phase transitions

Water in polymers acts as a plasticizer and depresses the glass transition temperature of the system [48-50]. The glass transition temperatures of dry and completely hydrated PEO_x-T6T6T copolymers were measured with DSC (10 ºC/min) and the results are given in Table 5.2.

Table 5.2: Thermal properties of dry and hydrated PEO_x-T6T6T copolymers.

			dry			*hydrated*		
PEO (*x*) [g/mol]	Conc. PEO [wt%]	WA [wt%]	T_g [ºC]	T_m PEO [ºC]	ΔH_m PEO [J/g]	T_g [ºC]	T_m PEO [ºC]	ΔH_m PEO [J/g]
600	49.0	18	-42	-	-	-58	-	-
1000	61.6	35	-54	-	-	-69	-	-
1500	70.6	69	-57	-8	31	-70	-52	18
2000	76.2	91	-53	14	40	-70	-39	31
3400	84.5	127	-55	32	62	-73	-28	n.d.
4600	88.1	170	-51	44	84	-72	-18	n.d.

In Figure 5.4 the glass transition temperatures of dry and hydrated PEO_x-T6T6T copolymers are given as a function of the PEO segment length. The relatively high T_g of PEO_{600}-T6T6T can be explained by the high physical crosslink density in the copolymer. The T_g values of the copolymers with a PEO segment length of 1000 g/mol or higher are more or less constant. The T_g values shift to lower temperatures when the copolymers absorb water. This phenomenon is due to the plasticizing effect of water on the PEO segments. The difference in T_g between dry and wet copolymer is almost independent of the PEO length, despite that longer PEO segments absorb more water.

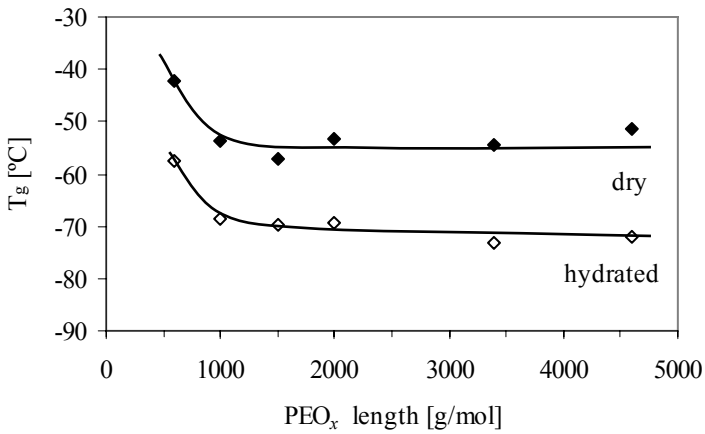

Figure 5.4: Glass transition temperature as a function of the PEO length (x) of PEO_x-T6T6T copolymers (♦, dry; ◊, hydrated).

Generally, the depression in glass transition temperature by the presence of a small molecule, in this case water, can be predicted by the Fox-Flory relationship [41]. However, the Fox-Flory equation can only be used for systems that are homogenously mixed. In the case of PEO_x-T6T6T copolymers it is assumed that the water molecules are present in the form of clusters, indicating that there is no homogenous mixture of PEO and water.

According to the results described in Chapter 2 of this thesis, an increase in PEO segment length results in an increased PEO melting temperature. The effect of the water in the copolymer on the PEO melting temperature and crystallinity is studied with DSC. In Table 5.2 the thermal properties of the PEO phase of dry and fully hydrated PEO_x-T6T6T copolymers are given. An increase in the PEO segment length from 1500 to 4600 g/mol results in an increase in the PEO melting temperature and enthalpy of the dry copolymer, indicating an increase in PEO crystallinity. When the copolymers are fully hydrated with water, the PEO melting temperature and enthalpy are strongly reduced. The melting point depression by the presence of a small molecule, in this case water, can be described by the Flory solvent theory [18,51].

Water present in a polymer, showing a melting and crystallisation temperature corresponding to pure water, is known as freezing water. For comparison, DSC results of pure demineralised water, recorded with a rate of 10 ºC/min, show a melting and crystallisation peak at approximately 3 and -20 ºC respectively (Figure 5.5).

The second heating scans of PEO_{4600}-T6T6T, containing different volume fractions of water, are given in Figure 5.5. Dry PEO_{4600}-T6T6T shows a PEO melting peak at approximately 44 ºC. With increasing water content the PEO melting temperature decreases. When the copolymer contains a water content of ~32 vol%, a small melting peak of freezing water is observed at approximately 3 ºC (see enlargement Figure 5.5). With a further increase of the water content in the copolymer, the amount of freezing water increases strongly. The fully hydrated PEO_{4600}-T6T6T copolymer contains 66 vol% water and shows two melting peaks of freezing water close to each other. This might be explained by an extra crystalline transition of water present in the copolymer [15,23,50,52-54]. Freezing bound water, which should give a melting peak below freezing water, was not observed in these copolymers.

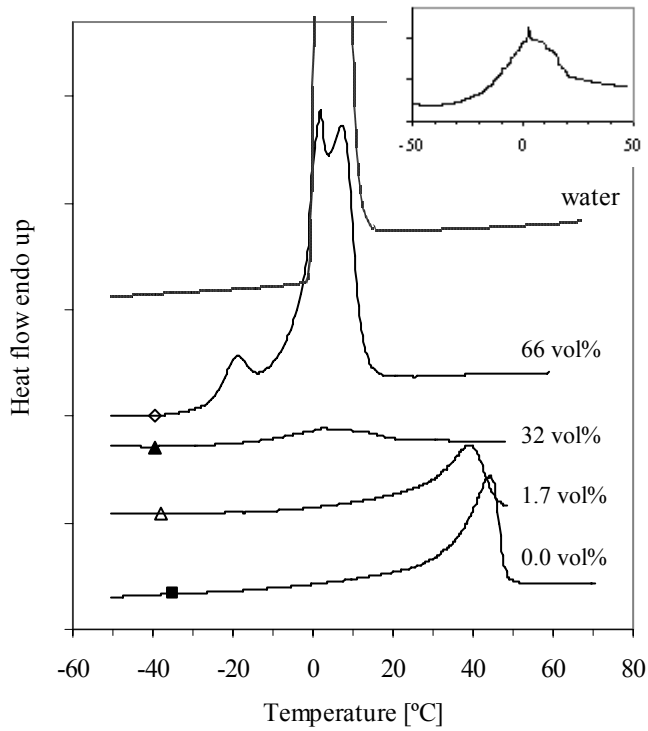

Figure 5.5: DSC second heating scans of PEO_{4600}-T6T6T containing different volume fractions of water: ■, 0 vol%; Δ, 1.7 vol%; ▲, 32 vol%; ◊, 66 vol%, (dotted line represents pure water). Enlargement of 32 vol% in right upper corner.

The phase transitions of PEO_{4600}-T6T6T and PEO_{2000}-T6T6T copolymers containing different volume fractions of water are reported in Table 5.3. In Figure 5.6 the glass transition temperatures and PEO melting temperatures of both copolymers as a function of the volume fraction of water are given.

Table 5.3: DSC results of PEO_{2000}-T6T6T and PEO_{4600}-T6T6T copolymers at different water vapour activities (a).

	PEO_{2000}-T6T6T					*PEO_{4600}-T6T6T*				
a	φ_{water} [vol%]	T_g [ºC]	T_m PEO [ºC]	ΔH_m PEO [J/g PEO]	T_m water [ºC]	φ_{water} [vol%]	T_g [ºC]	T_m PEO [ºC]	ΔH_m PEO [J/g PEO]	T_m water [ºC]
0.00	0.0	-53	14	40	-	0.0	-51	44	84	-
0.31	4.5	-56	7	31	-	1.7	-54	43	58	-
0.54	5.2	-57	8	31	-	2.8	-56	39	69	-
0.85	26	-67	-20	9	-	32	-66	5	n.d.[1]	~3
1.00	51	-70	-39	12	~3	66	-72	-18	n.d.[1]	~3

[1] *could not be determined*

Dry PEO_{4600}-T6T6T and PEO_{2000}-T6T6T copolymers have a PEO melting temperature of 44 and 14 ºC respectively. The dry PEO_{4600}-T6T6T copolymer has a higher PEO melting temperature and enthalpy than PEO_{2000}-T6T6T since PEO_{4600} is more crystalline than PEO_{2000}. The PEO melting temperatures of both copolymers decrease with increasing volume fraction of water. Also the PEO melting enthalpies are reduced when the copolymers absorb water, suggesting that the PEO crystallinity is decreased. The water absorption of PEO_{4600}-T6T6T at low activities ($a \leq 0.54$) is restricted by the presence of a semi-crystalline PEO phase at room temperature. This explains why PEO_{4600}-T6T6T has a lower water absorption than PEO_{2000}-T6T6T at an activity of 0.54.

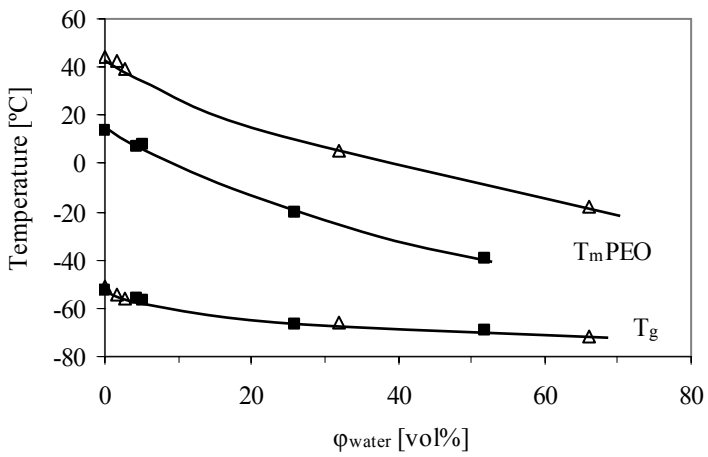

Figure 5.6: Phase transitions of (■) PEO_{2000}-T6T6T and (Δ) PEO_{4600}-T6T6T copolymers as a function of the volume fraction of water.

The glass transition temperatures of PEO_{2000}-T6T6T and PEO_{4600}-T6T6T copolymers are reduced with increasing volume fraction of water absorbed. Similar T_g values are observed for both copolymers, indicating than the amount of water present in the copolymer has an influence on the decrease in T_g. With increasing water content the reduction in T_g is less strong compared to the reduction in PEO melting temperature. This indicates that with increasing amount of water absorbed in the copolymer the T_g/T_m ratio increases from 0.77 to 0.81 for PEO_{2000}-T6T6T and from 0.70 to 0.79 for PEO_{4600}-T6T6T. Usually, a higher T_g/T_m ratio results in a reduced crystallisation rate and crystallinity [41] and this might explain a lowering of the PEO crystallinity with increasing water content. Another reason might be that PEO and water mix exothermically and thereby lowering the melting enthalpy [15].

Since the PEO and freezing water melting peaks overlap partly, the cooling scan was used to determine the crystallisation enthalpy of freezing water. Pure demineralised water shows a crystallisation peak at approximately -20 ºC as determined by DSC at a cooling rate of 10 ºC/min. All PEO_x-T6T6T copolymers show a crystallisation peak at approximately -20 ºC, corresponding to freezing water. An extra crystallisation peak is observed for PEO_x-T6T6T copolymers with a PEO segment length above 1000 g/mol, located at a temperature close to the crystallisation temperature of freezing water. This can be explained by an extra crystalline transition of water present in the copolymer [15,23,50,52-54].

The fully hydrated PEO_{600}-T6T6T copolymer contains approximately 18 vol% water (H_2O/EO ratio of 1.0) and shows a crystallisation peak of freezing water. PEO_{2000}-T6T6T contains approximately 26 vol% at a water vapour activity of 0.85 shows no crystallisation peak of freezing water. This copolymer has a H_2O/EO ratio of 0.9. This indicates that copolymers contain freezing water when the H_2O/EO ratio is above 0.9, i.e. when the PEO phase contains more than 30 vol% water.

The percentage of freezing water (w_f) in PEO-based copolymers can be calculated using Equation 5.2.

$$w_f = \frac{\Delta H}{\Delta H_w} \times 100\% \qquad [\%] \qquad \text{(Equation 5.2)}$$

where ΔH is the measured crystallisation enthalpy of water in a fully hydrated copolymer and ΔH_w the heat of fusion of pure water (334 J/g). It is assumed that no freezing bound water is present. The amount of bound water (w_b) can be calculated by subtracting w_f from the total water absorption. The number of bound water molecules per ethylene oxide repeating unit (H_2O/EO bound) can be calculated by using Equation 5.3 [22].

$$H_2O / EO\ bound = \frac{(w_b \times \varphi_{water})}{18} \times \frac{44}{\varphi_{PEO}} \qquad [-] \qquad \text{(Equation 5.3)}$$

where φ_{water} and φ_{PEO} are the weight fraction of water and PEO in the copolymer respectively. The amounts of freezing and bound water as well as the number of (bound) water molecules per EO unit are given in Table 5.4.

Table 5.4: DSC results of fully hydrated PEO_x-T6T6T copolymers (water vapour activity of 1).

PEO length (x) [g/mol]	WA [wt%]	φ_{water} [wt%]	φ_{water} [vol%]	ΔH_c [J/g]	w_f [%]	w_b [%]	H_2O/EO bound [-]	H_2O/EO [-]
600	18	15	18	13	26	74	0.7	0.9
1000	35	26	30	21	24	76	1.1	1.4
1500	69	41	45	25	18	82	2.0	2.4
2000	91	48	51	27	17	83	2.4	2.9
3400	127	56	59	-[1]	-	-	-	3.7
4600	170	63	66	-[1]	-	-	-	4.7

[1] *could not be determined*

The crystallisation enthalpies of water in fully hydrated PEO_x-T6T6T copolymers increase with increasing PEO segment length and thus with increasing volume fraction of water. By using Equation 5.2 the amount of freezing water was calculated. The PEO_x-T6T6T copolymers show a small decrease in freezing water percentage with increasing PEO length. This is not expected as the WA increases with PEO segment length and thus PEO concentration. The amount of freezing water in the PEO_x-T6T6T copolymers is between 17 to 26% of the total concentration of water absorbed by the copolymer.

The crystallisation enthalpy of freezing water for the PEO_{3400}-T6T6T and PEO_{4600}-T6T6T copolymers could not be determined as the crystallisation peak of freezing water overlaps with the crystallisation peak of PEO.

Stress-strain behaviour

The tensile properties of the PEO-T6T6T segmented copolymers are determined by stress-strain measurements. At small deformation the stress increases linearly with the strain. Above the yield point the stress gradually increases. At higher strains, above 300%, strain-induced crystallisation of the polyether segments can take place, which results in a higher fracture stress [55]

The PEO-T6T6T copolymers have a semi-crystalline PEO phase when the PEO length is 1000 g/mol or longer [38]. Water reduces the melting temperature of PEO and strain-induced crystallisation of the PEO segments will become more difficult. To study the influence of water on the tensile properties of PEO-T6T6T copolymers, strain-induced crystallisation of the PEO segments must be restricted to exclude other effect besides water. Therefore, the tensile tests were performed on $(PEO_{600}/T)_y$-T6T6T copolymers, where the PEO_{600} segments

are extended with terephthalic units to a desired flexible segment length (y) [39]. The PEO melting temperature and crystallinity of these copolymers are partly suppressed. The $(PEO_{600}/T)_y$-T6T6T copolymers contain an amorphous PEO phase at room temperature and, therefore, the change in tensile properties is likely mainly due to a change in T6T6T concentration and amount of water absorbed by the copolymer.

For applications in an aqueous environment, it is necessary to maintain good mechanical properties of the polymer. Therefore, the stress-strain behaviour is determined for both dry and fully hydrated $(PEO_{600}/T)_y$-T6T6T copolymers. The tensile properties of the copolymers are given in Table 5.5.

Table 5.5: Tensile properties of dry and hydrated $(PEO_{600}/T)_y$-T6T6T copolymers.

y [g/mol]	WA [wt%]	Conc. T6T6T [wt%]	η_{inh} [dL/g]	E [MPa]	σ_y [1] [MPa]	ε_y [1] [%]	σ_f [MPa]	ε_f [%]	σ_{true} [2] [MPa]
600	0	51.0	1.4	263	15.5	17	32	490	189
	18	43.2		216	16.8	16	36	520	223
1250	0	33.3	1.6	233	10.8	13	27	710	219
	30	25.6		130	8.7	21	26	780	229
2500	0	20.0	1.7	81	5.9	24	19	1080	224
	49	13.4		22	4.2	40	9.6	650	72
5000	0	11.0	1.4	66	3.2	35	7.7	900	77
	66	6.6		9	2.4	63	2.6	90	26
10,000	0	5.9	1.5	21	1.5	38	2.1	100	4
	75	3.4		-	-	-	-	-	-

[1] *Yield stress and strain were determined using the Considère method* [56]

[2] *True fracture stress (σ_{true}) was calculated by $\sigma_f \times (1 + (\varepsilon_f /100))$*

The tensile behaviour of segmented block copolymers at small strains is characterised by the initial E-modulus. The E-modulus is related to the storage modulus (G') according to Equation 5.4.

$$G' = \frac{E}{2}(1+\nu) \qquad \text{(Equation 5.4)}$$

where υ is the Poisson constant. In the case of an ideal elastomer, the Poisson constant equals 0.5 and thus $G' = 3E$. The E- and G'-modulus as a function of T6T6T content of dry

$(PEO_{600}/T)_y$-T6T6T copolymers are given in Figure 5.7. Most copolymers show a ratio of approximately *G' = 3E*.

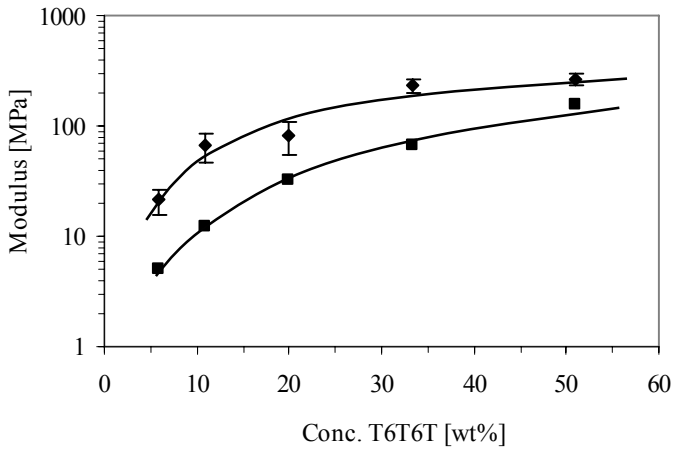

Figure 5.7: The (♦) E-modulus and (■) storage modulus (G') of dry $(PEO_{600}/T)_y$-T6T6T copolymers as a function of T6T6T content.

The E-modulus depends on the modulus of the soft phase, the physical network density and the reinforcement of the amorphous matrix by the crystallites [57]. The reinforcement of the crystallites depends on the crystalline content, the aspect ratio of the crystals and the stiffness of the crystals. In Figure 5.8 the E-moduli of dry and hydrated $(PEO_{600}/T)_y$-T6T6T copolymers are given as a function of the T6T6T concentration.

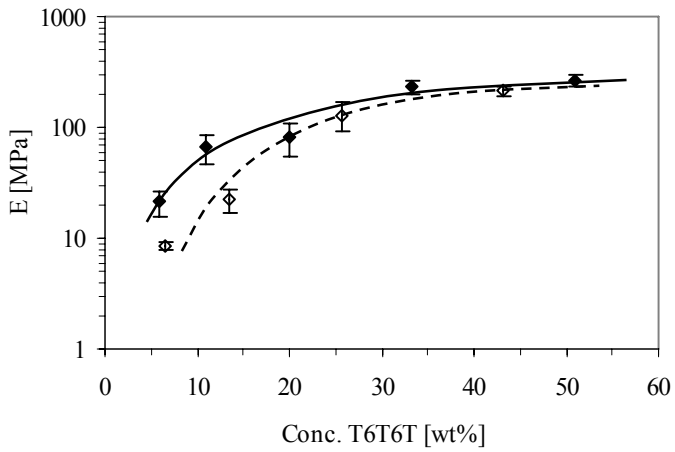

Figure 5.8: E-modulus of $(PEO_{600}/T)_y$-T6T6T copolymers as a function of the actual T6T6T content: ♦, dry copolymers; ◊, hydrated copolymers.

By increasing the T6T6T content of dry and hydrated $(PEO_{600}/T)_y$-T6T6T copolymers the modulus increases. The actual T6T6T content in hydrated copolymers is calculated by

correcting for the dilution of the polymer in water. Above a T6T6T content of approximately 20 wt% there is hardly any difference in E-modulus between dry and hydrated copolymers. Below this concentration, the hydrated copolymers have a lower E-modulus compared to that of dry copolymers. It is assumed that the crystalline T6T6T phase is not affected by water. Most likely, the modulus of the polyether phase is lowered when water is present.

The yield point of segmented block copolymer is usually the beginning of breaking up the crystalline structure. Before the yield point the deformation is mainly elastic. In semi-crystalline polymers the yield stress is determined by the crystallinity in the copolymer and, therefore, depends mainly on the T6T6T content. The yield stress of segmented block copolymers is linearly related to rigid segment concentration [58,59]. In Figure 5.9a the fracture stress and yield stress of the copolymers are given as a function of the T6T6T concentration and in Figure 5.9b the yield strain of the copolymers is given as a function of the T6T6T content.

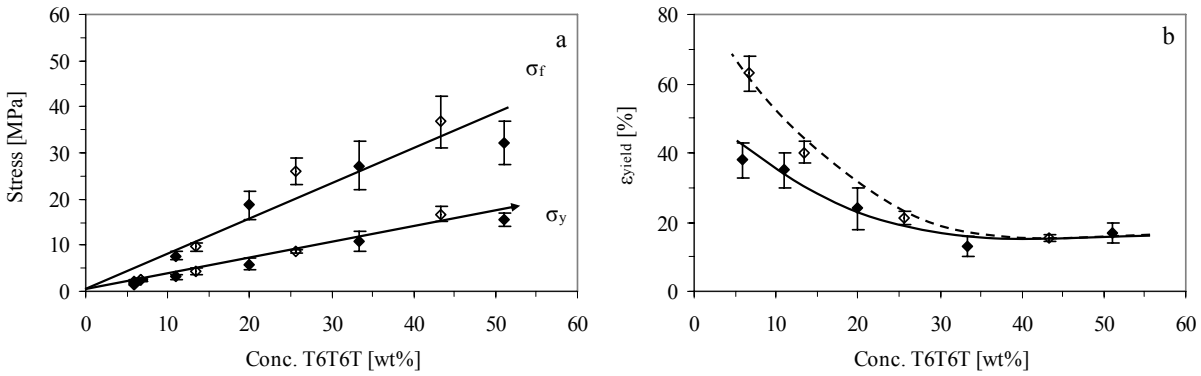

Figure 5.9: (a) Fracture and yield stress and (b) yield strain as a function of the actual T6T6T content for $(PEO_{600}/T)_y$-T6T6T copolymers: ♦, dry copolymers; ◊, hydrated copolymers.

A linear increase in yield stress with actual T6T6T concentration is observed for dry and hydrated $(PEO_{600}/T)_y$-T6T6T copolymers and there is no difference between both copolymers. The fracture stress is higher than the yield stress, indicating that some strain-induced crystallisation of the polyether segments has taken place. The fracture properties of segmented block copolymers depend strongly on whether strain-induced crystallisation of the flexible segments can take place. When strain-induced crystallisation is taken place the polyether crystallinity and the melting temperature increase.

The yield strain increases with decreasing T6T6T content. The hydrated copolymers show a higher yield strain than the corresponding dry copolymers. This can be explained by the

plasticizing effect of water on the PEO segments. Due to the presence of water, the crystalline content decreases and the amorphous PEO chains become more mobile. As a result, the modulus is lower but the yield strain higher.

A linear increase in true fracture stress with inherent viscosity is observed for PTMO-T6T6T copolymers [59]. These copolymers have a high molecular weight and showed strain-induced crystallisation of the PTMO segments. Strain-induced crystallisation is taking place above 300% strain and is influenced by the type of polyether segment and the molecular weight of the copolymer. When the flexible segment cannot crystallise and strain-induced crystallisation is absent, the fracture stress is directly related to the rigid segment content.

The inherent viscosity of the $(PEO_{600}/T)_y$-T6T6T copolymers varies within a small range from 1.4 to 1.7 dL/g, indicating that the difference in fracture stress between the copolymers cannot be explained by the molecular weight. The increase in fracture stress with increasing T6T6T content is similar for both dry and hydrated $(PEO_{600}/T)_y$-T6T6T copolymers (Figure 5.9a). This indicates that the fracture stress depends on both the T6T6T content and strain-induced crystallisation of polyether segments. The fracture strains of all $(PEO_{600}/T)_y$-T6T6T copolymers are high except the copolymer with a low T6T6T content (<6.6 wt%). A reason for this is as yet not clear.

Segmented block copolymer with mixed polyether segments

Segmented block copolymers based on mixed hydrophilic PEO_{2000} and hydrophobic $PTMO_{2000}$ segments and monodisperse T6T6T segments were synthesised. The compositions of the copolymers in this series are given in Table 5.6.

Table 5.6: Polymer composition and water absorption of $PEO_{2000}/PTMO_{2000}$-T6T6T copolymers.

Ratio PEO/PTMO	Conc. PEO [wt%]	Conc. PTMO [wt%]	Conc. T6T6T [wt%]	WA [wt%]	φ_{water} [vol%]	H_2O/EO [-]
0/100	0.0	76.2	23.8	1.2	1.2	-
20/80	15.2	61.0	23.8	9.8	10	1.6
40/60	30.5	45.7	23.8	24	22	1.9
50/50	38.1	38.1	23.8	33	28	2.1
60/40	45.7	30.5	23.8	42	33	2.3
80/20	61.0	15.2	23.8	60	41	2.4
100/0	76.2	0.0	23.8	91	51	2.9

The synthesis and thermal mechanical properties of these copolymers are described in Chapter 4. The PEO/PTMO ratio was altered while the T6T6T concentration remained constant (23.8 wt%). Copolymers with PEO/PTMO ratios of 0/100 and 100/0 are also denoted as $PTMO_{2000}$-T6T6T and PEO_{2000}-T6T6T respectively.

Previous results revealed that the H_2O/EO ratio is determined by the crosslink density in the copolymer and the presence of hydrophobic units in the PEO phase. In Figure 5.10 the water absorption (WA) and volume fraction of water (φ_{water}) of the $PEO_{2000}/PTMO_{2000}$-T6T6T copolymers are given as a function of the PEO/PTMO ratio.

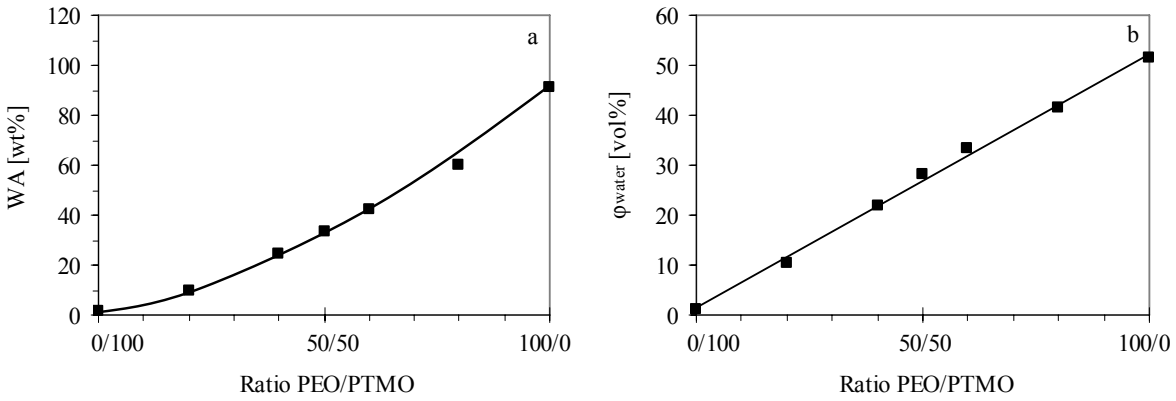

Figure 5.10: (a) Water absorption and (b) volume fraction of water of $PEO_{2000}/PTMO_{2000}$-T6T6T copolymers as a function of the PEO/PTMO ratio.

An increase in WA of the copolymers is observed with increasing PEO/PTMO ratio. When φ_{water} is given as a function of the PEO/PTMO ratio, a linear relation is observed. The T6T6T concentration has no influence on this relation as it is similar for all copolymers in this series. The H_2O/EO ratio increases from 1.6 to 2.9 with increasing PEO/PTMO ratio (Table 5.6), indicating that the presence of hydrophobic PTMO units decreases the amount of water per EO unit. When there is no interaction between the PEO and PTMO the number of water molecules per EO unit would have given a constant value.

To examine whether the PEO and PTMO segments in the copolymers are phase separated or form one homogeneous mixed polyether phase in an aqueous environment, the AFM technique is used. The surface morphology of dry and fully hydrated PEO/PTMO-T6T6T copolymers is studied with AFM tapping mode. The AFM height images of $PEO_{2000}/PTMO_{2000}$-T6T6T (20/80) are recorded on a 1x1 μm scale and are given in three-dimensional (Figure 5.11).

The surface of the dry copolymer is not completely smooth but no separate phases can be distinguished. The surface of the hydrated copolymer shows some irregularities. It is clearly visible that the hydrated polymer sample swells inhomogeneously and there are clusters formed with a height of 10 – 50 nm and width of ~100 nm. Probably, these clusters consist of a swollen PEO segments. However, the dimensions of the clusters are relatively large compared to the PEO_{2000} segments used.

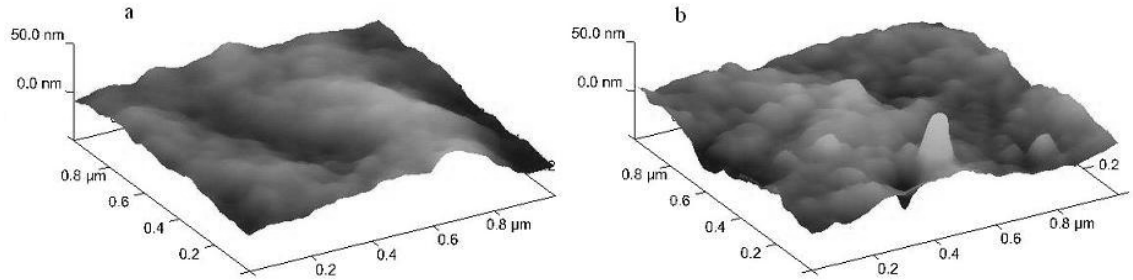

Figure 5.11: AFM height image (3D) of PEO_{2000}/$PTMO_{2000}$-T6T6T (20/80) at 1x1 µm: left, dry copolymer; right, hydrated copolymer.

Effect of water on polyether transitions

Previous results show that water in PEO-T6T6T segmented block copolymers acts as a plasticizer and depresses the T_g of the polymer. Furthermore, the PEO melting temperature and crystallinity were reduced when the copolymer absorbs water. The influence of water on the phase transitions of copolymers with mixed PEO and PTMO segments was studied with DSC and the results are given in Table 5.7.

Table 5.7: DSC results of dry and hydrated PEO_{2000}/$PTMO_{2000}$-T6T6T copolymers on heating (10 ºC/min).

Ratio PEO/PTMO	φ_{water} [vol%]	*dry* T_g [ºC]	*dry* T_m ether [ºC]	*dry* ΔH_m ether [J/g]	*hydrated* T_g [ºC]	*hydrated* T_m ether [ºC]	*hydrated* ΔH_c[1] ether [J/g]	*hydrated* T_m water [ºC]	*hydrated* ΔH_c[1] water [J/g]
0/100	1.2	-73	-2	20	-76	-2	20	-	-
20/80	10	-68	-4	16	-72	-4	14	1	4
40/60	22	-64	-3	17	-69	2	<1	2	12
50/50	28	-65	0	21	-71	- [2]	- [2]	6	14
60/40	33	-60	1	21	-73	- [2]	- [2]	3	19
80/20	41	-56	8	25	-71	- [2]	- [2]	6	21
100/0	51	-53	14	40	-70	- [2]	- [2]	6	27

[1] *Determined using the DSC cooling scan*
[2] *could not be determined*

In Figure 5.12 the glass transition temperatures of dry and hydrated $PEO_{2000}/PTMO_{2000}$-T6T6T copolymers are given as a function of the PEO/PTMO ratio.

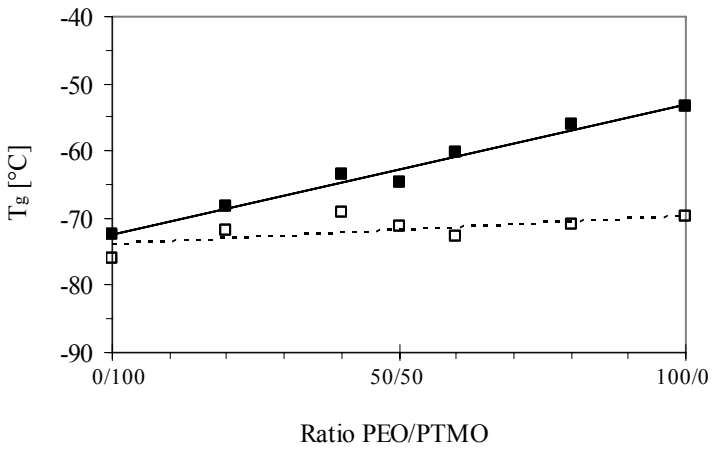

Figure 5.12: Glass transition temperature of $PEO_{2000}/PTMO_{2000}$-T6T6T copolymers as a function of the ratio PEO/PTMO: ■, dry copolymers; □, hydrated copolymers.

In dry conditions, one T_g is observed for the copolymers, which increases linearly with PEO/PTMO ratio. This linear relation suggests that PEO and PTMO form a homogenous mixed polyether phase. The difference between dry $PTMO_{2000}$-T6T6T and dry PEO_{2000}-T6T6T is due to a higher T_g of the PEO prepolymers (-72 to -65 ºC) [60] compared to the PTMO prepolymers (-86 ºC) [41].

The T_g of hydrated PTMO-T6T6T is only slightly lower compared to dry PTMO-T6T6T, while that of hydrated PEO-T6T6T is strongly lowered (~17 ºC). Hydrated PEO/PTMO-T6T6T copolymers show also a linear increase in T_g with increasing PEO/PTMO ratio. However, this increase in T_g is less strong than that of dry copolymers. The T_g is stronger reduced when the polymer absorbs more water, which is the case for copolymers with a higher PEO/PTMO ratio. Since the T_g of hydrated PTMO-T6T6T and PEO-T6T6T copolymers are close together no conclusions concerning the structure of the polyether phase can be drawn. The AFM images of hydrated PEO/PTMO-T6T6T copolymers indicate that inhomogeneous swelling has taken place in water, which suggests that two different polyether phases are present.

The influence of water on the melting temperature and crystallinity of the polyether phase of PEO/PTMO-T6T6T copolymers is determined by using DSC. Furthermore, the state of water present in the copolymer is determined and the amount of freezing and bound water was

calculated. In Figure 5.13 the DSC heating and cooling scans of fully hydrated PEO/PTMO-T6T6T copolymers are given. Pure demineralised water gives a melting peak and crystallisation peak at approximately 3 and -20 ºC respectively (Figure 5.5).

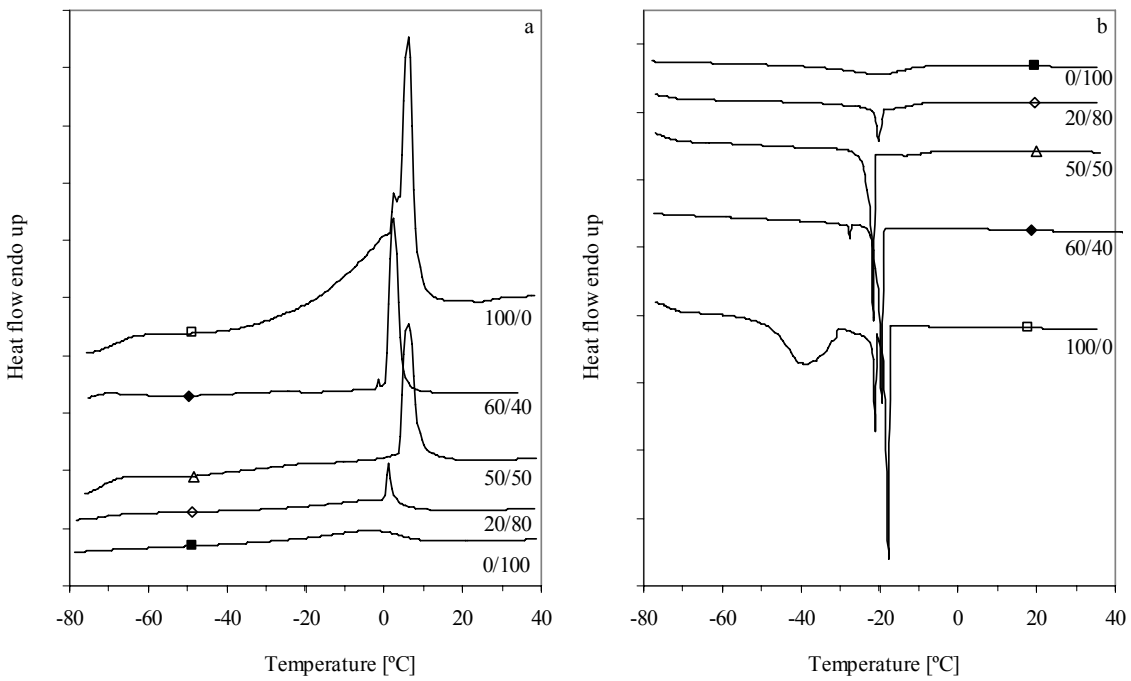

Figure 5.13: DSC (a) heating and (b) cooling scans (10 ºC/min) of $PEO_{2000}/PTMO_{2000}$-T6T6T copolymers with different PEO/PTMO ratios: □, 100/0; ♦, 60/40; Δ, 50/50; ◊, 20/80; ■, 0/100.

In the DSC heating scan, all $PEO_{2000}/PTMO_{2000}$-T6T6T copolymers, with the exception of $PTMO_{2000}$-T6T6T, show a sharp melting peak at approximately 3 ºC. This peak corresponds to freezing water. Freezing bound water, which should give a melting peak below freezing water, was not observed in these copolymers. The melting enthalpy of freezing water in the copolymers increases with increasing PEO/PTMO ratio. The hydrated PTMO-T6T6T copolymer shows no freezing water but a broad polyether melting peak at approximately -2 ºC. When low amount of PEO are introduced in the copolymer, the polyether melting temperature remains unaffected but the melting enthalpy decreases (Table 5.7). At higher PEO/PTMO ratios, it becomes impossible to distinguish a polyether melting temperature since this peaks overlaps with the melting peak of freezing water.

The DSC cooling scans of copolymers with a high PEO/PTMO ratio give a more clear distinction between the polyether peak and freezing water since the PEO crystallisation peak is strongly reduced by water. Therefore, the crystallisation enthalpy of the polyether and freezing water can be determined by using the DSC cooling scan (Table 5.7).

The percentage of freezing water (w_f) in $PEO_{2000}/PTMO_{2000}$-T6T6T copolymers was calculated using Equation 5.2. The percentage of bound water (w_b) is calculated by subtracting w_f from the total water absorption. It is assumed that no freezing bound water is present. The number of bound water molecules per ethylene oxide repeating unit was calculated according to Equation 5.3. In Table 5.8 the amounts of freezing and bound water of PEO/PTMO-T6T6T copolymers as well as the H_2O/EO ratio are given.

Table 5.8: Amount of freezing and bound water of $PEO_{2000}/PTMO_{2000}$-T6T6T copolymers

Ratio PEO/PTMO	WA [wt%]	φ_{water} [wt%]	φ_{water} [vol%]	ΔH_c [J/g]	w_f [%]	w_b [%]	H_2O/EO bound [-]	H_2O/EO [-]
0/100	1.2	1.2	1.2	-	-	-	-	-
20/80	9.8	8.9	10	4	13	87	1.4	1.6
40/60	24	19	22	12	19	81	1.6	1.9
50/50	33	25	28	14	17	83	1.8	2.1
60/40	42	30	33	19	19	81	1.9	2.3
80/20	60	38	41	21	17	83	2.0	2.4
100/0	91	48	52	27	17	83	2.4	2.9

The $PEO_{2000}/PTMO_{2000}$-T6T6T copolymers have more or less comparable amount of freezing water (13 - 19%), despite different PEO contents. This suggests that the PEO concentration and the presence of PTMO have no significant influence on the amount of freezing water.
Previous results revealed that the PEO_x-T6T6T copolymers contain freezing water when the water concentration in the PEO phase is above ~30 vol%, which corresponds to a H_2O/EO ratio of at least 1.0. All PEO/PTMO-T6T6T copolymers contain freezing water since they all have a H_2O/EO ratio above 1.0.

Tensile properties

The tensile properties of $PEO_{2000}/PTMO_{2000}$-T6T6T copolymers in dry and wet conditions have been determined and the results are given in Table 5.9. At small deformation the stress increases linearly with the strain. Above the yield point the stress gradually increases. At higher strains (>300%) strain-induced crystallisation of the polyether segments can take place, which results in an increased fracture stress [55]. Since water lowers the melting temperature of PEO, strain-induced crystallisation of the hydrated PEO segments becomes more difficult. The crystalline PTMO phase is hardly affected by the presence of water.

Table 5.9: Tensile properties of dry and hydrated $PEO_{2000}/PTMO_{2000}$-T6T6T copolymers.

Ratio PEO/PTMO	η_{inh} [dL/g]	Conc. T6T6T [wt%]	WA [wt%]	G' [1] [MPa]	E [MPa]	σ_y [2] [MPa]	ε_y [2] [%]	σ_f [MPa]	ε_f [%]	σ_{true} [3] [MPa]
0/100	2.0	23.8	0	34	115	9.0	43	45	1000	495
		23.5	1.2	-	117	9.0	43	42	900	420
20/80	2.0	23.8	0	38	142	8.5	38	29	880	284
		21.7	9.8	-	142	8.2	36	28	870	272
40/60	2.1	23.8	0	31	123	7.4	41	26	680	203
		19.2	24	-	82	7.7	42	27	670	208
50/50	1.7	23.8	0	33	133	8.0	30	22	780	194
		17.9	33	-	60	6.5	40	17	620	122
60/40	1.8	23.8	0	33	120	7.5	34	21	620	151
		16.7	42	-	53	7.9	51	19	470	108
80/20	1.9	23.8	0	33	126	8.1	36	23	620	166
		14.9	60	-	28	7.6	60	19	490	112
100/0	1.9	23.8	0	38	117	6.3	27	27	920	275
		12.5	91	-	20	5.4	67	17	490	100

[1] *Storage modulus (G') determined by DMA at 20 °C* [40]

[2] *Yield stress and strain were determined using the Considère method* [56]

[3] *True fracture stress (σ_{true}) was calculated by $\sigma_f \times (1 + (\varepsilon_f / 100))$*

The initial E-moduli of segmented block copolymers with monodisperse T6T6T segments increase with increasing rigid segment concentration [38]. In Figure 5.14 the E-moduli of dry and hydrated PEO/PTMO-T6T6T copolymers is given as a function of the PEO/PTMO ratio.

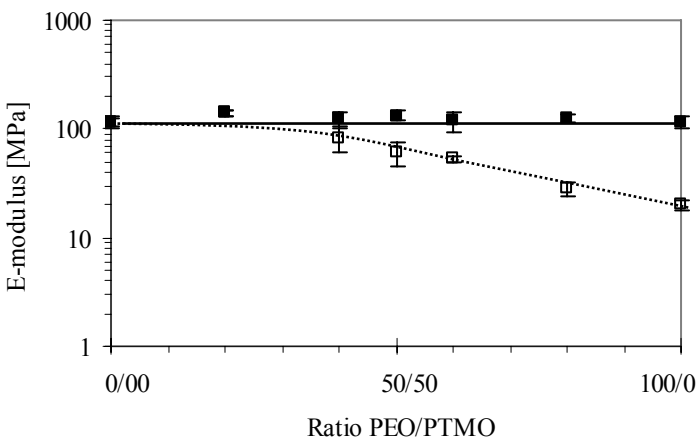

Figure 5.14: Initial E-modulus of $PEO_{2000}/PTMO_{2000}$-T6T6T as a function of the ratio PEO/PTMO: ■, dry copolymers; □, hydrated copolymers.

As the T6T6T concentration in dry $PEO_{2000}/PTMO_{2000}$-T6T6T copolymers is constant, the modulus is comparable for all copolymers. Moreover, it is assumed that the crystalline T6T6T phase is not affected by water. The initial E-modulus is related to the storage modulus (G') according to Equation 5.4. In the case of ideal elastomers the Poisson constant equals 0.5 and $G' = 3E$. This relation is observed for the PEO/PTMO-T6T6T copolymers (Table 5.9).
When taking the swelling of the copolymer into account, the actual T6T6T content can be calculated by correcting for the water absorption. On swelling, the T6T6T content in PEO-T6T6T decreases from 23.8 to 12.5 wt%. This decrease in T6T6T concentration in PEO-T6T6T would have resulted in a reduction of the modulus by a factor three [38]. However, the observed lowering of the modulus of hydrated PEO/PTMO-T6T6T copolymers is more than a factor three. Therefore, the lowering of the modulus is partly due to a lowering of the T6T6T concentration on swelling but, probably, also due to an increased flexibility of the hydrated PEO segments.

In semi-crystalline copolymers, the yield point is often the beginning of breaking up the crystalline structure. Before the yield point the deformation is mainly elastic. The yield stress increases linearly with increasing T6T6T concentration. In Figure 5.15a the yield stress and fracture stress of PEO/PTMO-T6T6T copolymers are given as a function of the PEO/PTMO ratio. Figure 5.15b shows the yield strain as a function of the PEO/PTMO ratio.

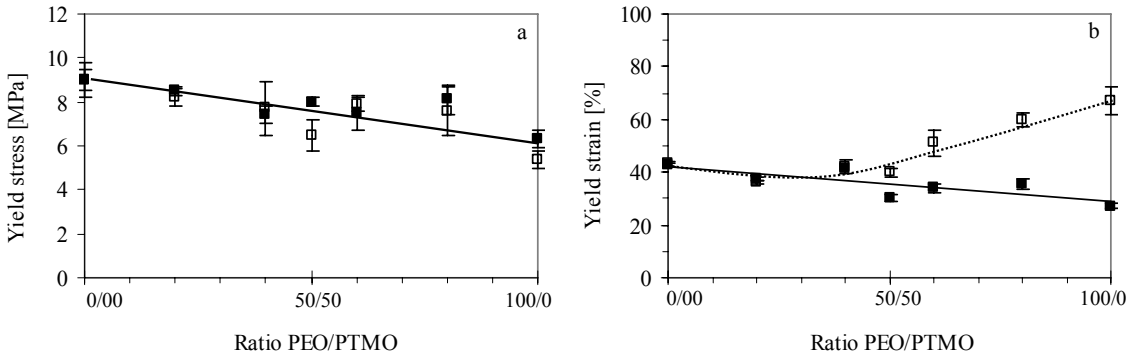

Figure 5.15: (a) Yield stress and (b) yield strain of $PEO_{2000}/PTMO_{2000}$-T6T6T as a function of the ratio PEO/PTMO: ■, dry copolymers; □, hydrated copolymers.

The yield stress of dry PEO_{2000}-T6T6T is lower than for $PTMO_{2000}$-T6T6T, 6.3 and 9.0 MPa respectively. This effect is as yet unknown since the T6T6T content and crystallinity is the same. With increasing PEO content in the PEO/PTMO-T6T6T copolymers the yield stress of both dry and hydrated copolymers decrease linearly. The swelling of the copolymers has no

effect, which is unexpected as the T6T6T concentration is reduced when the copolymer absorbs water. This would have resulted in a lower yield stress.

The yield strain of dry PEO_{2000}-T6T6T is lower than $PTMO_{2000}$-T6T6T, 27 and 43% respectively. An increase in the PEO content of PEO/PTMO-T6T6T copolymers results in a gradual decrease of the yield strain. In aqueous conditions, the yield strain of $PTMO_{2000}$-T6T6T is not changed while for PEO_{2000}-T6T6T an increase is observed. This increase can be explained by the plasticizing effect of water on the PEO segments. The yield strain of hydrated PEO/PTMO-T6T6T copolymers increases gradually with PEO content. Due to the presence of water, not only the crystalline content decreases but also the amorphous chains become more mobile. As a result the modulus is lower but the yield strain is higher.

Generally, the fracture properties of segmented block copolymers depend on the strain-induced crystallisation of the soft phase [57]. Strain-induced crystallisation is influenced by the type of soft segment and the molecular weight of the copolymer. Strain-induced crystallisation has taken place in both PEO_{2000}-T6T6T and $PTMO_{2000}$-T6T6T copolymers as the fracture stress is much higher than the yield stress. In Figure 5.16 the fracture stress of dry and hydrated PEO/PTMO-T6T6T copolymer is given as a function of the PEO/PTMO ratio.

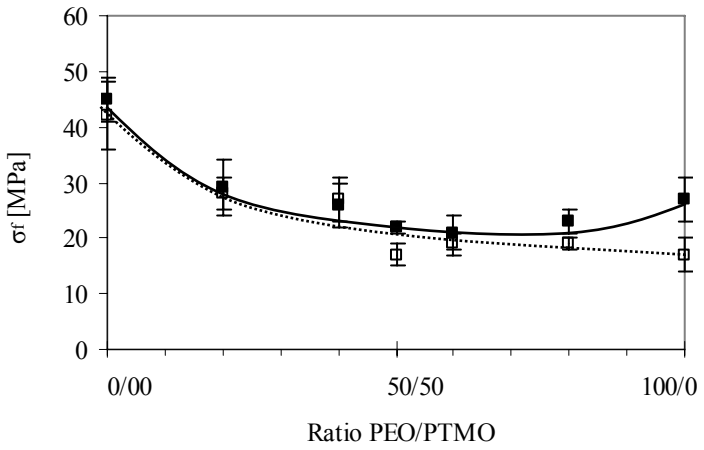

Figure 5.16: Fracture stress of PEO/PTMO of PEO_{2000}/$PTMO_{2000}$-T6T6T as a function of the PEO/PTMO ratio: ■, dry copolymers; □, hydrated copolymers.

The fracture stress of dry PEO_{2000}-T6T6T is considerably lower than dry $PTMO_{2000}$-T6T6T, 27 and 45 MPa respectively, despite the fact that the molecular weights are comparable. This indicates that the reinforcing effect obtained by strain-induced crystallisation of PEO is lower than PTMO. Copolymers that contain a mixture of PEO and PTMO segments have a lower

fracture stress compared to PEO-T6T6T or PTMO-T6T6T copolymers. Most likely, this is due to less strain-induced crystallisation as a result of the reduced polyether melting temperatures. There is hardly any difference between the fracture stress of dry and hydrated PEO/PTMO-T6T6T copolymers observed, except for PEO_{2000}-T6T6T. The fracture stress of hydrated PEO_{2000}-T6T6T is much lower compared to the dry copolymer, 17 and 27 MPa respectively. The PEO melting temperature is strongly reduced by water and, therefore, the strain-induced crystallisation of the PEO phase is suppressed, which results in a lower fracture stress.

By combining the fracture stress and strain, the true fracture stress can be calculated (Table 5.9). This true fracture stress decreases with increasing PEO and water concentration, from 495 MPa for dry $PTMO_{2000}$-T6T6T to 100 MPa for hydrated PEO_{1000}-T6T6T. This can be explained by a difference in the ability of strain-induced crystallisation of the polyether phase.

Conclusions

The influence of water on the physical and tensile properties of segmented block copolymers, containing a mixture of hydrophilic poly(ethylene oxide) (PEO) and/or hydrophobic poly(tetramethylene oxide) (PTMO) flexible segments and monodisperse T6T6T segments, is studied in this chapter.

The PEO_x-T6T6T, $(PEO_x/T)_y$-T6T6T and $PEO_{2000}/PTMO_{2000}$-T6T6T copolymers show an exponential increase in water absorption with increasing PEO content. An exponential increase in water absorption with increasing water vapour activity is observed for PEO-based copolymers, indicating that water clusters are formed. The water absorption of PEO-based copolymers depends on the PEO concentration. The number of water molecular per ethylene oxide unit (H_2O/EO) is determined by the crosslink density in the copolymer (i.e. the T6T6T concentration) and the presence of hydrophobic units (like PTMO or terephthalic units) in the PEO phase.

The glass transition temperature of PEO-based copolymers is strongly lowered when the copolymer is fully hydrated with water, compared to dry copolymers. This is due to the plasticizing effect of water on the PEO segments. The T_g's of hydrated PTMO-T6T6T and PEO-T6T6T are close together, which makes it difficult to draw conclusions concerning the structure of the polyether phase. However, the surface morphology of hydrated copolymers, recorded with AFM, reveals that copolymer surface swells inhomogeneous and clusters are formed. The PEO melting temperature and crystallinity are strongly reduced when the copolymer absorbs water, while the PTMO phase remains unaffected by water. Freezing

water is present in the PEO-based copolymer when the PEO phase contains approximately 30 vol% of water. The amount of freezing water is almost independent of the PEO concentration, the PEO molecular weight and the presence of hydrophobic PTMO segments in the PEO phase.

The tensile properties of the polyether-T6T6T copolymers are evaluated in dry and wet conditions. In an aqueous environment, the PEO melting temperature is strongly reduced and the ability of strain-induced crystallisation of the PEO segments is lowered. Hydrated copolymers have lower initial E-moduli but higher yield strains compared to dry copolymers. This can be explained by the lower T6T6T concentration in hydrated copolymers and an increase flexibility of the plasticized polyether phase. Taking into account the swelling of the copolymer, the yield stress and the fracture stress were similarly for the dry and wet samples and both decrease with T6T6T content.

References

1. Gebben, B., *J. Membr. Sci.* **1996**, 113, p. 323-329.
2. Stroeks, A. and Dijkstra, K., *Polymer* **2001**, 42, p. 117-127.
3. Metz, S.J., Mulder, M.H.V. and Wessling, M., *Macromolecules* **2004**, 37, p. 4590-4597.
4. Metz, S.J., Potreck, J., Mulder, M.H.V. and Wessling, M., *Desalination* **2002**, 148, p. 303-307.
5. Bondar, V.I., Freeman, B.D. and Pinnau, I., *J. Polym. Sci., Part B: Polym. Phys.* **1999**, 37, p. 2463-2475.
6. Bondar, V.I., Freeman, B.D. and Pinnau, I., *J. Polym. Sci., Part B: Polym. Phys.* **2000**, 38, p. 2051-2062.
7. Johnson, L. and Schultze, D., *Medical Device & Diagnostic Industry*, Breathable TPE films for medical applications, **2000**.
8. Schneider, N.S., Illinger, J.L. and Karasz, F.E., in *Polymers of biological and biomedical significance,* American Chemical Society, Washington D.C. **1994**.
9. Lee, D., Lee, S., Kim, S., Char, K., Park, J.H. and Bae, Y.H., *J. Polym. Sci., Part B: Polym. Phys.* **2003**, 41, p. 2365-2374.
10. Schneider, N.S., Langlois, D.A. and Byrne, C.A., *Polym. Mater. Sci. Eng.* **1993**, 69, p. 249-250.
11. Chen, C.T., Eaton, R.F., Chang, Y.J. and Tobolsky, A.V., *J. Appl. Polym. Sci.* **1972**, 16, p. 2105-2114.
12. Schneider, N.S., Illinger, J.L. and Karasz, F.E., *J. Appl. Polym. Sci.* **1993**, 47, p. 1419-1425.
13. Yilgör, I. and Yilgör, E., *Polymer* **1999**, 40, p. 5575-5581.
14. Schneider, N.S., Dusablon, L.V., Snell, E.W. and Prosser, R.A., *J. Macromol. Sci., Phys.* **1969**, B3, p. 623-644.
15. Kjellander, R. and Florin, E., *J. Chem. Soc., Faraday Trans. 1* **1981**, 77, p. 2053-2077.
16. Brown, G.L., in *Water in polymers,* ACS symposium series, Washington D.C. **1980**.
17. Barrie, A., in *Diffusion in polymers,* Academic Press, London **1968**.
18. Flory, P.J., in *Principles of polymer chemistry*, Cornell University Press, Ithaca **1967**.
19. Zimm, B.H. and Lundberg, J.L., *J. Phys. Chem.* **1956**, 60, p. 425-428.
20. Quinn, F.X., Kampff, E., Smyth, G. and Mcbrierty, V.J., *Macromolecules* **1988**, 21, p. 3191-3198.
21. Ping, Z.H., Nguyen, Q.T., Chen, C.T., Zhou, J.Q. and Ding, Y.D., *Polymer* **2001**, 42, p. 8461-8467.
22. Antonsen, K.P. and Hoffman, A.S., in *Poly(Ethylene Glycol) Chemistry; Biotechnical and Biomedical Applications,* Plenum Press, New York **1992**.
23. Graham, N.B., Zulfiqar, M., Nwachuku, N.E. and Rashid, A., *Polymer* **1989**, 30, p. 528-533.
24. Deschamps, A.A., Grijpma, D.W. and Feijen, J., *J. Biomater. Sci., Polym. Ed.* **2002**, 13, p. 1337-1352.
25. Sakkers, R.J.B., De Wijn, J.R., Dalmeyer, R.A.J., Brand, R. and Van Blitterswijk, C.A., *J. Mater. Sci.: Mater. Med.* **1998**, 9, p. 375-379.
26. Rault, J. and Le Huy, H.M., *J. Macromol. Sci., Phys.* **1996**, 35, p. 89-114.
27. Petrini, P., Fare, S., Piva, A. and Tanzi, M.C., *J. Mater. Sci.: Mater. Med.* **2003**, 14, p. 683-686.

28. Deschamps, A.A., Grijpma, D.W. and Feijen, J., *Polymer* **2001**, 42, p. 9335-9345.
29. Petrik, S., Hadobas, F., Simek, L. and Bohdanecky, M., *J. Appl. Polym. Sci.* **1993**, 47, p. 677-684.
30. Shibaya, M., Suzuki, Y., Doro, M., Ishihara, H., Yoshihara, N. and Enomoto, M., *J. Polym. Sci., Part B: Polym. Phys.* **2006**, 44, p. 573-583.
31. Okkema, A.Z., Grasel, T.G., Zdrahala, R.J., Solomon, D.D. and Cooper, S.L., *J. Biomater. Sci., Polym. Ed.* **1989**, 1, p. 43-62.
32. Vaidya, A. and Chaudhury, M.K., *J. Colloid Interface Sci.* **2002**, 249, p. 235-245.
33. Deslandes, Y., Pleizier, G., Alexander, D. and Santerre, P., *Polymer* **1998**, 39, p. 2361-2366.
34. Park, J.H. and Bae, Y.H., *J. Appl. Polym. Sci.* **2003**, 89, p. 1505-1514.
35. Park, J.H. and Bae, Y.H., *Biomaterials* **2002**, 23, p. 1797-1808.
36. Miller, J.A., Lin, S.B., Hwang, K.K.S., Wu, K.S., Gibson, P.E. and Cooper, S.L., *Macromolecules* **1985**, 18, p. 32-44.
37. Harrell, L.L., *Macromolecules* **1969**, 2, p. 607-612.
38. Chapter 2 of this thesis.
39. Chapter 3 of this thesis.
40. Chapter 4 of this thesis.
41. Van Krevelen, D.W., in *Properties of polymers*, Elsevier Science Publishers, New York **1990**.
42. Murthy, N.S., Stamm, M., Sibilia, J.P. and Krimm, S., *Macromolecules* **1989**, 22, p. 1261-1267.
43. Metz, S.J., van de Ven, W.J.C., Mulder, M.H.V. and Wessling, M., *J. Membr. Sci.* **2005**, 266, p. 51-61.
44. Pissis, P., Apekis, L., Christodoulides, C., Niaounakis, M., Kyritsis, A. and Nedbal, J., *J. Polym. Sci., Part B: Polym. Phys.* **1996**, 34, p. 1529-1539.
45. Kanapitsas, A., Pissis, P., Gomez Ribelles, J.L., Monleon Pradas, M., Privalko, E.G. and Privalko, V.P., *J. Appl. Polym. Sci.* **1999**, 71, p. 1209-1221.
46. Dolmaire, N., Espuche, E., Mechin, F. and Pascault, J.P., *J. Polym. Sc., Part B: Polym. Phys.* **2004**, 42, p. 473-492.
47. Valentova, H., Nedbal, J., Ilavsky and Pissis, P., *J. Non-Cryst. Solids* **2002**, 307-310, p.
48. Rault, J., Gref, R., Ping, Z.H., Nguyen, Q.T. and Néel, J., *Polymer* **1995**, 36, p. 1655-1661.
49. Rault, J., Ping, Z.H. and Nguyen, Q.T., *Journal of Non-Cryst. Solids* **1994**, 172, p. 733-736.
50. Hatakeyama, H. and Hatakeyama, T., *Thermochimica Acta* **1998**, 308, p. 3-22.
51. Flory, P.J., *Trans. Faraday Soc.* **1955**, 51, p. 848.
52. Huang, L. and Nishinari, K., *J. Polym. Sci., Part B: Polym. Phys.* **2001**, 39, p. 496-506.
53. Hager, S.I. and MacCrury, T.B., *J. Appl. Polym. Sci.* **1980**, 25, p. 1559-1571.
54. De Vringer, T., Joosten, J.G.H. and Junginger, H.E., *Colloid Poly. Sci.* **1986**, 264, p. 623-630.
55. Niesten, M.C.E.J. and Gaymans, R.J., *Polymer* **2001**, 42, p. 6199-6207.
56. McCrum, N.G., Buckley, C.P. and Bucknall, C.B., in *Principles of polymer engineering*, Oxford university press, New York **1997**.
57. Holden, G., Legge, N.R., Quirk, R.P. and Schroeder, H.E., in *Thermoplastic elastomers*, Hanser Publishers, Munich **1996**.
58. Biemond, G.J.E., Ph.D. Thesis '*Hydrogen bonding in segmented block copolymers*', University of Twente, The Netherlands **2006**.
59. Krijgsman, J. and Gaymans, R.J., *Polymer* **2004**, 45, p. 437-446.
60. Bailey, J.F.E. and Koleske, J.V., in *Poly(ethylene oxide)*, Acedemic Press, New York **1976**.

Chapter 6

Surface properties of polyether-based segmented block copolymers

---

Abstract

The surface properties of segmented block copolymers based on flexible polyether segments and monodisperse crystallisable tetra-amide segments are discussed in this chapter. The polyether phase consists of hydrophilic poly(ethylene oxide) (PEO) and/or hydrophobic poly(tetramethylene oxide) (PTMO) segments. The monodisperse crystallisable segments (T6T6T) are based on dimethyl terephthalate (T) and hexamethylenediamine (6). As the T6T6T crystallinity is high (~85%) there has maximally 15% of the total T6T6T concentration in the copolymer not crystallised and is partly dissolved in the polyether phase. This indicates that the polyether phase is rather pure.

The influence of the polyether phase composition on the surface hydrophilicity of the copolymers is investigated. In order to study the surface hydrophilicity of these highly hydrated polymers the static captive (air) bubble method was used.

Since the molecular weight of the T6T6T segments is low, the polyether content in the copolymers can reach a value of approximately 88 wt%. The contact angle (CA) decreases with increasing PEO content. A CA of ~29° can be obtained when the copolymer contains approximately 85 wt% PEO. An interesting combination of properties, i.e. a low CA combined with relatively low water absorption, was observed for the copolymer based on PEO segments with a molecular weight of 1000 g/mol. However, further characterisation of the copolymers as well as the PEO starting materials is required to explain the relation between the CA and the PEO molecular weight.

The surface morphology of hydrated PEO/PTMO-T6T6T copolymers, based on a mixture of hydrophilic PEO and hydrophobic PTMO segments, was studied with AFM. Inhomogeneous swelling of the hydrated surface was observed and this suggests that an amphiphilic surface was created. The CA of these PEO/PTMO-T6T6T copolymers decreased linearly with increasing PEO concentration, indicating that PEO was not preferentially present at the surface.

Introduction

Segmented block copolymers, consisting of alternating flexible and rigid segments, can find applications in many different fields like the coating, packaging or textile industry. The materials can be processed into complex shapes, have tunable properties and their surface composition can be modified. Therefore, they are also interesting materials for biomedical applications where the surface properties are important. One can think of applications like membranes for separation processes, contact lenses, catheters, wound dressings and coatings for blood and protein storage devices [1-6]. Several segmented block copolymers like polyurethanes [7-12] and polyesters [13-17] are applied as biomaterials. However, problems like surface-induced thrombosis, infections and calcification can still occur after short- or long-term contact with blood [1,18].

Poly(ethylene oxide) (PEO) based segmented block copolymers can be used to diminish protein adsorption at the polymer surface. PEO is a synthetic, water-soluble and non-toxic polymer. Polymers based on PEO have a high degree of hydration and a low interfacial free energy with water [2,5,19-21]. The blood compatible nature of PEO can be explained by several mechanisms [5,19,22]. The low interfacial energy between a biological fluid and PEO results in a low driving force for protein adsorption. Also the large excluded volume and mobility of hydrated PEO repel proteins approaching the polymer surface.

Polyurethane(urea) copolymers based on PEO have been evaluated as biomaterials due to their good biocompatibility and excellent mechanical properties [11,23-26]. The blood-compatibility of these copolymers is better than that of homopolymers consisting of only polyether or urethane(urea) components, which indicates that a phase separated structure affects the blood compatibility of the material [23,25]. Improvement of the phase separation between flexible and rigid segments leads to a better blood compatible material [22-25,27]. In biological fluids the polymer surface will be enriched with the lowest interfacial free energy component, which will be PEO.

A combination of hydrophilic and hydrophobic segments can be used to create an optimal hydrophilic-hydrophobic balance of the polymer surface [24,27-31]. The surface properties of these amphiphilic polymer systems can change with the environmental conditions like water content and pH or temperature of the medium. These environmentally responsive materials adjust spontaneously their surface composition in order to achieve a low interfacial free energy with the environment. This can be interesting for (selective) adsorption-desorption of proteins and the design of non-fouling membranes.

There are several possibilities to improve the blood compatibility of a polymer. One can apply surface treatments like physical adsorption or covalent grafting of PEO on a hydrophobic substrate. Physical adsorption is not sufficient for long-term applications as PEO can be replaced by other molecules which have a higher affinity for the surface. Covalent grafting of PEO on a hydrophobic bulk polymer is more adequate for long-term applications. PEO has been covalently grafted to (modified) polymeric substrates like poly(ethylene terephthalate) [20,32-34], polystyrene [35,36], polyethylene [4,22] or polyurethanes [10,37]. Grafting of PEO chains on a hydrophobic surface can be achieved by a method called plasma immobilization, described in detail by Hoffman et al. [38,39]. However, most of the grafting methods are practically limited as functional groups have to be generated on the surface and the procedure is often complex [5]. Moreover, when the surface is damaged, for instance by scratching, the hydrophobic bulk is exposed and the blood compatibility of the material reduced.
Another possibility to improve the blood compatibility of a surface is to use segmented block copolymers based on PEO. In this case PEO is present at the surface as well as in the bulk. The PEO-based copolymers are interesting for applications where swelling of the material is not essential. Compared to the PEO-grafts, the materials are easy to produce and process, and retain their low tendency for protein adsorption when subjected to surface damage or abrasion. However, the PEO segments in segmented block copolymers have a restricted mobility, which can restrict the blood compatibility of the surface. The hard segments, which are partly dissolved in the PEO phase, can also be present at the polymer surface. This must be avoided as the hard segments can induce protein adsorption at the polymer surface and can denature proteins [2].

By increasing the crystallinity of rigid segments in the copolymers the amount of non-crystallised rigid segments dissolved in the soft phase is reduced. The degree of crystallisation of the rigid segments can be improved by using monodisperse segments [40,41]. With monodisperse crystallisable segments a fast and more complete crystallisation is obtained than with random crystallisable segments. According to literature, an improved phase separation between hard and soft segments leads to better blood-contacting properties of the material [22-25,27].

This thesis deals with the synthesis and characterisation of segmented block copolymers with polyether segments and monodisperse crystallisable tetra-amide segments (T6T6T). The T6T6T segments are based on terephthalic acid (T) and hexamethylenediamine (6) [42]. As the T6T6T crystallinity in the copolymers is high (~85%), a maximum of 15% of the total T6T6T

concentration has not crystallised and is partly dissolved in the polyether phase. Copolymers with high PEO concentrations can be prepared which still have good mechanical properties. This is due to the low molecular weight of T6T6T (624 g/mol). However, the PEO-T6T6T copolymers absorb considerable amounts of water, which influences the mechanical properties of the material as was discussed in more detail in Chapter 5.

The surface properties of polyether-T6T6T segmented block copolymers will be studied by determining the contact angle using the static captive (air) bubble method. The influence of the polyether phase composition on the contact angle of three different polyether-T6T6T series will be discussed in this chapter. The first polymer series is based on PEO, denoted as PEO_x-T6T6T, where the PEO molecular weight (x) is varied from 1000 to 3400 g/mol. In Chapter 2 the synthesis and characterisation of these copolymers are described. The second polymer series contains PEO segments that are extended with terephthalic units (T) to create long flexible polyether segments that will not phase separate by liquid-liquid demixing. These copolymers are denoted as $(PEO_x/T)_y$-T6T6T, where both the PEO molecular weight (x) as well as the total molecular weight of the flexible segments (y) are varied. The synthesis and characterisation of these copolymers are reported in Chapter 3. The third polymer series is based on a mixture of hydrophilic PEO and hydrophobic poly(tetramethylene oxide) (PTMO) segments and is denoted as $PEO_x/PTMO_z$-T6T6T. The molecular weights of PEO (x) and/or PTMO (z) as well as the PEO/PTMO ratio are varied and, consequently, the swelling of the copolymer is tuned. In Chapter 4 the synthesis of these copolymers is presented. The morphology of dry and hydrated $PEO_x/PTMO_z$-T6T6T copolymers will be investigated by AFM.

Experimental

PEO_x-T6T6T block copolymers. The PEO_x-T6T6T copolymers were synthesised by a polycondensation reaction using PEO segments with a molecular weight (x) of 600 – 4600 g/mol and T6T6T [43].

$(PEO_x/T)_y$-T6T6T block copolymers. The $(PEO_x/T)_y$-T6T6T copolymers were synthesised by a poly-condensation reaction using PEO segments, which are extended with terephthalic units, and T6T6T [44]. The PEO molecular weight (x) and the total molecular weight of the flexible segment (y) were varied.

$PEO_x/PTMO_z$-T6T6T block copolymers. The $PEO_x/PTMO_z$-T6T6T block copolymers were synthesised by a polycondensation reaction using a mixture of PEO and PTMO segments and T6T6T [45]. The PEO molecular weight (x) was varied from 600 to 8000 g/mol and the PTMO molecular weight (z) from 650 to 2900 g/mol.

Water absorption (WA). The equilibrium WA was measured using pieces of injection-moulded polymer bars. The samples were placed in a desiccator filled with demineralised water for 4 wks at room temperature. The WA was defined as the weight gain of the polymer according to;

$$Water\ absorption = \frac{m - m_0}{m_0} \times 100\% \quad [wt\%] \qquad \text{(Equation 6.1)}$$

where m_0 is the weight of dry sample and m the weight of the sample after conditioning to equilibrium. The measurements were performed in duplicate. After 4 wks the samples were dried and m_0 was measured again to exclude weight loss during the experiment. The volume fraction of water (φ_{water}) was determined by using the PEO, PTMO, DMT and T6T6T density of 1.13, 0.98, 1.20 and 1.32 g/cm^3 respectively [46].

Contact angle (CA). Static captive (air) bubble (CB) contact angle measurements were performed by introducing a 10 µL air bubble from a micro-syringe below the surface of a polymer film, which is placed in an optical cuvet filled with demineralised water. The measurements were performed using a video-based Optical Contact Angle Meter OCA15 plus (DataPhysics Instruments). Static sessile drop (SD) contact angle measurements were performed by placing a water drop of approximately 10 µL on a dry polymer surface. The contact angles were calculated immediately after the droplet was placed on the surface (±10 s) by using SCA20 software, applying ellipse fitting. Results are the average of at least 20 measurements.

The polymer films were made by compression moulding and had a thickness of approximately 300 µm. Before the CA measurements the films were ultrasonically cleaned in *n*-hexane for 5 min. Subsequently, the films were wiped with cotton and rinsed with *n*-hexane. The films were then dried in a vacuum oven for 24 h to remove all *n*-hexane. Approximately 5 h before the measurements the films were placed in demineralised water to allow the materials to absorb water till equilibrium was reached.

Atomic Force Microscopy (AFM). AFM measurements were performed on a Bioscope AFM and Nanoscope IV controller. The AFM height images were recorded in tapping mode. The operating set point value (A/A_0) was 0.6 – 0.7 and the scan size was 1 µm. Solvent-cast samples of ~15 µm-thick films were prepared from a 4 wt% solution in TFA. The AFM measurements were first performed on dry samples using a TESP cantilever (k ~ 40 N/m). Subsequently, a drop of demineralised water was placed on the film and the measurements were performed using a DNP cantilever (k ~ 0.58 N/m). From the height images the RMS (root-mean-square) roughness (R_q) was calculated according to equation 6.2.

$$R_q = \sqrt{\frac{\sum (z_i)^2}{N}} \qquad \text{(Equation 6.2)}$$

where z_i is the height of a single value and N the number of points.

Results and discussion

In this chapter the surface hydrophilicity of several series of polyether-T6T6T segmented block copolymers will be determined to get more insight in the effect of the type of polyether, the polyether concentration and the polyether molecular weight on the contact angle (CA). The three series that will be discussed are PEO_x-T6T6T, $(PEO_x/T)_y$-T6T6T and $PEO_x/PTMO_z$-T6T6T. In dry conditions, the copolymers can contain a semi-crystalline polyether phase at room temperature when the PEO molecular weight is >2000 g/mol. The presence of polyether crystals in the copolymer can have an effect on the CA. However, when the copolymer is in contact with liquid water the PEO melting temperature is strongly reduced as was discussed in

Chapter 5. Therefore, during the CA measurements performed at room temperature the polyether phase was completely amorphous.

PEO_x-T6T6T copolymers

A polymer series based on PEO_x-T6T6T was made, in which the PEO molecular weight (x) was varied from 600 to 4600 g/mol. The composition, the water absorption and contact angle of these copolymers are given in Table 6.1.

The water absorption (WA) was influenced by both the PEO and the T6T6T concentration. With increasing PEO length, and thus decreasing T6T6T content, the water absorption increases. A higher T6T6T concentration limits the swelling of the copolymer as the physical crosslink density in the copolymer increases. Results reported in Chapter 5 reveal a linear increase in volume fraction of water (φ_{water}) with increasing PEO concentration.

Table 6.1: Composition, water absorption and contact angles of PEO_x-T6T6T copolymers.

PEO_x [g/mol]	Conc. T6T6T [wt%]	Conc. PEO [wt%]	WA [wt%]	φ_{water} [vol%]	CA ± sd [º]
600	51.0	49.0	18	18	46 ± 2
1000	38.4	61.6	35	30	33 ± 3
1500	29.4	70.6	69	45	33 ± 2
2000	23.8	76.2	91	51	36 ± 2
3400	15.5	84.5	127	59	35 ± 2
4600	11.9	88.1	170	66	31 ± 2

In Figure 6.1a the contact angle of PEO_x-T6T6T copolymers is given as a function of the PEO length. The CA decreases with increasing PEO molecular weight and this decrease is especially strong in the region from PEO_{600} to PEO_{1000}. When the PEO molecular weight is too low (<1000 g/mol) it seems that some hard segments are present at the polymer surface, which might explain the high CA of PEO_{600}-T6T6T. When the PEO molecular weight is ≥1000 g/mol the decrease in CA is rather small.

The T6T6T crystals are randomly distributed in the polyether matrix and expected not to be present at the polymer surface. However, the non-crystallised T6T6T, which are present in the amorphous phase for approximately 15 wt%, can be located at the polymer surface. With increasing PEO length the amount of T6T6T decreases and, consequently, the amount of non-crystallised T6T6T in the polyether phase decreases.

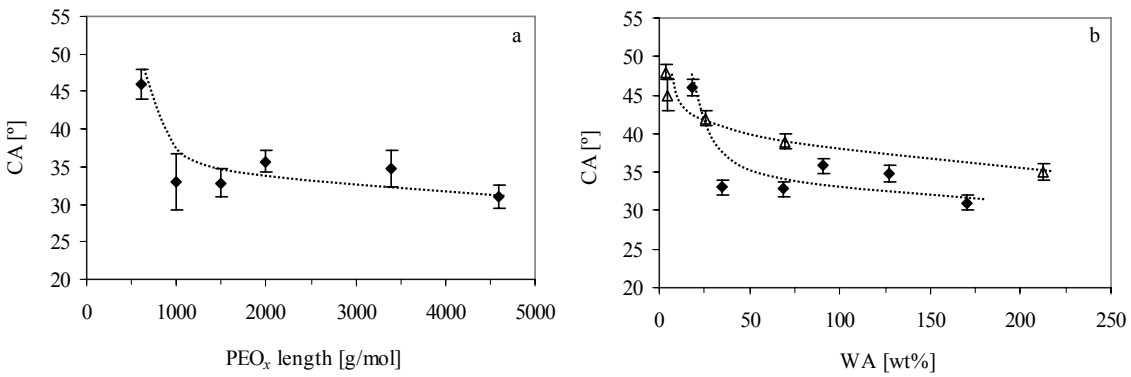

Figure 6.1: Contact angle as a function of (a) the PEO length and (b) the water absorption: ♦, PEO$_x$-T6T6T; Δ, PEO-PBT [15].

Deschamps et al. studied segmented block copolymers based on PEO and poly(butylene terephthalate) (PBT) rigid segments, using PEO lengths varying from 300 to 4000 g/mol and PBT contents varying from 30 to 70 wt% [15]. To compare the CA of PEO-PBT with that of the PEO$_x$-T6T6T copolymers, the CA is given as a function of the WA (Figure 6.1b). These PEO-PBT copolymers showed a decrease in CA with increasing water absorption, and thus increasing PEO concentration. The PBT crystallinity in these copolymers is rather low (~35%), indicting that approximately 65% non-crystallised PBT is present in the amorphous PEO phase. These non-crystallised PBT can be present at the polymer surface, resulting in a higher CA. At similar water absorption the CA of PEO$_x$-T6T6T is lower than that of the PEO-PBT, indicating a more hydrophilic polymer surface. This suggests that the use of monodisperse crystallisable segments results in a more hydrophilic surface.

Terephthalic extended PEO segments

The PEO molecular weight in segmented block copolymers is limited to 4600 g/mol. The use of higher PEO molecular weights results in phase separation by liquid-liquid demixing. A way to create longer flexible segments, without the occurrence of liquid-liquid demixing, is by extending the PEO segments with terephthalic units (T). These copolymers are denoted as (PEO$_x$/T)$_y$-T6T6T, where both the PEO molecular weight (x) as well as the molecular weight of the total flexible segment (y) can be varied. The terephthalic segments are amorphous and have a hydrophobic nature. Consequently, they might affect the hydrophilicity of the polymer surface.

Previous results discussed in Chapter 5, revealed that the WA of the (PEO$_x$/T)$_y$-T6T6T copolymers increases strongly with increasing PEO concentration. Furthermore, at similar PEO concentrations the (PEO$_x$/T)$_y$-T6T6T copolymers have a slightly lower water absorption

as compared to PEO_x-T6T6T copolymers. The presence of terephthalic units in the PEO phase slightly restricts the water absorption of the copolymer. The influence of terephthalic units present in the PEO phase on the hydrophilicity of the polymer surface is studied. The CA values of $(PEO_x/T)_y$-T6T6T copolymers with different soft phase compositions are given in Table 6.2.

Table 6.2: Water absorption and contact angles of $(PEO_x/T)_y$-T6T6T copolymers.

y [g/mol]	Conc. T6T6T [wt%]	Conc. PEO [wt%]	Conc. T [wt%]	η_{inh} [dl/g]	WA [wt%]	φ_{water} [vol%]	CA ± sd [º]
$(PEO_{300}/T)_y$-T6T6T							
2500	19.9	58.4	21.7	1.7	14	14	41 ± 3
$(PEO_{600}/T)_y$-T6T6T							
600	51.0	49.0	-	1.4	18	18	46 ± 2
1250	33.3	60.4	6.3	1.9	30	26	43 ± 2
2500	20.0	69.0	11.0	1.7	49	37	33 ± 2
5000	11.1	74.8	14.1	1.4	66	43	31 ± 1
$(PEO_{1000}/T)_y$-T6T6T							
1000	38.4	61.6	-	1.4	35	30	33 ± 3
3000	17.2	76.3	6.5	1.3	78	48	30 ± 1
5000	11.1	80.6	8.3	1.2	92	52	29 ± 1
$(PEO_{2000}/T)_y$-T6T6T							
2000	23.8	76.2	-	2.1	91	51	36 ± 2
4000	13.5	83.8	2.7	2.1	130	60	32 ± 2
6000	9.5	86.8	3.7	2.3	145	63	29 ± 2

In Figure 6.2 the contact angle of the different $(PEO_x/T)_y$-T6T6T series are given as a function of the PEO concentration. An increase in the total molecular weight of the flexible segment (*y*) results in a higher PEO concentration. With increasing PEO concentration the CA decreases linearly and this behaviour is observed for all terephthalic extended PEO series. However, there is no simple relation observed between the CA and the soft phase composition of the copolymers. All copolymer series show a linear decrease in CA with increasing PEO concentration but the slopes of these trend lines are different. The CA of $(PEO_{300}/T)_{2500}$-T6T6T falls on the same trend line observed for $(PEO_{600}/T)_y$-T6T6T. Despite the fact that the $(PEO_{2000}/T)_y$-T6T6T copolymers have a high PEO concentration, the CA values are not as low as expected.

At comparable PEO concentrations, the $(PEO_{1000}/T)_y$-T6T6T copolymers have the lowest CA of all the PEO extended copolymer series. This suggests that the CA is not only related to the PEO concentration but that also the type of PEO used has an influence. Therefore, further characterisation of the copolymers as well as the PEO starting materials is required to explain the relation between the CA and the soft phase composition.

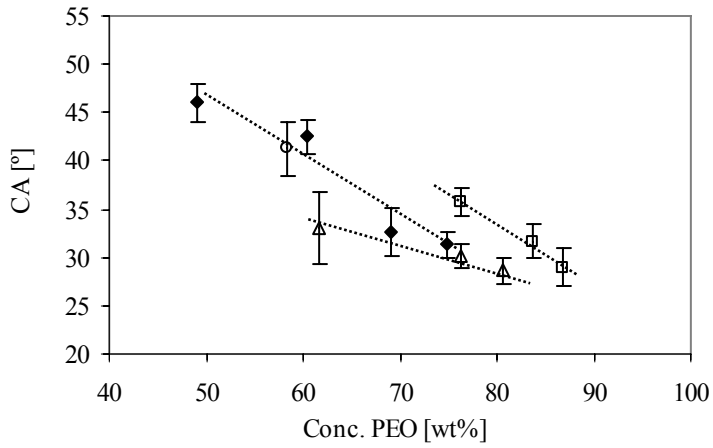

Figure 6.2: Contact angle as a function of the PEO content: ○, $(PEO_{300}/T)_y$-T6T6T; ♦, $(PEO_{600}/T)_y$-T6T6T; Δ, $(PEO_{1000}/T)_y$-T6T6T; □, $(PEO_{2000}/T)_y$-T6T6T.

At high PEO concentrations the CA of all copolymers seems to converge to one point. When extrapolated to 100 wt% PEO a CA of ~23º can be obtained. This corresponds well to a poly(ethylene terephthalate) film that has been covalently grafted with PEO and revealed a contact angle of approximately 23º [32,34].

PEO/PTMO mixed polyether phase

Segmented block copolymers based on a combination of hydrophilic PEO and hydrophobic PTMO segments can be used to tune the surface properties. The surface hydrophilicity of the $PEO_x/PTMO_z$-T6T6T copolymers is determined by contact angle measurements. These copolymers have a homogenously mixed amorphous polyether phase since only one glass transition temperature is observed [47].

Surface morphology

The surface morphology of dry and hydrated $PEO_{2000}/PTMO_{2000}$-T6T6T, with a PEO/PTMO ratio of 20/80, was studied with AFM tapping mode. The AFM height images of the

copolymer were recorded on a 1x1 μm scale and are given as three-dimensional images (Figure 6.3).

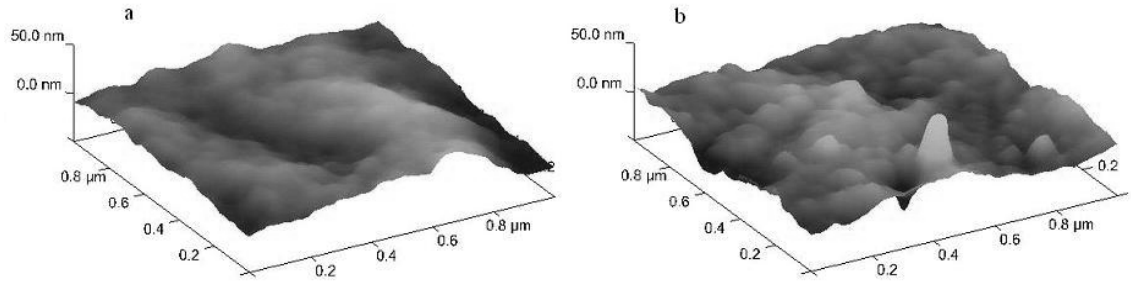

Figure 6.3: AFM height images (3D) of dry $PEO_{2000}/PTMO_{2000}$-T6T6T (20/80) at 1x1 μm: (a), dry sample; (b), hydrated sample.

The surface of the dry copolymer is not completely smooth but no separate phases can be distinguished. The surface of the hydrated copolymer contains some irregularities. The root-mean-square (RMS) roughness is calculated using Equation 6.2 and gives an average value for the difference between peak heights and depths. No clear distinction in RMS roughness between the dry (7.2 nm) and hydrated (7.5 nm) polymer sample is found. This indicates that the average heights and depths of both dry and hydrated samples are comparable. However, the AFM image of the hydrated polymer sample reveals that the surface swells inhomogeneously and there are clusters formed with a height of 10 - 50 nm and width of ~100 nm. Most likely, these clusters consist of a swollen PEO phase. However, the dimensions of the clusters are relatively large compared to the PEO_{2000} segments used.

Surface hydrophilicity

The surface hydrophilicity of the $PEO_x/PTMO_z$-T6T6T copolymers was determined by contact angle measurements. Generally, the contact angle of highly hydrated copolymers is determined by using the captive (air) method (CB). When the water absorption of the copolymer is relatively low the sessile drop (SD) method is preferred.

Both the CB and SD method are used to determine the CA of $PEO_{2000}/PTMO_{2000}$-T6T6T copolymers in order to study the effect of the applied method (Table 6.3). The CA values of $PEO_{1000}/PTMO_{1000}$-T6T6T copolymers are also given in this table. The CA values obtained by the sessile drop method are specifically denoted as CA (SD) and when the captive bubble method is applied only the term CA is used.

Table 6.3: Water absorption and (CB and SD) contact angles of $PEO_x/PTMO_z$-T6T6T copolymers.

Ratio PEO_x/ $PTMO_z$	Conc. T6T6T [wt%]	Conc. PEO [wt%]	Conc. PTMO [wt%]	WA [wt%]	φ_{water} [vol%]	CA ± sd (CB) [°]	CA ± sd (SD) [°]
$PEO_{2000}/PTMO_{2000}$-T6T6T							
0/100	23.8	0.0	76.2	1.2	1.2	55 ± 2	87 ± 2
20/80	23.8	15.2	61.0	9.8	10	50 ± 1	-
40/60	23.8	30.5	45.7	24	22	48 ± 2	61 ± 3
50/50	23.8	38.1	38.1	33	28	48 ± 2	-
60/40	23.8	45.7	30.5	42	33	45 ± 2	57 ± 2
80/20	23.8	61.0	15.2	60	41	39 ± 2	-
100/0	23.8	76.2	0.0	91	51	36 ± 2	41 ± 4
$PEO_{1000}/PTMO_{1000}$-T6T6T							
0/100	38.4	0.0	61.6	1.1	1.2	53 ± 2	-
30/70	38.4	18.5	43.1	8.1	8.8	51 ± 1	-
40/60	38.4	24.6	37.0	11	12	47 ± 2	-
60/40	38.4	37.0	24.6	20	19	44 ± 1	-
100/0	38.4	61.6	0.0	35	30	33 ± 3	-

Previous results discussed in Chapter 5, show an increase in WA of these copolymers with increasing PEO/PTMO ratio. The water absorption of $PEO_{1000}/PTMO_{1000}$-T6T6T is lower than $PEO_{2000}/PTMO_{2000}$-T6T6T. This is due to a higher T6T6T concentration of the $PEO_{1000}/PTMO_{1000}$-T6T6T copolymers, and thus a higher physical crosslink density in the copolymer.

When the PEO/PTMO ratio increases the CA of both series shows a linear decrease (Figure 6.4a). This linear decrease indicates that PEO is not preferentially present at the polymer surface or else a sharp decrease in CA would have been observed at low PEO contents. It was also not likely that PEO segments migrate towards the surface when the polymer is exposed to water since the T6T6T crystallinity is high and, as a result, the PEO mobility restricted.

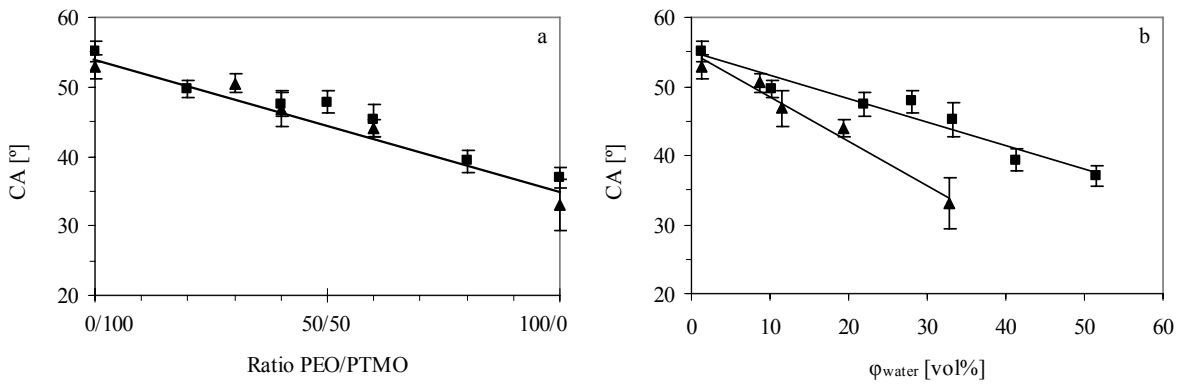

Figure 6.4: Contact angle as a function of the (a) ratio PEO/PTMO and (b) volume fraction of water: (■), $PEO_{2000}/PTMO_{2000}$-T6T6T; (▲), $PEO_{1000}/PTMO_{1000}$-T6T6T.

Both the $PEO_{1000}/PTMO_{1000}$-T6T6T and $PEO_{2000}/PTMO_{2000}$-T6T6T copolymers show a linear decrease in CA with increasing volume fraction of water (Figure 6.4b). At similar volume fractions of water the CA of $PEO_{1000}/PTMO_{1000}$-T6T6T is lower than that of $PEO_{2000}/PTMO_{2000}$-T6T6T. Also at similar PEO concentrations, the $PEO_{1000}/PTMO_{1000}$-T6T6T copolymers have a lower CA compared to that of the $PEO_{2000}/PTMO_{2000}$-T6T6T copolymers. Therefore, the $PEO_{1000}/PTMO_{1000}$-T6T6T copolymers are significantly different in terms of surface properties than $PEO_{2000}/PTMO_{2000}$-T6T6T since the water absorption is lower while the hydrophilicity of the polymer surface is comparable.

Contact angle measurements of $PEO_{2000}/PTMO_{2000}$-T6T6T were performed by using the captive bubble (CB) and sessile drop (SD) method. Both methods give different CA values (Table 6.3). The CA measured by using the CB method on hydrated surfaces is systematically lower than the CA measured by the SD method on dry surfaces. The difference in CA between SD and CB decreases with increasing PEO content. This indicates that the CA of a hydrated surface depends mainly on the nature of the polymer and the amount of water absorbed by the polymer. However, one has to keep in mind that the effect of time between the placement of a water droplet on a dry surface and the analysis of the angle has a large effect on the observed contact angle.

The influence of both the PEO_x and $PTMO_z$ molecular weight of $PEO_x/PTMO_z$-T6T6T copolymers on the surface hydrophilicity was also investigated. Two series, $PEO_x/PTMO_{1000}$-T6T6T and $PEO_{1000}/PTMO_z$-T6T6T, were made where x is varied from 600 to 8000 g/mol and z from 650 to 2900 g/mol (Table 6.4).

Despite the fact that the PEO concentration in $PEO_x/PTMO_{1000}$-T6T6T increases only slightly from 17 to 21 wt%, the water absorption increases strongly from 4.4 to 22 wt%. This is due to two effects: a decreased T6T6T content and a higher PEO molecular weight. In the $PEO_{1000}/PTMO_z$-T6T6T series, where the PTMO molecular weight was varied while the PEO concentration remained constant, the water absorption increases only slightly (18 – 23 wt%). This effect can be ascribed to a decreased T6T6T content.

Table 6.4: Water absorption and contact angles of $PEO_x/PTMO_z$-T6T6T copolymers.

Ratio $PEO_x/PTMO_z$	M_n PEO [g/mol]	M_n PTMO [g/mol]	Conc. T6T6T [wt%]	Conc. PEO [wt%]	Conc. PTMO [wt%]	WA [wt%]	φ_{water} [vol%]	CA ± sd [°]
$PEO_x/PTMO_{1000}$-T6T6T								
30/70	600	1000	42.9	17.1	40.0	4.4	4.6	50 ± 2
30/70	1000	1000	38.4	18.5	43.1	8.1	8.8	51 ± 1
30/70	3400	1000	33.0	20.1	46.9	18	18	46 ± 1
30/70	4600	1000	32.3	20.3	47.4	19	18	46 ± 1
30/70	8000	1000	31.5	20.6	47.9	22	20	40 ± 2
$PEO_{1000}/PTMO_z$-T6T6T								
65/36	1000	650	42.7	36.9	20.4	18	17	47 ± 2
60/40	1000	1000	38.4	37.0	24.6	20	19	44 ± 1
55/45	1000	2000	32.6	37.1	30.3	22	21	46 ± 1
53/47	1000	2900	30.2	37.0	32.8	23	21	47 ± 2

The CA of $PEO_x/PTMO_{1000}$-T6T6T decreases from 50 to 40° when the PEO molecular weight increases from 600 to 8000 g/mol, despite that the PEO concentration remains more or less the same. This suggests that the CA also depends on the PEO molecular weight. However, it is also possible to explain the decrease in the CA by the combination of a small increase in PEO content (from 17 to 21 wt%) and a decrease in T6T6T content (from 43 – 32 wt%). The $PEO_{1000}/PTMO_z$-T6T6T copolymers have almost a comparable CA, despite the change in PTMO segment length.

In Figure 6.5 the CA of the $PEO_x/PTMO_{1000}$-T6T6T and $PEO_{1000}/PTMO_z$-T6T6T is given as a function of the volume fraction of water. The $PEO_x/PTMO_{1000}$-T6T6T copolymers show a similar linear decrease in CA as observed previously for the $PEO_{1000}/PTMO_{1000}$-T6T6T copolymers (indicated by the dotted line in Figure 6.5). The CA of $PEO_{1000}/PTMO_z$-T6T6T is slightly higher than that of $PEO_{1000}/PTMO_{1000}$-T6T6T. Especially the $PEO_{1000}/PTMO_{2900}$-T6T6T copolymer, which has the highest water absorption of the series, has an unexpected

high CA. A possible explanation might be that there are PTMO crystals present at the polymer surface as $PTMO_{2900}$ is partly crystalline and these PTMO crystals are not soluble in water [47].

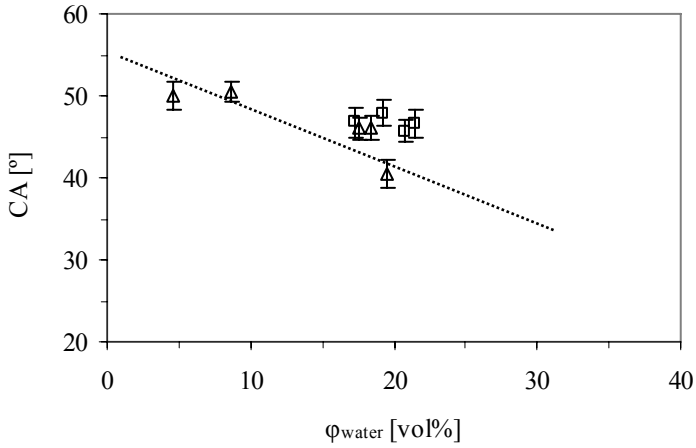

Figure 6.5: Contact angle as a function of the volume fraction of water (dotted line represents the $PEO_{1000}/PTMO_{1000}$-T6T6T copolymers): (Δ), $PEO_x/PTMO_{1000}$-T6T6T; (□), $PEO_{1000}/PTMO_z$-T6T6T.

Conclusions

The surface properties of polyether-T6T6T segmented block copolymers have been discussed in this chapter. The polyether phase consists of hydrophilic poly(ethylene oxide) (PEO) and/or hydrophobic poly(tetramethylene oxide) (PTMO) segments. The use of monodisperse T6T6T segments results in a well phase separated polymer morphology, where maximally 15% non-crystallised T6T6T is dissolved in the polyether phase. As the T6T6T segments have a low molecular weight the polyether concentration in the copolymer can reach a concentration of 88 wt% without phase separation by liquid-liquid demixing to occur.

The surface hydrophilicity is studied by using the captive (air) bubble method to determine the contact angle (CA). The CA measured according to this method is systematically lower than the CA measured by the sessile drop method. So, the CA of a hydrated surface depends mainly on the nature of the polymer and the amount of water absorbed by the polymer.

Generally, the CA of the copolymers decreases with higher PEO contents. An interesting combination of properties, i.e. a low CA combined with relatively low water absorption, is observed for copolymers based on PEO segments with a molecular weight of 1000 g/mol. However, further characterisation of the copolymers as well as the PEO starting materials is

required to explain the relation between the CA and the PEO molecular weight used in the copolymer.

At similar water absorptions, the PEO-T6T6T has a more hydrophilic surface compared to PEO-PBT segmented block copolymer. This is due to a high crystallinity of T6T6T in the copolymer, which results in a low amount of non-crystallised T6T6T segments in the PEO phase.

Segmented block copolymer based on a mixture of PEO and PTMO show a linear decrease in CA with increasing PEO content. This linear decrease indicates that there is no preferential diffusion of PEO towards the hydrated polymer surface. AFM results reveal that hydrated PEO/PTMO-T6T6T copolymers contain an inhomogeneous cluster-like structure.

References

1. Courtney, J.M., Lamba, N.M.K., Sundaram, S. and Forbes, C.D., *Biomaterials* **1994**, 15, p. 737-744.
2. Lee, J.H., Lee, H.B. and Andrade, J.D., *Prog. Polym. Sci.* **1995**, 20, p. 1043-1079.
3. Leininger, R.I., in *Biomedical and dental applications of polymers,* Plenum Press, New York **1981**.
4. Allmér, K., Hilborn, J., Larsson, P.H., Hult, A. and Ranby, B., *J. Polym. Sc., Part A: Polym. Chem.* **1990**, 28, p. 173-183.
5. Amiji, M. and Park, K., in *Polymers of biological and biomedical significance,* American Chemical Society, Washington DC **1994**.
6. Yoda, R., *J. Biomater. Sci., Polym. Ed.* **1998**, 9, p. 561-626.
7. Petrini, P., Fare, S., Piva, A. and Tanzi, M.C., *J. Mater. Sci.: Mater. Med.* **2003**, 14, p. 683-686.
8. Wheatley, D.J., Raco, L., Bernacca, G.M., Sim, I., Belcher, P.R. and Boyd, J.S., *Eur. J. Cardio-thorac.* **2000**, 17, p. 440-448.
9. Lamba, N.M.K., Woodhouse, K.A. and Cooper, S.L., in *Polyurethanes in biomedical applications*, CRC Press, Washinghton DC **1998**.
10. Brinkman, E., Poot, A., van der Does, L. and Bantjes, A., *Biomaterials* **1990**, 11, p. 200-205.
11. Ji, J., Barbosa, M.A., Feng, L. and Shen, J., *J. Mater. Sci.: Mater. Med.* **2002**, 13, p. 677-684.
12. Wesslén, B., Kober, M., Freij-Larsson, C., Ljungh, A. and Paulsson, M., *Biomaterials* **1994**, 15, p. 278-284.
13. Stapert, H.R., '*Environmentally degradable polyesters, poly(ester-amide)s and poly(ester-urethane)s*', **1998**.
14. Bezemer, J.M., Weme, P.O., Grijpma, D.W., Dijkstra, P.J., van Blitterswijk, C.A. and Feijen, J., *J. Biomed. Mater. Res.* **2000**, 52, p. 8-17.
15. Deschamps, A.A., Claase, M.B., Sleijster, W.J., Bruijn, d., J.D., Grijpma, D.W. and Feijen, J., *J. Controlled Release* **2002**, 78, p. 175-186.
16. Deschamps, A.A., van Apeldoorn, A.A., de Bruijn, J.D., Grijpma, D.W. and Feijen, J., *Biomaterials* **2003**, 24, p. 2643-2652.
17. Van Dijkhuizen-Radersma, R., Roosma, J.R., Kaim, P., Metairie, S., Peters, F., de Wijn, J., Zijlstra, P.G., de Groot, K. and Bezemer, J.M., *J. Biomed. Mater. Res.* **2003**, 67A, p. 1294-1304.
18. Leininger, R.I., in *Biomedical and dental applications of polymers,* Plenum Press, New York **1981**.
19. Kjellander, R. and Florin, E., *J. Chem. Soc., Faraday Trans. 1* **1981**, 77, p. 2053-2077.
20. Gombotz, W.R., Guanghui, W., Horbett, T.A. and Hoffman, A.S., *J. Biomed. Mater. Res.* **1991**, 25, p. 1547-1562.
21. Milton Harris, J., in *Poly(ethylene glycol) chemistry*, Plenum Press, New York **1992**.
22. Lee, J.H., Kopecek, J. and Andrade, J.D., *J. Biomed. Mater. Res.* **1989**, 23, p. 351-368.
23. Takahara, A., Jo, N.J. and Kajiyama, T., *J. Biomater. Sci., Polym. Ed.* **1989**, 1, p. 17-29.
24. Okkema, A.Z., Grasel, T.G., Zdrahala, R.J., Solomon, D.D. and Cooper, S.L., *J. Biomater. Sci., Polym. Ed.* **1989**, 1, p. 43-62.
25. Takahara, A., Tashita, J., Kajiyama, T. and Takayanagi, M., *Polymer* **1985**, 26, p. 987-996.

26. Takahara, A., Tashita, J., Kajiyama, T. and Takayanagi, M., *Polymer* **1985**, 26, p. 978-986.
27. Deslandes, Y., Pleizier, G., Alexander, D. and Santerre, P., *Polymer* **1998**, 39, p. 2361-2366.
28. Vaidya, A. and Chaudhury, M.K., *J. Colloid Interface Sci.* **2002**, 249, p. 235-245.
29. Park, J.H. and Bae, Y.H., *J. Appl. Polym. Sci.* **2003**, 89, p. 1505-1514.
30. Park, J.H. and Bae, Y.H., *Biomaterials* **2002**, 23, p. 1797-1808.
31. Ito, E., Suzuki, K., Yamato, M., Yokoyama, M., Sakurai, Y. and Okano, T., *J. Biomed. Mater. Res.* **1998**, 42, p. 148-155.
32. Desai, N.P. and Hubbell, J.A., *J. Biomed. Mater. Res.* **1991**, 25, p. 829-843.
33. Lin, Q., Unal, S., Fornof, A.R., Wei, Y.P., Li, H.M., Armentrout, R.S. and Long, T.E., *Macromol. Symp.* **2003**, 199, p. 163-172.
34. Gombotz, W.R., Guanghui, W. and Hoffman, A.S., *J. Appl. Polym. Sci.* **1989**, 37, p. 91-107.
35. Meng, F.H., Engbers, G.H.M. and Feijen, J., *J. Biomed. Mater. Res. Part A* **2004**, 70A, p. 49-58.
36. Grainger, D.W., Okano, T. and Kim, S.W., *J. Colloid Interface Sci.* **1989**, 132, p. 161-175.
37. Chen, Z., Ward, R., Tian, Y., Malizia, F., Gracias, D.H., Shen, Y.R. and Somorjai, G.A., *J. Biomed. Mater. Res.* **2002**, 62, p. 254-264.
38. Terlingen, J.G.A., Feijen, J. and Hoffman, A.S., *J. Biomater. Sci. Polym. Ed.* **1992**, 4, p. 31-33.
39. Sheu, M.S., Hoffman, A.S. and Feijen, J., in *Contact ange, wettability and adhesion,* VSP, Utrecht **1993**.
40. Miller, J.A., Lin, S.B., Hwang, K.K.S., Wu, K.S., Gibson, P.E. and Cooper, S.L., *Macromolecules* **1985**, 18, p. 32-44.
41. Harrell, L.L., *Macromolecules* **1969**, 2, p. 607-612.
42. Krijgsman, J., Husken, D. and Gaymans, R.J., *Polymer* **2003**, 44, p. 7043-7053.
43. Chapter 2 of this thesis.
44. Chapter 3 of this thesis.
45. Chapter 4 of this thesis.
46. Van Krevelen, D.W., in *Properties of polymers*, Elsevier Science Publishers, New York **1990**.
47. Chapter 5 of this thesis.

Chapter 7

Gas permeation properties of PEO-based segmented block copolymers

Abstract

In this chapter the gas permeation properties of PEO-based segmented block copolymers containing monodisperse crystallisable segments (T6T6T) are discussed. The PEO-T6T6T copolymers have a well phase separated polymer structure, consisting of a crystalline T6T6T phase and an amorphous or semi-crystalline PEO phase. Copolymers containing PEO segments with a molecular weight above 2000 g/mol have a semi-crystalline PEO phase at room temperature. A way to partly suppress the PEO crystallinity and reduce the PEO melting temperature of the copolymer is by extending low molecular weight PEO segments (300 or 600 g/mol) with terephthalic units (T). In this way, copolymers can be prepared with a high PEO concentration while the PEO crystallinity is partly suppressed.

The influence of the soft phase composition and the temperature on gas permeation properties (CO_2, N_2, He, CH_4, O_2 and H_2) and pure gas selectivities of PEO-T6T6T and PEO/T-T6T6T copolymers are studied. When the PEO phase is completely amorphous, the gas permeation properties of both types of copolymers decrease with decreasing temperature. When a crystalline PEO phase is present the decrease in gas permeability is even stronger. At low temperatures the PEO/T-T6T6T copolymers have higher gas permeabilities than PEO-T6T6T, despite the presence of hydrophobic terephthalic units in the PEO phase. This is due to a partly suppressed PEO crystallinity in the copolymer.

The CO_2/N_2, CO_2/H_2 and CO_2/O_2 selectivities at 35 °C of both the PEO-T6T6T and PEO/T-T6T6T copolymers are almost independent of the polymer composition. When the copolymers contain a PEO semi-crystalline phase the CO_2/H_2 and CO_2/He selectivities are reduced, which is due to a more size-sieving ability of the copolymer. The presence of a semi-crystalline PEO phase has no adverse effect on the CO_2 selectivity over larger gases like N_2, O_2 and CH_4.

Introduction

The removal of CO_2 from gas mixtures with light gases such as CH_4, N_2 and H_2 is important in a variety of industrial applications, like the CO_2 recovery from flue, synthetic or natural gases. Polyethylene oxide (PEO) based segmented block copolymers are interesting membrane materials for these gas separation applications since they combine a high polar/nonpolar gas selectivity with a high permeability [1].

So far, segmented block copolymers containing polar poly(ethylene oxide) (PEO) segments provide the best combination of high CO_2 permeability and CO_2/N_2 or CO_2/H_2 selectivities since these units interact favourably with CO_2 [1,2]. These copolymers, containing PEO flexible segments and polyamides [1,3-5], polyimide [6], polyurethane [7,8] or polyester [9] rigid segments, have a phase separated morphology. Phase separation can occur through liquid-liquid demixing or crystallisation. Usually, only a part of the rigid segments is phase separated while the other part is dissolved in the PEO phase. When phase separation occurs through crystallisation, the rigid segments provide the copolymer mechanical and heat stability and inhibit the PEO crystallisation partly.

In Table 7.1 the CO_2 permeability (P) and CO_2/N_2 selectivity (α) of some PEO-based segmented block copolymers are given.

Table 7.1: CO_2 permeability and CO_2/N_2 selectivity of PEO-based segmented block copolymers at 35 ºC.

Rigid segments [1]	Conc. PEO [wt%]	Pressure [bar]	P CO_2 [Barrer]	α(CO_2/N_2) [-]
Polyamide				
PA6 [1]	55.0	10	120	52
PA12 [1]	57.0	10	66	55
Polyester				
PBT [9]	64.0	4	108	45
Polyurethane				
MDI-BPA [7]	66.0	2	59	49
TDI-BPA [7]	64.5	2	47	51
Polyimide				
PMDA-PDDS [7]	68.6	2	238	49
BPDA-ODA [7]	62.3	2	117	51

[1] *MDI, 4,4-diphenyl-methane diisocyanate; TDI, 2,4-toluene-diisocyanate; BPA, bisphenol A; PMDA, pyromellitic dianhydride; PDDS, 4,4-diamino diphenyl sulfone; BPPA, 3,3,4,4-biphenyl tetracarboxylic dianhydride; ODA, 4,4-oxydianiline*

The CO_2/N_2 selectivity of all these materials is almost similar, while the CO_2 permeability varies significantly. This suggests that the PEO phase is the continuous phase for gas permeation. Furthermore, the PEO segment length, the PEO content, the type of rigid segment, the amount of dissolved non-crystallised rigid segment and the morphology of the rigid segments in the copolymer can have an influence on the gas permeation properties of the segmented block copolymers [1,3,7-10].

Metz et al. studied segmented block copolymers based on PEO and poly(butylene terephthalate) (PBT) rigid segments [9]. The copolymer composition was varied by changing the PEO and/or PBT block lengths. An increase in the PEO segment length, while the PEO-PBT ratio remains constant, enhances the chain flexibility of the PEO phase, thereby causing a higher gas permeability. The chain flexibility decreases with increasing PBT concentration due to a less pronounced phase separation between the PEO and PBT phase.

The crystallinity of the rigid segments in the existing segmented block copolymers is rather low (~30%) and a large amount of non-crystallised rigid is dissolved in the soft phase. It was reported that polymers with poor phase separation between the soft and hard phase show a decreased gas permeability and diffusivity [3,8]. This is most likely due to a reduced chain flexibility of the soft phase when non-crystallised rigid segments are incorporated in the soft phase.

The crystallinity of the rigid segments is improved when monodisperse crystallisable segments are used [11-16]. By using short monodisperse rigid segments (~4 nm) the phase separation is almost complete, the crystallisation of the copolymer fast and the amount of non-crystallised rigid segment in the soft phase low.

In Chapter 2 of this thesis the synthesis and characterisation of PEO-based segmented block copolymers and monodisperse crystallisable tetra-amide segments (T6T6T) are described. These copolymers are denoted as PEO_x-T6T6T, where x represents the PEO segment length. The PEO_x-T6T6T copolymers have a high T6T6T crystallinity (~85%) and, therefore, high PEO concentrations can be reached (up to 88 wt%) while still obtaining good thermal mechanical properties of the copolymers.

By increasing the PEO segment length, the PEO concentration in the copolymer increases, but at the same time the PEO crystallinity increases. With increasing PEO crystallinity the CO_2 permeability is lowered. Pure PEO has a high crystallinity (71 vol%) and, as a result, a very low CO_2 permeability (12 Barrer at 35 ºC) [17].

A way to increase the PEO content without increasing the PEO crystallinity is by extending short PEO segments (300 or 600 g/mol) with terephthalic units. These copolymers are denoted as $(PEO_x/T)_y$-T6T6T, where the PEO segments are extended with terephthalic units (T) to a desired flexible segment length (y) (Figure 7.1) [18].

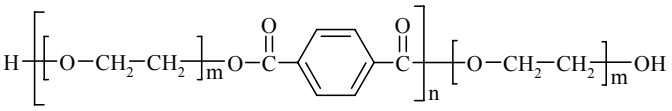

Figure 7.1: Structure of PEO extended with terephthalic units, where m represents the number of repeating ethylene oxide units and n the number of repeating PEO/T units.

The gas permeation properties (CO_2, N_2, He, CH_4, O_2 and H_2) and selectivities of PEO_x-T6T6T and $(PEO_x/T)_y$-T6T6T segmented block copolymers are investigated in a temperature range of -5 to 75 ºC. These copolymers might be interesting for gas separation processes at low temperatures since they have an almost complete phase separated morphology and a suppressed PEO crystallinity.

Background

The flux of a gas through a nonporous polymer membrane, resulting from a pressure difference over the membrane, can be described by Equation 7.1 [19];

$$J = \frac{P}{l} \Delta p \qquad \text{(Equation 7.1)}$$

where J is the gas flux through the membrane ($cm^3(STP)/(cm^2\ s)$), P the permeability coefficient (Barrer, 1 Barrer = 1 x 10^{-10} $cm^3(STP)/(cm^2\ s\ cmHg)$), l the membrane thickness (cm) and Δp the pressure difference over the membrane (cmHg).

Permeation through a nonporous polymer film is generally described by the solution-diffusion model [20]. Here, penetrant gas molecules sorb at the membrane side with the highest concentration of gas molecules, diffuse through the membrane and then desorb from the side with the lowest concentration of gas molecules. The rate-limiting step in this process is diffusion across the polymer film. The gas permeability through a nonporous polymeric material is given as the product of the solubility and the diffusivity;

$$P = S \times D \qquad \text{(Equation 7.2)}$$

where S is the solubility (cm^3(STP)/(cm^3 polymer cmHg)) and D the diffusivity (cm^2/s).
The solubility increases with increasing condensability of the gas (i.e. higher critical temperature) and also depends on the possible interactions with the polymer [19]. For example, the solubility of CO_2 in hydrophilic polymers is generally higher than in more hydrophobic polymers. The diffusivity is enhanced by decreasing molecular size of the gas molecule, increasing chain flexibility and decreasing interactions between the polymer and gas [19].
A measure of the ability of a polymer to separate pure gases is given by the ideal selectivity for gas A over gas B;

$$\alpha_{A/B} = \frac{P_A}{P_B} = \frac{S_A}{S_B} \times \frac{D_A}{D_B} \qquad \text{(Equation 7.3)}$$

where P_A and P_B are the permeability coefficients of pure gas A and B respectively, S_A/S_B the solubility selectivity and D_A/D_B the diffusivity selectivity.

Effect of temperature on gas permeation

The temperature has a large effect on the rate of gas permeability through polymer films. The gas permeability decreases with increasing temperature and its relation with temperature is often described by an Arrhenius type of equation [19];

$$P = P_0 \, e^{\frac{-E_p}{RT}} \qquad \text{(Equation 7.4)}$$

where P_0 is a pre-exponential factor, E_p the activation energy for permeation, R the gas constant and T the temperature. Since the permeability depends on the solubility (S) and diffusivity (D), both parameters must be used for understanding the temperature effect. The activation energy for permeation can be written as [19];

$$E_p = E_d + \Delta H_s \qquad \text{(Equation 7.5)}$$

where E_d represents the activation energy for diffusion and ΔH_s the heat of solution. The activation energy for diffusion is the energy required to create a diffusion gap of sufficient

size to accommodate a penetrant gas molecule. The diffusion of a gas molecule is inversely related to the molecular size and increases with increasing temperature. The kinetic diameter of some gases is given in Table 7.2.

Table 7.2: Kinetic diameter and critical temperature (T_c) of some gas molecules.

Gas molecule	Diameter [Å]	T_c [ºC]
He	2.60	-268
H_2	2.89	-240
CO_2	3.30	31
O_2	3.46	-119
N_2	3.64	-147
CH_4	3.80	-83

The heat of solution is determined by the heat of condensation of the penetrant gas molecule and the heat of mixing of the penetrant gas and polymer segments. The heat of solution can be positive or negative. Gases with a higher critical temperature are more condensable and, therefore, more soluble. The critical temperature of some gases is given in Table 7.2. For non-interactive gases, like N_2, He, CH_4 or H_2, the heat of solution has a small positive value, indicating that the solubility increases slightly with temperature. Polymers containing polar ether groups interact with gases like CO_2, which results in a higher solubility. In this case, the heat of sorption is negative and the solubility decreases with temperature.

For small non-interactive gases the temperature effect on the permeability coefficient is more determined by the diffusivity since the solubility does not change that much with temperature. For large interactive gases like CO_2 the temperature effect on the permeability coefficient is more complex since the two parameters, diffusion and solubility, are opposing.

Experimental

PEO$_x$-T6T6T block copolymers. The PEO$_x$-T6T6T copolymers were synthesised by a polycondensation reaction using PEO segments with a molecular weight (x) of 1000 and 2000 g/mol and T6T6T [13].

(PEO$_x$/T)$_y$-T6T6T block copolymers. The (PEO$_x$/T)$_y$-T6T6T copolymers were synthesised by a polycondensation reaction using PEO segments, which are extended with terephthalic units (T), and T6T6T [18]. The PEO molecular weight (x) (M_n of 300 or 600 g/mol) and the total molecular weight of the flexible segment (y) were varied.

Film preparation: Films of approximately 100 µm thickness have been prepared from dried copolymers using a Lauffer 40 press. The temperature was set approximately 40 ºC above the melting temperature of the copolymer. First, air was removed from the polymer in the mould by quickly pressurising the samples followed by depressurising. This procedure was repeated three times before actually pressing the samples at ~8.5 MPa for 5 min. Subsequently, the samples were cooled to room temperature while maintaining the pressure. To prevent sticking of the polymer onto the metal mould, glass-fibre reinforced PTFE sheets were used (Benetech type B105).

Differential scanning calorimetry (DSC). DSC spectra were recorded on a Perkin Elmer DSC7 apparatus, equipped with a PE7700 computer and TAS-7 software. Dry polymer samples (5 – 10 mg) were heated from -50 to 250 °C at a rate of 20 °C/min. Subsequently, a cooling scan from 250 to -50 °C at a rate of 20 °C/min followed by a second heating scan under the same conditions as the first heating were performed. The melting temperature (T_m) and enthalpy (ΔH_m) were determined from the endothermic peak in the second heating scan.

Gas permeation. The single gas permeation properties of the copolymer were determined with N_2, CH_4, O_2, He, H_2 and CO_2 in a temperature range of -5 to 75 °C. Single gas permeability values were calculated from the steady-state pressure increase in time in a calibrated volume at the permeate side, following the constant volume variable pressure method as described in detail elsewhere [21]. Pure gas selectivity values were calculated from the ratios of single gas permeability values. The experiments yielded an experimental error of <15% which falls within the systematic error for the characterisation equipment used.

Results and discussion

The gas permeation properties of two different copolymer series, the PEO_x-T6T6T and $(PEO_x/T)_y$-T6T6T series, will be discussed [13,18]. The soft phase composition of the copolymers is varied by changing the PEO molecular weight (x) and/or the molecular weight of the total flexible segment (y) (Table 7.3).

Previous DSC results of PEO_x-T6T6T copolymers revealed that the PEO_{600}-T6T6T copolymer has a fully amorphous PEO phase. By extending short PEO_{300} or PEO_{600} segments with terephthalic units, crystallisation of extended polyether segments (PEO/T) is taken place despite the fact that these short PEO prepolymers are amorphous. The hydrophobic terephthalic units are amorphous and dissolved in the PEO phase and, therefore, they might affect the gas permeability of the copolymers.

Thermal properties of PEO_x-T6T6T and $(PEO_x/T)_y$-T6T6T

In Table 7.3 the PEO melting temperature and crystallinity of the PEO_x-T6T6T and $(PEO_x/T)_y$-T6T6T copolymers, determined by DSC measurements, are given. Melting data from the second heating scan were used to exclude the influence of the thermal history of the samples.

Table 7.3: Thermal properties of PEO_x-T6T6T and $(PEO_x/T)_y$-T6T6T copolymers.

Polymer	Conc. T6T6T [wt%]	Conc. PEO [wt%]	Conc. T [wt%]	T_g [1] [°C]	T_m PEO [°C]	ΔH_m PEO [J/g PEO]	X_c [2] PEO [%]	T_m T6T6T [°C]
PEO_{1000}-T6T6T	38.4	61.6	-	-45	-2	20	10	195
PEO_{2000}-T6T6T	23.8	76.2	-	-48	21	53	25	167
$(PEO_{600}/T)_{2500}$-T6T6T	20.0	69.0	11.0	-44	-6	5	3	187
$(PEO_{600}/T)_{5000}$-T6T6T	11.1	74.8	14.1	-43	-3	6	3	171
$(PEO_{300}/T)_{2500}$-T6T6T	19.9	58.4	21.7	-28	-	-	-	205

[1] *Glass transition temperature is determined by dynamic mechanical analysis* [13,18]

[2] *PEO crystallinity (X_c) is calculated by using a PEO melting enthalpy of 197 J/g for 100% crystalline PEO* [22]

The glass transition temperature (T_g) depends on the crosslink density in the copolymer and the soft phase composition. It is assumed that the flexible segment length corresponds to the length between network points. A decrease in the flexible segment length leads to an increase in the network density and an increase in the T_g.

The PEO_x-T6T6T copolymers have a low T_g of the soft phase (Table 7.3), which is slightly higher than the T_g of the PEO prepolymer (-72 to -65 ºC) [23]. The soft phase of $(PEO_x/T)_y$-T6T6T copolymers consists of PEO, terephthalic units and non-crystallised T6T6T segments. Terephthalic units do not crystallise and belong to the amorphous phase [24]. The T_g's of $(PEO_x/T)_y$-T6T6T copolymers are slightly higher (~5 ºC) than those of PEO_x-T6T6T copolymers since the presence of terephthalic units in the soft phase restricts the mobility of the flexible segments. This was also observed for terephthalic extended PTMO-based copolymers with monodisperse T6T6T segments [14,25].

The T_g of $(PEO_{300}/T)_{2500}$-T6T6T is higher than the T_g's of corresponding copolymers with PEO_{600} extended segments (Table 7.3). This might be explained by a combination of a high terephthalic content (21.7 wt%) and a low PEO molecular weight used for the extension (300 g/mol).

By using monodisperse rigid segments the T6T6T crystallinity in the copolymer is high (~85%), indicating that approximately 15% of the T6T6T concentration has not crystallised and is present in the polyether phase. So, PEO_{1000}-T6T6T and PEO_{2000}-T6T6T contain approximately 3.6 and 5.8 wt% non-crystallised T6T6T in the PEO phase. As these concentrations are rather low it is expected that it has no significant influence on the T_g of the soft phase.

In Figure 7.2 the PEO melting temperature and crystallinity of the PEO_x-T6T6T and $(PEO_{600}/T)_y$-T6T6T copolymers are given.

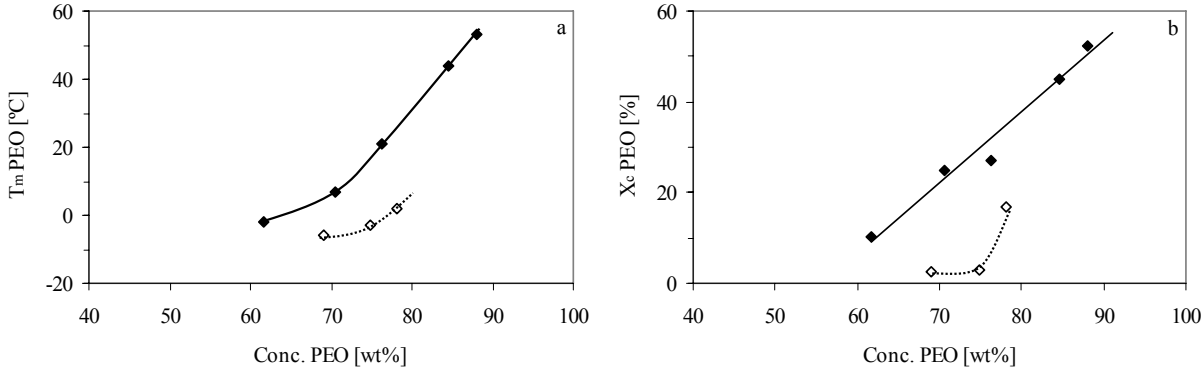

Figure 7.2: (a) PEO melting temperature and (b) PEO crystallinity (X_c) as a function of the PEO concentration: ♦, PEO_x-T6T6T [13]; ◊, $(PEO_{600}/T)_y$-T6T6T [18] .

An increase in PEO segment length of the PEO_x-T6T6T copolymers from 1000 to 4600 g/mol results in an increase in the PEO melting temperature from -2 to 53 ºC [13]. As the PEO_{600}-T6T6T copolymers shows no PEO melting peak it is assumed that the PEO phase in PEO_{600}-T6T6T is amorphous. The PEO crystallinity increases also strongly with increasing the PEO segment length, from 10% for PEO_{1000} to 52% for PEO_{4600}. Copolymers that exhibit PEO segments with a molecular weight >2000 g/mol have a polyether melting peak above room temperature.

Long flexible segments can be prepared, up to a molecular weight of 10,000 g/mol, by extending the PEO segments with terephthalic units. With increasing flexible segment length the polyether crystallinity increases despite using amorphous PEO prepolymers. However, by extending short PEO segments (M_n of 300 or 600 g/mol) the polyether melting temperature and crystallinity are lower than for the PEO_x-T6T6T copolymers at similar PEO concentrations (Figure 7.2). The PEO_{2000}-T6T6T and $(PEO_{600}/T)_{5000}$-T6T6T have more or less the same PEO concentration, 76.2 and 74.8 wt% respectively, but the PEO melting temperature of $(PEO_{600}/T)_{5000}$-T6T6T is approximately 24 ºC lower. Also the PEO crystallinity is much lower (25 and 3% respectively).

The DSC results of $(PEO_{300}/T)_{2500}$-T6T6T show no PEO melting peak and, therefore, it is assumed that the PEO phase is completely amorphous.

The T6T6T melting temperature of the copolymers depends strongly on the polyether concentration [13]. A decrease in melting temperature with increasing PEO concentration can be explained by the solvent effect theory proposed by Flory, which states that the soft phase acts as a solvent for the crystalline phase [26,27]. The presence and concentration of terephthalic units in the soft phase result in a less reduced T6T6T melting temperature of the copolymer and is discussed in more detail in Chapter 3. Most likely, terephthalic units present in the soft phase slightly restrict the function of the PEO phase as solvent for the crystalline phase.

Effect of the temperature on gas permeation properties

Figure 7.3 shows the influence of the temperature on the gas permeation properties of PEO_{2000}-T6T6T copolymers.

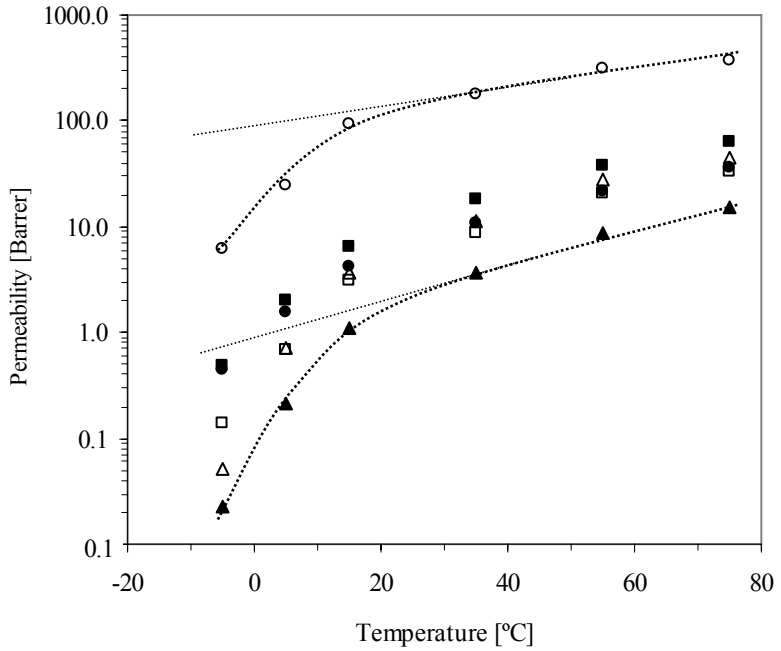

Figure 7.3: Gas permeability as a function of the temperature for PEO_{2000}-T6T6T: ○, $P(CO_2)$; ■, $P(H_2)$; ●, P (He); Δ, $P(CH_4)$; □, $P(O_2)$; ▲, $P(N_2)$.

All gasses show a linear increase in permeability with increasing temperature in the region from 30 to 75 °C. When the temperature is below the PEO_{2000} melting temperature (~20 ºC) the gas permeability is strongly reduced and the data no longer show a linear relation. The presence of crystalline PEO domains reduces the chain mobility of the amorphous segments and increases the size-sieving ability of the copolymer.

In Figure 7.4a the CO_2 permeabilities of PEO_{1000}-T6T6T and PEO_{2000}-T6T6T copolymers are compared at different temperatures and in Figure 7.4b the CO_2 permeabilities of PEO_{2000}-T6T6T is compared to $(PEO_{600}/T)_{5000}$-T6T6T.

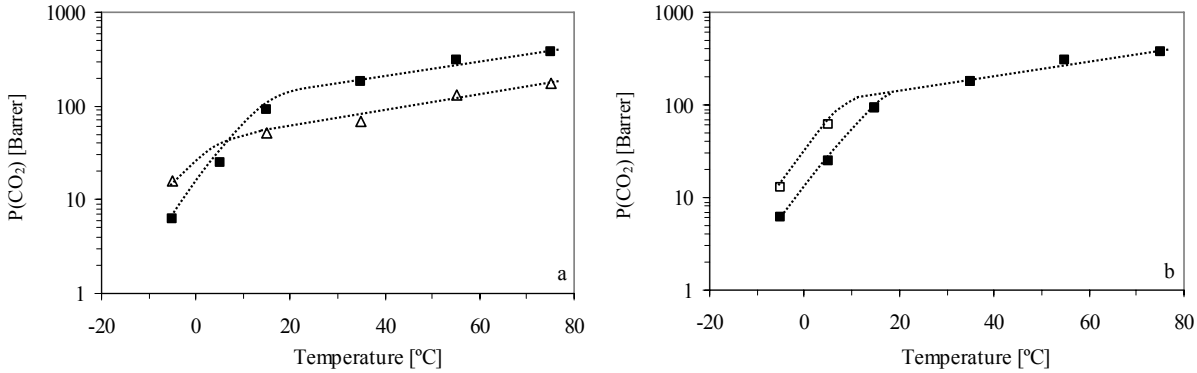

Figure 7.4: CO_2 permeability as a function of the temperature: (a) ■, PEO_{2000}-T6T6T and Δ, PEO_{1000}-T6T6T; (b) □, $(PEO_{600}/T)_{5000}$-T6T6T and ■, PEO_{2000}-T6T6T.

The PEO_{1000}-T6T6T copolymer has a lower CO_2 permeability compared to PEO_{2000}-T6T6T, which is due to a lower PEO concentration. A linear increase in CO_2 permeability of PEO_{1000}-T6T6T with increasing temperature is observed when the temperature is above -2 ºC since the PEO phase is completely amorphous above this temperature. The PEO_{2000}-T6T6T copolymers show a linear increase in CO_2 permeability with temperature above ~20 ºC. Below these temperatures the permeability is strongly reduced due to the presence of a semi-crystalline PEO phase. Therefore, PEO_{1000}-T6T6T is more suitable for applications requiring a relatively high CO_2 permeability at low temperatures than PEO_{2000}-T6T6T.

Above approximately 20 ºC, the CO_2 permeability of PEO_{2000}-T6T6T is comparable to $(PEO_{600}/T)_{5000}$-T6T6T since both copolymers have almost comparable PEO concentrations (Figure 7.4b). As the PEO melting temperature of $(PEO_{600}/T)_{5000}$-T6T6T is lower, compared to PEO_{2000}-T6T6T, the CO_2 permeability is higher at low temperatures.

At temperatures where the PEO phase is completely amorphous, the CO_2 permeabilities of $(PEO_{600}/T)_{2500}$-T6T6T and $(PEO_{300}/T)_{2500}$-T6T6T are lower than those of PEO_{2000}-T6T6T and $(PEO_{600}/T)_{5000}$-T6T6T since the PEO concentration is lower (data not given). However, at low temperatures the $(PEO_{600}/T)_{2500}$-T6T6T has the highest CO_2 permeability (29 Barrer at -5 ºC) as this copolymer has the lowest PEO melting temperature.

So, it is possible to create PEO-based segmented block copolymers that have a relatively high CO_2 permeability at low temperatures by partly suppressing the PEO crystallinity by using terephthalic extended PEO segments.

For each gas, the activation energy for permeation of PEO-T6T6T copolymers is determined using the obtained gas permeation properties at a temperature region were the PEO phase is completely amorphous (30 to 75 ºC). The activation energy for permeation (E_p) depends on the activation energy for diffusion and the heat of solution. In Table 7.4 the obtained activation energies for permeation of different gases through PEO_x-T6T6T and $(PEO_{600}/T)_y$-T6T6T copolymers are given.

Table 7.4: Activation energies for permeation (E_p in kJ/mol) of different gases through PEO_x-T6T6T and $(PEO_{600}/T)_y$-T6T6T copolymers (the kinetic diameter of the gases is given between brackets).

Polymer	CO_2 (3.30 Å)	He (2.60 Å)	H_2 (2.89 Å)	O_2 (3.46 Å)	N_2 (3.64 Å)	CH_4 (3.80 Å)
PEO_{1000}-T6T6T	21.2	28.6	28.2	29.7	32.1	30.7
PEO_{2000}-T6T6T	16.6	26.9	27.9	30.0	32.2	31.0
$(PEO_{600}/T)_{2500}$-T6T6T	22.9	31.8	33.8	41.1	45.3	41.2
$(PEO_{600}/T)_{5000}$-T6T6T	24.2	32.9	34.9	39.6	43.9	43.0

The E_p values for H_2 and He are lower than those for O_2, N_2 and CH_4 since the activation energies for diffusion are lower for smaller gases. The E_p value for CO_2 is lower than the value for O_2, N_2 and CH_4, which is due to difference in the sorption enthalpies between the gases.

The E_p values for the different gases through PEO_{1000}-T6T6T and PEO_{2000}-T6T6T are comparable. The E_p values for small gas molecules, like H_2 and He, are between 26.9 and 28.6 kJ/mol, while larger gases have E_p values between 29.7 and 32.2 kJ/mol. The E_p for CO_2 through PEO_{1000}-T6T6T is slightly higher than through PEO_{2000}-T6T6T.

The activation energies for permeation through $(PEO_{600}/T)_{2500}$-T6T6T and $(PEO_{600}/T)_{5000}$-T6T6T copolymers are also comparable. The E_p values of copolymers containing terephthalic extended PEO segments are slightly higher than for PEO_x-T6T6T copolymers (Table 7.4).

Effect of the polymer composition on the gas permeation properties

A standard temperature for evaluating the gas permeabilities of polymers is 35 °C. At this temperature, the PEO phase of the PEO-T6T6T copolymers is completely amorphous. When plotting the CO_2 permeability as a function of the PEO concentration of all copolymers studied, one relation is found (Figure 7.5a). This might suggest that the PEO molecular weight and the presence of terephthalic units in the PEO phase of these segmented block copolymers have hardly any influence on the CO_2 permeability.

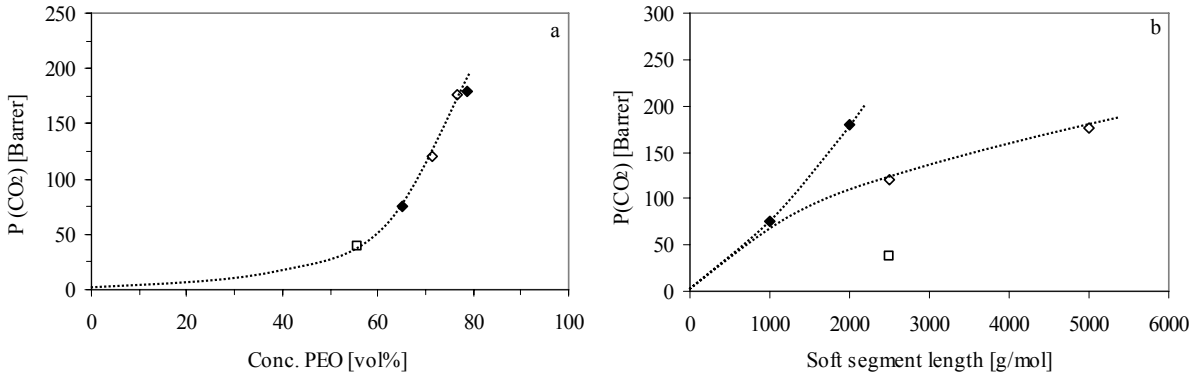

Figure 7.5: CO_2 permeability (35 ºC) as a function of (a) the PEO concentration and (b) the soft segment length: ♦, PEO-T6T6T; ◊, $(PEO_{600}/T)_y$-T6T6T; □, $(PEO_{300}/T)_{2500}$-T6T6T.

Previous studies on PEO-PBT segmented block copolymers revealed that the CO_2 permeability depends on the PEO molecular weight and the amount of dissolved rigid segments in the soft phase [9]. An increase of the PEO molecular weight results in a decreased network density of the copolymer and an increased chain flexibility of the PEO segments. Furthermore, it is expected that an increased amount of dissolved rigid segments in the PEO phase decreases the chain flexibility.

By plotting the CO_2 permeability of PEO_x-T6T6T and $(PEO_x/T)_y$-T6T6T copolymers as a function of the molecular weight of the total flexible segment (PEO or PEO/T), the effect of the network density and the effect of dissolved terephthalic units in the PEO phase can be shown (Figure 7.5b). Here, it is assumed that the crystalline T6T6T is impermeable for CO_2. An increase in the total molecular weight of the flexible segments results in an increased CO_2 permeability. However, at the same flexible segment length (i.e. the same network density) the CO_2 permeabilities decrease in the order of PEO_x-T6T6T > $(PEO_{600}/T)_y$-T6T6T > $(PEO_{300}/T)_y$-T6T6T. This might be explained by the present of terephthalic units in the PEO phase, which lowers the PEO chain flexibility. Furthermore, these results suggest that the

maximally attainable CO_2 permeability for copolymers is higher when PEO segments are used that are completely amorphous and are not extended with terephthalic units.
However, one has to keep in mind that there are only four polymers investigated and to verify these statements more extensive research has to be performed.

Effect of the polymer composition on gas selectivity

In Table 7.5 the gas permeabilities and gas selectivities at 35 ºC for the PEO_x-T6T6T and $(PEO_{600}/T)_y$-T6T6T copolymers are given. At this temperature the PEO phase of the copolymers is completely amorphous.

Table 7.5: Gas permeabilities and selectivities at 35 ºC of PEO_x-T6T6T and $(PEO_{600}/T)_y$-T6T6T copolymers.

Polymer	Conc. PEO	Permeability [Barrer]						Selectivity [-]		
	[wt%]	CO_2	He	H_2	O_2	N_2	CH_4	CO_2/H_2	CO_2/O_2	CO_2/N_2
PEO_{1000}-T6T6T	61.6	75	6.3	10.4	4.7	1.8	5.5	7.2	16	41
PEO_{2000}-T6T6T	76.2	180	10.9	17.9	8.8	3.6	11.3	10	21	49
$(PEO_{600}/T)_{2500}$-T6T6T	69.0	121	9.4	14.6	6.2	2.5	7.1	8.3	20	49
$(PEO_{600}/T)_{5000}$-T6T6T	74.8	176	12.2	19.6	8.7	3.3	10.2	9.0	20	53

The CO_2/H_2 selectivity is mainly influenced by the solubility selectivity (CO_2 is easier condensable than H_2). Polymers containing polar PEO segments have interactions with CO_2 that enhance the solubility selectivity. Besides, these copolymers have a very weak size-sieving ability since the amorphous PEO segments are highly flexible. The CO_2/H_2 selectivity for PEO-T6T6T copolymers is around 7.2 to 10 and almost independent of the soft phase composition.
The CO_2/O_2 selectivity is important for packaging materials of fruit and vegetables. The PEO-T6T6T copolymers have a CO_2/O_2 selectivity of approximately 20 at 35 ºC and this selectivity is independent of the soft phase composition.
The PEO-based copolymers are more permeable for CO_2 than CH_4 or N_2, since the diffusivity and solubility of CO_2 are higher (smaller molecule and more easy to condensate). The CO_2/N_2 selectivity of all the PEO-T6T6T copolymers studied is almost similar (~48), while the CO_2 permeabilities vary significantly. The CO_2/CH_4 selectivity at 35 ºC of PEO-T6T6T copolymers is also more or less a constant value, approximately 16. The soft phase composition, i.e. the presence of terephthalic units or the PEO length, seems to have only little effect on the CO_2/N_2 selectivity. Commercially available PEO-based segmented block

copolymers exhibit more or less the same CO_2/N_2 selectivity, approximately 50 (Table 7.1). The CO_2 permeability of PEO_{1000}-T6T6T is lower than expected.

Effect of the temperature on gas selectivity

The temperature effect on the pure gas selectivities is studied for the PEO_{1000}-T6T6T and PEO_{2000}-T6T6T copolymers at a temperature range of -5 to 75 ºC. A decrease in temperature from 75 to -5 °C results in an increase in CO_2/H_2 selectivity from 5.2 to 19.7 for PEO_{1000}-T6T6T (Figure 7.6). At the same time the CO_2 permeability decreases from 193 to 18 Barrer.

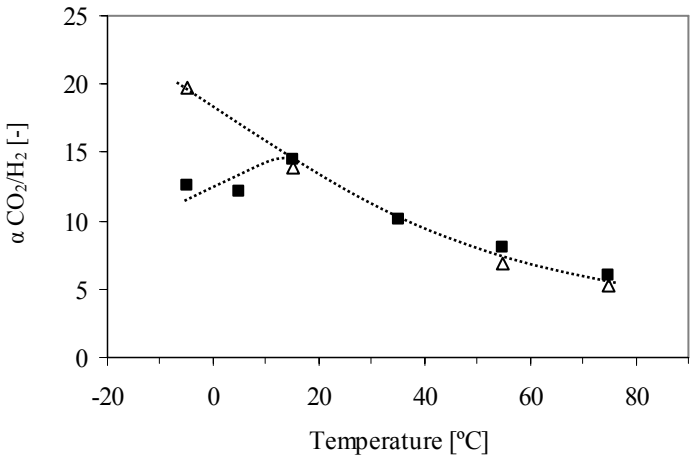

Figure 7.6: CO_2/H_2 selectivity as a function of the temperature: Δ, PEO_{1000}-T6T6T; ■, PEO_{2000}-T6T6T.

The PEO_{2000}-T6T6T copolymer also shows an increase in CO_2/H_2 selectivity when decreasing the temperature to approximately 20 ºC. At lower temperatures a PEO semi-crystalline phase is present and the gas permeability and CO_2/H_2 selectivity are reduced (Figure 7.6). This lowering of the CO_2/H_2 selectivity might be due to a more pronounced size-sieving ability of the copolymer when crystalline PEO domains are present in the soft phase. A similar behavior is observed for the CO_2/He selectivity for both copolymers.

The CO_2/H_2 selectivity of PEO-T6T6T copolymers is mainly determined by the temperature. The polymer composition has no influence on the selectivity, indicating that the copolymer has a well phase separated polymer morphology and a rather pure PEO phase. This behaviour is not observed for PEO-PBT [9] or PEBAX [1] segmented block copolymers. The CO_2/H_2 selectivity of these copolymers depends on both the temperature as well as the polymer composition (i.e. the PEO molecular weight and concentration).

The influence of the temperature on the CO_2 selectivity over larger gases, like N_2, and CH_4, is also examined for PEO_{1000}-T6T6T and PEO_{2000}-T6T6T copolymers. The PEO-based copolymers are more permeable for CO_2 than CH_4 or N_2 since the diffusivity and solubility for CO_2 are higher. In Figure 7.7a the CO_2/N_2 selectivity for both copolymers is given as a function of the temperature.

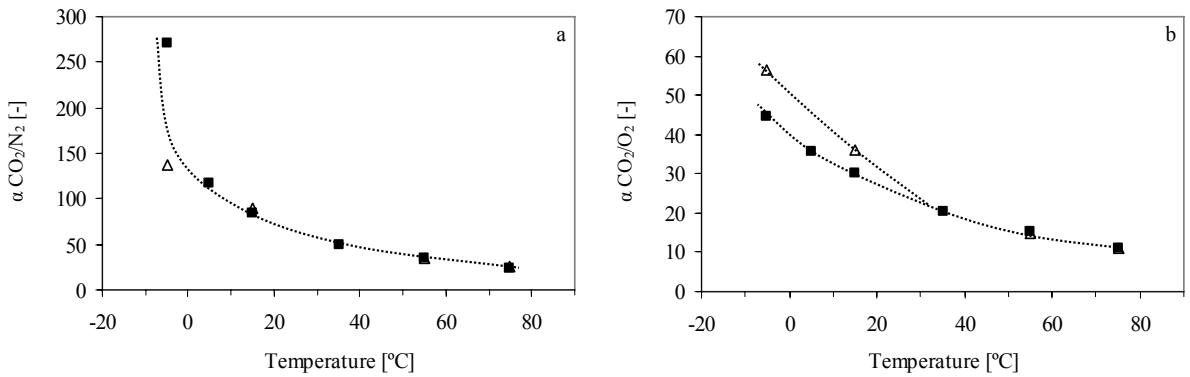

Figure 7.7: (a) CO_2/N_2 and (b) CO_2/O_2 selectivity as a function of the temperature: Δ, PEO_{1000}-T6T6T; ■, PEO_{2000}-T6T6T.

As expected for PEO-based copolymers, the CO_2/N_2 selectivity increases with decreasing temperature. Despite the fact that PEO_{2000}-T6T6T contains a semi-crystalline PEO phase at temperatures below ~20 ºC the CO_2/N_2 selectivity remains high. The size-sieving ability of copolymers is more dominant when crystalline PEO domains are present. As N_2 and CH_4 molecules are larger than CO_2, the gas permeability of these gases is more restricted by the presence of crystalline PEO domains. Consequently, the CO_2/N_2 and CO_2/CH_4 selectivities increase when a semi-crystalline PEO phase is present.

At temperatures above ~20 ºC the CO_2/O_2 selectivity of PEO_{1000}-T6T6T is comparable to that of PEO_{2000}-T6T6T since the PEO phase of both copolymers is amorphous (Figure 7.7b). When the temperature decreases, the PEO_{1000}-T6T6T shows a slightly higher CO_2/O_2 selectivity than PEO_{2000}-T6T6T. The kinetic diameter of O_2 is almost comparable to that of CO_2. Therefore, the size-sieving ability of the PEO crystalline domains affects the CO_2 as well as the O_2. Commercially available PEBAX materials have a CO_2/O_2 selectivity at 23 ºC of 9.6 and 11.1 for MV3000 and MV6100 respectively [28]. The PEO-T6T6T copolymers have a much higher CO_2/O_2 selectivity, approximately 30, at the same temperature.

In this paper an attempt is made to evaluate whether well phase-separated PEO-T6T6T segmented block copolymers are interesting materials for gas separation applications. However, more extensive research is necessary for this evaluation. It might be advisable to replace the hydrophobic terephthalic units by a more polar extender to improve the CO_2 permeability of the segmented block copolymers.

Conclusion

PEO-based segmented block copolymers are interesting membrane materials for gas separation applications since they have a high CO_2 permeability and CO_2/N_2 or CO_2/H_2 selectivity values. However, PEO has a strong tendency for crystallisation and with increasing PEO crystallinity the gas permeability is reduced. The gas permeation properties at low temperatures of PEO-based copolymers can be improved by suppressing the PEO crystallinity.

In general, the phase separation in segmented block copolymers is incomplete and a high concentration of non-crystallised rigid segment is incorporated in the soft phase. The crystallinity of the rigid segments in the copolymer is improved when monodisperse crystallisable segments (T6T6T) are used. These PEO-T6T6T copolymers exhibit an almost complete phase separated structure and only a small amount of non-crystallised T6T6T is present in the PEO phase. An increased PEO segment length results in an increased PEO crystallinity of the copolymer. A way to create long flexible segments while the PEO crystallisation is partly suppressed is by extending low molecular weight PEO segments (300 or 600 g/mol) with terephthalic units (T).

When the PEO phase is completely amorphous, the gas permeation properties are similar for PEO-T6T6T and PEO/T-T6T6T copolymers containing similar PEO concentrations. At low temperatures, the PEO/T-T6T6T copolymers have higher gas permeabilities than the PEO-T6T6T copolymers since the PEO crystallinity is partly suppressed.

An increase in CO_2 permeability from 75 to 180 Barrer (35 ºC), with increasing PEO concentration from 61.6 to 76.2 wt%, is observed for both PEO-T6T6T and PEO/T-T6T6T copolymers.

An increase in the total molecular weight of the flexible segments results in an increased CO_2 permeability through the copolymer. However, at the same flexible segment length (i.e. the same network density) the CO_2 permeability of $(PEO_x/T)_y$-T6T6T is lower than that of PEO_x-

T6T6T, which might be explained by the presence of terephthalic units in the PEO phase that lower the chain flexibility of the PEO segments.

For both the PEO-T6T6T and PEO/T-T6T6T copolymers the CO_2/N_2, CO_2/H_2 and CO_2/O_2 selectivities at 35 ºC are almost similar, 48, 8.6 and 20 respectively. The CO_2/X selectivity of PEO-T6T6T and PEO/T-T6T6T copolymers, where X represents N_2, He, CH_4, O_2 or H_2, increases with decreasing temperature. When the copolymers contain a PEO semi-crystalline phase the CO_2/H_2 and CO_2/He selectivities are reduced. This reduction is probably due to the increased size-sieving ability of the copolymer when crystalline PEO domains are present in the soft phase. The presence of a semi-crystalline PEO phase has no adverse effect on the CO_2 selectivity over larger gases, like N_2, O_2 and CH_4.

References

1. Bondar, V.I., Freeman, B.D. and Pinnau, I., *J. Polym. Sci., Part B: Polym. Phys.* **2000**, 38, p. 2051-2062.
2. Lin, H. and Freeman, B.D., *J. Mol. Struct.* **2005**, 739, p. 57-74.
3. Barbi, V., Funari, S.S., Gehrke, R., Scharnagl, N. and Stribeck, N., *Macromolecules* **2003**, 36, p. 749-758.
4. Bondar, V.I., Freeman, B.D. and Pinnau, I., *J. Polym. Sci., Part B: Polym. Phys.* **1999**, 37, p. 2463-2475.
5. Kim, J.H., Ha, S.Y. and Lee, Y.M., *J. Membr. Sci.* **2001**, 190, p. 179-193.
6. Okamoto, K., Fujii, M., Okamyo, S., Suzuki, H., Tanaka, K. and Kita, H., *Macromolecules* **1995**, 28, p. 6950-6956.
7. Yoshino, M., Ito, K., Kita, H. and Okamoto, K., *J. Polym. Sc., Part B: Polym. Phys.* **2000**, 38, p. 1707-1715.
8. Damian, C., Espuche, E., Escoubes, M., Cuney, S. and Pascault, J.P., *J. Appl. Polym. Sci.* 65, p. 2579-2587.
9. Metz, S.J., Mulder, M.H.V. and Wessling, M., *Macromolecules* **2004**, 37, p. 4590-4597.
10. Petropoulos, J.H., *J. Polym. Sc., Polym. Phys. Ed* **1985**, 23, p. 1309-1324.
11. Van der Schuur, M., Ph.D. Thesis '*Poly(propylene oxide) based segmented blockcopolymers*', University of Twente, The Netherlands **2004**.
12. Biemond, G.J.E., Ph.D. Thesis '*Hydrogen bonding in segmented block copolymers*', University of Twente, The Netherlands **2006**.
13. Chapter 2 of this thesis.
14. Krijgsman, J., Husken, D. and Gaymans, R.J., *Polymer* **2003**, 44, p. 7573-7588.
15. Harrell, L.L., *Macromolecules* **1969**, 2, p. 607-612.
16. Miller, J.A., Lin, S.B., Hwang, K.K.S., Wu, K.S., Gibson, P.E. and Cooper, S.L., *Macromolecules* **1985**, 18, p. 32-44.
17. Lin, H. and Freeman, B.D., *J. Membr. Sci.* **2004**, 239, p. 105-117.
18. Chapter 3 of this thesis.
19. Mulder, M., in *Basic principles of membrane technology*, Kluwer Academic Publishers, Dordrecht **1991**.
20. Wijmans, J.G. and Baker, R.W., *J. Membr. Sci.* **1995**, 107, p. 1-21.
21. Bos, A., Punt, I.G.M., Wessling, M. and Strathmann, H., *J. Polym. Sci., Polym. Phys. Ed.* 36, p. 1547-1556.
22. Wunderlich, B., in *Thermal Analysis of Polymeric Materials*, Springer, Berlin Heidelberg New York **2005**.
23. Bailey, J.F.E. and Koleske, J.V., in *Poly(ethylene oxide)*, Acedemic Press, New York **1976**.
24. Niesten, M.C.E.J., Feijen, J. and Gaymans, R.J., *Polymer* **2000**, 41, p. 8487-8500.
25. Niesten, M.C.E.J., ten Brinke, J.W. and Gaymans, R.J., *Polymer* **2001**, 42, p. 1461-1469.
26. Flory, P.J., *Trans. Faraday Soc.* **1955**, 51, p. 848.
27. Flory, P.J., in *Principles of polymer chemistry*, Cornell University Press, Ithaca **1967**.
28. PEBAX General Brochure; PEBAX® Breathable Film Grades.

Chapter 8

Water vapour transmission through polyether-based segmented block copolymers

Abstract

In this chapter the rate of water vapour transmission (WVT) through monolithic films of segmented block copolymers with flexible polyether segments and monodisperse crystallisable amide segments will be discussed. The polyether phase of the copolymers consists of hydrophilic poly(ethylene oxide) (PEO) and/or hydrophobic poly(tetramethylene oxide) (PTMO) segments. The monodisperse crystallisable segments (T6T6T) are based on dimethyl terephthalate (T) and hexamethylenediamine (6).

The WVT was determined according to the ASTM E96BW standard, also known as the inverted cup method. By using this method there is direct contact between the polymer film and the water in the cup. The WVT experiments were performed in a climate-controlled chamber at a temperature of 30 ºC and a relative humidity of 50%.

A linear relation was found between the WVT and the reciprocal film thickness of polyether-T6T6T segmented block copolymers. The WVT of a 25 µm-thick film of $PTMO_{2000}$-T6T6T or PEO_{2000}-T6T6T copolymers is 3.1 and 153 kg/m^{2}d respectively. The WVT values of polyether-T6T6T copolymers increase exponentially with the PEO content or volume fraction of water. The volume fraction of water in the copolymers depends on the PEO concentration. The number of water molecules per ethylene oxide unit (H_2O/EO) was related to the crosslink density in the copolymer and the presence of hydrophobic units in the soft phase (like PTMO or terephthalic units).

Introduction

Segmented block copolymers are often used in breathable film applications in markets like construction, medical, hygiene, textile and food packaging. A breathable film is characterised by a high permeability toward water vapour and is impermeable for water.

One type of breathable film is a monolithic (homogeneous) film made from a hydrophilic polymer. These films have good mechanical properties in dry conditions, are non-fouling, and have a selective permeability. However, hydrophilic polymers often swell in the presence of water and with an increased amount of absorbed water the mechanical properties like modulus and fracture stress are reduced [1-6].

The transport of water vapour molecules through a monolithic film is usually described by the solution-diffusion model [7]. Water sorbed at the film side with the highest concentration of water molecules. Subsequently, water diffuses through the film and desorbs from the side with the lowest concentration of water molecules. The driving force for diffusion is the concentration difference across the film. The transport of water vapour molecules through a monolithic film can be described by Fick's first law (Equation 8.1) [8];

$$J = -D\frac{da}{dx} \qquad \text{(Equation 8.1)}$$

where J is the water vapour flux through the film, D is the diffusion coefficient or diffusivity and da/dx the activity gradient over the film with a certain thickness (x).

According to the solution-diffusion model, the permeability of water vapour through a polymer film is the product of diffusivity and solubility. In hydrophilic polymers these parameters are strongly influenced by the interaction between water and the polar groups in the polymer through hydrogen bonding.

Solubility is a thermodynamic parameter that represents a measure for the amount of water sorbed by the polymer film [8]. With increasing number of polar groups in the polymer the solubility for water increases. However, this relation is influenced by other factors like the accessibility of the polar groups for water molecules and the degree of crystallinity of the polymer matrix [9].

Diffusivity is a kinetic parameter that indicates how fast water vapour molecules are transported through the polymer film [8]. Generally, the water vapour diffusivity of polar polymers increases with increasing water sorbed in the polymer due to the plasticizing effect.

However, when clustering of water molecules in the polymer takes place, the diffusivity decreases [8-11]. Since water molecules experience strong hydrogen bonding with each other, the molecules can form clusters during diffusion, which results in reduced mobility.
Adriaensens et al. reported that in polyamide copolymers the diffusion coefficient of water increases linearly with the water absorption of the copolymer [12], indicating that water absorption has a direct effect on both the water solubility and diffusivity.

The breathability of a polymer film can be defined as the ability to pass water vapour. Generally, the rate of water vapour transmission (WVT) is used as a measure for the breathability. The WVT can be expressed in the measuring unit kg/m^2d, meaning the amount of water vapour transported through one square meter of film in one day.
A large variety of methods is available for determining the WVT [13]. There are many differences in test conditions between the methods, like humidity on both sides of the film, temperature, indirect or direct contact of the film with water, etc. The test methods and conditions are often adjusted to the demands of the application market of the film. It was found that the WVT results obtained with different test methods were not comparable [13,14], however, it is possible to make a correlation between these WVT results [13,14].
The ASTM E96 standard gives a description of different methods that can be used for the measurements of WVT through polymer films. Two of these methods, the E96BW (inverted cup) and the E96B (upright cup) method, are frequently applied. By using the inverted cup method the water in the cup is in direct contact with the film, while with the upright cup method an air layer between the film and water in the cup exists. This air layer acts as an extra resistant boundary layer that affects the WVT. Consequently, the WVT values obtained with the E96BW method are significantly higher than when the E96B method is applied. To obtain WVT values that are characteristic for the polymer, the diffusion of water vapour through the film must be the main rate determining step. Therefore, the E96BW method is more suitable than the E96B method as the WVT values obtained by the E96B method are limited by a resistant air layer. The ASTM E96BW is not suitable for measuring the WVT of highly permeable thin films since the resistance of the boundary layers becomes more dominant than the diffusion of water vapour through the film [15,16].

There are several polyether-based segmented block copolymers available, containing urethane [10,17-19], ester [20,21] or amide groups [22], which can be used for (monolithic) breathable film applications. A hydrophilic polyether segment is suitable for monolithic breathable film

applications. The polyether hydrophilicity increases in the order of poly(tetramethylene oxide) (PTMO), poly(propylene oxide) (PPO) and poly(ethylene oxide) (PEO).
Metz et al. observed an increase in the water vapour flux through poly(ether ester) segmented block copolymers (PEO-PBT) with increasing PEO concentration [11]. Furthermore, the diffusion coefficient for PEO-PBT decreases with increasing water vapour concentration in the film due to the presence of water clusters [11].

In Table 8.1 the WVT of some commercially available segmented block copolymers are given [15,22]. The WVT of these materials were measured using the ASTM E96BW method at a temperature of 38 ºC, a relative humidity of 50% and a film thickness of 25 µm. The use of a more hydrophilic polyether segment resulted in increased water absorption (WA) and WVT.

Table 8.1: WVT of some commercially available segmented block copolymers (ASTM E96BW, T = 38 ºC, RH = 50%) [15,22,23].

Polymer	Trade name (company)	Type of polyether	WA [wt%]	WVT (25 µm) [kg/m^{2}d]
poly(ether ester)	Arnitel PM380 [1] (DSM)	PPO	5.7 [1]	4.0
poly(ether ester)	Arnitel EM400 [1] (DSM)	PTMO	0.5 [1]	1.9
poly(ether amide)	PEBAX 3533 [2] (Arkema)	PTMO	1.2 [2]	2.5
poly(ether amide)	PEBAX MV1041 [2] (Arkema)	PEO	12	>10
poly(ether amide)	PEBAX MV3000 [2] (Arkema)	PEO	-	20
poly(ether amide)	PEBAX MV1074 [2] (Arkema)	PEO	48	>20

[1] *determined according to ISO62*
[2] *determined according to ASTM D570*

In general, the crystallinity of the rigid segments of these PEO-based segmented block copolymers is rather low (~30%). This means that a relatively high amount of rigid segments is required to obtain good mechanical properties of the copolymer. Consequently, the PEO concentration decreases and thus the water vapour transmission is reduced. Moreover, a large amount of non-crystallised hydrophobic rigid segment is present in the polyether phase, which can affect the rate of water vapour transmission.
With the use of short monodisperse crystallisable segments one can avoid liquid-liquid demixing and improve the crystallinity of the rigid segments in the copolymer [24-26]. As a result, segmented block copolymers are obtained that have a good phase separation between the rigid and flexible segments and, therefore, contain a low concentration of non-crystallised rigid segment in the soft phase.

This thesis reports the synthesis and characterisation of segmented block copolymers with polyether flexible segments and monodisperse crystallisable tetra-amide segments (T6T6T) will be discussed. The polyether phase consists of hydrophilic PEO and/or hydrophobic PTMO segments. The T6T6T segments are based on dimethyl terephthalic (T) and hexa-methylenediamine (6) [27]. The polyether-T6T6T copolymers have a high T6T6T crystallinity (~85%). A high polyether concentration can be reached, while still obtaining good mechanical properties of the copolymer. The influence of the soft phase composition of the polyether-T6T6T copolymers on the rate of water vapour transmission (WVT) is studied. The WVT is determined according to the ASTM E96BW standard, using a temperature of 30 ºC and a relative humidity of 50%.

Three different copolymer series have been studied, which vary in the PEO concentration, the hydrophobic segment concentration (PTMO or terephthalate units) and the T6T6T concentration. The first polymer series was based on a mixture of hydrophilic PEO and hydrophobic PTMO segments and is denoted as $PEO_x/PTMO_z$-T6T6T [28]. The molecular weights of PEO (x) and PTMO (z) are varied as well as the PEO/PTMO ratio. The second polymer series, denoted as PEO_x-T6T6T, is based on PEO flexible segments with varying PEO molecular weight (x) (1000 to 3400 g/mol) [29]. The third polymer series contains PEO segments that are extended with terephthalic units (T) to create long flexible polyether segments that will not phase separate by liquid-liquid demixing. These copolymers are denoted as $(PEO_x/T)_y$-T6T6T, where the PEO molecular weight (x) and the total molecular weight of the flexible segments (y) are varied [30].

Experimental

$PEO_x/PTMO_z$-T6T6T block copolymers. The $PEO_x/PTMO_z$-T6T6T block copolymers were synthesised by a polycondensation reaction using a mixture of PEO and PTMO segments and T6T6T [28]. The PEO molecular weight (x) was varied from 600 to 8000 g/mol and the PTMO molecular weight (z) from 650 to 2900 g/mol.

PEO_x-T6T6T block copolymers. The PEO_x-T6T6T copolymers were synthesised by a polycondensation reaction using PEO segments with a molecular weight (x) of 1000 – 3400 g/mol and T6T6T [29].

$(PEO_x/T)_y$-T6T6T block copolymers. The $(PEO_x/T)_y$-T6T6T copolymers were synthesised by a polycondensation reaction using PEO segments that are extended with terephthalic units (T) and T6T6T [30]. The PEO molecular weight (x) and the total molecular weight of the flexible segment (y) were varied.

Film preparation: Films of approximately 100 µm thicknesses were prepared from dried copolymers using a Lauffer 40 press. The temperature was set approximately 40 ºC above the melting temperature of the copolymer. First, air was removed from the polymer in the mould by quickly pressurising the samples followed by depressurising. This procedure was repeated three times before actually pressing the samples at ~8.5 MPa for

5 min. Subsequently, the samples were cooled to room temperature while maintaining the pressure. It was possible to vary the film thickness from 50 – 300 μm by using metal moulds of appropriate thickness. To prevent sticking of the polymer onto the metal mould, glass-fibre reinforced PTFE sheets were used (Benetech type B105). The dry film thickness was the average measured on ten different places.

Water absorption (WA). The equilibrium water absorption was measured using pieces of injection-moulded polymer bars. The samples were placed in a desiccator filled with demineralised water for 4 wks at room temperature. The water absorption was defined as the weight gain of the polymer according to;

$$WA = \frac{m - m_0}{m_0} \times 100\% \quad [wt\%] \quad \text{(Equation 8.2)}$$

where m_0 is the weight of dry sample and m the weight of the sample after conditioning to equilibrium. The measurements were performed in duplicate. After 4 wks the samples were dried and m_0 was measured again to exclude weight loss during the experiment. The volume fraction of water in the polymer (φ_{water}) was determined by using a PEO, PTMO, DMT and T6T6T density of 1.13, 0.98, 1.20 and 1.32 g/cm^3 respectively [9].

Rate of water vapour transmission (WVT). The WVT through films was determined according to the ASTM E96BW standard (inverted cup method). A cup filled with demineralised water (250 ml) was sealed with a completely hydrated polymer film and placed upside-down in a climate-controlled chamber. In this chamber the temperature was 30 ± 1 ºC, the relative humidity was 50 ± 2% and there was a constant air circulation. A sealant (butyl rubber) was used to prevent leakage of water when the cup was placed in the inverted position. After steady-state conditions were reached (~2 hours), the weight of the cup was periodically measured (periods of ~2 h) for at least 5 times. The WVT was calculated using the following Equation;

$$WVT = \frac{(G/t)}{A} \quad [kg/m^2 d] \qquad \text{(Equation 8.3)}$$

where G is the weight loss (kg), t the time in days (d), A the test area of the cup (0.00503 m^2) and WVT the rate of water vapour transmission (kg/m^{2}d). The WVT experiments were performed in duplicate.

Results and discussion

In this chapter several series of polyether-T6T6T segmented block copolymers were investigated to obtain more insight in the effect of the type of polyether, the polyether molecular weight and the polyether concentration on the WVT. The three polymer series that will be discussed are PEO$_x$-T6T6T, (PEO$_x$/T)$_y$-T6T6T and PEO$_x$/PTMO$_z$-T6T6T.

The WVT measurements were performed using the inverted cup method described by the ASTM E96BW standard, where there is direct contact between water in the cup and the polymer film. For the calculation of the WVT the thickness of the dry film was used.

The setup was allowed to reach steady-state conditions, i.e. the film was allowed to adjust to the temperature and humidity in the climate controlled chamber, before the WVT data points were collected. After approximately 2 hours, steady-state conditions were obtained and the weight loss as a function of time could be measured (Figure 8.1). From the slope of the

weight loss versus time plot, the vapour flux through the film was determined. By dividing the water vapour flux by the test area, the rate of water vapour transmission was calculated using Equation 8.3.

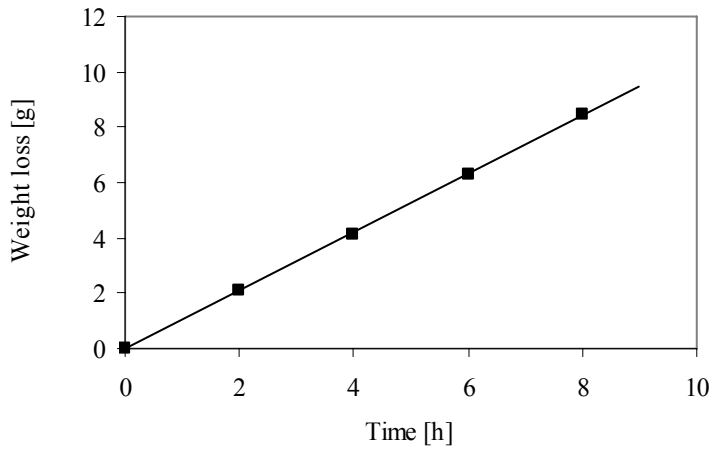

Figure 8.1: Weight loss (g) as a function of the time (h) at steady-state conditions of $PEO_{2000}/PTMO_{2000}$-T6T6T (40/60) (dry film thickness ~119 µm).

Influence of the film thickness on WVT

According to Fick's first law (Equation 8.1) the water vapour flux is inversely related to the thickness of a monolithic film [31], assuming that the diffusion coefficient is constant. The influence of the film thickness on the WVT was examined using the $PEO_{2000}/PTMO_{2000}$-T6T6T (40/60) copolymer, which consists of mixed PEO_{2000} and $PTMO_{2000}$ segments with a weight percentage ratio of 40/60 and monodisperse crystallisable T6T6T segments. The WVT of the films with varying thicknesses between 69 - 216 µm are given in Table 8.2.

Table 8.2: Influence of the film thickness (dry) and the water content in the cup on the WVT of $PEO_{2000}/PTMO_{2000}$-T6T6T (40/60).

Film thickness [µm]	1/thickness [1] [μm^{-1}]	Water in cup [ml]	WVT [kg/m^2d]	$WVT_{(25\ \mu m)}$ [kg/m^2d]
69	0.0145	250	9.3	25.8
92	0.0109	250	7.3	26.9
119	0.0084	250	5.0	23.7
132	0.0076	250	4.5	23.9
216	0.0046	250	2.8	23.8
105	0.0095	75	6.4	26.9

[1] *thickness of the dry film*

As expected, a linear relation is observed between the reciprocal film thickness and the WVT (Figure 8.2a). To compare the WVT of films with different thicknesses (l), a normalised WVT can be calculated by using a reference thickness (l_{ref}) according to Equation 8.4.

$$WVT_{(25\mu m)} = WVT \times \left(\frac{l}{l_{ref}} \right) \quad [kg/m^2 d] \qquad \text{(Equation 8.4)}$$

The $WVT_{(25\ \mu m)}$ indicates the normalised rate of water vapour transmission for a 25 µm-thick film (kg/m^{2}d). In Table 8.2 the WVT values of $PEO_{2000}/PTMO_{2000}$-T6T6T (40/60) with different film thicknesses are normalised to a 25 µm-thick film. An average $WVT_{(25\ \mu m)}$ of 25 kg/m^{2}d is calculated with a standard deviation of 1.6 kg/m^{2}d.

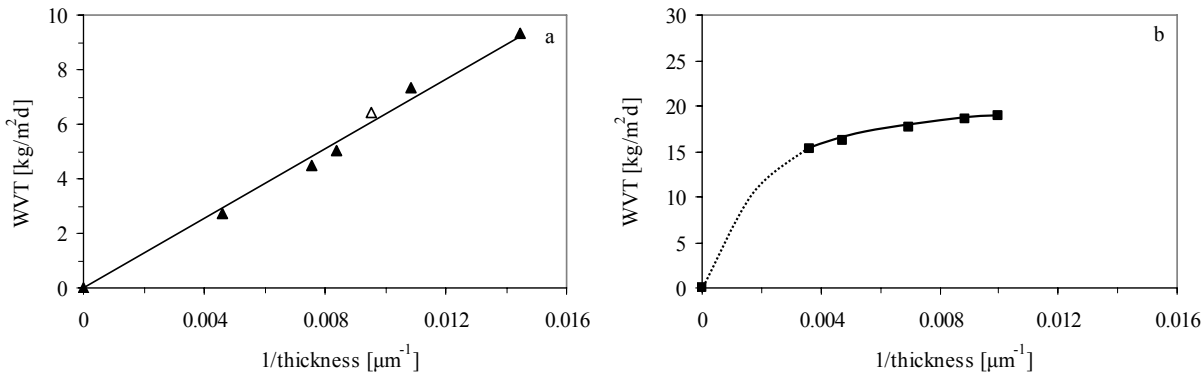

Figure 8.2: Influence of film thickness (dry) and water content in the cup on the WVT: (a) $PEO_{2000}/PTMO_{2000}$-T6T6T (40/60); ▲, 250 ml water; Δ, 75 ml water, (b) PEO_{2000}-T6T6T.

The influence of the film thickness on the WVT was also studied for a highly water vapour permeable PEO_{2000}-T6T6T segmented block copolymer. The film thickness of this copolymer was varied from 100 - 277 µm. In contrast with the $PEO_{2000}/PTMO_{2000}$-T6T6T (40/60) copolymer, no linear relation is observed between the reciprocal film thickness and the WVT (Figure 8.2b). This is probably due to a shortcoming of the used inverted cup method. When the amount of water in the cup decreases strongly due to a high water vapour flux, the pressure in the cup reduces. Due to this reduced pressure, the film deforms into a hollow shape and this deformation becomes stronger when the water vapour flux is higher, which is the case for thin films. It is expected that the reduced pressure in the cup decreases the water vapour flux and consequently reduces the WVT values. It is possible to lower the water vapour flux by increasing the film thickness and shorten the time of measuring. It is also

possible that the ventilation inside the climate-controlled chamber is insufficient for controlling the humidity below the film.
The WVT experiments of highly breathable films were performed by using thick films and a relatively short time period of measuring to prevent the occurrence of creating a low pressure in the cup. With the used experimental set-up it was not possible to measure the WVT of films that were thicker than 300 μm as the sealing of the cup failed and leakage of water took place.

To examine whether the weight of water on top of the film has an influence on the WVT, the water content in the cup was varied (250 and 75 ml). This effect was studied using the $PEO_{2000}/PTMO_{2000}$-T6T6T (40/60) copolymer (Table 8.2). At a similar film thickness, the WVT of the experiment using 75 ml water is comparable to the WVT of the experiment using 250 ml water (Figure 8.2a). This indicates that the amount of water present in the cup (between 75 and 250 ml) has no measurable influence on the WVT.

WVT of PEO/PTMO-T6T6T copolymers

The hydrophilic nature of the polyether segments has a large influence on the WVT of segmented block copolymers. The WVT of PTMO-based copolymers was significant lower compared to PEO-based copolymers. The hydrophilicity of the copolymers can be varied by using a mixture of hydrophilic PEO and hydrophobic PTMO segments [6]. These copolymers are denoted as $PEO_x/PTMO_z$-T6T6T, where *x* and *z* represents the PEO and PTMO molecular weights (Table 8.3). The soft phase composition was varied by changing both the PEO/PTMO ratio and the polyether molecular weights. Copolymers with $PEO_x/PTMO_z$ ratios of 0/100 and 100/0 were also defined as $PTMO_x$-T6T6T and PEO_z-T6T6T respectively. The WVT results of the $PEO_{2000}/PTMO_{2000}$-T6T6T and $PEO_{1000}/PTMO_{1000}$-T6T6T series are given in Table 8.3.
As shown before, the water absorption (WA) of $PEO_x/PTMO_z$-T6T6T copolymers depends on the PEO concentration [6]. The number of water molecules per ethylene oxide unit (H_2O/EO) was calculated using the PEO and water concentration. The H_2O/EO ratio was related to the crosslink density in the copolymer, i.e. the modulus of the copolymer, and the presence of hydrophobic segments like PTMO or terephthalic units [6]. The incorporation of PTMO segments in the PEO phase results in a decreased H_2O/EO ratio (Table 8.3).

Table 8.3: $WVT_{(25\ \mu m)}$ of $PEO_x/PTMO_z$-T6T6T copolymers.

PEO_x/ $PTMO_z$ [ratio]	Conc. T6T6T [wt%]	Conc. PEO [wt%]	Conc. PTMO [wt%]	$G'_{20°C}$ [1] [MPa]	WA [wt%]	H_2O/EO [-]	φ_{water} [vol%]	$WVT_{(25\ \mu m)}$ ± sd [kg/m²d]
$PEO_{2000}/PTMO_{2000}$-T6T6T								
0/100	23.8	0.0	76.2	34	1.2	-	1.2	3.1 ± 0.5
20/80	23.8	15.2	61.0	38	9.8	1.6	10	7.5 ± 1.4
40/60	23.8	30.5	45.7	31	24	1.9	22	25 ± 2
50/50	23.8	38.1	38.1	33	33	2.1	28	42 ± 7
60/40	23.8	45.7	30.5	33	42	2.3	33	62 ± 10
80/20	23.8	61.0	15.2	33	60	2.4	41	101 ± 17
100/0	23.8	76.2	0.0	38	91	2.9	51	153 ± 12
$PEO_{1000}/PTMO_{1000}$-T6T6T								
0/100	38.4	0.0	61.6	89	1.1	-	1.2	1.7 ± 0.2
30/70	38.4	18.5	43.1	80	8.1	1.1	8.8	3.5 ± 0.2
40/60	38.4	24.6	37.0	111	11	1.1	12	6.2 ± 0.9
60/40	38.4	37.0	24.6	103	20	1.3	19	14 ± 2
100/0	38.4	61.6	0.0	85	35	1.4	30	57 ± 9

[1] *storage modulus determined at 20 ºC using dynamic mechanical analysis* [6]

With increasing PEO concentration in the $PEO_{2000}/PTMO_{2000}$-T6T6T copolymers an exponential increase in $WVT_{(25\ \mu m)}$ is observed (Figure 8.3a). The $WVT_{(25\ \mu m)}$ of $PTMO_{2000}$-T6T6T (3.1 kg/m²d) is much lower compared to PEO_{2000}-T6T6T (153 kg/m²d), since PEO is more hydrophilic compared to PTMO. The continuous increase in $WVT_{(25\ \mu m)}$ with PEO concentration indicates that no phase inversion between the PEO and PTMO is noticeable or else an S-shape curve would have been observed [19]. Phase inversion might occur when the PEO and PTMO phases are separated.

The $PEO_{1000}/PTMO_{1000}$-T6T6T copolymers also show an exponential increase in $WVT_{(25\ \mu m)}$ with increasing PEO concentrations (Figure 8.3a). At similar PEO concentrations, the $WVT_{(25\ \mu m)}$ of $PEO_{1000}/PTMO_{1000}$-T6T6T is lower compared to that of $PEO_{2000}/PTMO_{2000}$-T6T6T, which is most likely due to a higher T6T6T concentration. A higher T6T6T concentration results in a higher modulus of the copolymer and a lower WA and $WVT_{(25\ \mu m)}$.

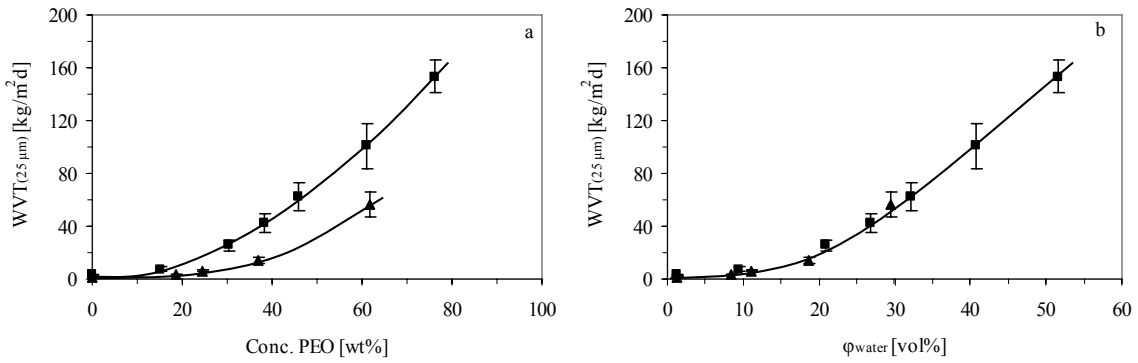

Figure 8.3: $WVT_{(25\ \mu m)}$ as a function of (a) the PEO concentration and (b) the volume fraction of water: ■, $PEO_{2000}/PTMO_{2000}$-T6T6T; ▲, $PEO_{1000}/PTMO_{1000}$-T6T6T.

When the $WVT_{(25\ \mu m)}$ of both series are plotted as a function of the volume fraction of water in the copolymer (φ_{water}) the data coincide in one exponential curve (Figure 8.3b). This suggests that the WVT is directly correlated to the amount of absorbed water, i.e. the hydrophilicity, of the copolymer. Although the $PEO_{2000}/PTMO_{2000}$-T6T6T copolymers have higher H_2O/EO values than $PEO_{1000}/PTMO_{1000}$-T6T6T, the WVT values are comparable at similar volume fractions of water.

Previous results showed an exponential increase in the water vapour sorption isotherm of PEO_{1000}-T6T6T and PEO_{2000}-T6T6T copolymers [6]. This exponentially increase was explained by the presence of water clusters in the copolymer. As the increase of PEO_{2000}-T6T6T was stronger than for PEO_{1000}-T6T6T it was assumed that the number of water clusters in the former copolymer was higher. It is reported that the diffusion coefficient of water vapour was decreased when water clusters were present in the copolymer [8-11]. However, it seems that at the conditions where the WVT experiments were performed, the presence of water clusters has no significant influence on the WVT of the polyether-T6T6T copolymers.

The $WVT_{(25\ \mu m)}$ was also determined for other $PEO_x/PTMO_z$-T6T6T copolymers containing different soft phase compositions (Table 8.4). Two series, denoted as $PEO_x/PTMO_{1000}$-T6T6T and $PEO_{1000}/PTMO_z$-T6T6T, were studied where the PEO (x) or PTMO (z) molecular weight was varied. In the $PEO_x/PTMO_{1000}$-T6T6T series the PEO_x length was varied from 600 to 8000 g/mol, while the PEO concentration was more or less constant (17.1 – 20.6 wt%). In the $PEO_{1000}/PTMO_z$-T6T6T series the PTMO length was varied from 650 to 2900 g/mol.

Table 8.4: $WVT_{(25\ \mu m)}$ of $PEO_x/PTMO_z$-T6T6T copolymers.

PEO_x/ $PTMO_z$ [ratio]	M_n PEO [g/mol]	M_n PTMO [g/mol]	Conc. T6T6T [wt%]	Conc. PEO [wt%]	Conc. PTMO [wt%]	$G'_{20°C}$ [1] [MPa]	WA [wt%]	H_2O/EO [-]	φ_{water} [vol%]	$WVT_{(25\ \mu m)}$ ± sd [kg/m²d]
$PEO_x/PTMO_{1000}$-T6T6T										
30/70	600	1000	42.9	17.1	40.0	113	4.4	0.6	4.6	1.8 ± 0.2
30/70	1000	1000	38.4	18.5	43.1	80	8.1	1.1	8.8	3.5 ± 0.2
30/70	3400	1000	33.0	20.1	46.9	73	18	2.2	18	8.5 ± 0.9
30/70	4600	1000	32.3	20.3	47.4	85 (80 [2])	19	2.3	19	12 ± 1
30/70	8000	1000	31.5	20.6	47.9	109 (70 [2])	22	2.6	20	8.9 ± 0.8
$PEO_{1000}/PTMO_z$-T6T6T										
64/36	1000	650	42.7	36.9	20.4	74	18	1.2	17	16 ± 2
60/40	1000	1000	38.4	37.0	24.6	103	20	1.3	19	14 ± 2
55/45	1000	2000	32.6	37.1	30.3	49	22	1.4	21	19 ± 3
53/47	1000	2900	30.2	37.0	32.8	41	23	1.5	21	22 ± 3

[1] *storage modulus determined at 20 ºC using dynamic mechanical analysis* [28]
[2] *storage modulus of the rubbery plateau determined at 55 ºC* [28]

In the $PEO_x/PTMO_{1000}$ series the H_2O/EO ratio increases from 0.6 to 2.6. The increase in WA is mainly due to a decreased T6T6T concentration and, to a small extent, to the increased PEO concentration and molecular weight. In the $PEO_{1000}/PTMO_z$-T6T6T series, where the PEO length and concentration were constant, the water absorption increases only slightly with increasing PTMO length. The PTMO molecular weight seems to have only a small effect on the WA.

At room temperature and at dry conditions, the copolymers contain a semi-crystalline PEO phase when the PEO molecular weight is above 2000 g/mol. The storage modulus ($G'_{20\ °C}$) increases when the copolymer contains a crystalline PEO phase at room temperature (Table 8.4). To obtain the storage modulus of the rubbery plateau, the G' is determined at 50 ºC since at this temperature all PEO crystals are molten. The presence of polyether crystals in the copolymer can have an effect on the WVT. However, when the copolymer absorbs water the PEO melting temperature was strongly reduced, as was discussed in Chapter 5. Therefore, during the WVT measurement, where the films were saturated with water, the polyether phase was completely amorphous.

In Figure 8.4 the $WVT_{(25\ \mu m)}$ of both copolymers series are given as a function of the volume fraction of water. A comparison is made with the $PEO_{1000}/PTMO_{1000}$-T6T6T copolymers.

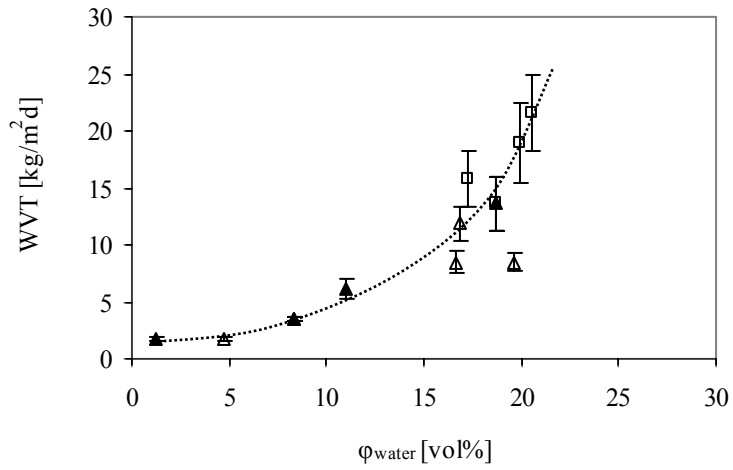

Figure 8.4: $WVT_{(25\ \mu m)}$ as a function the volume fraction of water: ▲, $PEO_{1000}/PTMO_{1000}$-T6T6T, Δ, $PEO_x/PTMO_{1000}$-T6T6T; □, $PEO_{1000}/PTMO_z$-T6T6T.

A similar exponential increase in WVT with increasing volume fraction of water is observed for all PEO/PTMO-based copolymers. However, the $PEO_{8000}/PTMO_{1000}$-T6T6T shows a significantly lower WVT value than indicated by the trend line (Figure 8.4). A reason for the lower WVT value of this copolymer is as yet not known.

PEO-T6T6T copolymers

In the previous series, a combination of PEO and PTMO polyether segments was used to control the hydrophilicity of the copolymer. It is also possible to create polyether-T6T6T copolymers that are based on only PEO flexible segments and monodisperse crystallisable T6T6T (Table 8.5). In this series, denoted as PEO_x-T6T6T, the PEO molecular weight (x) was varied from 1000 to 3400 g/mol [28,29]. It was not possible to make a polymer film by compression moulding with a PEO molecular weight below 1000 g/mol as the film was too brittle. When the PEO molecular weight was higher than 3400 g/mol, the WA of the copolymer was too high (>127 wt%) and the wet film teared during clamping in the cup.

A way to obtain copolymers with a high PEO concentration is by extending the PEO segments with terephthalic units (T) [30]. These copolymers are denoted as $(PEO_x/T)_y$-T6T6T, where y is the total molecular weight of the flexible segment (Table 8.5).

Table 8.5: $WVT_{(25\ \mu m)}$ of PEO_x-T6T6T and $(PEO_x/T)_y$-T6T6T copolymers.

x or *y* [g/mol]	Conc. T6T6T [wt%]	Conc. PEO [wt%]	Conc. T [wt%]	$G'_{20°C}$ [1] [MPa]	WA [wt%]	H_2O/EO [-]	φ_{water} [vol%]	$WVT_{(25\ \mu m)}$ ± sd [kg/m²d]
PEO_x-T6T6T								
1000	38.4	61.6	-	86	35	1.4	30	57 ± 9
1500	29.4	70.6	-	57	69	2.4	45	117 ± 10
2000	23.8	76.2	-	38	91	2.9	51	153 ± 12
3400	15.5	84.5	-	72 (18 [2])	127	3.7	59	188 ± 14
$(PEO_{300}/T)_y$-T6T6T								
2500	19.9	58.4	21.7	46	14	0.6	14	13 ± 3
$(PEO_{600}/T)_y$-T6T6T								
1250	33.3	60.4	6.3	68	30	1.2	26	25 ± 5
2500	20.0	69.0	11.0	32	49	1.7	37	58 ± 8
5000	11.1	74.8	14.1	12	66	2.2	43	124 ± 11

[1] *storage modulus determined at 20 °C using dynamic mechanical analysis* [6]
[2] *storage modulus of the rubbery plateau determined at 55 °C* [6]

The WA of the PEO_x-T6T6T copolymers is influenced by both the PEO and T6T6T concentration. With increasing soft segment length, and thus with decreasing T6T6T content, the water absorption was increased. For all these copolymers, a linear relation was found between the volume fraction of water (φ_{water}) and the PEO concentration when the PEO concentration was above 49 wt% [28]. Slightly lower water absorptions were observed for copolymers with terephthalic extended PEO segments. The reduction of water absorption was stronger when copolymers contained higher concentrations of terephthalic unit. The presence of hydrophobic terephthalic groups in the soft phase lowers the H_2O/EO ratio in a similar way as was observed when PTMO was present.

In Figure 8.5 the $WVT_{(25\ \mu m)}$ of the PEO_x-T6T6T and $(PEO_x/T)_y$-T6T6T copolymers are given as a function of the volume fraction of water. At similar φ_{water} values, there is no difference in the $WVT_{(25\ \mu m)}$ values between PEO_x-T6T6T, $(PEO_x/T)_y$-T6T6T and $PEO_x/PTMO_z$-T6T6T copolymers. This indicates again that there is a strong correlation between the water absorption, and thus the hydrophilicity of the copolymer, and the WVT.

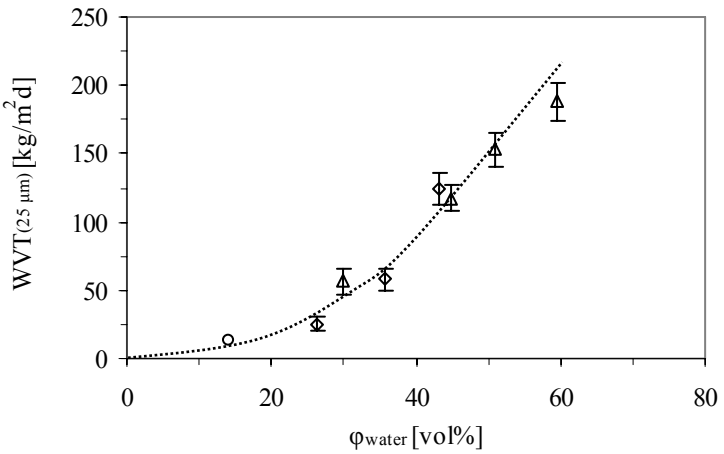

Figure 8.5: $WVT_{(25\ \mu m)}$ as a function the volume fraction of water (line represents the $PEO_{2000}/PTMO_{2000}$-T6T6T copolymers): Δ, PEO_x-T6T6T; ◊, $(PEO_{600}/T)_y$-T6T6T; ○,$(PEO_{300}/T)_{2500}$-T6T6T).

Conclusions

The rate of water vapour transmission (WVT) through polyether-T6T6T films was determined by using the inverted cup method described by the ASTM E96BW standard. The experiments were performed in a climate-controlled chamber at a temperature of 30 ºC and a relative humidity of 50%.

A linear relation was found between the WVT and the reciprocal film thickness of the polyether-T6T6T copolymers. Therefore, it is possible to calculate a normalised WVT value for a 25 μm-thick film. With increasing PEO concentration in the copolymer, a strong exponential increase in $WVT_{(25\ \mu m)}$ was observed. The $WVT_{(25\ \mu m)}$ for $PTMO_{2000}$-T6T6T and PEO_{2000}-T6T6T is 3.1 and 153 kg/m^{2}d respectively. The WVT of polyether-T6T6T segmented block copolymers is mainly determined by the volume fraction of absorbed water.

References

1. Sakkers, R.J.B., De Wijn, J.R., Dalmeyer, R.A.J., Brand, R. and Van Blitterswijk, C.A., *J. Mater. Sci.: Mater. Med.* **1998**, 9, p. 375-379.
2. Petrini, P., Fare, S., Piva, A. and Tanzi, M.C., *J. Mater. Sci.: Mater. Med.* **2003**, 14, p. 683-686.
3. Rault, J. and Le Huy, H.M., *J. Macromol. Sci., Phys.* **1996**, 35, p. 89-114.
4. Chen, C.T., Eaton, R.F., Chang, Y.J. and Tobolsky, A.V., *J. Appl. Polym. Sci.* **1972**, 16, p. 2105-2114.
5. Deschamps, A.A., Grijpma, D.W. and Feijen, J., *J. Biomater. Sci., Polym. Ed.* **2002**, 13, p. 1337-1352.
6. Chapter 5 of this thesis.
7. Wijmans, J.G. and Baker, R.W., *J. Membr. Sci.* **1995**, 107, p. 1-21.
8. Mulder, M., in *Basic principles of membrane technology*, Kluwer Academic Publishers, Dordrecht **1991**.
9. Van Krevelen, D.W., in *Properties of polymers*, Elsevier Science Publishers, New York **1990**.
10. Schneider, N.S., Dusablon, L.V., Snell, E.W. and Prosser, R.A., *J. Macromol. Sci., Phys.* **1969**, B3, p. 623-644.

11. Metz, S.J., van de Ven, W.J.C., Mulder, M.H.V. and Wessling, M., *J. Membr. Sci.* **2005**, 266, p. 51-61.
12. Adriaensens, P., Pollaris, A., Rulkens, R., Litvinov, V.M. and Gelan, J., *Polymer* **2001**, 42, p. 7943-7952.
13. McCullough, E.A., Kwon, M. and Shim, H., *Meas. Sci. Technol.* **2003**, 14, p. 1402-1408.
14. Stroeks, A., *Polymer* **2001**, 42, p. 9903-9908.
15. Nguyen, Q.T., Germain, Y., Clement, R. and Hirata, Y., *Polymer Testing* **2001**, 20, p. 901-911.
16. Hu, Y., Topolkaraev, V., Hiltner, A. and Baer, E., *J. Appl. Polym. Sci.* **2001**, 81, p. 1624-1633.
17. Dolmaire, N., Espuche, E., Mechin, F. and Pascault, J.P., *J. Polym. Sc., Part B: Polym. Phys.* **2004**, 42, p. 473-492.
18. Petrik, S., Hadobas, F., Simek, L. and Bohdanecky, M., *Eur. Polym. J.* **1992**, 28, p. 15-18.
19. Yilgör, I. and Yilgör, E., *Polymer* **1999**, 40, p. 5575-5581.
20. Gebben, B., *J. Membr. Sci.* **1996**, 113, p. 323-329.
21. Metz, S.J., Potreck, J., Mulder, M.H.V. and Wessling, M., *Desalination* **2002**, 148, p. 303-307.
22. Stroeks, A. and Dijkstra, K., *Polymer* **2001**, 42, p. 117-127.
23. PEBAX data information sheet (http://mymatweb.com).
24. Harrell, L.L., *Macromolecules* **1969**, 2, p. 607-612.
25. Miller, J.A., Lin, S.B., Hwang, K.K.S., Wu, K.S., Gibson, P.E. and Cooper, S.L., *Macromolecules* **1985**, 18, p. 32-44.
26. Van der Schuur, M., Ph.D. Thesis '*Poly(propylene oxide) based segmented blockcopolymers*', University of Twente, The Netherlands **2004**.
27. Krijgsman, J., Husken, D. and Gaymans, R.J., *Polymer* **2003**, 44, p. 7043-7053.
28. Chapter 4 of this thesis.
29. Chapter 2 of this thesis.
30. Chapter 3 of this thesis.
31. Jonquières, A., Clément, R. and Lochon, P., *Prog. Polym. Sci.* **2002**, 27, p. 1803-1877.

Chapter 9

Use of monofunctional PEO in segmented block copolymers containing monodisperse crystallisable segments

---

Abstract

In this chapter the synthesis and characterisation of segmented block copolymers that are end-capped with monofunctional PEO (mPEO) have been discussed. The mid-blocks of these copolymers consist of flexible polyether segments (PEO or PTMO) and monodisperse crystallisable segments (T6T6T). The ratio between the mPEO end-blocks and the difunctional polyether (mid-)blocks was varied. The influence of the mPEO concentration on the polymer molecular weight, the thermal mechanical properties, the water absorption, the surface properties and the tensile properties was studied. Moreover, the effect of the molecular weight of the mPEO end-blocks, which was varied from 350 to 5000 g/mol, on the surface hydrophilicity was investigated.

Copolymers that exhibit mPEO end-blocks have a higher PEO melting temperature and crystallinity than copolymers containing difunctional PEO (mid-)blocks. Besides, the copolymers with mPEO end-blocks have a slightly lower glass transition temperature and a slightly increased modulus and T6T6T melting temperature as compared to corresponding copolymers that were not end-capped with mPEO.

The water absorption of PTMO-T6T6T copolymers end-capped with mPEO is slightly higher than for PEO/PTMO-T6T6T copolymers that are based on difunctional PEO segments. For the mPEO end-capped polymers, the mPEO and PTMO segments are probably partly phase separated and, therefore, PTMO will not decrease the water absorption as effectively as when PEO and PTMO are not phase separated.

A more hydrophilic polymer surface, indicated by a lower contact angle, is obtained by using mPEO segments instead of difunctional PEO segments. The molecular weight of the mPEO segments has a strong influence on both the bulk as well as the surface properties of the copolymer.

An increased mPEO concentration results in a reduced polymer molecular weight and, consequently, a reduction of the fracture properties of the copolymer. By introducing a trifunctional carboxylate ester, the polymer molecular weight is increased, resulting in good fracture properties, while the mPEO concentration is relatively high.

Introduction

Polymer surfaces that exhibit a low degree of protein adsorption are interesting biomaterials, which can be used for applications like contact lenses, wound dressings and catheters [1-3]. These biomaterials have many requirements like biocompatibility, manufacturability, and sterilizability. Besides, they need suitable physical, mechanical and surface properties.

Biomaterials are often based on poly(ethylene oxide) (PEO) that is known for its ability to reduce protein adsorption. PEO is a synthetic, water-soluble and non-toxic polymer [4]. The biocompatible nature of PEO can be explained by several mechanisms [5-7]. The low interfacial free energy between a biological fluid and PEO results in a low driving force for protein adsorption. Also, the large excluded volume and mobility of hydrated PEO repel proteins approaching the polymer surface.

Polymers based on PEO have a high degree of hydration and a low interfacial free energy with water [4,6-9]. The surface concentration of an adsorbed protein depends on the type of protein, its concentration in solution, the adsorption time and the characteristics of the polymer surface. For PEO-containing polymers, the density of the PEO segments on the surface, the PEO molecular weight and the polymer morphology will influence the protein adsorption behaviour.

An approach to create a PEO-based polymer with improved biocompatibility (i.e. low protein adsorption) for long-term applications is by covalently grafting PEO onto a hydrophobic substrate. The grafted PEO segments are effective due to a high mobility as they are bound at only one side. PEO has been covalently grafted to (modified) polymeric substrates like poly(ethylene terephthalate) [9-11], polystyrene [12-14], polyethylene [2,5] and poly(methyl methacrylate) [15,16]. Grafting of PEO chains on a hydrophobic surface can be achieved by a method called plasma immobilization, described in detail by Hoffman et al. [17,18]. However, most of the grafting methods are practically limited as functional groups have to be generated on the surface and the grafting procedure is often complex.

Another approach to improve the biocompatibility of a polymer surface is to use PEO-based segmented block copolymers. Accordingly, PEO is built into the polymer main chain and is present at the surface as well as in the bulk. Benefits of using PEO-based segmented block copolymers as biomaterials are the ease of processing into complex shapes, the ability to tune properties and the ability to modify the surface composition.

Several PEO-containing segmented block copolymers, like polyurethanes [19-27] and polyesters [28-33], have been studied for application as biomaterials. These copolymers are interesting due

to their good mechanical properties and biocompatibility. However, problems like surface-induced thrombosis, infections and calcification can still occur after contact with biological fluids [3,34,35]. The presence of hard segments at the polymer surface can limit the biocompatibility of segmented block copolymers since it can induce protein adsorption and denature proteins [8].

PEO-based segmented block copolymers absorb considerable amounts of water and, as a result, they swell. This leads to a decrease in the tensile properties like, E-modulus, yield stress and fracture stress [19,36-40]. Therefore, the water absorption of PEO-based copolymers should be minimized. An ideal biomaterial should have a very hydrophilic surface and low bulk water absorption.

According to literature, an improved phase separation between the rigid and flexible segments of the copolymer leads to an improved biocompatible material [5,24,26,27,41]. By increasing the crystallinity of the rigid segments the amount of non-crystallised rigid segments in the soft phase is reduced and phase separation will be enhanced. The crystallisation of the rigid segments can be improved considerably by using monodisperse rigid segments [42,43]. In earlier chapters of this thesis, the synthesis and properties of segmented block copolymers with hydrophilic PEO and/or hydrophobic poly(tetramethylene oxide) (PTMO) flexible polyether segments and monodisperse crystallisable tetra-amide segments (T6T6T) were described. The T6T6T segments are based on dimethyl terephthalate (T) and hexamethylene-diamine (6).

A water contact angle of approximately 29º was observed for PEO-T6T6T copolymers with a high PEO concentration (~88 wt%), indicating a high surface hydrophilicity [44]. However, the water absorption of this copolymer is high, approximately 92 wt%. It is known that grafted PEO segments or PEO end-blocks can be used to create polymers with a low contact angle. PEO end-blocks have a high mobility as these segments are bound at only one side. In literature, PEO-endcapped segmented block copolymers have only been reported for linear poly(ethylene terephthalate) [45]. In this case monofunctional PEO was used (mPEO). The presence of the mPEO end-blocks results in an increased polymer surface hydrophilicity and decreased protein adsorption. However, by using mPEO end-blocks the molecular weight of the copolymer was strongly reduced, which leads to a lowering of the fracture properties.

It is interesting to study the effect of PEO end-blocks in polyether-T6T6T segmented block copolymers that have a well phase separated polymer morphology, on the water absorption, the contact angle and the mechanical properties.

Aim

In this chapter the synthesis and characterisation of segmented block copolymers that are endcapped with monofunctional PEO (mPEO) segments are described. The polymer mid-blocks consist of hydrophobic difunctional $PTMO_{2000}$ segments and monodisperse crystallisable T6T6T. The copolymers are denoted as $mPEO_{2000}/PTMO_{2000}$-T6T6T and the ratio between mPEO end-blocks and PTMO (mid-)blocks is varied.

The influence of the $mPEO_{2000}$ concentration on the polymer molecular weight, the thermal mechanical properties, the water absorption, the surface properties and the tensile properties will be studied. Furthermore, the influence of the mPEO molecular weight, which was varied from 350 to 5000 g/mol, on the surface properties will be examined.

To increase the polymer molecular weight, while the mPEO concentration remains relatively high (11 wt%), a trifunctional carboxylate ester is incorporated to create a branched polymer structure. These copolymers are based on $mPEO_{550}$ end-blocks and -(PEO_{1000}-T6T6T)- mid-blocks. The influence of the trifunctional carboxylate ester on the polymer molecular weight, the thermal mechanical properties, the water absorption, the surface properties and the tensile properties will be studied.

Experimental

Materials. *N*-methyl-2-pyrrolidone (NMP) was purchased from Merck. Tetra-isopropyl orthotitanate (Ti(*i*-$OC_3H_7)_4$) was obtained from Aldrich and diluted in *m*-xylene (0.05 M) received from Fluka. Trimethyl trimesate (TMTM) was obtained from Aldrich and Irganox 1330 from CIBA. Difunctional poly(ethylene glycol) (M_n of 1000 g/mol) was obtained from Aldrich and difunctional poly(tetramethylene oxide) (M_n of 2000 g/mol) was a gift from Dupont. Monofunctional poly(ethylene glycol) (M_n of 350, 550, 1100, 2000 and 5000 g/mol) was obtained from Fluka. T6T6T-dimethyl was synthesised as described before [46].

$PEO_{2000}/PTMO_{2000}$-T6T6T block copolymers. These copolymers were synthesised by a polycondensation reaction using a mixture of flexible difunctional PEO and PTMO segments and T6T6T. Both polyether segments had a molecular weight of 2000 g/mol and the weight percentage ratio between PEO and PTMO was varied (see Chapter 4 of this thesis).

$mPEO_b/PTMO_{2000}$-T6T6T block copolymers. The $mPEO_b/PTMO_{2000}$-T6T6T copolymers were synthesised by a polycondensation reaction using mPEO segments of a certain molecular weights (*b*), $PTMO_{2000}$ segments (M_n of 2000 g/mol) and T6T6T. The weight percentage ratio between mPEO and PTMO was varied. The synthesis of $mPEO_b/PTMO_{2000}$-T6T6T with b = 2000 g/mol and an mPEO/PTMO ratio of 33/67 is given as an example.

The reaction was carried out in a 50 mL glass vessel equipped with a magnetic stirrer and nitrogen inlet. The vessel contained T6T6T-dimethyl (5 mmol, 3.43 g), $mPEO_{2000}$ (2 mmol, 4.00 g), $PTMO_{2000}$ (4 mmol, 8.00 g), Irganox 1330 (0.12 g), 25 mL NMP and catalyst solution (0.6 mL of 0.05 M Ti-(*i*-$(OC_3H_7)_4$) in *m*-xylene). The reaction mixture was heated to 180 °C under a nitrogen flow in an oil bath and after 30 min the temperature was

increased to 250 °C in 1 h. After 2 h at 250 °C the pressure was slowly reduced (P < 21 mbar) to remove all NMP. Subsequently, the pressure was further reduced (P < 1 mbar) to allow melt polycondensation for 1 h. The polymer melt was cooled down to room temperature while maintaining the vacuum. Then the reaction vessel was broken and the polymer was removed. The polymer was crushed and dried in a vacuum oven at 50 ºC for 24 h.

$mPEO_{550}/PEO_{1000}$/TMTM-T6T6T block copolymers. The $mPEO_{550}/PEO_{1000}$/TMTM-T6T6T copolymers were synthesised by a polycondensation reaction using a trifunctional trimethyl trimesate (TMTM) monomer. The reactants for the polymerisation were $mPEO_{550}$ (4 mmol, 2.2 g), PEO_{1000} (11.1 mmol, 11.1 g), T6T6T-dimethyl (10.1 mmol, 6.93 g) and TMTM (2 mmol, 0.50 g), 25 mL NMP and catalyst solution (2.6 mL of 0.05 M Ti-(*i*-$(OC_3H_7)_4$) in *m*-xylene). The polymerisation was comparable to the method described for the $mPEO_b/PTMO_{2000}$-T6T6T copolymers.

Viscometry. The inherent viscosity (η_{inh}) of the polymers was determined at 25 °C using a capillary Ubbelohde type 1B. The polymer solution had a concentration of 0.1 dL/g in a 1/1 (molar ratio) mixture of phenol/1,1,2,2-tetrachloroethane.

Injection-moulding. Samples for dynamic mechanical analysis, differential scanning calorimetry and compression set were prepared on an Arburg-H manual injection-moulding machine. The barrel temperature was set approximately 80 °C above the melting temperature of the block copolymer and the mould temperature was set at 70 °C.

Differential scanning calorimetry. DSC spectra were recorded on a Perkin Elmer DSC7 apparatus, equipped with a PE7700 computer and TAS-7 software. Dry polymer samples obtained from injection-moulding (5 – 10 mg) were heated from -50 to 250 °C at a rate of 20 °C/min. Subsequently, a cooling scan from 250 to -50 °C at a rate of 20 °C/min followed by a second heating scan under the same conditions as the first heating scan were performed. The melting temperature (T_m) and melting enthalpy (ΔH_m) were determined from the second heating scan.

Dynamic mechanical analysis. The torsion behaviour (storage modulus G' and loss modulus G" as a function of temperature) was measured using a Myrenne ATM3 torsion pendulum at a frequency of 1 Hz and 0.1% strain. Before use, samples (70x9x2 mm) were dried in a vacuum oven at 50 °C overnight. Samples were cooled to -100 °C and then heated at a rate of 1 °C/min. The glass transition temperature (T_g) was defined as the maximum of the loss modulus and the flow temperature (T_{flow}) as the temperature where the storage modulus reached 1 MPa. The temperature where the rubber plateau starts is denoted as the flex temperature (T_{flex}) and the storage modulus at 20 ºC is given as $G'_{20\,°C}$.

Water absorption (WA). The equilibrium water absorption was measured using pieces of injection-moulded polymer bars. The samples were placed in a desiccator filled with demineralised water for 4 wks at room temperature. The water absorption was defined as the weight gain of the polymer according to;

$$WA = \frac{m - m_0}{m_0} \times 100\% \quad [wt\%] \quad \text{(Equation 9.1)}$$

where m_0 is the weight of dry sample and m the weight of the sample after conditioning to equilibrium. The measurements were performed in duplicate. The volume fraction of water in the copolymer (φ_{water}) can be determined by using a (m)PEO, PTMO, TMTM and T6T6T density of 1.13, 0.98, 1.26 and 1.32 g/cm^3 respectively [47].

Contact angle. Static captive (air) bubble (CB) contact angle measurements were performed by introducing a 10 µL air bubble from a micro-syringe below the surface of a polymer film, which is placed in an optical cuvet filled with demineralised water. The measurements were performed using a video-based Optical Contact Angle Meter OCA15 plus (DataPhysics Instruments). Static sessile drop (SD) contact angle measurements were performed by placing a water drop of approximately 10 µL on a dry polymer surface. The contact angles (CA) were calculated immediately after the droplet was placed on the surface (± 10 s) by using SCA20 software, applying ellipse fitting. Results are the average of at least 20 measurements.

The polymer films were made by compression moulding and had a thickness of approximately 300 µm. Before the CA measurements the films were ultrasonically cleaned in *n*-hexane for 5 min. Subsequently, the films were wiped with cotton and rinsed with *n*-hexane. The films were then dried in a vacuum oven for 24 h to remove all *n*-hexane. Approximately 5 h before the measurements the films were placed in demineralised water to allow the materials to absorb water till equilibrium was reached.

Tensile test. Tensile tests were performed on a Zwick Z020 universal tensile machine equipped with a 500 N load cell, using compression-moulded polymer bars with a thickness of ~1 mm cut to dumbbells (ISO 37 type 2). The strain was measured with extensometers. Standard stress-strain curves were obtained at a test speed of 60 mm/min. The tensile test, preformed in 5-fold, is according to the ISO 37 standard. Tensile tests were also performed on hydrated polymers samples. In this case the samples were placed in demineralised water for 1 d to reach an equilibrium state of water absorption.

Results and discussion

Three different polymer series will be discussed in this chapter; $mPEO_{2000}/PTMO_{2000}$-T6T6T, $mPEO_b/PTMO_{2000}$-T6T6T and $mPEO_{550}/PEO_{1000}$/TMTM-T6T6T.

In the first polymer series a comparison is made between the use of monofunctional PEO_{2000} and difunctional PEO_{2000}. The (wt%) ratio between mPEO and PTMO is varied and the influence of the $mPEO_{2000}$ concentration on the polymer molecular weight, the thermal mechanical properties, the water absorption, the surface properties and the tensile properties are studied.

In the second polymer series, the influence of the mPEO molecular weight (*b*) on the surface properties is examined. The mPEO molecular weight was varied from 350 to 5000 g/mol while the polymer molecular weight remains constant (~11,000 g/mol).

In the third polymer series, the polymer molecular weight is increased by using a trifunctional carboxylate ester (TMTM), while the mPEO concentration remains high (~11 wt%). The copolymers are based on $mPEO_{550}$ end-blocks and -(PEO_{1000}-T6T6T)- mid-blocks. The influence of the presence of TMTM in the copolymer on the polymer molecular weight, the thermal mechanical properties, the water absorption, the surface properties and the tensile properties are studied.

$mPEO_{2000}/PTMO_{2000}$-T6T6T segmented block copolymers

A polymer series is made based on monofunctional PEO_{2000} ($mPEO_{2000}$), difunctional $PTMO_{2000}$ and monodisperse crystallisable T6T6T segments. The hydrophilic mPEO segments will be present at the polymer chain ends, while the more hydrophobic PTMO segments are expected to be mainly present as mid-blocks. The series is denoted as $mPEO_{2000}/PTMO_{2000}$-T6T6T. The (wt%) ratio between mPEO and PTMO is varied and the compositions of these copolymers are given in Table 9.1.

Table 9.1: Composition and inherent viscosity of $(m)PEO_{2000}/PTMO_{2000}$-T6T6T copolymers.

Ratio (m)PEO/PTMO	Conc. T6T6T [wt%]	Conc. (m)PEO [wt%]	Conc. PTMO [wt%]	η_{inh} [dL/g]
$mPEO_{2000}/PTMO_{2000}$-T6T6T				
0/100	23.8	-	76.2	2.2
6/94	23.2	4.8	72.0	1.6
17/83	22.2	13.0	64.8	1.3
22/78	21.7	17.4	60.9	1.2
33/67	20.6	26.5	52.9	1.0
50/50	19.0	40.5	40.5	0.6
100/0	13.5	86.5	-	0.3
$PEO_{2000}/PTMO_{2000}$-T6T6T				
0/100	23.8	-	76.2	2.2
20/80	23.8	15.2	61.0	2.0
40/60	23.8	30.5	45.7	2.1
50/50	23.8	38.1	38.1	1.7
60/40	23.8	45.7	30.5	1.8
80/20	23.8	61.0	15.2	1.9
100/0	23.8	76.2	-	2.1

High molecular weight segmented block copolymers made by a polycondensation reaction are only obtained when a high degree of conversion is reached [48]. The inherent viscosity of a polymer solution gives an indication of the polymer molecular weight. Generally, an inherent viscosity of 2.0 – 3.0 dL/g is obtained for polyether-T6T6T copolymers [49-51].

Unpublished results on $PTMO_{1000}$ segments extended with terephthalic units to a flexible segment length of 6,000 g/mol revealed that these extended segments have an inherent viscosity of 0.6 dL/g. With ^{1}H NMR the obtained molecular weight was verified. When adequate solvents are used for inherent viscosity measurements, the inherent viscosity of these

copolymers often increases linearly with the molecular weight [52]. An inherent viscosity of 1.0 dL/g corresponds to a molecular weight (M_n) of approximately 10,000 g/mol.

The mPEO segments are chain-stoppers for the polycondensation reaction and limit the formation of high molecular weight copolymers. An increased mPEO concentration results in an increased number of polymer end-blocks and thus a reduced molecular weight. This explains the decrease in inherent viscosity from 2.2 to 0.3 dL/g with increasing mPEO concentration.

The $mPEO_{2000}/PTMO_{2000}$-T6T6T copolymers were compared with $PEO_{2000}/PTMO_{2000}$-T6T6T copolymers, which contain difunctional PEO and PTMO segments. The synthesis and thermal mechanical properties of the $PEO_{2000}/PTMO_{2000}$-T6T6T copolymers are described in Chapter 4. In this series the PEO/PTMO ratio is varied, while the T6T6T concentration remains constant (Table 9.1). The polycondensation reaction of $PEO_{2000}/PTMO_{2000}$-T6T6T copolymers is not limited by the presence of monofunctional segments as only difunctional polyether segments are used. Therefore, these copolymers have a high inherent viscosity (~2.0 dL/g) and thus a high molecular weight.

Differential scanning calorimetry

DSC measurements on polyether prepolymers were performed to determine their melting temperature and crystallinity. The DSC results of difunctional $PTMO_{2000}$ and PEO_{2000} and monofunctional PEO_{2000} prepolymers are given in Table 9.2. The crystallinity of the prepolymers was calculated by assuming a melting enthalpy of 100% crystalline (m)PEO and PTMO of 197 and 200 J/g respectively[53].

Table 9.2: DSC results of polyether prepolymers (20 ºC/min).

Type Polyether	Type endgroups	T_m [ºC]	ΔH_m [J/g]	X_c [%]
$PTMO_{2000}$	-OH	29	99	50
PEO_{2000}	-OH	55	168	85
$mPEO_{2000}$	-OH, $-OCH_3$	58	131	66

The melting temperature and degree of crystallinity of the $(m)PEO_{2000}$ prepolymers are higher than those of $PTMO_{2000}$. No significant difference was observed in melting temperature

between monofunctional PEO_{2000} and difunctional PEO_{2000}. However, the melting enthalpy of the PEO_{2000} prepolymer was somewhat higher than that of $mPEO_{2000}$.
The crystallisation of the polyether segments in the copolymers is expected to depend on the location of the segment in the polymer chain, i.e. mid-block or end-block, and on the polymer molecular weight. Monofunctional segments are bound at only one side and, therefore, are more able to diffuse and crystallise than difunctional segments. It is also expected that a reduced polymer molecular weight increases the mobility of the polyether segments.

The melting and crystallisation behaviour of the $mPEO_{2000}/PTMO_{2000}$-T6T6T copolymers was studied with DSC (Figure 9.1, Table 9.3). The melting data of the second heating scan was used to exclude the influence of the thermal history of the copolymers. Three melting peaks are observed in the DSC heating scans of $mPEO_{2000}/PTMO_{2000}$-T6T6T copolymers, corresponding to PTMO, mPEO and T6T6T.

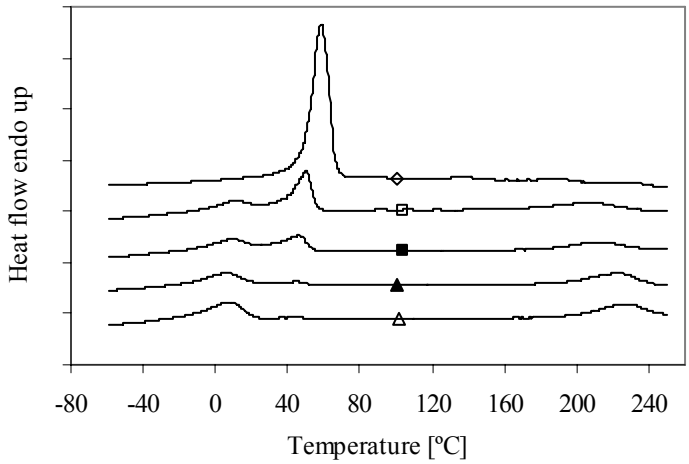

Figure 9.1: DSC second heating scan (20 ºC/min) of $mPEO_{2000}/PTMO_{2000}$-T6T6T copolymers with different mPEO/PTMO ratios: ◊, 100/0; □, 50/50; ■, 33/67; ▲, 17/83; Δ, 6/94.

The copolymer with an mPEO/PTMO ratio of 0/100, also known as $PTMO_{2000}$-T6T6T, has a PTMO melting temperature of 2 °C (Table 9.3). On increasing the mPEO/PTMO ratio, the PTMO concentration decreases while the PTMO melting temperature is slightly increased (Figure 9.2). This increase might be due to co-crystallisation of PTMO and mPEO segments and/or to an improved PTMO crystallisation as the polymer molecular weight decreases. However, from previous results on PEO/PTMO-T6T6T copolymers, based on difunctional PEO segments, it is not likely that co-crystallisation of PEO and PTMO takes place [54].

Table 9.3: DSC results of $mPEO_{2000}/PTMO_{2000}$-T6T6T copolymers (20 ºC/min).

Ratio mPEO/PTMO	mPEO T_m [°C]	mPEO ΔH_m [J/g mPEO]	mPEO X_c [%]	PTMO T_m [°C]	PTMO ΔH_m [J/g PTMO]	PTMO X_c [%]	T6T6T T_m [°C]	T6T6T ΔH_m [J/g T6T6T]	T6T6T X_c [%]	T6T6T $X_{c\,(FTIR)}$ [1] [%]
0/100	-	-	-	2	22	11	227	134	88	85
6/94	42	21	11	8	32	16	228	161	>99	85
17/83	45	31	16	6	31	16	224	133	88	89
33/67	46	87	44	9	60	30	215	133	88	85
50/50	50	104	53	10	57	29	208	146	96	-
100/0	59	136	69	-	-	-	- [2]	- [2]	-	-

[1] *crystallinity determined by FTIR technique described in Chapter 4*
[2] *not observed*

The mPEO phase has a separate melting temperature that appears approximately 40 °C higher than the PTMO phase. The $mPEO_{2000}$-T6T6T-$mPEO_{2000}$ (100/0) copolymer has a melting peak at 59 ºC, which is more or less at the same temperature as the melting temperature of $mPEO_{2000}$ prepolymer (Table 10.1). The $mPEO_{2000}$ segments in this copolymer seem to be as mobile as the prepolymer. The mPEO melting temperature decreases with decreasing mPEO/PTMO ratio, which is probably due to the reduced PEO concentration and/or the increased polymer molecular weight (Figure 9.2).

The melting temperature of the T6T6T phase in the copolymer decreases with increasing mPEO concentration. The DSC results of the $mPEO_{2000}$-T6T6T-$mPEO_{2000}$ (100/0) copolymer show no clear T6T6T melting temperature as probably the T6T6T concentration is too low.

Table 9.4: DSC results of $PEO_{2000}/PTMO_{2000}$-T6T6T copolymers (20 ºC/min) [55].

Ratio PEO/PTMO	Polyether T_m [°C]	Polyether ΔH_m [J/g ether]	Polyether X_c [1] [%]	T6T6T T_m [°C]	T6T6T ΔH_m [J/g T6T6T]	T6T6T X_c [%]	T6T6T $X_{c\,(FTIR)}$ [2] [%]
0/100	2	22	11	227	134	88	85
20/80	0	20	10	220	105	69	86
40/60	7	21	11	207	84	55	87
50/50	10	28	14	203	113	75	86
60/40	12	33	17	196	97	64	87
80/20	15	39	20	184	84	55	84
100/0	21	52	27	167	67	44	84

[1] *crystallinity determined by using the PEO and PTMO concentrations and corresponding melting enthalpies of 100% crystalline polyether (PEO = 197 J/g and PTMO = 200 J/g) [53]*
[2] *crystallinity determined by FTIR technique described in Chapter 4*

The polyether melting temperature and crystallinity of $mPEO_{2000}/PTMO_{2000}$-T6T6T copolymers (Table 9.3) are compared to $PEO_{2000}/PTMO_{2000}$-T6T6T copolymers based on difunctional PEO (Table 9.4). In Chapter 4 of this thesis it was reported that $PEO_{2000}/PTMO_{2000}$-T6T6T copolymers show only one polyether melting temperature. This melting temperature increases with increasing PEO/PTMO ratio but is lower than in the case of ideal co-crystallisation as a non-linear relation was found (Figure 9.2). This indicates that the crystallinity of the polyether segments was disturbed by the presence of the other polyether segment.

There is a significant difference in (m)PEO melting temperature between both series. The mPEO melting temperature of the mPEO-based series is approximately 40 ºC higher than the difunctional PEO-based series. This is most likely due to location of the PEO segments in the copolymer. Monofunctional PEO segments that are only bound at one side are more able to diffuse and crystallise than difunctional segments.

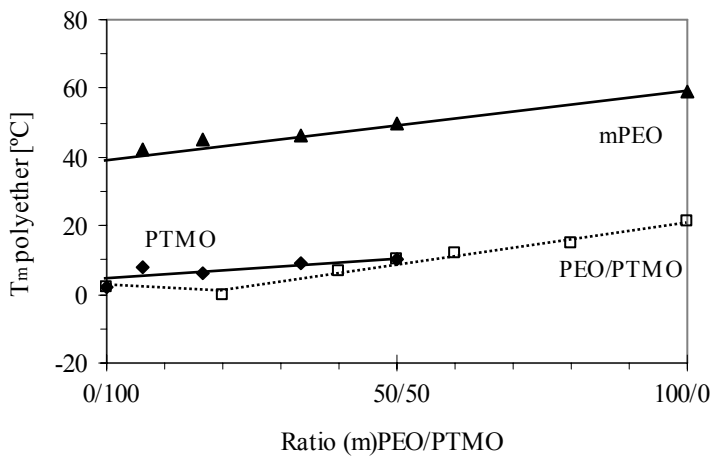

Figure 9.2: Polyether melting temperature as a function of the (m)PEO/PTMO ratio: □, $PEO_{2000}/PTMO_{2000}$-T6T6T; ▲, T_m mPEO of $mPEO_{2000}/PTMO_{2000}$-T6T6T; ♦, T_m PTMO of $mPEO_{2000}/PTMO_{2000}$-T6T6T.

By splitting the overlapping mPEO and PTMO melting peaks it was possible to determine the separate polyether melting enthalpies and to calculate the separate polyether crystallinities (X_c) (Table 9.3). The polyether crystallinities were calculated assuming a melting enthalpy of 197 and 200 J/g for 100% crystalline mPEO and PTMO respectively [53].

The PTMO and mPEO crystallinities increase with increasing mPEO concentration. The mPEO heat of fusion of the $mPEO_{2000}$-T6T6T-$mPEO_{2000}$ (100/0) copolymer is comparable to that of the $mPEO_{2000}$ prepolymer. So, $mPEO_{2000}$ end-blocks in a copolymer have a similar

melting temperature and crystallinity as the $mPEO_{2000}$ prepolymers. This is not observed for the PEO mid-blocks and the difunctional PEO_{2000} prepolymer.

The melting temperature of the crystalline T6T6T phase in the copolymers depends on the polyether concentration and the type of polyether used, as was discussed in Chapter 2. An increased polyether concentration results in a decreased melting temperature of the copolymer, which was explained by the solvent effect theory proposed by Flory [56,57]. Furthermore, the T6T6T melting temperature of PEO_{2000}-T6T6T is approximately 50 ºC lower compared to $PTMO_{2000}$-T6T6T, despite the same polyether concentration. This is probably due to a different interaction between the polyether and T6T6T segments [49].

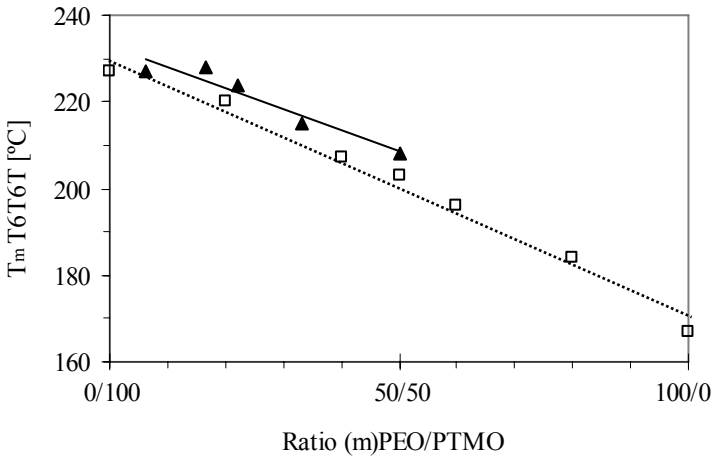

Figure 9.3: T6T6T melting temperature as a function of the (m)PEO/PTMO ratio: □, PEO_{2000}/$PTMO_{2000}$-T6T6T; ▲, $mPEO_{2000}$/$PTMO_{2000}$-T6T6T.

When the (m)PEO/PTMO ratio increases, the T6T6T melting temperature decreases (Figure 9.3). The $mPEO_{2000}$/$PTMO_{2000}$-T6T6T copolymers have a slightly higher T6T6T melting temperature and enthalpy than the PEO_{2000}/$PTMO_{2000}$-T6T6T copolymers, which is probably due to the lower molecular weight. A lower molecular weight can result in a higher T6T6T crystallinity in the copolymer, as was observed for PTMO-T6T6T copolymers [50].

The T6T6T crystallinity was calculated assuming a melting enthalpy of 152 J/g for 100% crystalline T6T6T [46]. The T6T6T crystallinity of all $mPEO_{2000}$/$PTMO_{2000}$-T6T6T copolymers is high and comparable, approximately 92% (Table 9.3). A decrease in T6T6T crystallinity from 88 to 44% with increasing PEO concentration is observed for PEO_{2000}/ $PTMO_{2000}$-T6T6T copolymers (Table 9.4).

The T6T6T crystallinity of the copolymers can also be determined by FTIR measurements, using the method described in Chapter 4 of this thesis. According to this method, the T6T6T crystallinity of all $PEO_{2000}/PTMO_{2000}$-T6T6T copolymers is high (~86%) and independent of the PEO concentration. The T6T6T crystallinity of the $mPEO_{2000}/PTMO_{2000}$-T6T6T copolymers determined by DSC and FTIR is almost constant (Table 9.3).
Unexplained as yet is the low T6T6T melting enthalpy for the $PEO_{2000}/PTMO_{2000}$-T6T6T copolymers with increasing PEO concentration, suggesting a low T6T6T crystallinity although that with FTIR experiments a high T6T6T crystallinity was found (~85%) [49]. The higher T_{flow} of the $mPEO_{2000}/PTMO_{2000}$-T6T6T copolymers than that of $PEO_{2000}/PTMO_{2000}$-T6T6T might be explained by the slightly higher T6T6T crystallinity.

Dynamic mechanical analysis

The storage and loss moduli of the $mPEO_{2000}/PTMO_{2000}$-T6T6T copolymers are given as a function of the temperature in Figure 9.4. The corresponding thermal mechanical properties of these copolymers are given in Table 9.5.

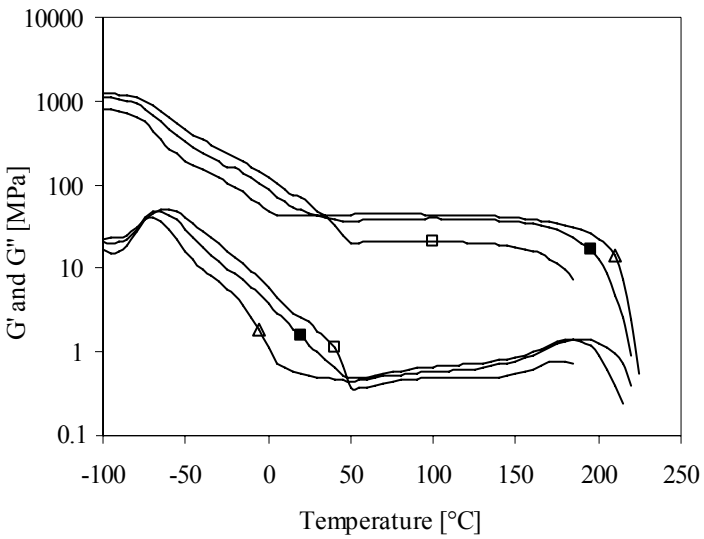

Figure 9.4: Storage (G') and loss modulus (G'') versus temperature of $mPEO_{2000}/PTMO_{2000}$-T6T6T with different mPEO/PTMO ratios: □, 50/50; ■, 33/67; Δ 6/94.

The molecular weight of the copolymer with an mPEO/PTMO ratio of 100/0 was too low to be processed by injection or compression moulding. All copolymers have a low glass transition temperature, a broad and an almost temperature independent rubbery plateau and a sharp flow temperature. This is common for copolymers with crystallisable segments of

monodisperse length [49-51,58]. For the $mPEO_{2000}/PTMO_{2000}$-T6T6T copolymers, three clear phase transitions are observed: a glass transition temperature of the soft phase, a broad melting transition of the polyether phase and a melting transition of the T6T6T phase.

Table 9.5: Dynamic mechanical properties of $(m)PEO_{2000}/PTMO_{2000}$-T6T6T copolymers.

	Conc. T6T6T [wt%]	Conc. (m)PEO [wt%]	Conc. PTMO [wt%]	T_g [°C]	T_{flex} [°C]	$G'_{20\,°C}$ [MPa]	$G'_{50\,°C}$ [MPa]	T_{flow} [°C]
$mPEO_{2000}/PTMO_{2000}$-T6T6T								
0/100	23.8	-	76.2	-70	4	34	35	226
6/94	23.2	4.8	72.0	-70	6	43	44	224
17/83	22.2	13.0	64.8	-68	10	41	42	218
33/67	20.6	26.5	52.9	-66	40	49	37	220
50/50	19.0	40.5	40.5	-64	50	69	20	~200
$PEO_{2000}/PTMO_{2000}$-T6T6T								
0/100	23.8	-	76.2	-70	4	34	35	226
20/80	23.8	15.2	61.0	-67	2	38	39	217
40/60	23.8	30.5	45.7	-63	6	31	31	212
50/50	23.8	38.1	38.1	-61	9	33	35	204
60/40	23.8	45.7	30.5	-57	8	33	35	199
80/20	23.8	61.0	15.2	-52	15	33	35	187
100/0	23.8	76.2	-	-48	20	38	38	174

Low temperature properties

One T_g is observed in the loss modulus of $mPEO_{2000}/PTMO_{2000}$-T6T6T copolymers, which increases and seems to broaden with higher mPEO concentrations (Figure 9.4). As the T_g of pure PTMO (-86 ºC) [47] is lower compared to that of the PEO prepolymer (-72 to -65 ºC) [59], the observed decrease in T_g with decreasing mPEO/PTMO ratio can be explained.

Both copolymer series show a linear increase in T_g with (m)PEO concentration (Figure 9.5). This increase is lower for $mPEO_{2000}/PTMO_{2000}$-T6T6T copolymers than for $PEO_{2000}/PTMO_{2000}$-T6T6T. It is expected that the T_g of mPEO is slightly lower compared to difunctional PEO as the mobility of the former is higher. Therefore, the increase in T_g of mPEO-based copolymers is smaller than that of difunctional PEO-based copolymers.

Most likely, the difference in T_g between PTMO and mPEO is rather small, which makes it difficult to determine whether one or two glass transitions are present in the copolymer. There

is a broadening in the glass transition observed for copolymers with a high mPEO concentration and this might indicate that mPEO and PTMO are partly phase separated.
There is another explanation possible for the low T_g of the $mPEO_{2000}/PTMO_{2000}$-T6T6T copolymers. The T6T6T crystallinity of $mPEO_{2000}/PTMO_{2000}$-T6T6T copolymers is slightly higher than for $PEO_{2000}/PTMO_{2000}$-T6T6T copolymers as the molecular weight is lower. A higher T6T6T crystallinity results in a lower amount of non-crystallised T6T6T dissolved in the polyether phase and thus a slightly lower T_g of the soft phase.

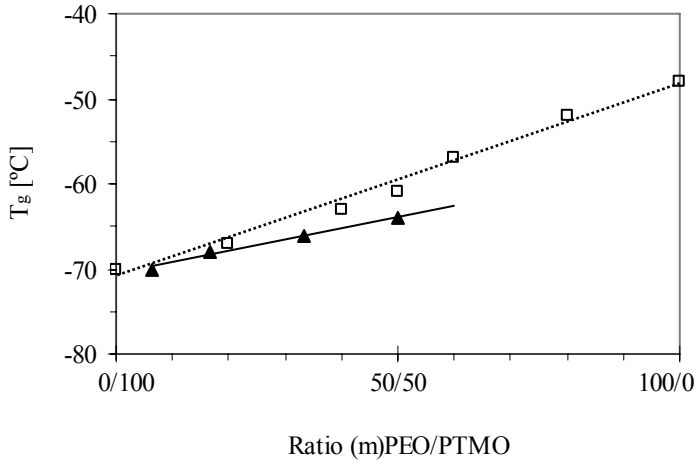

Figure 9.5: Glass transition temperature as a function of the (m)PEO/PTMO ratio: □, $PEO_{2000}/PTMO_{2000}$-T6T6T; ▲, $mPEO_{2000}/PTMO_{2000}$-T6T6T.

The melting of the crystalline polyether phase can be seen as a shoulder in the loss modulus curve (Figure 9.4). In the loss moduli versus temperature plot of the copolymer with an mPEO/PTMO ratio of 50/50, two shoulders can be observed, suggesting the existence of two crystalline polyether phases.
The flex temperature (T_{flex}), defined as the temperature where the rubbery plateau starts, is strongly related to the polyether melting temperature [49]. With increasing the mPEO/PTMO ratio a strong increase in T_{flex} of the $mPEO_{2000}/PTMO_{2000}$-T6T6T copolymers is observed. This is in agreement with the DSC results, which reveal that an increased mPEO/PTMO ratio results in an increased mPEO melting temperature and crystallinity.

Storage modulus and flow temperature

The modulus of the rubbery plateau of polyether-T6T6T copolymers depends mainly on the T6T6T concentration [49]. The modulus increases with crystalline content due to a higher physical crosslink density in the copolymer and the reinforcing filler effect of the crystalline

domains. The type of polyether segment used has no influence on the modulus of the copolymer [49]. However, the presence of a semi-crystalline polyether phase at room temperature resulted in an increased storage modulus and thus a reduced flexibility of the copolymer. The storage modulus of the rubbery plateau is determined at 50 ºC ($G'_{50\ ^oC}$) as at this temperature all polyether crystals are molten (Table 9.5).

The storage modulus at room temperature (G'_{20^oC}) of all the $PEO_{2000}/PTMO_{2000}$-T6T6T copolymers is more or less constant (~34 MPa) as the T6T6T concentration is constant and a crystalline polyether phase is absent. The T6T6T concentration of the $mPEO_{2000}/PTMO_{2000}$-T6T6T copolymers increases with increasing mPEO/PTMO ratio. As a result, the modulus of the rubbery plateau (G'_{50^oC}) increases slightly. The G'_{20^oC} is higher for the 50/50 and 33/67 ratios as these copolymers contain a semi-crystalline mPEO phase at room temperature.

Despite the same T6T6T concentration, the $mPEO_{2000}/PTMO_{2000}$-T6T6T copolymers have a slightly higher storage modulus than the $PEO_{2000}/PTMO_{2000}$-T6T6T copolymers, which is probably due to a higher T6T6T crystallinity. The higher crystallinity might be explained by the lower molecular weight of the mPEO containing copolymers.

The flow temperature determined with DMA corresponds well with melting temperature of the copolymers measured with DSC. In previous DSC results of $PEO_{2000}/PTMO_{2000}$-T6T6T copolymers it was found that the flow temperature (T_{flow}) of the copolymers depends strongly on the polyether concentration and the type of polyether segments used. The T_{flow} of $mPEO_{2000}/PTMO_{2000}$-T6T6T and $PEO_{2000}/PTMO_{2000}$-T6T6T decreases with increasing (m)PEO content, and is for both series comparable. Here, no effect of the polymer molecular weight on the T_{flow} is observed.

Water absorption

The water absorption of PEO-based segmented block copolymers is high due to the hydrophilic nature of the PEO segments [55]. The PTMO-T6T6T copolymer hardly absorbs water (~1.2 wt%). The water absorption (WA) of PEO-based copolymers depends on the PEO content. The number of water molecules per ethylene oxide unit (H_2O/EO ratio) decreases with increasing crosslink density in the copolymer and concentration of hydrophobic PTMO units in the soft phase [55].

An exponential increase in WA of $(m)PEO_{2000}/PTMO_{2000}$-T6T6T copolymers is observed with increasing (m)PEO concentration (Table 9.6, Figure 9.6a). A linear relation is observed for the copolymers when the volume fraction of water versus PEO concentration is plotted

(Figure 9.6b). The $mPEO_{2000}/PTMO_{2000}$-T6T6T copolymers have a higher WA compared to the $PEO_{2000}/PTMO_{2000}$-T6T6T copolymers.

Table 9.6: Water absorption (WA) and contact angle (CA) of (m)$PEO_{2000}/PTMO_{2000}$-T6T6T copolymers.

Ratio (m)PEO/PTMO	Conc. T6T6T [wt%]	Conc. (m)PEO [wt%]	Conc. PTMO [wt%]	WA [wt%]	H_2O/EO [-]	φ_{water} [vol%]	CA ± sd [°]
$mPEO_{2000}/PTMO_{2000}$-T6T6T							
0/100	23.8	-	76.2	1.2	-	1.2	55 ± 2
6/94	23.2	4.8	72.0	3.9	2.0	3.9	50 ± 2
17/83	22.2	13.0	64.8	12	2.3	11	47 ± 1
22/78	21.7	17.4	60.9	18	2.5	16	44 ± 1
33/67	20.6	26.5	52.9	26	2.4	22	40 ± 2
50/50	19.0	40.5	40.5	43	2.6	32	35 ± 2
$PEO_{2000}/PTMO_{2000}$-T6T6T							
0/100	23.8	-	76.2	1.2	-	1.2	55 ± 2
20/80	23.8	15.2	61.0	9.8	1.6	10	50 ± 1
40/60	23.8	30.5	45.7	24	1.9	22	48 ± 2
50/50	23.8	38.1	38.1	33	2.1	28	48 ± 2
60/40	23.8	45.7	30.5	42	2.3	33	45 ± 2
80/20	23.8	61.0	15.2	60	2.4	41	39 ± 2
100/0	23.8	76.2	-	91	2.9	52	36 ± 2

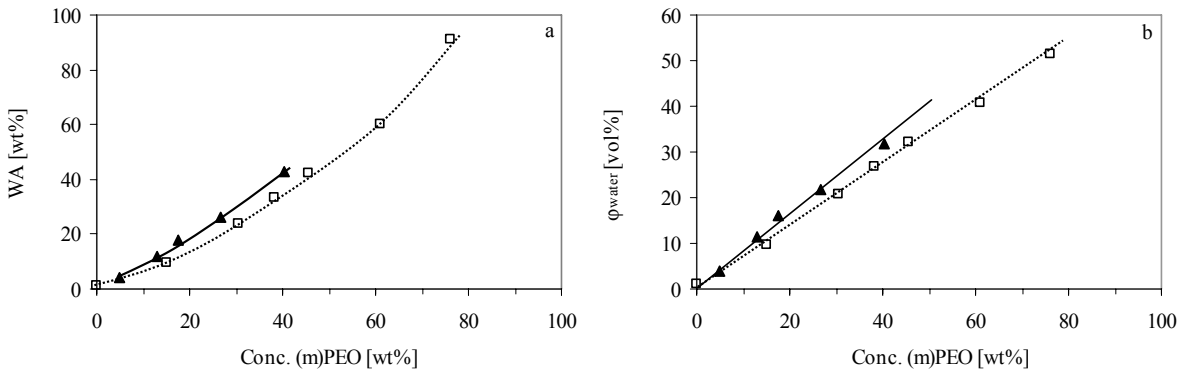

Figure 9.6: (a) Water absorption (WA) and (b) volume fraction of water (φ_{water}) as a function of the (m)PEO concentration: □, $PEO_{2000}/PTMO_{2000}$-T6T6T; ▲, $mPEO_{2000}/PTMO_{2000}$-T6T6T.

The H_2O/EO ratio of $mPEO_{2000}/PTMO_{2000}$-T6T6T decreases linearly with decreasing mPEO/PTMO ratio, suggesting that the presence of PTMO reduces the water absorption (Figure 9.7). At similar (m)PEO/PTMO ratios the H_2O/EO ratio is higher for $mPEO_{2000}/PTMO_{2000}$-T6T6T than for $PEO_{2000}/PTMO_{2000}$-T6T6T (Figure 9.7). This indicates

that PTMO decreases the water absorption to a lower extent when it is present in $mPEO_{2000}/PTMO_{2000}$-T6T6T than when it is incorporated in $PEO_{2000}/PTMO_{2000}$-T6T6T. A possible explanation is that the mPEO and PTMO segments are partly phase separated. The interaction between water and EO units is reduced when PTMO is present. When the (m)PEO and PTMO phases are well phase separated the interaction between water and EO units is less disturbed than when both phases are mixed and the phase separation is less complete.

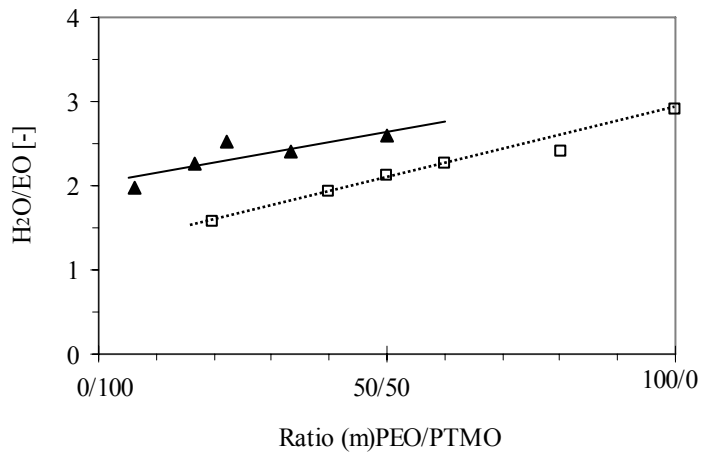

Figure 9.7: Number of water molecules per ethylene oxide unit (H_2O/EO) as a function of the (m)PEO/PTMO ratio: □, $PEO_{2000}/PTMO_{2000}$-T6T6T; ▲, $mPEO_{2000}/PTMO_{2000}$-T6T6T.

Surface properties

The surface properties of highly hydrated segmented block copolymers are studied by using the static captive (air) bubble technique. The obtained contact angle (CA) is a measure for the surface hydrophilicity; a lower CA indicates a more hydrophilic polymer surface. During the CA measurement, the polyether phase is completely amorphous as the PEO melting temperature is strongly reduced when the copolymer is fully hydrated with water [44].

Previous results obtained with segmented block copolymers based on a mixture of PEO and PTMO show a linear decrease of the CA with increasing PEO content [44]. This linear decrease indicates that there was no preferential diffusion of PEO towards the hydrated polymer surface. The CA of the $mPEO_{2000}/PTMO_{2000}$-T6T6T series has been determined to study the effect of the location of the PEO segments in the copolymers on the surface hydrophilicity (Table 9.6).

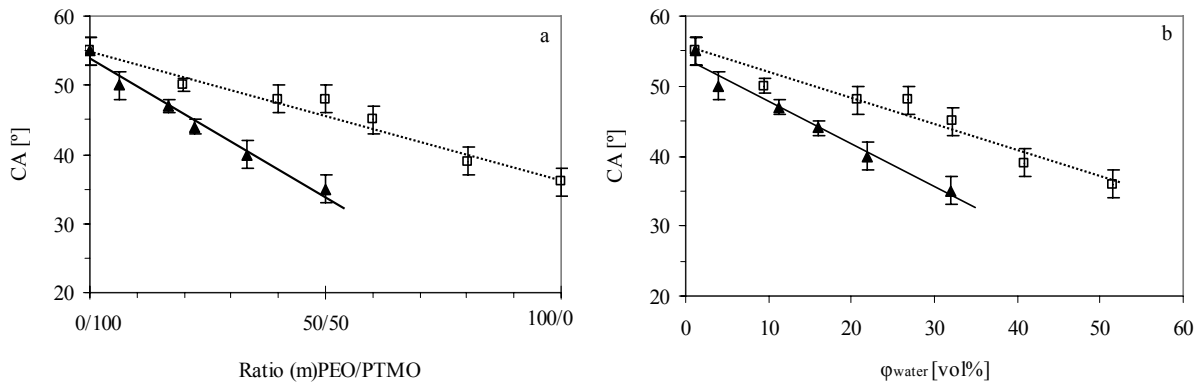

Figure 9.8: Contact angle (CA) as a function of (a) the (m)PEO/PTMO ratio and (b) the volume fraction of water: □, $PEO_{2000}/PTMO_{2000}$-T6T6T; ▲, $mPEO_{2000}/PTMO_{2000}$-T6T6T.

When the (m)PEO/PTMO ratio or volume fraction of water increases, the CA of both copolymer series show a linear decrease (Figure 9.8). This linear decrease indicates that PEO is not preferentially present at the polymer surface or else a sharp decrease in CA would have been observed at low PEO contents. The T6T6T crystalline phase restricts diffusion of the PEO segments and, therefore, the migration of PEO towards the surface.

At a similar (m)PEO/PTMO ratio or volume fraction of water, the $mPEO_{2000}/PTMO_{2000}$-T6T6T copolymers have a significantly lower CA than the $PEO_{2000}/PTMO_{2000}$-T6T6T copolymers. This is most likely due to the higher mobility of mPEO segments compared to difunctional PEO segments.

Tensile properties

The tensile properties of dry and fully hydrated $mPEO_{2000}/PTMO_{2000}$-T6T6T segmented block copolymers were studied by using injection moulded bars cut to dumbbells (Table 9.7). In general, it is known that water lowers the mechanical properties of the copolymer, like the initial E-modulus, yield stress and fracture stress [19,36-40]. The presence of polyether crystals at room temperature results in an increased modulus, yield stress and fracture stress. However, in an aqueous environment the PEO melting temperature is strongly reduced and the PEO phase is completely amorphous at room temperature [55].

At small deformations the stress increases linearly with the strain. Above the yield point the stress gradually increases. At higher strains (>300%) strain-induced crystallisation of the polyether segments can take place, which results in an increased fracture stress [60]. As water lowers the melting temperature of PEO, strain-induced crystallisation of the hydrated PEO segments becomes more difficult [55]. The PTMO segments are hardly affected by the

presence of water. Taking into account the swelling of the copolymer in water, the actual T6T6T concentration was calculated by correcting for the water absorption.

Table 9.7: Tensile properties of dry and hydrated $mPEO_{2000}/PTMO_{2000}$-T6T6T copolymers.

Ratio mPEO/PTMO	η_{inh} [dL/g]	WA [wt%]	Conc. T6T6T [wt%]	$\sigma_{10\%}$ [MPa]	σ_y [1] [MPa]	ε_y [1] [%]	σ_f [MPa]	ε_f [%]	σ_{true} [2] [MPa]
6/94	1.6	0	23.2	7.0	11.1	45	26	710	207
		3.9	22.3	5.8	9.7	39	20	560	133
17/83	1.3	0	22.2	5.9	10.0	38	13	300	52
		12	19.8	4.9	8.4	38	12	310	48
22/78	1.2	0	21.7	5.7	9.7	40	12	230	41
		18	18.4	4.2	7.6	38	9	110	18
33/67	1.0	0	20.6	5.7	-	-	10	60	15
		26	16.6	-	-	-	3	10	3

[1] *Yield stress and strain were determined using the Considère method* [61]
[2] *True fracture stress (σ_{true}) was calculated by $\sigma_f \times (1 + (\varepsilon_f / 100))$*

The stress at 10% strain ($\sigma_{10\%}$), which is a measure for the tensile behaviour at low strains, depends mainly on the T6T6T concentration [51]. A small increase in $\sigma_{10\%}$ is observed for the $mPEO_{2000}/PTMO_{2000}$-T6T6T copolymers with decreasing mPEO/PTMO ratio since the T6T6T concentration increases. The $\sigma_{10\%}$ of hydrated copolymers is slightly lower compared to dry copolymers. This difference is due to a lower T6T6T concentration of hydrated copolymers and an increased flexibility of hydrated PEO segments.

In segmented block copolymers, the yield point is often the beginning of breaking up the crystalline structure [62]. Before the yield point the deformation is mainly elastic. The yield stress of polyether-T6T6T copolymers depends on the T6T6T content. Generally, a linear increase in yield stress is observed with increasing rigid segment concentration [51,55].

There is a small increase in the yield stress of dry $mPEO_{2000}/PTMO_{2000}$-T6T6T copolymers with decreasing mPEO/PTMO ratio since the T6T6T concentration increases. When the copolymers absorb water, the T6T6T concentration is slightly reduced and the strain-induced crystallisation of the PEO segments is reduced.

Previous results on hydrated polyether-T6T6T copolymers revealed that the yield strain increases with decreasing concentration T6T6T and increasing water absorption. This was explained by the plasticizing effect of water on the PEO segments [55]. There was no remarkable difference observed in the yield strain between the dry $mPEO_{2000}/PTMO_{2000}$-

T6T6T copolymers despite the small changes in the T6T6T concentration. Moreover, no difference is observed in yield strain between dry and hydrated copolymers.

The fracture stress of polyether-based segmented block copolymers depends on the polymer molecular weight and the strain-induced crystallisation of the polyether phase [60,62,63]. Strain-induced crystallisation is taking place above 300% strain and is influenced by the type of polyether segment and the molecular weight. At comparable molecular weights, the reinforcing effect obtained by strain-induced crystallisation of PEO-based copolymers was lower than of PTMO-based copolymers, resulting in a lower fracture stress (27 and 45 MPa respectively) [55].

An increased mPEO/PTMO ratio of $mPEO_{2000}/PTMO_{2000}$-T6T6T copolymers leads to an increased number of polymer end-blocks and, consequently, a decreased molecular weight. With increasing the mPEO/PTMO ratio the fracture stress and strain are strongly reduced. The 6/94 copolymer has still a high fracture strain (710%) and strain-induced crystallisation was taken place, giving a high fracture stress (26 MPa). Upon further increasing the mPEO/PTMO ratio, the molecular weights decrease and thus the fracture stress and strain decrease. The copolymer with a ratio of 33/67 has a relatively low molecular weight (~11,000 g/mol), a fracture stress of 10 MPa and a fracture strain of 60%.

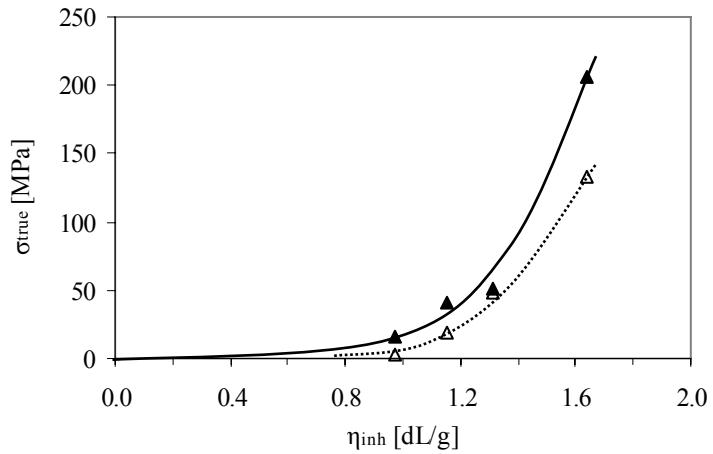

Figure 9.9: True fracture stress (σ_{true}) as a function of the inherent viscosity (η_{inh}) of $mPEO_{2000}/PTMO_{2000}$-T6T6T copolymers: (▲) dry and (Δ) hydrated copolymers.

The fracture stress and fracture strain can be combined into a single parameter; the true fracture stress (σ_{true}). The σ_{true} of the copolymers decreases with decreasing molecular weight and ability of strain-induced crystallisation of the polyether phase. In Figure 9.9 the σ_{true} is

given as a function of the inherent viscosity of $mPEO_{2000}/PTMO_{2000}$-T6T6T copolymers. When the inherent viscosity is approximately 1.6 dL/g a strong increase in σ_{true} is observed. The fracture properties, and thus the true fracture stress, are lowered when the copolymer absorbs water.

$mPEO_b/PTMO_{2000}$-T6T6T segmented block copolymers

The previous results show that end-capping $PTMO_{2000}$-T6T6T copolymers with monofunctional PEO_{2000} segments results in an increased polymer surface hydrophilicity. An $mPEO_b/PTMO_{2000}$-T6T6T copolymer series is made, where *b* represents the molecular weight of the mPEO segments, which is varied from 350 to 5000 g/mol (Table 9.8). All the copolymers have more or less the same inherent viscosity and thus comparable molecular weights (~11,000 g/mol).

Table 9.8: Polymer composition, inherent viscosity, water absorption and contact angle of $mPEO_b/PTMO_{2000}$-T6T6T copolymers.

M_n mPEO [g/mol]	Ratio mPEO/PTMO	Conc. T6T6T [wt%]	Conc. mPEO [wt%]	Conc. PTMO [wt%]	η_{inh} [dL/g]	WA [wt%]	H_2O/EO [-]	φ_{water} [vol%]	CA ± sd [°]
-	0/100	23.8	-	76.2	2.2	1.2	-	1.2	55 ± 2
350	8/92	26.4	5.9	67.7	1.1	1.2	0.5	1.3	56 ± 2
550	12/88	25.6	9.0	65.4	1.0	1.4	0.4	1.5	54 ± 2
1100	22/78	23.4	16.5	60.1	1.1	12	1.8	11	42 ± 2
2000	33/67	20.6	26.5	52.9	1.0	26	2.4	22	40 ± 2
5000	56/44	14.8	47.3	37.9	1.2	64	3.3	41	36 ± 4

An increase in the mPEO molecular weight from 350 to 5000 g/mol results in an increased mPEO concentration in the copolymer, from 5.9 to 47.3 wt%. Hence, the water absorption also increases from 1.2 to 64 wt% (Table 9.8). A linear relation is observed between the volume fraction of water and the mPEO concentration when the mPEO molecular weight is ≥1100 g/mol (Figure 9.10a). When *b* is below 1100 g/mol, the volume fraction of water deviates from the observed linear relation. The number of water molecules per ethylene oxide unit depends strongly on the molecular weight of mPEO. A linear increase in H_2O/EO ratio is observed with increasing mPEO/PTMO ratio and thus mPEO length (Figure 9.10b).

Copolymers with short mPEO segments have a low water absorption and a low H_2O/EO ratio. The strong increase in the H_2O/EO ratio with increasing mPEO/PTMO ratio is most likely due to the mPEO molecular weight and not to the mPEO concentration.

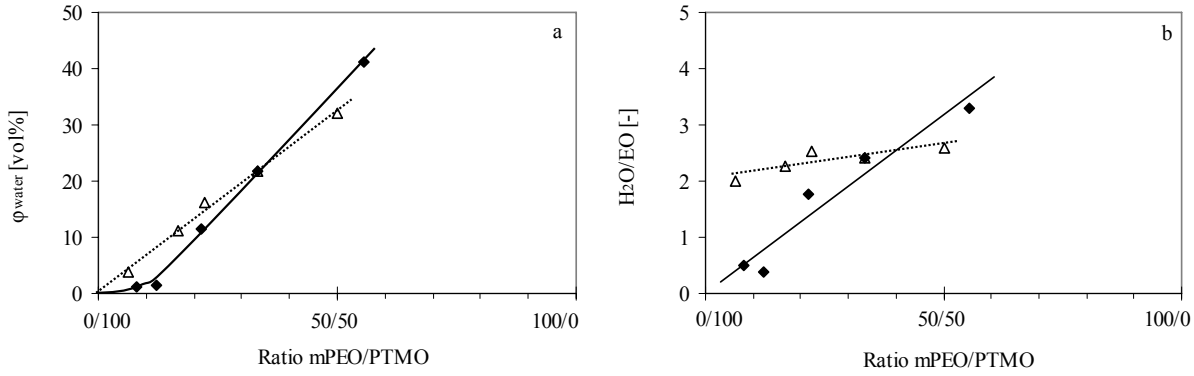

Figure 9.10: (a) Volume fraction of water (φ_{water}) and (b) number of water molecules per EO unit as a function of the mPEO/PTMO ratio: Δ, $mPEO_{2000}/PTMO_{2000}$-T6T6T; ♦, $mPEO_b/PTMO_{2000}$-T6T6T.

The influence of the molecular weight of mPEO in the $mPEO_b/PTMO_{2000}$-T6T6T copolymers on the surface hydrophilicity is studied (Table 9.8). The CA values of these copolymers are compared to the $mPEO_{2000}/PTMO_{2000}$-T6T6T copolymers, where the mPEO molecular weight was constant (2000 g/mol) and the mPEO/PTMO ratio was varied (Table 9.6).

A linear decrease in CA was observed for the $mPEO_{2000}/PTMO_{2000}$-T6T6T series with increasing mPEO/PTMO ratio (Figure 9.11a). The $mPEO_b/PTMO_{2000}$-T6T6T series shows a different behaviour. The use of $mPEO_{350}$ and $mPEO_{550}$ has no significant effect on lowering the CA and the CA is comparable to $PTMO_{2000}$-T6T6T. It seems that the surface concentration of short $mPEO_{350}$ and $mPEO_{550}$ end-blocks is relatively low and, therefore, these end-blocks are not effective to increase the surface hydrophilicity. The use of $mPEO_{1100}$ is effective in reducing the CA. A further increase of the mPEO molecular weight has only little effect on reducing the CA, despite the increased mPEO concentration.

The CA of $mPEO_{2000}/PTMO_{2000}$-T6T6T copolymers decreases linearly with the volume fraction of water (Figure 9.11b). The $mPEO_{350}$ and $mPEO_{550}$ copolymers have a comparable CA and water absorption compared to $PTMO_{2000}$-T6T6T. The use of $mPEO_{1100}$ results in an effective lowering of the CA combined with a low water absorption. The further decrease in CA by using $mPEO_{2000}$ and $mPEO_{5000}$ is minimal while the increase in water absorption is strong. This means that the copolymer with $mPEO_{1100}$ has the most optimal properties; a relatively low CA combined with relatively low water absorption. It can be concluded that the

molecular weight of the mPEO segments has a strong effect on both the bulk and surface properties of the copolymer.

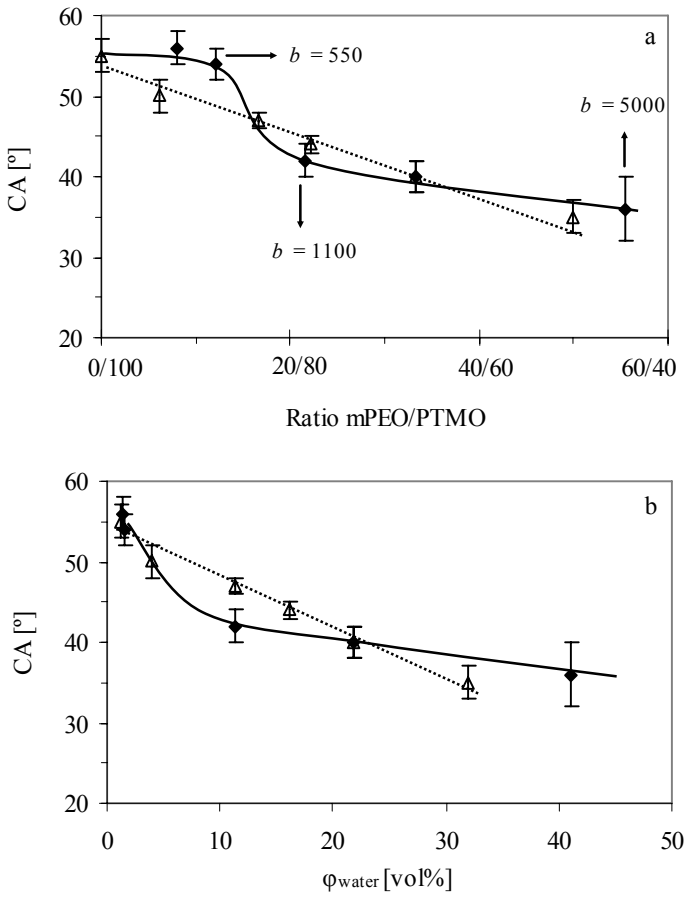

Figure 9.11: Contact angle (CA) as a function of (a) the mPEO/PTMO ratio and (b) the volume fraction of water: Δ, $mPEO_{2000}/PTMO_{2000}$-T6T6T; ♦, $mPEO_b/PTMO_{2000}$-T6T6T.

Trifunctional monomer incorporated in $mPEO_{550}/PEO_{1000}$-T6T6T copolymers

So far, it was found that end-capping of PTMO-based copolymers with monofunctional PEO segments results in an increased surface hydrophilicity. When mPEO segments were introduced in the copolymer, the polymer molecular weight was reduced, which result in a lowering of the fracture properties.

By introducing a trifunctional carboxylate ester in the copolymer, a branched structure is formed and the molecular weight increases without decreasing the mPEO concentration. An example of a trifunctional carboxylate ester is trimethyl trimesate (TMTM, Figure 9.12). This monomer has been introduced in mPEO-PET copolymers with a TMTM concentration of 3 mol%, resulting in an increased polymer surface hydrophilicity and decreased protein adsorption [45].

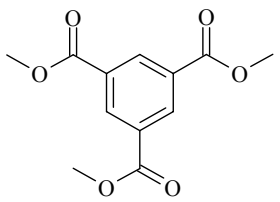

Figure 9.12: Structure of trimethyl trimesate (TMTM).

A relatively low contact angle (33º) and water absorption (35 wt%) have been observed for PEO_{1000}-T6T6T [44]. A copolymer based on PEO_{1000}-T6T6T has been end-capped with $mPEO_{550}$ segments to examine whether the surface hydrophilicity could be improved. Furthermore, an $mPEO_{550}/PEO_{1000}$-T6T6T copolymer has been synthesised containing 1.6 wt% TMTM and this copolymer is denoted as $mPEO_{550}/PEO_{1000}$/TMTM-T6T6T (Table 9.9).

The TMTM concentration should not be too high or else crosslinking takes place, resulting in a copolymer that is not soluble and melt-processable anymore. By end-capping PEO_{1000}-T6T6T with 11 wt% $mPEO_{550}$, a decrease in the inherent viscosity of 1.4 to 0.6 dL/g is observed (Table 9.9). As expected, the $mPEO_{550}/PEO_{1000}$/TMTM-T6T6T copolymer has a much higher inherent viscosity (2.5 dL/g) since this copolymer contains branches.

Table 9.9: Polymer composition and thermal mechanical properties of PEO_{1000}-T6T6T, $mPEO_{550}/PEO_{1000}$-T6T6T and $mPEO_{550}/PEO_{1000}$/TMTM-T6T6T.

Polymer type	Conc. TMTM [wt%]	Conc. T6T6T [wt%]	Conc. mPEO [wt%]	Conc. PEO [wt%]	η_{inh} [dL/g]	T_g [°C]	T_{flex} [°C]	$G'_{20\,°C}$ [MPa]	T_{flow} [°C]
PEO	-	38.4	-	61.6	1.4	-45	-13	85	199
mPEO/PEO	-	38.1	11.0	50.9	0.6	-45	0	110	204
mPEO/PEO/TMTM	1.6	31.7	11.0	55.7	2.5	-45	3	73	196

Generally, the glass transition temperature of the soft phase is influenced by the crosslink density in the copolymer [64]. By introducing TMTM in the copolymer branching points are formed and, at the same time, the physical crosslink density of the T6T6T segments is lowered due to a reduced T6T6T concentration. There is no difference in the T_g observed between PEO_{1000}-T6T6T, $mPEO_{550}/PEO_{1000}$-T6T6T and $mPEO_{550}/PEO_{1000}$/TMTM-T6T6T copolymers (Table 9.9).

Previous results discussed in this chapter revealed that the PEO crystallinity and melting temperature increases when the PEO segments are present as end-blocks instead of mid-

blocks. Therefore, the flex temperatures of both the $mPEO_{550}/PEO_{1000}$-T6T6T and $mPEO_{550}/PEO_{1000}$/TMTM-T6T6T copolymers are higher than that of PEO_{1000}-T6T6T. The high polymer molecular weight of $mPEO_{550}/PEO_{1000}$/TMTM-T6T6T does not lower the flex temperature.

The storage modulus (G') of the polyether-T6T6T copolymers depends mainly on the T6T6T concentration. With increasing T6T6T concentrations the physical crosslink density increases, which results in a higher modulus. Moreover, the storage modulus ($G'_{20\ °C}$) increases when mPEO crystals are present. The storage modulus of $mPEO_{550}/PEO_{1000}$/TMTM-T6T6T, which contains physical crosslinks as well as branching points, is lower than that of PEO_{1000}-T6T6T since the T6T6T concentration is lower. Introducing branching points at the cost of the T6T6T concentration lowers the storage modulus.

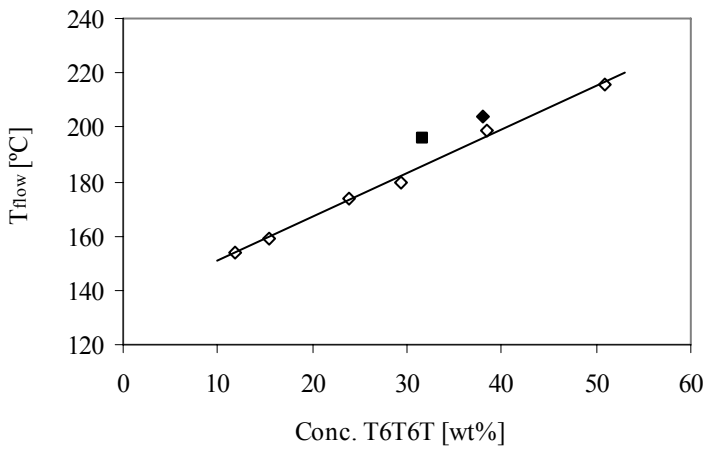

Figure 9.13: The flow temperature as a function of the T6T6T concentration: ◊, PEO_xT6T6T [49]; ♦, $mPEO_{550}/PEO_{1000}$-T6T6T; ■, $mPEO_{550}/PEO_{1000}$/TMTM-T6T6T.

At similar T6T6T concentrations, the $mPEO_{550}/PEO_{1000}$-T6T6T copolymers have a slightly higher modulus at room temperature than the PEO_x-T6T6T copolymers. At room temperature the polyether phase of the $mPEO_{550}/PEO_{1000}$-T6T6T copolymers is completely amorphous and, thus, there is no contribution of an additional crystalline phase to explain this difference in modulus. Previous results discussed in this chapter, revealed that a lower molecular weight results a higher storage modulus of the copolymer, which is probably due to a higher T6T6T crystallinity. This might explain why the $mPEO_{550}/PEO_{1000}$-T6T6T copolymer has a higher modulus than PEO_x-T6T6T copolymers.

At a comparable T6T6T concentration the flow temperatures of $mPEO_{550}/PEO_{1000}$-T6T6T and $mPEO_{550}/PEO_{1000}$/TMTM-T6T6T copolymers are slightly higher compared to the PEO_x-T6T6T copolymers (Figure 9.13). For the $mPEO_{550}/PEO_{1000}$-T6T6T copolymer this might be due to the lower molecular weight. However, the $mPEO_{550}/PEO_{1000}$/TMTM-T6T6T copolymer has a high molecular weight and, therefore, the slightly higher T_{flow} cannot be explained by this effect. An explanation for this is still not available.

Table 9.10: Water absorption (WA) and contact angle (CA) of PEO_{1000}-T6T6T, $mPEO_{550}/PEO_{1000}$-T6T6T and $mPEO_{550}/PEO_{1000}$/TMTM-T6T6T.

Polymer type	Conc. TMTM [wt%]	Conc. T6T6T [wt%]	Conc. mPEO [wt%]	Conc. PEO [wt%]	WA [wt%]	H_2O/EO [-]	φ_{water} [vol%]	CA ± sd [º]
PEO	-	38.4	-	61.6	35	1.4	30	33 ± 3
mPEO/PEO	-	38.1	11.0	50.9	33	1.3	28	28 ± 1
mPEO/PEO/TMBCT	1.6	31.7	11.0	55.7	45	1.6	35	29 ± 1

In Table 9.10 the water absorption and H_2O/EO ratio of PEO_{1000}-T6T6T, $mPEO_{550}/PEO_{1000}$-T6T6T and $mPEO_{550}/PEO_{1000}$/TMTM-T6T6T are given. In Figure 9.14 the linear relation between the volume fraction of water and PEO concentration of PEO_x-T6T6T copolymers is given.

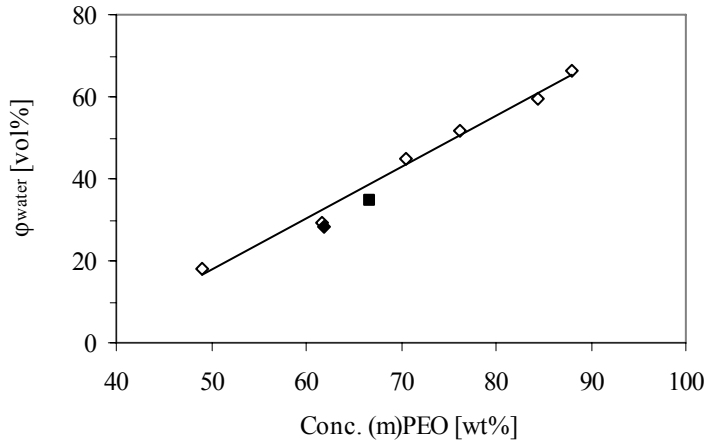

Figure 9.14: Volume fraction of water (φ_{water}) as a function of the (m)PEO concentration: ◊, PEO_xT6T6T [49]; ♦, $mPEO_{550}/PEO_{1000}$-T6T6T; ■, $mPEO_{550}/PEO_{1000}$/TMTM-T6T6T.

The water absorption of the $mPEO_{550}/PEO_{1000}$-T6T6T copolymers is more or less similar as that for PEO_x-T6T6T. This indicates that end-capping the copolymers with $mPEO_{550}$

segments does not result in a higher water absorption. Also, the presence of TMTM (1.6 wt%) in the copolymer has no significant influence on the water absorption.

The surface hydrophilicity of the copolymers is studied by determining the contact angle. The contact angles of $mPEO_{550}/PEO_{1000}$-T6T6T and $mPEO_{550}/PEO_{1000}$/TMTM-T6T6T copolymers are lower compared to PEO_{1000}-T6T6T (Table 9.10). This suggests that even $mPEO_{550}$ segments can be used to improve the hydrophilicity of PEO_{1000}-based polymer surfaces.
Previous results discussed in this chapter suggested that the surface concentration of $mPEO_{550}$ end-blocks is relatively low and insufficient for reducing of the CA of $mPEO_{550}/PTMO_{2000}$-T6T6T. The presence of 1.6 wt% TMTM in the $mPEO_{550}/PEO_{1000}$-T6T6T copolymer has no adverse effect on the surface hydrophilicity. The combination of a low contact angle (29º) and a relatively low water absorption (45 wt%) for $mPEO_{550}/PEO_{1000}$/TMTM-T6T6T copolymers is an improvement compared to the $(PEO_{1000}/T)_{5000}$-T6T6T copolymers, which have a comparable contact angle but a much higher water absorption (92 wt%) [44].

Incorporation of mPEO segments in polyether-T6T6T copolymers improves the surface hydrophilicity but decreases the polymer molecular weight. A reduced molecular weight results in a reduction of the fracture properties. The molecular weight can be increased while the mPEO concentration remains high by incorporation of a trifunctional carboxylate ester (TMTM). The introduction of 1.6 wt% TMTM leads to an increase of the inherent viscosity from 0.6 to 2.5 dL/g (Table 9.9). The tensile properties of dry and fully hydrated $mPEO_{550}/PEO_{1000}$/TMTM-T6T6T copolymers have been determined to study the effect of incorporated TMTM (Table 9.11).
The fracture stress and strain of the dry $mPEO_{550}/PEO_{1000}$-T6T6T copolymer are low, 11 MPa and 4% respectively (Table 9.11). When this copolymer was fully hydrated with water the samples could not be measured anymore. By introducing 1.6 wt% TMTM in the copolymer the tensile properties are significantly improved since the molecular weight is higher. The tensile properties of $mPEO_{550}/PEO_{1000}$/TMTM-T6T6T are also compared to the high molecular weight PEO_{1000}-T6T6T copolymer.
The actual T6T6T concentration in the hydrated copolymer was calculated by correcting the T6T6T concentration for the water absorption. The stress at 10% strain ($\sigma_{10\%}$), which depends mainly on the T6T6T concentration, is significantly reduced for hydrated PEO_{1000}-T6T6T copolymers compared to the dry copolymers, 14 to 7.8 MPa respectively. This difference is

due to a lower T6T6T concentration in hydrated copolymers and an increased flexibility of the hydrated PEO segments. The TMTM-based copolymer has a lower T6T6T concentration than PEO_{1000}-T6T6T and, therefore, the $\sigma_{10\%}$ of dry as well as hydrated copolymers is lower.

Table 9.11: Tensile properties of dry and hydrated PEO_{1000}-T6T6T, $mPEO_{550}/PEO_{1000}$-T6T6T and $mPEO_{550}/PEO_{1000}$/TMTM-T6T6T.

Polymer type	Conc. TMTM [wt%]	η_{inh} [dL/g]	WA [wt%]	Conc. T6T6T [wt%]	$\sigma_{10\%}$ [MPa]	σ_y [1] [MPa]	ε_y [1] [%]	σ_f [MPa]	ε_f [%]	σ_{true} [2] [MPa]
PEO	-	1.4	0	38.4	14	17	18	27	410	138
			35	28.4	7.8	10	23	14	150	35
mPEO/PEO	-	0.6	0	38.1	-	-	-	11	4	11
			33	28.6	-	-	-	-	-	-
mPEO/PEO/TMTM	1.6	2.5	0	31.7	11	15	27	19	290	74
			45	21.9	4.5	8	31	8.2	50	12

[1] *Yield stress and strain were determined using the Considère method* [61]
[2] *True fracture stress (σ_{true}) was calculated by $\sigma_f \times (1 + (\varepsilon_f / 100))$*

Generally, a linear increase in yield stress is observed for dry polyether-T6T6T copolymers with increasing rigid segment concentration. However, this increase is smaller for hydrated copolymers [51,55]. The polyether-T6T6T copolymers show a linear increase in yield strain with decreasing T6T6T concentration [51,55]. Furthermore, the yield strain of the copolymers increases with increasing amount of absorbed water in the equilibrium state.

The decrease in yield stress and increase in yield strain of the hydrated copolymer is due to a lower T6T6T concentration and the plasticizing effect of water on the PEO segments. The same effects are observed for the $mPEO_{550}/PEO_{1000}$/TMTM-T6T6T copolymer; when the copolymer absorbs water the yield stress decreases and the yield strain increases (Table 9.11). A lower yield stress and a higher yield strain are observed for the TMTM-based copolymer compared to the PEO_{1000}-T6T6T, which can be explained by the lower T6T6T concentration.

As was discussed before in this chapter, the true fracture stress (σ_{true}) decreases with decreasing polymer molecular weight and decreasing ability of strain-induced crystallisation of the polyether phase [60,62,63]. When TMTM is incorporated in the copolymer the molecular weight increases and, consequently, the fracture stress and strain increase (Figure 9.15).

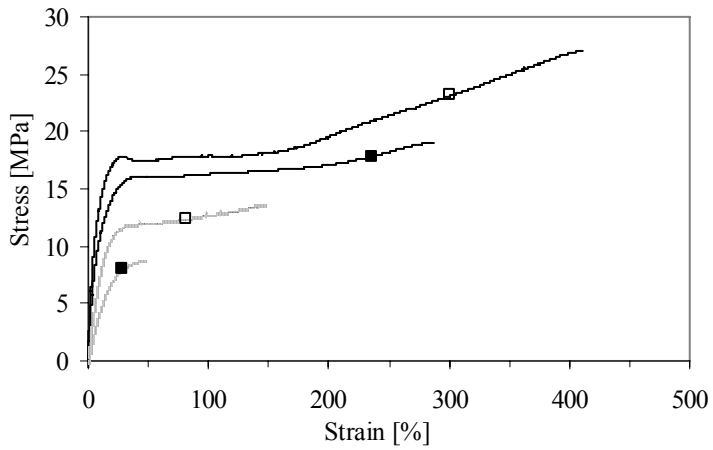

Figure 9.15: Stress-strain behaviour of dry (solid lines) and hydrated (dotted lines) copolymers: ■, mPEO$_{550}$/PEO$_{1000}$/TMTM-T6T6T; □, PEO$_{1000}$-T6T6T.

Strain-induced crystallisation of the polyether phase of the mPEO$_{550}$/PEO$_{1000}$/TMTM-T6T6T copolymer starts at ~200% (Figure 9.15), which results in an improved fracture stress. The fracture properties decrease when the copolymer absorbs water. Consequently, the true fracture stress of the hydrated copolymer is lower compared to the dry copolymer (Table 9.11). Despite the fact that the molecular weight of mPEO$_{550}$/PEO$_{1000}$/TMTM-T6T6T is higher than that of PEO$_{1000}$-T6T6T, the fracture stress and strain are lower. The mPEO$_{550}$/PEO$_{1000}$/TMTM-T6T6T copolymer shows less strain-induced crystallisation of the polyether phase than the PEO$_{1000}$-T6T6T copolymer and, therefore, the fracture properties are lower (Figure 9.15). This might be due to the presence of branching points, which partly restrict the strain-induced crystallisation of the polyether phase.

Conclusions

Segmented block copolymers end-capped with monofunctional PEO (mPEO) can be synthesised. The mid-blocks of these copolymers consist of polyether flexible segments and monodisperse crystallisable segments (T6T6T). Copolymers that contain PEO end-blocks have a higher PEO melting temperature and crystallinity than copolymers containing PEO mid-blocks. Moreover, copolymers with mPEO end-blocks have a slightly lower glass transition temperature and a slightly increased modulus and T6T6T melting temperature as compared to corresponding copolymers which were not end-capped with mPEO.

Most likely, the mPEO and PTMO phases in mPEO/PTMO-T6T6T copolymers are partly phase separated. In this case, PTMO will not decrease the water absorption of the copolymer as effectively as when PEO and PTMO are not phase separated.

The polymer surface hydrophilicity is improved when mPEO end-blocks are used instead of difunctional PEO (mid-)blocks. Segmented block copolymers end-capped with mPEO have a low contact angle (29º) combined with a relatively low water absorption (35 vol%). Preferential diffusion of the PEO segments towards the polymer surface was not observed.

The molecular weight of the mPEO end-blocks has a strong effect on both the bulk and surface properties of the copolymer. The surface concentration of short $mPEO_{350}$ and $mPEO_{550}$ end-blocks is probably low and, therefore, these end-blocks are not effective to increase the surface hydrophilicity. The use of $mPEO_{1100}$ is effective in increasing the surface hydrophilicity. A further increase of the mPEO molecular weight has only little effect on reducing the contact angle, while the water absorption increases strongly.

A disadvantage of using the mPEO segments is a decreased polymer molecular weight, which leads to a strong reduction of the fracture properties of the copolymer. By incorporating a trifunctional carboxylate ester, the molecular weight can be increased, resulting in good fracture properties, while the mPEO concentration can be relatively high (11 wt%).

References

1. Yoda, R., *J. Biomater. Sci., Polym. Ed.* **1998**, 9, p. 561-626.
2. Allmér, K., Hilborn, J., Larsson, P.H., Hult, A. and Ranby, B., *J. Polym. Sc., Part A: Polym. Chem.* **1990**, 28, p. 173-183.
3. Courtney, J.M., Lamba, N.M.K., Sundaram, S. and Forbes, C.D., *Biomaterials* **1994**, 15, p. 737-744.
4. Milton Harris, J., in *Poly(ethylene glycol) chemistry*, Plenum Press, New York **1992**.
5. Lee, J.H., Kopecek, J. and Andrade, J.D., *J. Biomed. Mater. Res.* **1989**, 23, p. 351-368.
6. Amiji, M. and Park, K., in *Polymers of biological and biomedical significance,* American Chemical Society, Washington DC **1994**.
7. Kjellander, R. and Florin, E., *J. Chem. Soc., Faraday Trans. 1* **1981**, 77, p. 2053-2077.
8. Lee, J.H., Lee, H.B. and Andrade, J.D., *Prog. Polym. Sci.* **1995**, 20, p. 1043-1079.
9. Gombotz, W.R., Guanghui, W., Horbett, T.A. and Hoffman, A.S., *J. Biomed. Mater. Res.* **1991**, 25, p. 1547-1562.
10. Desai, N.P. and Hubbell, J.A., *J. Biomed. Mater. Res.* **1991**, 25, p. 829-843.
11. Gombotz, W.R., Guanghui, W. and Hoffman, A.S., *J. Appl. Polym. Sci.* **1989**, 37, p. 91-107.
12. Meng, F.H., Engbers, G.H.M. and Feijen, J., *J. Biomed. Mater. Res. Part A* **2004**, 70A, p. 49-58.
13. Grainger, D.W., Okano, T. and Kim, S.W., *J. Colloid Interface Sci.* **1989**, 132, p. 161-175.
14. Sun, Y.H., Feng, L.X. and Zheng, X.X., *J. Appl. Polym. Sci.* **1999**, 74, p. 2826-2831.
15. Guo, S., Shen, L. and Feng, L., *Polymer* **2001**, 42, p. 1017-1022.
16. Andrade, J.D., Nagaoka, S., Cooper, S., Okano, T. and Kim, W., *Trans. Am. Soc. Artif. Intern. Organs* **1987**, XXXIII, p. 75-84.
17. Terlingen, J.G.A., Feijen, J. and Hoffman, A.S., *J. Biomater. Sci. Polym. Ed.* **1992**, 4, p. 31-33.
18. Sheu, M.S., Hoffman, A.S. and Feijen, J., in *Contact ange, wettability and adhesion,* VSP, Utrecht **1993**.
19. Petrini, P., Fare, S., Piva, A. and Tanzi, M.C., *J. Mater. Sci.: Mater. Med.* **2003**, 14, p. 683-686.
20. Lamba, N.M.K., Woodhouse, K.A. and Cooper, S.L., in *Polyurethanes in biomedical applications*, CRC Press, Washinghton DC **1998**.
21. Brinkman, E., Poot, A., van der Does, L. and Bantjes, A., *Biomaterials* **1990**, 11, p. 200-205.

22. Ji, J., Barbosa, M.A., Feng, L. and Shen, J., *J. Mater. Sci.: Mater. Med.* **2002**, 13, p. 677-684.
23. Wesslén, B., Kober, M., Freij-Larsson, C., Ljungh, A. and Paulsson, M., *Biomaterials* **1994**, 15, p. 278-284.
24. Takahara, A., Tashita, J., Kajiyama, T. and Takayanagi, M., *Polymer* **1985**, 26, p. 987-996.
25. Takahara, A., Tashita, J., Kajiyama, T. and Takayanagi, M., *Polymer* **1985**, 26, p. 978-986.
26. Takahara, A., Jo, N.J. and Kajiyama, T., *J. Biomater. Sci., Polym. Ed.* **1989**, 1, p. 17-29.
27. Okkema, A.Z., Grasel, T.G., Zdrahala, R.J., Solomon, D.D. and Cooper, S.L., *J. Biomater. Sci., Polym. Ed.* **1989**, 1, p. 43-62.
28. Stapert, H.R., '*Environmentally degradable polyesters, poly(ester-amide)s and poly(ester-urethane)s*', **1998**.
29. Bezemer, J.M., Weme, P.O., Grijpma, D.W., Dijkstra, P.J., van Blitterswijk, C.A. and Feijen, J., *J. Biomed. Mater. Res.* **2000**, 52, p. 8-17.
30. Deschamps, A.A., Claase, M.B., Sleijster, W.J., Bruijn, d., J.D., Grijpma, D.W. and Feijen, J., *J. Controlled Release* **2002**, 78, p. 175-186.
31. Deschamps, A.A., van Apeldoorn, A.A., de Bruijn, J.D., Grijpma, D.W. and Feijen, J., *Biomaterials* **2003**, 24, p. 2643-2652.
32. Van Dijkhuizen-Radersma, R., Roosma, J.R., Kaim, P., Metairie, S., Peters, F., de Wijn, J., Zijlstra, P.G., de Groot, K. and Bezemer, J.M., *J. Biomed. Mater. Res.* **2003**, 67A, p. 1294-1304.
33. Van Dorp, A.G.M., Verhoeven, M.C.H., Koerten, H.K., Blitterswijk, v., C.A. and Ponec, M., *J. Biomed. Mater. Res.* **1999**, 47, p. 292-300.
34. Leininger, R.I., in *Biomedical and dental applications of polymers,* Plenum Press, New York **1981**.
35. Leininger, R.I., in *Biomedical and dental applications of polymers,* Plenum Press, New York **1981**.
36. Deschamps, A.A., Grijpma, D.W. and Feijen, J., *J. Biomater. Sci., Polym. Ed.* **2002**, 13, p. 1337-1352.
37. Sakkers, R.J.B., De Wijn, J.R., Dalmeyer, R.A.J., Brand, R. and Van Blitterswijk, C.A., *J. Mater. Sci.: Mater. Med.* **1998**, 9, p. 375-379.
38. Rault, J. and Le Huy, H.M., *J. Macromol. Sci., Phys.* **1996**, 35, p. 89-114.
39. Deschamps, A.A., Grijpma, D.W. and Feijen, J., *Polymer* **2001**, 42, p. 9335-9345.
40. Chen, C.T., Eaton, R.F., Chang, Y.J. and Tobolsky, A.V., *J. Appl. Polym. Sci.* **1972**, 16, p. 2105-2114.
41. Deslandes, Y., Pleizier, G., Alexander, D. and Santerre, P., *Polymer* **1998**, 39, p. 2361-2366.
42. Miller, J.A., Lin, S.B., Hwang, K.K.S., Wu, K.S., Gibson, P.E. and Cooper, S.L., *Macromolecules* **1985**, 18, p. 32-44.
43. Harrell, L.L., *Macromolecules* **1969**, 2, p. 607-612.
44. Chapter 6 of this thesis.
45. Lin, Q., Unal, S., Fornof, A.R., Wei, Y.P., Li, H.M., Armentrout, R.S. and Long, T.E., *Macromol. Symp.* **2003**, 199, p. 163-172.
46. Krijgsman, J., Husken, D. and Gaymans, R.J., *Polymer* **2003**, 44, p. 7043-7053.
47. Van Krevelen, D.W., in *Properties of polymers*, Elsevier Science Publishers, New York **1990**.
48. Odian, G., in *Principles of polymerization*, John Wiley & Sons, Inc., New York **1991**.
49. Chapter 2 of this thesis.
50. Krijgsman, J., Husken, D. and Gaymans, R.J., *Polymer* **2003**, 44, p. 7573-7588.
51. Biemond, G.J.E., Ph.D. Thesis '*Hydrogen bonding in segmented block copolymers*', University of Twente, The Netherlands **2006**.
52. Vieweg, R., in *Kunststoff-Handbuch*, Hanser, Munchen **1963**.
53. Wunderlich, B., in *Thermal Analysis of Polymeric Materials*, Springer, Berlin Heidelberg New York **2005**.
54. Chapter 4 of this thesis.
55. Chapter 5 of this thesis.
56. Flory, P.J., *Trans. Faraday Soc.* **1955**, 51, p. 848.
57. Flory, P.J., in *Principles of polymer chemistry*, Cornell University Press, Ithaca **1967**.
58. Van der Schuur, M., Ph.D. Thesis '*Poly(propylene oxide) based segmented blockcopolymers*', University of Twente, The Netherlands **2004**.
59. Bailey, J.F.E. and Koleske, J.V., in *Poly(ethylene oxide)*, Academic Press, New York **1976**.
60. Niesten, M.C.E.J. and Gaymans, R.J., *Polymer* **2001**, 42, p. 6199-6207.
61. McCrum, N.G., Buckley, C.P. and Bucknall, C.B., in *Principles of polymer engineering*, Oxford university press, New York **1997**.
62. Holden, G., Legge, N.R., Quirk, R.P. and Schroeder, H.E., in *Thermoplastic elastomers*, Hanser Publishers, Munich **1996**.
63. Krijgsman, J. and Gaymans, R.J., *Polymer* **2004**, 45, p. 437-446.
64. Cowie, J.M.G., in *Polymers: chemistry & physics of modern materials*, Chapman & Hall, Cheltenham **1991**.

Summary

Segmented block copolymers consist of alternating flexible segments and crystallisable rigid segments. The flexible segments have a low glass transition temperature and are used to obtain flexible materials. The rigid segments can crystallise and act as thermal-reversible physical crosslinks, giving the material dimensional stability and solvent resistance.
The ***aim*** of the research described in this thesis, is to study the synthesis and structure-property relations of polyether-based segmented block copolymers containing monodisperse bisester tetra-amide segments (T6T6T). The polyether phase consists of hydrophilic poly(ethylene oxide) (PEO) and/or hydrophobic poly(tetramethylene oxide) (PTMO) segments. The T6T6T segments are prepared from dimethyl terephthalate (T) and hexa-methylenediamine (6). Well phase-separated polymer structures are obtained by using monodisperse crystallisable segments, resulting in a rather pure polyether phase.

The synthesis and thermal mechanical properties of PEO-T6T6T segmented block copolymers are described in ***Chapter 2***. The PEO segment length is varied from 600 to 4600 g/mol, thereby increasing the PEO concentration in the copolymer from 49 to 88 wt%. All copolymers have a high molecular weight, are melt-processable, solvent resistant and transparent. By using monodisperse rigid segments the crystallisation of the copolymers is fast and a high crystallinity is obtained (~85%). The copolymers have a low glass transition temperature, an almost temperature independent rubbery plateau and a sharp melting temperature. The copolymers have an almost complete phase separated morphology, indicating that only a small amount of non-crystallised T6T6T is present in the PEO phase. As the T6T6T concentration increases (12 – 51 wt%), the storage modulus of the rubbery plateau increases from 12 to 159 MPa and the flow temperature from 154 – 216 °C. The PEO crystallinity and melting temperature increase with increasing PEO segment length. When the PEO segment length is >2000 g/mol, PEO crystals are present at room temperature, which results in a reduced elasticity of the copolymer.

In ***Chapter 3*** the synthesis and thermal mechanical properties of PEO/T-T6T6T segmented block copolymers, where the PEO segments are extended with terephthalic units (T), are reported. Introduction of terephthalic units in the soft phase has no disturbing effect on the

storage modulus of the copolymer and leads to a slightly higher flow temperature. The use of terephthalic extended PEO segments influences the low temperature properties of the copolymer. The glass transition temperature of the soft phase is approximately 5 ºC higher when terephthalic units are present due to a reduced mobility of the PEO chains. Furthermore, by using PEO/T flexible segments the PEO melting temperature is reduced and the PEO crystallinity partly suppressed.

The synthesis and thermal mechanical properties of segmented block copolymers based on mixed hydrophilic PEO and hydrophobic PTMO flexible segments and monodisperse T6T6T segments are discussed in ***Chapter 4***. The PEO/PTMO-T6T6T copolymers have one glass transition temperature of the soft phase, indicating that both polyether segments form one homogenously mixed amorphous phase. The glass transition temperature of the copolymers increases linearly with increasing PEO content. The PEO/PTMO-T6T6T copolymers have a single polyether crystalline phase when both polyether segments have molecular weights of 2000 g/mol or less. However, when either PEO or PTMO is longer than 2000 g/mol two polyether crystalline phases are present. The polyether melting temperatures and crystallinities of the copolymers are lower than in the case of ideal co-crystallisation, indicating that the polyether segments hinder each other in their crystallisation.

In ***Chapter 5*** the influence of water on the physical and tensile properties of PEO-T6T6T, PEO/T-T6T6T and PEO/PTMO-T6T6T segmented block copolymers is studied. All the copolymers show an exponential increase in water absorption with increasing PEO concentration. The number of water molecules per ethylene oxide unit (H_2O/EO) decreases with increasing crosslink density of the copolymer and concentration of hydrophobic units in the PEO phase, like PTMO or terephthalic units. The glass transition temperature of hydrated PEO/PTMO-T6T6T copolymers decreases strongly with increasing PEO concentration and approaches the glass transition temperature of the hydrated PTMO-T6T6T copolymer. It is expected that the PEO and PTMO segments are phase separated in an aqueous environment, although it is not possible to verify this with DSC measurement. The PEO melting temperature and crystallinity decrease strongly when the copolymer absorbs water, while the PTMO crystalline phase remains unaffected.
Freezing water is present in the PEO-based copolymers when the PEO phase contains at least 30 vol% of water. Approximately 80% of the total amount of water absorbed by the PEO-

based copolymer is bound water. The PEO concentration and/or the presence of hydrophobic PTMO segments in the PEO phase have only little effect on the amount of bound water.
Hydrated copolymers have lower initial E-moduli but higher yield strains compared to dry copolymers. This can be explained by the lower T6T6T concentration in hydrated copolymers, an increased flexibility of the plasticized polyether phase and less strain-induced crystallisation of the hydrated PEO segments. After correction the T6T6T concentration for the swelling, the yield stress and the fracture stress were similar for the dry and hydrated copolymers and both decrease with decreasing T6T6T content.

The surface properties of polyether-T6T6T segmented block copolymers have been determined by contact angle measurements (captive air bubble method) and are reported in ***Chapter 6***. The contact angle of PEO-based copolymers decreases with increasing PEO concentration, indicating that the surface becomes more hydrophilic. Due to an excellent phase separation the amount of non-crystallised T6T6T in the copolymer is low and, as a result, the surface hydrophilicity is high. An interesting combination of properties, i.e. a low contact angle combined with relatively low water absorption, is observed for copolymers based on PEO segments with a molecular weight of 1000 g/mol. The PEO/PTMO-T6T6T copolymers show a linear decrease in contact angle with increasing PEO content, which indicates that there is no preferential diffusion of PEO towards the hydrated polymer surface.

The gas permeation properties and pure gas selectivities of PEO-T6T6T and PEO/T-T6T6T segmented block copolymers are examined in ***Chapter 7***. The chain flexibility of the soft phase is high since the amount of non-crystallised T6T6T in the PEO phase is low. Furthermore, the PEO crystallinity is partly suppressed by using short PEO segments (M_n of 300 or 600 g/mol) that are extended with terephthalic units. At low temperatures, the PEO/T-T6T6T copolymers have higher gas permeabilities than the PEO-T6T6T copolymers since the PEO crystallinity is partly suppressed. However, at similar amorphous flexible segment length, the CO_2 permeability of the PEO/T-based copolymers is lower than for PEO-based copolymers due to reduced chain flexibility when hydrophobic terephthalic units are present in the PEO phase.
The CO_2/N_2, CO_2/H_2 and CO_2/O_2 selectivities at 35 ºC of both the PEO-T6T6T and PEO/T-T6T6T copolymers are similar, approximately 48, 8.6 and 20 respectively. The CO_2/X selectivity of PEO-T6T6T and PEO/T-T6T6T copolymers, where X represents N_2, He, CH_4, O_2 or H_2, increases with decreasing temperature. When the copolymers contain a PEO semi-

crystalline phase the CO_2/H_2 and CO_2/He selectivities are reduced due to a more enhanced size-sieving ability of the copolymer. The presence of a semi-crystalline PEO phase has no adverse effect on the CO_2 selectivity over larger gases, like N_2, CH_4 and O_2.

The rate of water vapour transmission (WVT) through polyether-T6T6T films is described in ***Chapter 8***. The WVT is determined by using the inverted cup method (ASTM E96BW) at 30 ºC and 50% relative humidity. A linear relation is observed between the WVT and the reciprocal film thickness of the copolymer. Therefore, the WVT value can be normalised to a certain film thickness (e.g. 25 μm). The WVT of a 25 μm-thick $PTMO_{2000}$-T6T6T and PEO_{2000}-T6T6T film is 3.1 and 153 kg/m^{2}d respectively. With increasing PEO concentration in the copolymer the WVT increases exponentially. All PEO-T6T6T, PEO/T-T6T6T and PEO/PTMO-T6T6T copolymers show the same exponential increase in WVT with increasing volume fraction of absorbed water.

In ***Chapter 9*** the synthesis and properties of PTMO-T6T6T segmented block copolymers end-capped with monofunctional PEO (mPEO) are reported. Copolymers that exhibit PEO end-blocks have a higher PEO melting temperature and crystallinity than copolymers containing difunctional PEO blocks. Most likely, the mPEO and PTMO segments are partly phase separated and, therefore, PTMO will not decrease the water absorption of the copolymer as effectively as when PEO and PTMO are not phase separated.
The polymer surface hydrophilicity is improved when mPEO end-blocks are used instead of difunctional PEO mid-blocks. Preferential diffusion of the PEO segments towards the polymer surface was not observed. The molecular weight of mPEO has a strong effect on both the bulk and surface properties of the copolymer. A disadvantage of using mPEO segments is a decreased polymer molecular weight, which leads to a strong reduction of the fracture properties of the copolymer. By incorporating a trifunctional carboxylate ester, the molecular weight increases, resulting in good fracture properties, while the mPEO concentration is relatively high (11 wt%).

Samenvatting

Gesegmenteerde blokcopolymeren bestaan uit alternerende flexibele en kristalliseerbare stijve segmenten. De flexibele segmenten hebben een lage glasovergangstemperatuur (T_g) en worden gebruikt om de materialen elastisch te maken. De stijve segmenten kunnen kristalliseren en gedragen zich als thermische-reversibele fysische knooppunten die het materiaal vormvastheid en oplosmiddelbestendigheid geven.
Het ***doel*** van het onderzoek, beschreven in dit proefschrift, is om de synthese en de structuur-eigenschap relaties van gesegmenteerde blokcopolymeren, gebaseerd op flexibele polyether segmenten en monodisperse bisester tetra-amide segmenten (T6T6T), te bestuderen. De polyether fase bestaat uit hydrofiele poly(ethylene oxide) (PEO) en/of hydrofobe poly(tetramethylene oxide) (PTMO) segmenten. De T6T6T segmenten zijn gesynthetiseerd uit dimethyl terephthalate (T) en hexamethylenediamine (6). Een goed fasegescheiden structuur van het polymeer is verkregen door het gebruik van monodisperse kristalliseerbare segmenten, wat resulteert in een zeer zuivere polyether fase.

De synthese en (thermisch) mechanische eigenschappen van de PEO-T6T6T gesegmenteerde blokcopolymeren zijn beschreven in ***Hoofdstuk 2***. De lengte van het PEO segment is gevarieerd van 600 tot 4600 g/mol. Hierdoor neemt de PEO concentratie in het copolymeer toe van 49 tot 88 wt%. Alle copolymeren hebben een hoog molgewicht, zijn verwerkbaar in de smelt, oplosmiddelbestendig en transparant. Het gebruik van monodisperse stijve segmenten resulteert in een snelle kristallisatie van het copolymeer en er wordt een hoge kristalliniteit verkregen (~85%). De copolymeren hebben een lage T_g, een bijna temperatuuronafhankelijk rubber plateau en een scherp smeltpunt. De fasescheiding van de copolymeren is bijna compleet, waardoor er slechts een kleine hoeveelheid niet-gekristalliseerd T6T6T aanwezig is in de PEO fase. Een toename van de T6T6T concentratie (12 – 51 wt%) resulteert in een toename van de opslagmodulus van het rubber plateau van 12 tot 159 MPa en de vloeitemperatuur van 154 – 216 ºC. De PEO kristalliniteit en smelttemperatuur nemen toe met toenemende PEO lengte. Het copolymeer bevat PEO kristallen bij kamertemperatuur als de PEO lengte groter dan 2000 g/mol, wat leidt tot een verminderde elasticiteit van het materiaal.

Hoofdstuk 3 beschrijft de synthese en (thermisch) mechanische eigenschappen van PEO/T-T6T6T gesegmenteerde blokcopolymeren, waarvan de PEO segmenten zijn verlengd met tereftalaat units (T). De aanwezigheid van tereftalaat units in the zachte fase heeft geen storend effect op de opslagmodulus van het copolymeer en leidt tot een lichte toename van de vloeitemperatuur. Het gebruik van tereftalaat verlengde PEO segmenten beïnvloed de lage temperatuur eigenschappen van het copolymeer. De T_g van de zachte fase is ~5 ºC hoger wanneer tereftalaat units aanwezig zijn doordat de mobiliteit van de PEO ketens is verminderd. Door het gebruik van PEO/T flexibele segmenten is bovendien de PEO smelttemperatuur verlaagd en de PEO kristalliniteit gedeeltelijk onderdrukt.

De synthese en (thermisch) mechanische eigenschappen van gesegmenteerde blok-copolymeren, gebaseerd op gemengde hydrofiele PEO en hydrofobe PTMO flexibele segmenten en monodisperse T6T6T segmenten, worden toegelicht in ***Hoofdstuk 4***. De polyether segmenten vormen een homogeen gemengde amorfe fase aangezien deze copolymeren één T_g van de zachte fase vertonen. De T_g neemt lineair toe met toenemende PEO concentratie. De PEO/PTMO-T6T6T copolymeren hebben een enkele polyether kristallijne fase als de lengte van de polyether segmenten kleiner of gelijk is aan 2000 g/mol. Wanneer het PEO of het PTMO segment groter is dan 2000 g/mol, dan zijn er twee polyether kristallijne fasen aanwezig. De polyether smelttemperatuur en kristalliniteit van de copolymeren zijn lager dan in het geval van ideale co-kristallisatie. Dit betekent dat de polyether segmenten elkaar hinderen in hun kristallisatie.

In ***Hoofdstuk 5*** wordt de invloed water op de fysische en trek-rek eigenschappen van PEO-T6T6T, PEO/T-T6T6T en PEO/PTMO-T6T6T gesegmenteerde blokcopolymeren bestudeerd. Alle copolymeren vertonen een exponentiele toename in waterabsorptie met toenemende PEO concentratie. Het aantal watermoleculen per ethylene oxide unit (H_2O/EO) neemt af bij een toenemende netwerkdichtheid van het copolymeer en een toenemende concentratie van hydrofobe units zoals PTMO of tereftalaat units. De T_g van gezwollen PEO/PTMO-T6T6T copolymeren neemt sterk af bij een toenemende PEO concentratie en nadert de T_g van een gezwollen PTMO-T6T6T copolymeer. Verwacht wordt dat in een waterige omgeving de PEO en PTMO segmenten fasegescheiden zijn. Het is echter niet mogelijk dit te bevestigen met DSC experimenten. De PEO smelttemperatuur en kristalliniteit nemen sterk af wanneer het copolymeer water absorbeert, terwijl de kristallijne PTMO fase onveranderd blijft.

‘Vrij water’ is aanwezig in een PEO gebaseerd copolymeer wanneer de PEO fase tenminste 30 vol% water bevat. Ongeveer 80% van de totale hoeveelheid geabsorbeerd water door het copolymeer is ‘gebonden water’. De PEO concentratie en/of de aanwezigheid van hydrofobe PTMO segmenten in de PEO fase hebben weinig effect op de hoeveelheid ‘gebonden water’. Gezwollen copolymeren hebben een lagere E-modulus maar een hogere vloeirek vergeleken met droge copolymeren. Dit kan worden verklaard door een lagere T6T6T concentratie in een gezwollen copolymeer en een toegenomen flexibiliteit van de gezwollen polyether fase. Na correctie van de T6T6T concentratie in het copolymeer voor het zwellen blijkt dat de vloei- en breukspanning van droge en gezwollen copolymeren gelijk zijn. Beide nemen af bij een afnemende T6T6T concentratie.

De oppervlakte eigenschappen van polyether-T6T6T gesegmenteerde blokcopolymeren vermeldt in ***Hoofdstuk 6*** zijn bepaald door contacthoekmetingen (‘captive bubble’ methode). De contacthoek van PEO gebaseerde copolymeren neemt af bij een toenemende PEO concentratie, wat aangeeft dat het oppervlak meer hydrofiel wordt. Vanwege een zeer goede fasescheiding is de concentratie niet-gekristalliseerd T6T6T in het copolymeer laag en daardoor de oppervlakte hydrofiliciteit hoog. Copolymeren bestaande uit PEO segmenten met een molgewicht van 1000 g/mol hebben een interessante combinatie van eigenschappen, dat wil zeggen een lage contacthoek en relatief lage water absorptie. De PEO/PTMO-T6T6T copolymeren vertonen een lineaire afname in contacthoek bij een toenemende PEO concentratie. Dit geeft aan dat er nauwelijks diffusie van PEO naar het gezwollen polymeer oppervlak plaatsvindt.

De permeatie van pure gassen en de bijbehorende selectiviteiten van PEO-T6T6T en PEO/T-T6T6T gesegmenteerde blokcopolymeren zijn bestudeerd in ***Hoofdstuk 7***. De ketenflexibiliteit van de zachte fase is groot aangezien de hoeveelheid niet-gekristalliseerd T6T6T in the PEO fase klein is. Bovendien, de PEO kristalliniteit is gedeeltelijk onderdrukt wanneer er gebruik wordt gemaakt van korte PEO segmenten (M_n van 300 of 600 g/mol) verlengd met tereftalaat units. Bij lage temperaturen hebben de PEO/T-T6T6T copolymeren een hogere gas permeabiliteit dan PEO-T6T6T copolymeren aangezien de PEO kristalliniteit gedeeltelijk is onderdrukt. Echter, bij een gelijke lengte van het totale amorfe flexibele segment is de CO_2 permeabiliteit van de PEO/T-T6T6T copolymeren lager dan de PEO-T6T6T copolymeren. Dit komt doordat de ketenflexibiliteit is verminderd wanneer er hydrofobe tereftalaat units aanwezig zijn in de PEO fase. Bij 35 ºC zijn de CO_2/N_2, CO_2/H_2 en

CO_2/O_2 selectiviteiten van zowel de PEO-T6T6T als de PEO/T-T6T6T copolymeren gelijk, respectievelijk 48, 8.6 en 20. De CO_2/X selectiviteit van PEO-T6T6T and PEO/T-T6T6T copolymeren, waarbij *X* het gas N_2, He, CH_4, O_2 of H_2 voorstelt, neemt toe bij een afnemende temperatuur. De CO_2/H_2 and CO_2/He selectiviteiten verminderen wanneer het copolymeer een PEO semi-kristallijne fase bevat omdat dit copolymeer in staat is om de gassen te scheiden op basis van grootte. De aanwezigheid van een semi-kristallijne PEO fase heeft geen nadelig effect op de CO_2 selectiviteit betreffende grotere gassen, zoals N_2, CH_4 en O_2.

Het transport van waterdamp (WVT) door polyether-T6T6T films wordt beschreven in ***Hoofdstuk 8***. De WVT is bepaald door middel van de 'omgekeerde cup' methode (ASTM E96BW) bij 30 ºC en 50% relatieve vochtigheid. Een lineair verband is gevonden tussen de WVT en de reciproke film dikte van het copolymeer. De WVT waarde kan dus worden genormaliseerd tot een bepaalde filmdikte (bijvoorbeeld 25 μm). De WVT waarden van een film (25 μm) van $PTMO_{2000}$-T6T6T en PEO_{2000}-T6T6T zijn 3.1 en 153 kg/m^2d respectievelijk. Bij een toenemende PEO concentratie in het copolymeer nemen de WVT waarden exponentieel toe. Alle PEO-T6T6T, PEO/T-T6T6T en PEO/PTMO-T6T6T copolymeren vertonen dezelfde exponentiele toename in WVT bij een toenemend volume fractie geabsorbeerd water.

De synthese en eigenschappen van PTMO-T6T6T gesegmenteerde blokcopolymeren die zijn geblokt met monofunctioneel PEO (mPEO) staan vermeld in ***Hoofdstuk 9***. Copolymeren die bestaan uit PEO eindblokken hebben een hogere PEO smelttemperatuur en kristalliniteit dan copolymeren die difunctionele PEO blokken bevatten. Waarschijnlijk zijn de mPEO en PTMO segmenten gedeeltelijk fasegescheiden waardoor de aanwezigheid van PTMO de waterabsorptie van het copolymeer minder effectief verlaagt dan wanneer PEO en PTMO niet fasegescheiden zijn.
De hydrofiliciteit van het copolymeer oppervlak is verbeterd wanneer mPEO eindblokken zijn gebruikt i.p.v. difunctionele PEO mid-blokken. Diffusie van PEO naar het polymeer oppervlak is niet waargenomen. Het molgewicht van de mPEO segmenten heeft een groot effect op zowel de bulkeigenschappen als de oppervlakte eigenschappen van het copolymeer. Een nadeel van het gebruik van mPEO is de verlaging van het molgewicht, met als gevolg een sterke afname van de breukeigenschappen van het polymeer. Door het toevoegen van een trifunctioneel carboxylate ester neemt het polymeer molgewicht toe dat leidt tot goede breukeigenschappen terwijl de mPEO concentratie relatief hoog is (11 wt%).

Curriculum Vitea

Debby Husken is geboren op 14 april 1978 in Enschede. Na het behalen van haar HAVO diploma begon ze in 1997 aan de studie Chemie aan de Saxion Hogeschool in Enschede met als hoofdrichting analytische chemie. Deze studie is afgerond in 2001 met het uitvoeren van de afstudeeropdracht 'gesegmenteerde blokcopolymeren met een hoge hitte- en oplosmiddel-bestendigheid' bij de vakgroep Synthese en Technologie van Engineering Plastics (STEP) geleid door dr. R.J. Gaymans.

Aansluitend heeft zij een jaar als technicus gewerkt in dezelfde groep waar zij een begin heeft gemaakt met het onderzoek naar 'hydrofiele gesegmenteerde blokcopolymeren' en 'segmenteerde blokcopolymeren met gedefinieerde eindblokken'. In september 2002 is haar een promotieplaats aangeboden in de STEP groep met als onderwerp 'hydrophilic segmented block copolymers based on poly(ethylene oxide)'. Haar promotieonderzoek is uitgevoerd onder begeleiding van dr. R.J. Gaymans en prof. J. Feijen als promotor en is onderdeel van het onderzoeksprogramma van het Dutch Polymer Institute (DPI), project #313. Het resultaat van dit werk staat beschreven in het proefschrift dat nu voor u ligt. Met dit proefschrift hoopt zij op 7 december 2006 te promoveren.

Vanaf 1 november 2006 zal zij werkzaam zijn bij DSM Coating Resins in Zwolle waar zij de functie van R&D Chemist zal uitvoeren.